SEX DIFFERENCES AND SEX STEROIDS EFFECTS IN MUSCULOSKELETAL HEALTH

EDITED BY: Abdul Malik Tyagik and Sadiq Umar
PUBLISHED IN: Frontiers in Endocrinology

frontiers Research Topics

ISSN 1664-8714
ISBN 978-2-83250-342-3
DOI 10.3389/978-2-83250-342-3

About Frontiers

Frontiers is more than just an open-access publisher of scholarly articles: it is a pioneering approach to the world of academia, radically improving the way scholarly research is managed. The grand vision of Frontiers is a world where all people have an equal opportunity to seek, share and generate knowledge. Frontiers provides immediate and permanent online open access to all its publications, but this alone is not enough to realize our grand goals.

Frontiers Journal Series

The Frontiers Journal Series is a multi-tier and interdisciplinary set of open-access, online journals, promising a paradigm shift from the current review, selection and dissemination processes in academic publishing. All Frontiers journals are driven by researchers for researchers; therefore, they constitute a service to the scholarly community. At the same time, the Frontiers Journal Series operates on a revolutionary invention, the tiered publishing system, initially addressing specific communities of scholars, and gradually climbing up to broader public understanding, thus serving the interests of the lay society, too.

Dedication to Quality

Each Frontiers article is a landmark of the highest quality, thanks to genuinely collaborative interactions between authors and review editors, who include some of the world's best academicians. Research must be certified by peers before entering a stream of knowledge that may eventually reach the public - and shape society; therefore, Frontiers only applies the most rigorous and unbiased reviews.
Frontiers revolutionizes research publishing by freely delivering the most outstanding research, evaluated with no bias from both the academic and social point of view. By applying the most advanced information technologies, Frontiers is catapulting scholarly publishing into a new generation.

What are Frontiers Research Topics?

Frontiers Research Topics are very popular trademarks of the Frontiers Journals Series: they are collections of at least ten articles, all centered on a particular subject. With their unique mix of varied contributions from Original Research to Review Articles, Frontiers Research Topics unify the most influential researchers, the latest key findings and historical advances in a hot research area! Find out more on how to host your own Frontiers Research Topic or contribute to one as an author by contacting the Frontiers Editorial Office: frontiersin.org/about/contact

SEX DIFFERENCES AND SEX STEROIDS EFFECTS IN MUSCULOSKELETAL HEALTH

Topic Editors:
Abdul Malik Tyagi, Central Drug Research Institute (CSIR), India
Sadiq Umar, University of Illinois at Chicago, United States

Citation: Tyagi, A. M., Umar, S., eds. (2022). Sex Differences and Sex Steroids Effects in Musculoskeletal Health. Lausanne: Frontiers Media SA. doi: 10.3389/978-2-83250-342-3

Table of Contents

frontiers | Frontiers in Endocrinology

TYPE Editorial
PUBLISHED 13 September 2022
DOI 10.3389/fendo.2022.991989

OPEN ACCESS

Edited and reviewed by
Jonathan H. Tobias,
University of Bristol, United Kingdom

*CORRESPONDENCE
Abdul Malik Tyagi
abdultyagi@gmail.com

SPECIALTY SECTION
This article was submitted to Bone Research, a section of the journal Frontiers in Endocrinology

RECEIVED 12 July 2022
ACCEPTED 10 August 2022
PUBLISHED 13 September 2022

CITATION
Tyagi AM and Umar S (2022) Editorial: Sex differences and sex steroid effects on musculoskeletal health. *Front. Endocrinol.* 13:991989. doi: 10.3389/fendo.2022.991989

Editorial: Sex differences and sex steroid effects on musculoskeletal health

Abdul Malik Tyagi[1]* and Sadiq Umar[2]

[1]Division of Endocrinology, Council of Scientific And Industrial Research-Central Drug Research Institute (CSIR-CDRI) Lucknow, Uttar Pradesh, India, [2]Department of Oral Biology, College of Dentistry, University of Illinois, Chicago, IL, United States

KEYWORDS

sex steroids, osteoblast, osteoclast, osteoporosis, bone mass

Editorial on the Research Topic
Sex differences and sex steroid effects on musculoskeletal health

This Research Topic published original research articles and reviews from both human studies and animal models to discuss the effect of sex steroid hormones on musculoskeletal health. A total of 11 articles were included in this Research Topic and were divided into four categories: (1) original articles from *in vitro* studies, (2) original articles from animal studies, (4) original articles from human studies, and (4) review articles. Out of these 11 articles, one article was an *in vitro* study, four articles were from studies in animal models of bone loss, five articles were from human studies, and two were review articles. The role of sex steroid hormones on bones has been extensively studied. Estrogen deficiency-induced bone loss in women is defined as primary osteoporosis. There are several mechanisms involved in bone loss of sex steroid–deficient conditions such as increased reactive oxygen species, increased osteoclastogenesis and life span of osteoclast, increased osteoblast apoptosis, and immune system activation. However, in men, it is the testosterone (T) hormone that regulates bone mass. Even though we have ample information about the pathophysiology of osteoporosis and its treatment, this Research Topic provides novel insights into the role of sex steroid hormones on musculoskeletal health.

Article from *in vitro* study

Wisanwattana et al. showed that prenylated flavonoid 14 promotes osteoblast differentiation by activating the cGMP/PKG/SHP2/Src/ERK cascade *via* phosphodiesterase 5 (PDE5) inhibition, thereby leading to the localized production of estrogen by stimulating aromatase expression. This study provides new insights into the use of PDE5-inhibiting drugs to mimic the anabolic effects of mechanical bone stimulation in the treatment of osteoporosis.

Articles from animal studies

Saul et al. studied the effect of two lipoxygenase inhibitors, baicalein and zileuton, on ovariectomy (OVX)-induced bone loss in female rats and showed that the oral administration of baicalein did not improve either the vertebra or the femur. Zileuton showed a favorable effect on the trabecular vertebra, while the femur was negatively affected. Deng et al. utilized bioinformatics tools to study the mechanism of estrogen deficiency-induced bone loss. They observed 38 downregulated and 30 upregulated differentially expressed genes (DEGs). Through gene ontology analysis, the authors found that downregulated DEGs were mainly enriched in myeloid cell differentiation and cytokine-related functions, while upregulated DEGs were enriched in immune-related biological processes, pathways like Notch signaling and mitogen-activated phosphate kinase activation.

Zhou et al. studied the estrogenic effect of water extract of *Rhizoma Drynariae* (RD) administered with tamoxifen. The authors showed the interactions between RD and tamoxifen in the bone, brain, and uterus of OVX rats, while RD did not alter their responses to tamoxifen. The study further revealed that RD selectively exerts estrogenic actions differently from tamoxifen. Moreover, RD interacts with tamoxifen without altering its effects in OVX rats. Zhou et al. studied the effect of a single or combined administration with parathyroid hormone (PTH) and zoledronate acid (ZOL) on implant loosening in a rat model of osteoporosis. In this study, the authors showed that the combined treatment and monotherapy of PTH and ZOL enhanced the periprosthetic bone volume and bone–implant contact and the intramedullary implant stability in a debris wear-induced periprosthetic osteolysis under a condition of osteoporosis. Moreover, the combined PTH and ZOL therapy revealed an additive effect on preventing periprosthetic osteolysis and improving prosthetic anchorage, exhibiting a greater improvement than monotherapy that was even similar to or higher than that of the normal control group. Their findings indicate that combination or monotherapy with PTH and/or ZOL might be a promising strategy for preventing early-stage implant loosening in patients with severe osteoporosis.

Articles from human studies

Kim et al. studied the effect of tissue-specific estrogen complex (TSEC) treatment on hip geometry in postmenopausal women from Korea. They reported improvement in bone geometry in postmenopausal women after 12 months of treatment with TSEC, and it can be utilized for the prevention of fracture as well as osteoporosis in postmenopausal women. As sex steroids are thought to play a critical role in the pathogenesis of osteoarthritis (OA), Yan et al. studied the effect of sex steroids on site- and sex-specific OA and the risk of joint replacement surgery using the Mendelian randomization (MR) method. Their data showed a positive causal association between serum T levels and risks of hip OA. Serum dihydrotestosterone level was also positively associated with the risk of hip replacement. Horwath et al. examined the effect of moderate-dose T administration on molecular regulators of muscle protein turnover and mitochondrial remodeling in muscle samples collected from young women. The authors found that the improvements in muscle size and oxidative capacity in young women in response to moderate-dose T administration cannot be explained by alterations in the total expression of molecular factors known to regulate muscle protein turnover or mitochondrial remodeling. Xu et al. assessed the association of bone mineral density (BMD) with sex hormones (including T and estradiol) and sex hormone-binding globulin (SHBG) in adolescent boys and girls aged 12–19 years. Based on these findings, an appropriate increase in serum testosterone levels may be beneficial for skeletal development in girls because of the inverted U-shaped relationship (with the inflection point at 25.4 ng/dl of testosterone), and a high testosterone level might be detrimental to BMD. Furthermore, keeping the estradiol levels below a certain level in boys (24.3 pg/ml) may need to be considered.

Review articles

Another interesting study by Lin et al. reviewed the relationship between breast cancer and osteoporosis. They concluded that neuropeptide Y and its associated factors play a vital role in the development of osteoporosis and breast cancer and can be a novel diagnostic and therapeutic target for osteoporosis and breast cancer. Parker et al. reviewed the current evidence regarding the impact of relaxin on the incidence of soft tissue hip injuries in women. They found that at molecular levels, relaxin activates matrix metalloproteinases (MMPs) including collagenases MMP-1/-13 and gelatinases MMP 2/-9 to loosen pelvic ligaments for parturition. The authors concluded that menstrual cycle peaks of relaxin activate MMPs, which locally degrade collagen and gelatin. Women have relaxin receptors in multiple joints, including the hip and knee, and increased relaxin correlates with increased musculoskeletal injuries. Relaxin has paracrine effects in the female pelvis on ligaments adjacent to hip

structures, such as acetabular labral cells, which express high levels of relaxin-targeted MMPs.

This Research Topic covers many important aspects of sex steroids and skeletal health with current updates and therapeutic strategies, which provide a better understanding of the disease diagnosis and treatment options in musculoskeletal health.

Author contributions

AT and SU wrote the manuscript. AT and SU corrected and approved the final manuscript. All authors contributed to the article and approved the submitted version.

Conflict of interest

The authors declare that the research was conducted in the absence of any commercial or financial relationships that could be construed as a potential conflict of interest.

Publisher's note

frontiers in Endocrinology

ORIGINAL RESEARCH
published: 11 March 2021
doi: 10.3389/fendo.2021.649952

Effect of Tissue-Selective Estrogen Complex on Hip Structural Geometry in Postmenopausal Women: A 12-Month Study

Bo Mi Kim, Sung Eun Kim, Dong-Yun Lee and DooSeok Choi*

Department of Obstetrics and Gynecology, Samsung Medical Center, Sungkyunkwan University School of Medicine, Seoul, South Korea

OPEN ACCESS

Edited by:
Katherine A. Staines, University of Brighton, United Kingdom

Reviewed by:
Hasmik Jasmine Samvelyan, University of Brighton, United Kingdom
Fiona Saunders, University of Aberdeen, United Kingdom

****Correspondence:***
Dong-Yun Lee
dongyun0406.lee@samsung.com

Specialty section:
This article was submitted to Bone Research, a section of the journal Frontiers in Endocrinology

Received: *05 January 2021*
Accepted: *17 February 2021*
Published: *11 March 2021*

Citation:
Kim BM, Kim SE, Lee D-Y and Choi D (2021) Effect of Tissue-Selective Estrogen Complex on Hip Structural Geometry in Postmenopausal Women: A 12-Month Study. Front. Endocrinol. 12:649952. doi: 10.3389/fendo.2021.649952

Background: Hip structural analysis (HSA) is a method for evaluating bone geometry reflecting bone structural and biomechanical properties. However, tissue-selective estrogen complex (TSEC) treatment effects on HSA have not been investigated.

Objective: This study was performed to evaluate the effect of TSEC treatment on hip geometry in postmenopausal Korean women. The treatment was given for 12 months, and hip geometry was measured by HSA.

Materials and Methods: A total of 40 postmenopausal women who received TSEC containing conjugated estrogen 0.45 mg and bazedoxifene 20 mg for treating vasomotor symptoms were included in this retrospective cohort study. The changes in bone mineral density and parameters of HSA including the outer diameter, cross-sectional area, cross-sectional moment of inertia, cortical thickness, section modulus, and buckling ratio as determined by dual-energy X-ray absorptiometry were compared before and after 12 months of TSEC treatment.

Results: Mean age and years since menopause were 55.1 and 4.5 years, respectively. Total hip bone mineral density significantly increased by 0.74% after treatment (P=0.011). The changes in HSA were mainly demonstrated in the narrow femoral neck: cross-sectional area (P=0.003) and cortical thickness (P<0.001) increased significantly. For the shaft region, only SM decreased significantly after treatment (P=0.009). However, most parameters did not change significantly with TSEC treatment in the intertrochanteric and shaft regions.

Conclusions: Our findings demonstrate that 12 months of TSEC treatment could improve bone geometry as measured by HSA. The findings suggest that TSEC might be an interesting option for the prevention of fracture as well as osteoporosis in postmenopausal women.

Keywords: tissue-selective estrogen complex (TSEC), bone mineral density, hip structural analysis, menopause, hormone therapy (HT)

INTRODUCTION

Menopausal hormone therapy (MHT), estrogen alone, or estrogen-progestin combination, is effective for the prevention of osteoporosis and fractures in postmenopausal women (1, 2). However, occurrence of adverse side effects and concerns about risks associated with MHT have deterred use of MHT for this purpose. Experimental evidence suggests that most of the side effects and risks are related to the progestogen component, and a combined therapy of conjugated estrogen (CE) and bazedoxifene was developed recently and used worldwide as an alternative to conventional MHT. This new progestin-free tissue-selective estrogen complex (TSEC) would be a useful MHT option especially in women who cannot tolerate the side effects related to progestogens or who have a higher risk for breast cancer (1), and also showed beneficial effects on bone mineral density (BMD) in previous studies (3–5).

Estrogen regulates bone metabolism *via* effects on osteocytes, osteoblast, and osteoclasts, and its main effect is inhibition of bone remodeling (6). MHT reduced all major osteoporotic fractures including hip and non-vertebral fractures (7, 8), and bazedoxifene reduced spinal fractures and even prevented hip fractures in postmenopausal women at higher risk of hip fracture (9). Therefore, TSEC, a combination of these two regimens, can also be expected to have beneficial effects on fracture risk. However, fracture risk has not been adequately assessed for low doses of CE (< 0.625 mg), although the effect of estrogen on bone is dose-dependent. Moreover, the effect of TSEC on fracture risk has never been evaluated because the study duration was short (12–24 months) and the subjects were young (subject mean age was in their 50s) in previous studies (3–5).

Hip structural analysis (HSA) is a method for evaluating bone geometry reflecting bone structural and biomechanical properties using dual energy X-ray absorptiometry (DXA) scan of the proximal femur. HSA is a software method to extract information, a line of pixel values across the proximal femur bone axis, from image data of DXA bone mass (10). The profile of a mass projection could be used to estimate geometric relevance. In spite of several limitations such as high correlation with BMD or 2D nature (11, 12), HSA has been applied to assess bone mechanical strength, and therefore, to evaluate the effect of osteoporosis treatment on fracture risk (13–15). However, TSEC treatment effects on HSA have not been investigated.

Therefore, this study evaluated the change in HSA after 12 months of TSEC treatment in postmenopausal Korean women.

MATERIALS AND METHODS

Study Population

All postmenopausal women who received MHT for relieving vasomotor symptoms at the Menopause Clinic at Samsung Medical Center were considered for inclusion. Menopause was diagnosed when women had no spontaneous menstruation over 12 months without any specific cause for amenorrhea.

The inclusion criteria were: postmenopausal women (1) with an intact uterus, (2) who received TSEC, (3) who were over 40 years old, (4) who were diagnosed with osteopenia at the femoral neck or total hip using DXA, and (5) who had results of bone densitometry and geometry before and after 12 months of TSEC use.

Exclusion criteria were: (1) use of MHT other than TSEC; (2) use of any medication that could affect bone metabolism, e.g., bisphosphonate, glucocorticoids, anti-convulsants, or heparin; (3) having a history of any disease that could affect bone metabolism, e.g., hyperthyroidism or hyperparathyroidism; (4) having been lost to follow-up before 12 months of TSEC treatment; and (5) having a history of hip fracture.

A total of 40 postmenopausal women were included for the analysis in this retrospective cohort study. The study protocol was approved by the Institutional Review Board of Samsung Medical Center, Seoul, Korea. Informed consent from participants was exempted by the Institutional Review Board because of the retrospective nature of the analysis.

Treatment and Measurement

Women received TSEC (Duavive®, Pfizer Ireland Pharmaceuticals, Newbridge, Ireland) for relief of vasomotor symptoms based on the preferences of both patients and doctors. Each TSEC tablet contained CE 0.45 mg and bazedoxifene 20 mg.

The baseline characteristics of the study population, i.e., age, body mass index, years since menopause, and parity, were obtained from medical records. In addition, the results of bone densitometry and hip geometry were also obtained.

BMD was measured at the hip using DXA (Delphi Q; Hologic Inc., Bedford, MA, USA). The *in vivo* coefficient of variation was 1.0% for the hip. For the evaluation of hip bone geometry, the HSA™ program was used for three regions, the femoral narrow neck, intertrochanter, and shaft. These were displayed on the DXA image. At each region, the HSA™ program produced geometric parameters including the outer diameter (OD), cross-sectional area (CSA), cross-sectional moment of inertia (CSMI), cortical thickness (CT), section modulus (SM), and buckling ratio (BR).

Statistical Analysis

All statistical analyses were performed using SPSS Statistics 25 software (SPSS Inc., Chicago, IL). Data are presented as mean ± standard error of the mean or number (percent). The normality assumption of the data was confirmed using the Levene's test for homogeneity of variances before statistical analysis. Changes in BMD and various parameters of HSA were compared before and after treatment using paired t tests. In addition, differences in HSA parameters between responders (no change or increase in BMD from baseline at 12 months) and non-responders (decrease in BMD from baseline at 12 months) were compared by t test or Mann–Whitney test. $P < 0.05$ was considered statistically significant.

RESULTS

Table 1 demonstrates the baseline characteristics of the study participants. The mean age and years since menopause were 55.1

TABLE 1 | Baseline characteristics of the study population.

Variables	N = 40
Age (year)	55.1 ± 0.5
Body mass index (kg/m^2)	21.5 ± 0.4
Age at menopause (year)	50.7 ± 0.5
Years since menopause (year)	4.5 ± 0.4
Age at menarche (year)	14.5 ± 0.3
Parity	1.9 ± 0.2
Nulliparous	4 (10)
Multiparous	36 (90)
Type of menopause	
Natural	40 (100)
Surgical	0

Data are presented as mean ± standard error or number (percent).

and 4.5 years, respectively. The mean body index was 21.5 kg/m^2, and only two women were obese.

Figure 1 depicts the change in BMD after 12 months of TSEC treatment. Both BMDs at the femoral neck (from 0.624 to 0.631 g/cm^2, P = 0.022) and total hip (from 0.770 to 0.776 g/cm^2, P = 0.011) increased significantly by 1.26% and 0.74%, respectively. In addition, T-score also improved significantly at the femoral neck (from -1.68 to -1.59, P = 0.004) and total hip (from -0.72 to -0.65, P = 0.006).

Table 2 shows the changes in various parameters of HSA after 12 months of TSEC treatment. For the narrow neck of the femur, CSA (P = 0.003) and CT (P<0.001) increased significantly. In addition, although not statistically significant, CSMI and SM tended to increase and BR tended to decrease. However, OD did not change. For the intertrochanteric region, women had a wider diameter after treatment (P = 0.041). However, other parameters such as CSA, CSMI, SM, CT, and BR did not change significantly after treatment. For the shaft region, only SM decreased significantly after treatment (P = 0.009), and OD, CSA, CSMI, CT, and BR did not differ.

Table 3 presents the changes in HSA according to BMD response. Responders were women with no change or increase in total hip BMD after treatment. Because the number of each group was relatively small, some parameters in **Table 3** did not meet the normality assumption. In these contexts, t test or Mann–Whitney test were used where indicated. For the narrow femoral neck, percent changes in OD, CSA, and CSMI were significantly higher in responders than in non-responders. Values were significantly decreased in OD and CSMI or only slightly increased in CSA in non-responders after treatment. Although not statistically significant, BR also decreased in responders in contrast to a minimal increase in non-responders. For the intertrochanteric region, OD and BR decreased in responders and increased in non-responders, and the changes were significantly different between responders and non-responders (P = 0.031 for OD and P=0.026 for BR). For the shaft region, CSA and CT increased in responders and decreased in non-responders after treatment, showing a significant difference of percent changes between the two groups (P = 0.005 for CSA and P = 0.042 for CT).

DISCUSSION

This study evaluated the changes in BMD and HSA after 12 months of TSEC treatment in postmenopausal Korean women. This study demonstrated that, with TSEC treatment, hip BMD significantly increased, and some parameters of HSA were improved with TSEC treatment.

In the present study, total hip BMD significantly increased by 0.7% after treatment. This finding is similar to previous studies that demonstrated an approximate 1% (SMART-1), 0.84% (SMART-4), and 0.5% (SMART-5) increase of total hip BMD after 12 months of TSEC treatment (3–5). Since our study population was osteopenic postmenopausal women who were at low risk for bone loss or fracture, this amount of BMD increase could maintain women's bone health (16). In addition, the percentage of total hip BMD responders was 65% in the present study. This is comparable to the 61.5% of SMART-4 (4) and 70% of SMART-1 responders (3). The amount of total hip BMD increase in the current study was similar to that seen with bazedoxifene alone (9). This suggests that the combination

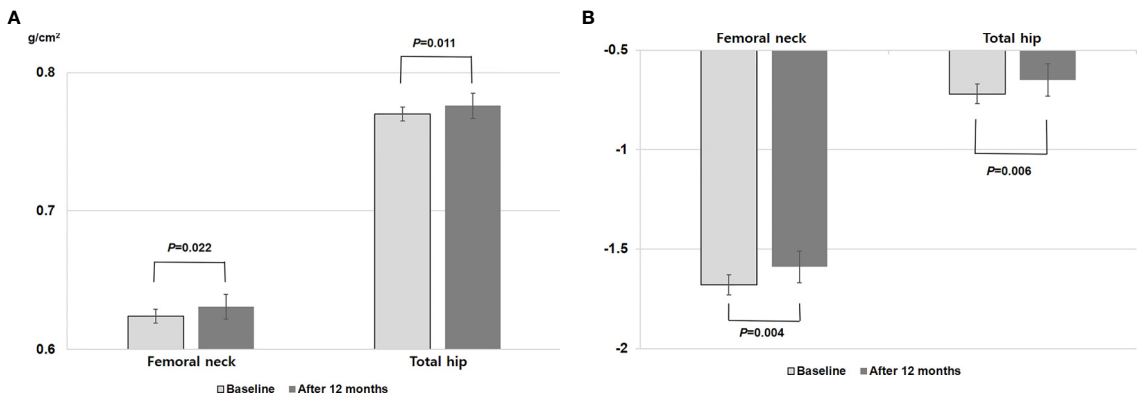

FIGURE 1 | Changes in **(A)** bone mineral density and **(B)** T-score at the femoral neck and total hip after 12 months of TSEC treatment. P value by paired t test.

TABLE 2 | Changes in parameters of hip structural analysis at three regions after 1 year of TSEC treatment.

Site	Variables	Baseline	After treatment	*P*-value
Narrow neck	OD (cm)	3.28 ± 0.045	3.25 ± 0.036	0.380
	CSA (cm^2)	2.41 ± 0.026	2.46 ± 0.025	**0.003**
	CSMI (cm^4)	2.06 ± 0.042	2.09 ± 0.042	0.075
	SM (cm^3)	1.14 ± 0.019	1.16 ± 0.017	0.055
	CT (cm)	0.15 ± 0.002	0.16 ± 0.002	**<0.001**
	BR	12.4 ± 0.324	11.9 ± 0.244	0.074
Intertrochanter	OD (cm)	5.40 ± 0.041	5.51 ± 0.054	**0.041**
	CSA (cm^2)	4.18 ± 0.060	4.27 ± 0.061	0.105
	CSMI (cm^4)	11.06 ± 0.273	11.52 ± 0.285	0.061
	SM (cm^3)	3.48 ± 0.076	3.57 ± 0.070	0.088
	CT (cm)	0.35 ± 0.006	0.36 ± 0.007	0.318
	BR	9.20 ± 0.176	9.21 ± 0.200	0.918
Femur shaft	OD (cm)	2.86 ± 0.026	2.88 ± 0.026	0.274
	CSA (cm^2)	3.64 ± 0.045	3.63 ± 0.051	0.507
	CSMI (cm^4)	2.94 ± 0.069	2.90 ± 0.061	0.166
	SM (cm^3)	1.97 ± 0.032	1.93 ± 0.030	**0.009**
	CT (cm)	0.49 ± 0.010	0.49 ± 0.011	0.187
	BR	3.10 ± 0.095	3.19 ± 0.120	0.104

Data are presented as mean ± standard error. P-value by paired t test. NS, not significant; TSEC, tissue-selective estrogen complex; OD, outer diameter; CSA, cross-sectional area; CSMI, cross-sectional moment of inertia; SM, section modulus; CT, cortical thickness; BR, buckling ratio.
In bold: statistically significant p-values.

TABLE 3 | Percent changes in parameters of hip structural analysis at three regions after 1 year of TSEC treatment, according to the response of bone mineral density at the total hip.

Site	Variables	Responder (n = 26)	Non-responder (n = 14)	*P*-value
Narrow neck	OD (cm)	3.06 ± 0.75	−4.33 ± 1.37	**0.001**
	CSA (cm^2)	3.83 ± 0.77	0.38 ± 0.85	**0.005**
	CSMI (cm^4)	4.47 ± 1.43	−0.13 ± 1.47	**0.031**
	SM (cm^3)	2.98 ± 1.17	2.40 ± 2.36	0.827
	CT (cm)	1.53 ± 1.65	5.81 ± 2.34	0.142
	BR	−6.18 ± 3.01	0.40 ± 2.32	0.091
Intertrochanter	OD (cm)	−0.01 ± 0.99	4.01 ± 1.49	**0.031**
	CSA (cm^2)	2.11 ± 1.30	2.72 ± 2.34	0.820
	CSMI (cm^4)	2.03 ± 2.57	8.26 ± 3.94	0.194
	SM (cm^3)	2.17 ± 1.77	4.16 ± 2.49	0.519
	CT (cm)	2.18 ± 1.85	1.62 ± 2.67	0.864
	BR	−2.14 ± 1.03	2.34 ± 1.62	0.026
Femur shaft	OD (cm)	0.14 ± 0.61	1.04 ± 0.73	0.349
	CSA (cm^2)	0.95 ± 0.65	−1.68 ± 0.58	**0.005**
	CSMI (cm^4)	−2.65 ± 1.46	0.35 ± 1.47	0.157
	SM (cm^3)	−2.64 ± 0.99	−1.20 ± 1.00	0.315
	CT (cm)	0.70 ± 1.39	−3.42 ± 1.37	**0.042**
	BR	0.25 ± 2.02	5.93 ± 2.59	0.092

Data are presented as mean ± standard error. P-value by t test or Mann–Whitney test as indicated. NS, not significant. TSEC, tissue-selective estrogen complex.
Responder, no change or increase in bone mineral density from baseline at 12 months; non-responder, decrease in bone mineral density from baseline at 12 months.
OD, outer diameter; CSA, cross-sectional area; CSMI, cross-sectional moment of inertia; SM, section modulus; CT, cortical thickness; BR, buckling ratio.
In bold: statistically significant p-values.

of bazedoxifene 20 mg and CE 0.45 mg did not produce an additional BMD gain by adding the estrogen component. One possible explanation is that, since both CE and bazedoxifene bind to the estrogen receptor and CE has a more potent effect, addition of bazedoxifene to CE may attenuate the BMD response (3, 5).

The risk of hip fracture is low in young postmenopausal women who usually take TSEC, and the study duration in previous studies regarding TSEC was too short (≤ 24 months). Therefore, fracture risk related to TSEC use has never really been addressed. In addition, either low-dose CE (0.45 mg) or bazedoxifene therapy has not been proven to reduce the hip fracture risk in postmenopausal women at low risk. In these contexts, HSA was assessed as a possible surrogate marker to evaluate beneficial effects of TSEC on fracture risk in this study.

In the present study, the changes in HSA parameters, indicating geometry-related improvement, were mainly observed in the narrow femoral neck region. The femoral neck is the most common location of fractures. Our findings are consistent with the 3-year retrospective study in postmenopausal women with osteoporosis (mean age: 67.4 years). Those researchers reported that treatment with bazedoxifene was associated with significant increases in CSA and SM in the narrow femoral neck and in CSA in the trochanter region. Also, almost no significant change in the

shaft region compared with placebo was demonstrated (17). Besides bazedoxifene results, results from the following three studies regarding MHT are also similar to our study findings. In a prospective study analyzing about 600 current hormone users, CSA and CT increased compared to never users (18). In addition, in the 3-year randomized clinical trial in women over the age of 65 years, MHT using CE 0.625 mg (n = 93) increased CSA and SM in the narrow femoral neck region, and BR decreased after treatment (19). From the Women's Health Initiative study (20), CSA and CT increased and BR decreased in the narrow neck region at year 1 among hormone users compared with placebo. Favorable changes in HSA parameters in the intertrochanter or shaft region were also not observed. No significant differences in the geometric changes were found between estrogen alone and estrogen-progestin treatment, suggesting that the effect of estrogen was responsible for the changes.

The beneficial effect of estrogen seems to be associated with increases in cortical thickness and section moduli *via* direct effects on bone (18). The load sensitivity can be increased by estrogen on bone tissue. In addition, estrogen has a positive effect on muscle strength; this may play an indirect role on bone strength (21). However, we could not conclude that the combination of bazedoxifene and CE had additional benefits on hip structural geometry compared with estrogen or bazedoxifene alone. Differences in treatment (dose, type, duration) and study population (age, baseline BMD, history of fracture, or other risk factors) have a considerable impact on bone health; therefore, the degree of beneficial effects will differ across studies.

This is the first study to evaluate the change in HSA with TSEC treatment in young osteopenic postmenopausal women. Although previous studies showed a significant increase in BMD and significant decreases in bone turnover markers, HSA has never been assessed in TSEC users. In addition, previous studies evaluated the effects of MHT on HSA in older women (over 65 years old); but, from recent guidelines, MHT is no longer recommended for bone health in older women (1, 2). The current main indication for MHT is young postmenopausal women having vasomotor symptoms who are younger than 60 years or within 10 years from menopause onset. This is similar to our study population. Therefore, the current study could provide real world evidence regarding TSEC on hip geometry.

However, this study had several limitations. This was not a prospective clinical trial, and duration of treatment and sample size may not have been adequate to assess the effects of TSEC on HSA. In a post-hoc power analysis, this study had a power of about 30% to detect differences in the changes of HSA parameters with an alpha error of 0.05. This study did not contain a control group who had osteopenia but did not use TSEC. However, it already has been shown that parameters of HSA did not change significantly in placebo group during one year (20). In addition, although intake of calcium and vitamin D was encouraged for all patients and daily supplementation was provided if necessary, we could not ascertain that all patients consumed sufficient calcium and vitamin D for maintaining bone health. Finally, the clinical implication of our findings is not clear in young postmenopausal women at low risk of hip fracture, and therefore, the results should be interpreted with caution.

In conclusion, this pilot study demonstrates that a combination of CE and bazedoxifene could enhance improvements in bone strength evaluated by HSA and suggests that TSEC may be a treatment option for prevention of fracture and osteoporosis in postmenopausal women. Further long-term, large-scale study is necessary to draw a clear conclusion.

DATA AVAILABILITY STATEMENT

The raw data supporting the conclusions of this article will be made available by the authors, without undue reservation.

ETHICS STATEMENT

The studies involving human participants were reviewed and approved by Samsung medical center. Written informed consent for participation was not required for this study in accordance with the national legislation and the institutional requirements.

AUTHOR CONTRIBUTIONS

BK, SK, D-YL, and DC were responsible for the concept and design of the study, searching for and analyzing data, and the writing of the manuscript. All authors contributed to the article and approved the submitted version.

REFERENCES

1. Baber RJ, Panay N, Fenton A, IMS Writing Group. 2016 IMS Recommendations on women's midlife health and menopause hormone therapy. *Climacteric* (2016) 19:109–50. doi: 10.3109/13697137.2015.1129166
2. The NAMS 2017 Hormone Therapy Position Statement Advisory Panel. The 2017 hormone therapy position statement of The North American Menopause Society. *Menopause* (2017) 24:728–53. doi: 10.1097/GME.0000000000000921
3. Lindsay R, Gallagher JC, Kagan R, Pickar JH, Constantine G. Efficacy of tissue-selective estrogen complex of bazedoxifene/conjugated estrogens for osteoporosis prevention in at-risk postmenopausal women. *Fertil Steril* (2009) 92:1045–52. doi: 10.1016/j.fertnstert.2009.02.093
4. Mirkin S, Komm BS, Pan K, Chines AA. Effects of bazedoxifene/conjugated estrogens on endometrial safety and bone in postmenopausal women. *Climacteric* (2013) 16:338–46. doi: 10.3109/13697137.2012.717994
5. Pinkerton JV, Harvey JA, Lindsay R, Pan K, Chines AA, Mirkin S, et al. Effects of bazedoxifene/conjugated estrogens on the endometrium and bone: a randomized trial. *J Clin Endocrinol Metab* (2014) 99:E189–98. doi: 10.1210/jc.2013-1707
6. Khosla S, Oursler MJ, Monroe DG. Estrogen and the skeleton. *Trends Endocrinol HSMetab* (2012) 23:576–81. doi: 10.1016/j.tem.2012.03.008

7. Jackson RD, Wactawski-Wende J, LaCroix AZ, Pettinger M, Yood RA, Watts NB, et al. Effects of conjugated equine estrogen on risk of fractures and BMD in postmenopausal women with hysterectomy: results from the women's health initiative randomized trial. *J Bone Miner Res* (2006) 21:817–28. doi: 10.1359/jbmr.060312
8. Cauley JA, Robbins J, Chen Z, Cummings SR, Jackson RD, LaCroix AZ, et al. Effects of estrogen plus progestin on risk of fracture and bone mineral density: the Women's Health Initiative randomized trial. *JAMA* (2003) 290:1729–38. doi: 10.1001/jama.290.13.1729
9. Silverman SL, Christiansen C, Genant HK, Vukicevic S, Zanchetta JR, de Villiers TJ, et al. Efficacy of bazedoxifene in reducing new vertebral fracture risk in postmenopausal women with osteoporosis: results from a 3-year, randomized, placebo-, and active-controlled clinical trial. *J Bone Miner Res* (2008) 23:1923–34. doi: 10.1359/jbmr.080710
10. Martin RB, Burr DB. Non-invasive measurement of long bone cross-sectional moment of inertia by photon absorptiometry. *J Biomech* (1984) 17:195–201. doi: 10.1016/0021-9290(84)90010-1
11. Beck TJ, Broy SB. Measurement of Hip Geometry-Technical Background. *J Clin Densitom* (2015) 18:331–7. doi: 10.1016/j.jocd.2015.06.006
12. Choi YJ. Dual-Energy X-Ray Absorptiometry: Beyond Bone Mineral Density Determination. *Endocrinol Metab* (2016) 31:25–30. doi: 10.3803/EnM.2016.31.1.25
13. Rivadeneira F, Zillikens MC, De Laet CE, Hofman A, Uitterlinden AG, Beck TJ, et al. Femoral Neck BMD Is a Strong Predictor of Hip Fracture Susceptibility in Elderly Men and Women Because It Detects Cortical Bone Instability: The Rotterdam Study. *J Bone Miner Res* (2007) 22:1781–90. doi: 10.1359/jbmr.070712
14. Kaptoge S, Beck TJ, Reeve J, Stone KL, Hillier TA, Cauley JA, et al. Prediction of Incident Hip Fracture Risk by Femur Geometry Variables Measured by Hip Structural Analysis in the Study of Osteoporotic Fractures. *J Bone Miner Res* (2008) 23:1892–904. doi: 10.1359/jbmr.080802
15. LaCroix AZ, Beck TJ, Cauley JA, Lewis CE, Bassford T, Jackson R, et al. Hip structural geometry and incidence of hip fracture in postmenopausal women: what does it add to conventional bone mineral density? *Osteoporos Int* (2010) 21:919–29. doi: 10.1007/s00198-009-1056-1
16. Gallagher JC, Palacios S, Ryan KA, Yu CR, Pan K, Kendler DL, et al. Effect of conjugated estrogens/bazedoxifene on postmenopausal bone loss: pooled analysis of two randomized trials. *Menopause* (2016) 23:1083–91. doi: 10.1097/GME.0000000000000694
17. Beck TJ, Fuerst T, Gaither KW, Sutradhar S, Levine AB, Hines T, et al. The effects of bazedoxifene on bone structural strength evaluated by hip structure analysis. *Bone* (2015) 77:115–9. doi: 10.1016/j.bone.2015.04.027
18. Beck TJ, Stone KL, Oreskovic TL, Hochberg MC, Nevitt MC, Genant HK, et al. Effects of current and discontinued estrogen replacement therapy on hip structural geometry: the study of osteoporotic fractures. *J Bone Miner Res* (2001) 16:2103–10. doi: 10.1359/jbmr.2001.16.11.2103
19. Greenspan SL, Beck TJ, Resnick NM, Bhattacharya R, Parker RA. Effect of hormone replacement, alendronate, or combination therapy on hip structural geometry: a 3-year, double-blind, placebo-controlled clinical trial. *J Bone Miner Res* (2005) 20:1525–32. doi: 10.1359/JBMR.050508
20. Chen Z, Beck TJ, Cauley JA, Lewis CE, LaCroix A, Bassford T, et al. Hormone therapy improves femur geometry among ethnically diverse postmenopausal participants in the Women's Health Initiative hormone intervention trials. *J Bone Miner Res* (2008) 23:1935–45. doi: 10.1359/jbmr.080707
21. Jacobsen DE, Samson MM, Kezic S, Verhaar HJJ. Postmenopausal HRT and tibolone in relation to muscle strength and body composition. *Maturitas* (2007) 58:7–18. doi: 10.1016/j.maturitas.2007.04.012

Conflict of Interest: The authors declare that the research was conducted in the absence of any commercial or financial relationships that could be construed as a potential conflict of interest.

frontiers in Endocrinology

ORIGINAL RESEARCH
published: 12 March 2021
doi: 10.3389/fendo.2021.636784

Inhibition of Phosphodiesterase 5 Promotes the Aromatase-Mediated Estrogen Biosynthesis in Osteoblastic Cells by Activation of cGMP/PKG/SHP2 Pathway

Wisanee Wisanwattana[1,2†], Kanjana Wongkrajang[3†], Dong-yi Cao[1,2], Xiao-ke Shi[1,2], Zhong-hui Zhang[4], Zong-yuan Zhou[1,2], Fu Li[1], Qing-gang Mei[1], Chun Wang[1], Apichart Suksamrarn[5], Guo-lin Zhang[1] and Fei Wang[1*]*

[1] Center for Natural Products Research, Chengdu Institute of Biology, Chinese Academy of Sciences, Chengdu, China, [2] University of Chinese Academy of Sciences, Beijing, China, [3] Department of Chemistry, Faculty of Science and Technology, Pibulsongkram Rajabhat University, Phitsanulok, Thailand, [4] College of Chemical Engineering, Sichuan University, Chengdu, China, [5] Department of Chemistry and Center of Excellent for Innovation in Chemistry, Faculty of Science, Ramkhamhaeng University, Bangkok, Thailand

OPEN ACCESS

Edited by:
Abdul Malik Tyagi,
Emory University, United States

Reviewed by:
Hamid Yousf Dar,
Emory University, United States
Subhashis Pal,
Emory University, United States

***Correspondence:**
Fei Wang
wangfei@cib.ac.cn
Guo-lin Zhang
zhanggl@cib.ac.cn

[†]These authors have contributed equally to this work

Specialty section:
This article was submitted to Bone Research, a section of the journal Frontiers in Endocrinology

Received: 02 December 2020
Accepted: 15 February 2021
Published: 12 March 2021

Citation:
Wisanwattana W, Wongkrajang K, Cao D-y, Shi X-k, Zhang Z-h, Zhou Z-y, Li F, Mei Q-g, Wang C, Suksamrarn A, Zhang G-l and Wang F (2021) Inhibition of Phosphodiesterase 5 Promotes the Aromatase-Mediated Estrogen Biosynthesis in Osteoblastic Cells by Activation of cGMP/PKG/SHP2 Pathway. Front. Endocrinol. 12:636784. doi: 10.3389/fendo.2021.636784

Mechanical stimulation induces bone growth and remodeling by the secondary messenger, cyclic guanosine 3', 5'-monophosphate (cGMP), in osteoblasts. However, the role of cGMP in the regulation of estrogen biosynthesis, whose deficiency is a major cause of osteoporosis, remains unclear. Here, we found that the prenylated flavonoids, 3-*O*-methoxymethyl-7-*O*-benzylicaritin (13), 7-*O*-benzylicaritin (14), and 4'-*O*-methyl-8-isopentylkaempferol (15), which were synthesized using icariin analogs, promoted estrogen biosynthesis in osteoblastic UMR106 cells, with calculated EC_{50} values of 1.53, 3.45, and 10.57 μM, respectively. 14 and 15 increased the expression level of the bone specific promoter I.4-driven aromatase, the only enzyme that catalyzes estrogen formation by using androgens as substrates, in osteoblastic cells. 14 inhibited phosphodiesterase 5 (PDE5), stimulated intracellular cGMP level and promoted osteoblast cell differentiation. Inhibition of cGMP dependent-protein kinase G (PKG) abolished the stimulatory effect of 14 on estrogen biosynthesis and osteoblast cell differentiation. Further, PKG activation by 14 stimulated the activity of SHP2 (Src homology 2 domain-containing tyrosine phosphatase 2), thereby activating Src and ERK (extracellular signal-regulated kinase) signaling and increasing ERK-dependent aromatase expression in osteoblasts. Our findings reveal a previously unknown role of cGMP in the regulation of estrogen biosynthesis in the bone. These results support the further development of 14 as a PKG-activating drug to mimic the anabolic effects of mechanical stimulation of bone in the treatment of osteoporosis.

Keywords: icariin analogs, aromatase, osteoblast, PDE5, estrogen biosynthesis

INTRODUCTION

Osteoporosis is a major global public health problem caused by the reduced estrogen level in postmenopausal women (1). In humans, aromatase cytochrome P450 (CYP19A1) catalyzes the formation of estrogens from C19 androgens (2). The aromatase expression at various sites is regulated by tissue-specific promoters through the alternative splicing mechanisms (3). In bone, class I cytokines such as TGF-β1, IL-1β, and TNF-α drive aromatase expression by the usage of promoter I.4 (4). Aromatase activity is a key factor in skeletal development and mineralization, and is crucial to estrogen production in the bone (5). Aromatase activity may decline with an increase in during aging, and the contribution of such decline to age-related bone loss is similar in magnitude to that of sex steroid deficiency in both women and men (6, 7). Therefore, agonists of aromatase expression or activity in the bone would be a new therapeutic means for preventing and treating osteoporosis.

Mechanical stimulation is a primary determinant of bone growth and remodeling, through generating the shear stress that stimulates osteoblasts and osteocytes and enhances their anabolic activity. In mechanically stimulated osteoblasts the NO/cGMP/PKG signaling pathway activates Erk-1/2 and a proliferative response through the recruitment of PKGII, Src, and SHP-1/2 into an integrin β3-containing mechanosome membrane complex (8). NO, which is increased by estrogen exposure, also mediates estrogen-stimulated human and rodent osteoblast proliferation and differentiation (9). Src kinase has also been found to regulate aromatase activity by directly phosphorylating aromatase or indirectly regulating aromatase expression through the MAPK pathway (10). In osteocyte, 17β-estradiol is found to prevent the bone loss by increasing its survival through NO/cGMP-mediated stimulation of Akt and Akt- and PKG-dependent phosphorylation of the pro-apoptotic Bcl-2 protein BAD (11). However, the role of cGMP in the regulation of estrogen biosynthesis in osteoblasts is still not well understood. An inhibitor of PDE5, which is responsible for cGMP degradation, has been found to increase aromatase expression and estrogen biosynthesis in human adipocytes and ovarian granulosa cells (12, 13). Thus, it will be of interest to investigate the crosstalk of cGMP signaling on aromatase expression in osteoblastic cells, which may provide new insights into the underlying mechanism of cGMP-mediated signaling in osteoblast proliferation and differentiation.

It is unclear whether natural medicinal plants exert their antiosteoporotic effects by modulating estrogen biosynthesis in the bone. Previously we found that icariin from *Epimedium brevicornum*, a widely used antiosteoporotic medicinal plant, promotes the production of estrogen in human ovarian granulosa cells and osteoblastic cells, with an underlying mechanism that remains unclear (14). Icariin and its analogs are found to be the inhibitors of PDE5 (15). We showed that the PDE5 inhibitors, sildenafil and icariin analogs, promote aromatase expression in human ovarian granulosa-like KGN cells by activating the cAMP/CREB pathway (13). Thus, further investigating the effect and mechanism of icariin analogs on aromatase regulation in bone tissue will be important for developing new therapeutic means to prevent and treat osteoporosis.

MATERIALS AND METHODS

Chemicals and Reagent

The 18 icariin analogs were synthesized and identified as described previously (16, 17, **Figure S1**). The compounds were dissolved in DMSO (Sigma-Aldrich, Shanghai, China) and stored at -20°C. Testosterone was purchased from Sigma-Aldrich. The magnetic particle-based 17β-estradiol enzyme-linked immunosorbent assay (ELISA) kit was purchased from Bio-Ekon Biotechnology (Beijing, China). NSC-87877, KT5823, PD98059 and Rp-8-pCPT-cGMPS were obtained from Tocris Bioscience (MN, USA). Antibodies used in this study as follow: aromatase (1:1,000, ab64881, Abcam, Shanghai, China), Src (1:1,000, 11097-1-AP, Proteintech, Wuhan, China), shp2 (1:2,000, 20145-1-AP, Proteintech, Wuhan, China), phospho-Src-Tyr^{418} (1:1,000, 11091, SAB, Nanjing, China), phospho-Src-Tyr^{529} (1:1,000, 11153-1, SAB, Nanjing, China), ERK1/2 (1:1,000, 48504-1, SAB, Nanjing, China), phospho-ERK1/2 (1:1,000, 12082-1, SAB, Nanjing, China) and PDE5A (1:1,000, 37810, SAB, Nanjing, China).

Cell Culture

The rat osteoblast-like cell line (UMR106), murine osteoblast-like cell line (MC3T3-E1), human embryonic kidney 293T (HEK293T) and 293A (HEK293A) cell lines were obtained from the Cell Bank of Chinese Academy of Sciences (Shanghai, China). UMR106, HEK293T, and HEK293A cells were maintained in DMEM/High glucose medium supplemented with 10% (v/v) fetal bovine serum and 1% (v/v) penicillin/streptomycin at 37°C in 5% CO_2. MC3T3-E1 cells were maintained in α-MEM medium supplemented with 10% (v/v) fetal bovine serum and 1% (v/v) penicillin/streptomycin at 37°C in 5% CO_2. Aromatase-overexpressing HEK293A cells as described before (18).

Cell-Based Estrogen Biosynthesis Assay

The assay was conducted as described previously (19). The UMR106 cells or MC3T3-E1 cells were seeded overnight in 24-well plates. After that the medium was replaced with serum-free medium, and the cells were pretreated for 24 h with the test chemicals. Testosterone (10 nM) was then added to each well, the cells were incubated for an additional 48 h. The magnetic particle-based ELISA kit was used to quantify the 17β-estradiol in the culture medium according to the manufacturer's instructions (Bio-Ekon Biotechnology). The results were normalized to the total cellular protein content, and expressed as percentages of the control. The BCA protein assay kit was used for protein determination (Bestbio, Shanghai, China).

Western Blotting

Immunoblotting was performed as described (19). Cells cultured were harvested in RIPA buffer supplemented with a protease inhibitor cocktail (Sigma). Proteins lysate was loaded and separated on a sodium dodecyl sulfate-polyacrylamide gel

electrophoresis. After that, the proteins were blotted onto nitrocellulose membranes and then incubated with each specific antibody, then enhanced chemiluminescence detection (Amersham Biosciences, Piscataway, NJ, USA).

Real-Time Quantitative Reverse Transcription-PCR

The qRT-PCR analysis was performed as described (19). TRIzol reagent was used to isolated total cellular RNA according to the manufacturer's protocol (Invitrogen, Carlsbad, CA, USA). SuperScript III Reverse Transcriptase (Invitrogen, Carlsbad, CA, USA) was used to reverse-transcribe total RNA (2 μg) with oligo dT15 primer. Equal amounts (1 μL) of cDNA were subjected qRT-PCR with the florescent dye SYBR Green I, according to the manufacturer's protocol (TransGen Biotech, Beijing, China). The following primer pairs were used: *aromatase*, 5'- ATGTTTCTGGAAATGCTGAACCCGAT GCATT -3' (forward) and 5'- CTGTTTCAGATATTTTT CGCTGTTGCGCGG -3' (reverse); aromatase *promoter I.4*, 5'–CACTGGTCAGCCCATCAA–3' (forward) and 5'-ACGATGCTGGTGATGTTATAATGT–3' (reverse); *GAPDH*,:5'-GGTCAGTGCCGGCCTCGTCTCATAGACA–3' (forward) and 5'-GAGGGTGCAGCGAACTTTATTGA–3'(reverse); *Runt-related transcription factor 2* (*Runx2*), 5'–ATGCTGCATAGCCCGCATAAACAGCCGCAG–3' (forward) and 5'- GTTCGCATCCGGCGCCTGCGGCACGCTCTG–3' (reverse); *Osteocalcin* (*OCN*), 5'–ATGCGCACCCTGAGCCT GCTGACC–3' (forward) and 5'–CACGGTGGTGCCAT AAATGCGTTTA–3' (reverse); *Osterix (Osx)*, 5'–ATGG CGAGCAGCCTGCTGGAAGAAGAAG–3' (forward) and 5'–AATTTCCAGCAGGTTGCTCTGTTCCGG–3' (reverse); *Alkaline phosphatase (ALP)*, 5'–ATGATTCTGCCGTTTC TGGTGCTGGC–3' (forward) and 5'–AAACAGGGTGCGC AGCGGAAACAG–3' (reverse); *Osteoprotegerin (OPG)*, 5'–CTGTGCGTGCCGTGCCCGGATTATAGCTA–3' (forward) and 5'–CAGGCAGCTAATTTTCACGCTCTGCA–3' (reverse); *Receptor activator of nuclear factor kappa-B ligand (RANKL)*, 5'–ATGCGCCGCGCGAACCGCGATTATG–3' (forward) and 5'–ATCAATATCCTGCACTTTAAACGCG–3' (reverse), and *β-actin*, 5'–ATGGATGATGATATTGCGGCGCTGG–3' (forward) and 5'– AAAGCATTTGCGATGCACAATGCTCG–3' (reverse). The thermal cycling conditions consisted of an initial denaturation step at 95 °C for 10 s, followed by 40 cycles of 95 °C for 60 s, 54 °C for 30 s, and 72 °C for 30 s. The relative quantity (n-Fold) of *aromatase*, *CYP19I.4*, *RUNX2*, *OCN*, *Osx*, *ALP*, and *OPG*/*RANKL* mRNA was calculated by the Δ(ΔCt) method using GAPDH as a reference amplified from the same sample.

Measurement of Intracellular cGMP Level

UMR106 cells seeded in 6-well plates overnight were treated with **14** and sildenafil for the indicated time. The pre-cooled PBS buffer (120-150 μL) was added in 1×10^6 cells to keep the cells suspended. The cells were lysed with the repeated freeze-thaw process. After centrifugation for 10 min at 1500 × g at 2-8°C, the supernatants were collected to carry out the assay. The cGMP concentration was determined with a commercial cGMP enzyme immunoassay kit (Elabscience, Wuhan, China). Thereafter, the results were measured with Thermo Scientific Verioskan Flash Multimode Reader at a wavelength of 450 nm ± 2 nm.

Alkaline Phosphatase (ALP) Activity Assay

ALP activity was performed as described (20). UMR-106 cells were seeded in serum-free medium in a 24-well plate overnight and treated with the test compounds for 48 h. After that a kit using para-nitrophenyl phosphate as substrate was used to assay the cell lysate. The OD value was measured at 405 nm with Thermo Scientific Verioskan Flash Multimode Reader. The results were expressed as percentages of the control and normalized on a protein basis.

SHP2 Activity Assay

SHP2 was immunoprecipitated and its activity is assayed as described previously (21). UMR106 cells were lysed in RIPA buffer that contained a complete protease inhibitor cocktail after treatment with **14** and SHP2 inhibitor (NSC-87877) for 30 min. The lysates were incubated on ice for 10 min and centrifuged at 20,000 × g for 15 min at 4°C. SHP2 antibody was incubated with cleared lysates overnight at 4°C with agitation, followed by the incubation with the Protein A/G agarose (Santa Cruz Biotech, TX, USA). The immunoprecipitates were resuspended gently in reaction buffer (100 μL) and transferred to a 96-well plate. The DiFMUP was used as the substrate of SHP2 to measure its activity with a plate reader (Thermo Scientific Varioskan® Flash).

Cellular Thermal Shift Assay

Cellular thermal shift assay was conducted as described previously (21). HEK293T cells were collected in PBS supplemented with protease inhibitor cocktail. The freeze-thawed cell lysates were centrifuged at 20,000 g for 20 min at 4°C, diluted with PBS and divided into two aliquots; one aliquot was treated with DMSO while the other was treated with **14** (100 μM). For temperature response experiments, 50 μL of lysate was transferred to PCR tubes and heated for 3 min to various temperatures. After that the cell lysates were centrifuged at 20,000 g for 20 min at 4°C to separate the soluble fractions from the precipitates. The supernatants were dissolved in loading buffer and analyzed by western blotting. The dose effect of **14** on the stability of PDE5A or vinculin was evaluated in the same manner.

Measuring Recombinant Expressed PDE5 Activity

The activity of recombinant expressed PDE5 (Enzo Biochem, Madison, USA) was evaluated using the PDE-Glo™ Phosphodiesterase assay (Promega Corporation, Madison, WI, USA). Aliquots of PDE-Glo™ reaction buffer containing appropriate amounts of purified human recombinants PDE5A were added to a 96-well plate. After the addition of diluted compounds to each well, cGMP™ solution was added to initiate the reaction. After an appropriate incubation, Kinase-Glo® reagent was pipetted into each well and 10 min later

luminescence was measured using a plate reader (Thermo Scientific Varioskan® Flash).

Molecular Docking

The crystal structure of PDE5 [PDB code: 2H42] was obtained from the Protein Data Bank. During the process, all water molecules were removed, and hydrogen atoms were added to the protein molecule. Autodock 4 was used to predict the interactions between compounds and protein structure of PDE5 according to the binding energy with the default setting.

Cell Viability Assay

UMR 106 cells were plated at 0.5×10^4 cells/well in 96-well plates with 100 μL medium. The different concentrations of **13**, **14**, and **15** were used to treat the cultured cells for 24 h. After that the medium was added with 10 μL of the Alamar blue reagent and incubated for another 2–4 h with the measurement of the relative fluorescence intensity in each well.

Statistical Analysis

Statistical analysis was analyzed by GraphPad Prism 6 (GraphPad, La Jolla, CA, USA). The results are expressed as mean ± standard error of the mean (S.E.M.) of three independent experiments with individual values. Data were compared by one-way ANOVA followed by Dunnett's *post hoc* test. A p-value of less than 0.05 was considered to indicate a significant difference relative to the control.

RESULTS

Effect of Icariin Analogs on Estrogen Biosynthesis

To search for small molecules that modulate estrogen biosynthesis, we examined the effects of icariin analogs (16, 17, **Figure S1**) and their effects on estrogen biosynthesis in the rat osteoblast-like cell line, UMR106. The chemical structure of the icariin (**Figure 1A**, compound 2) and its analogs are presented in **Figure 1A**. As shown in **Figure 1B**, testosterone supplementation significantly increased 17β-estradiol production in UMR106 cells, which was further enhanced by dexamethasone treatment, thereby aligning with previous reports (22, 23). To examine the effect of icariin and its analogs on 17β-estradiol biosynthesis, UMR106 cells were incubated for 24 h with different concentrations of the test compounds followed by a further 24-h incubation with testosterone. Among the 18 compounds, 11 could increase the production of 17β-estradiol; these 9 compounds were the flavonoids icariside I (**3**), 7-*O*-methylkaempferol (**6**), kaempferide (**9**), 3-*O*-methoxymethyl-4′-*O*-methyl-7-*O*-benzylkaempferol (**11**), 3-*O*-methoxymethyl-4′-*O*-methyl-5-*O*-isopentenyl-7-*O*-benzylkaempferol (**12**), 3-*O*-methoxymethyl-7-*O*-benzylicaritin (**13**), 7-*O*-benzylicaritin (**14**), 4′-*O*-methyl-8-isopentylkaempferol (**15**), 4′-*O*-methyl-5-*O*-isopentenyl-7-*O*-benzylkaempferol (**16**), 4-benzyloxy-2,3,3-trimethyl-7-(4-methoxyphenyl)-8-methoxymethoxy-2,3-dihydrofuro[2,3-*f*]chromen-9-one (**17**) and 3-*O*-(2‴′,3‴′,4‴′-tri-*O*-acetyl-α-L-rhamnopyranosyl)-7-*O*-(2‴,3‴,4‴,6‴-tetra-*O*-acetyl-β-D-glucopyranosyl)icaritin (**18**). Compounds **13**, **14**, and **15** promoted 17β-estradiol biosynthesis in a concentration-dependent manner, with EC_{50} values of 1.53, 3.45, and 10.57 μM, respectively (**Figure 1C**). They also had no effect on the viability of UMR106 cells (**Figure 1D**). These results indicate that the icariin analogs, such as compounds **13**, **14**, and **15**, could potently promote estrogen biosynthesis in rat osteoblast-like cells.

Effect of Icariin Analogs on Aromatase Expression

To determine whether compounds **14** and **15** promoted 17β-estradiol biosynthesis by affecting aromatase, we examined the mRNA and protein levels of aromatase in UMR106 cells treated with the selected compounds. Compounds **14** and **15** significantly increased aromatase transcript levels in a concentration-dependent manner (**Figure 2A**). **14** increased 58% of the aromatase mRNA levels at 10 μM while **15** increased 60% of the aromatase mRNA levels at 25 μM compared in the DMSO-treated control cells. **14** and **15** also significantly increased the bone specific aromatase promoter I.4 transcript in a concentration-dependent manner (**Figure 2A**, **Figure S2**). **14** and **15** also significantly increased aromatase protein expression in UMR106 and MC3T3-E1 cells in a concentration-dependent manner (**Figures 2B–D**). Furthermore, in aromatase-overexpressing HEK293A cells, letrozole, a specific inhibitor of aromatase enzymatic activity, significantly inhibited 17β-estradiol biosynthesis; however, **14** had no apparent effect on 17β-estradiol production compared to the DMSO-treated cells (**Figure 2E**), western blot also showed **14** had no effect on aromatase protein expression (**Figure S3**). These results excluding the probability that **14** directly modulates the enzymatic activity of aromatase protein. Actinomycin D, an RNA polymerase inhibitor, significantly suppressed **14**-induced aromatase mRNA transcription (**Figure S4**). These results indicate that **14** and **15** promoted estrogen biosynthesis by affecting aromatase at the transcriptional level.

Inhibitory Effect of 14 on PDE5A Activity

Previously, the icariin analogs were found to be potent inhibitors of PDE5 (15); thus, we opted to use recombinant-expressed PDE5A to examine whether **14** inhibits PDE5 activity. As shown in **Figure 3A** and **Figure S5**, **14** significantly inhibited PDE5 activity in a concentration-dependent manner with the IC_{50} value of 9.914 μM, a finding similar to that obtained with the specific PDE5 inhibitor, sildenafil. **14** had no effect on the PDE5 expression in both UMR106 cells and MC3T3-E1 cells (**Figure S6**). Thereafter, we proceeded to perform a cellular thermal shift assay to examine whether **14** directly interacts with PDE5A in cells (24). Compared to the DMSO control, the presence of **14** markedly increased the accumulation of PDE5A in the soluble fraction at the temperatures examined (**Figure 3B**). We also tested the concentration-response of **14** on PDE5A stability at increased temperatures. An increase in **14** concentration resulted in a marked increase in PDE5A accumulation (**Figure 3C**). We then examined the effect of **14** on

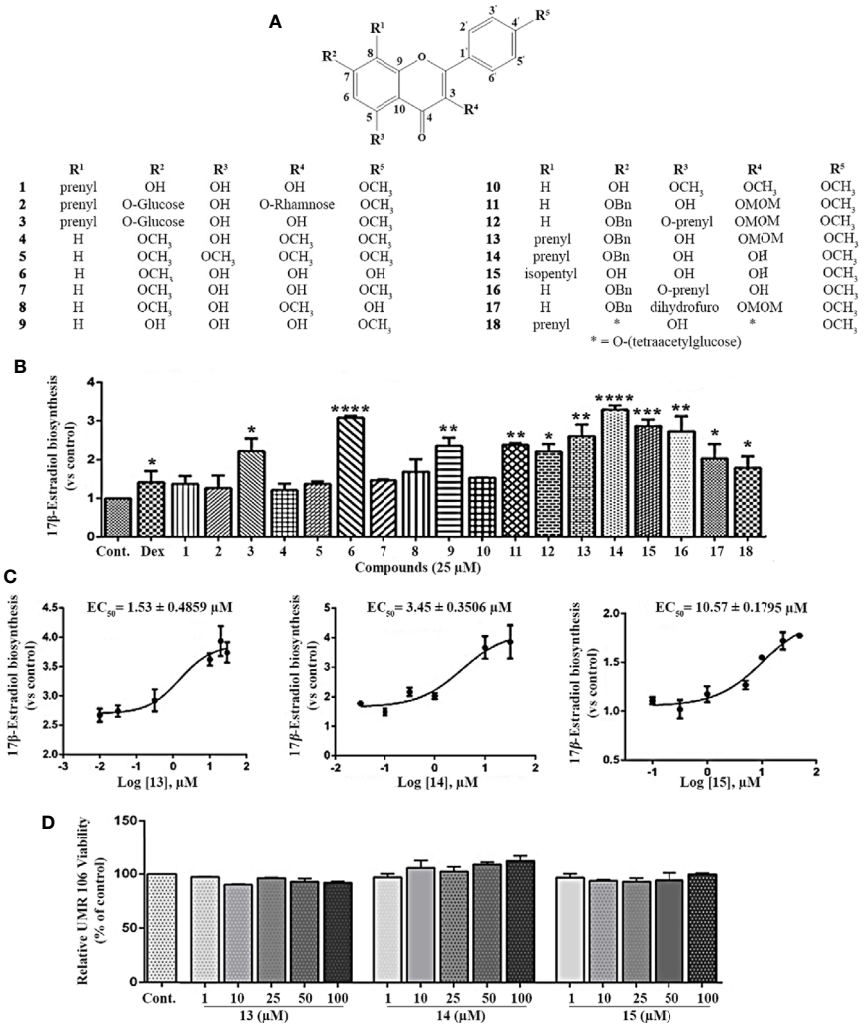

	R1	R2	R3	R4	R5
1	prenyl	OH	OH	OH	OCH_3
2	prenyl	O-Glucose	OH	O-Rhamnose	OCH_3
3	prenyl	O-Glucose	OH	OH	OCH_3
4	H	OCH_3	OH	OCH_3	OCH_3
5	H	OCH_3	OCH_3	OCH_3	OCH_3
6	H	OCH_3	OH	OH	OH
7	H	OCH_3	OH	OH	OCH_3
8	H	OCH_3	OH	OCH_3	OH
9	H	OH	OH	OH	OCH_3
10	H	OH	OCH_3	OCH_3	OCH_3
11	H	OBn	OH	OMOM	OCH_3
12	H	OBn	O-prenyl	OMOM	OCH_3
13	prenyl	OBn	OH	OMOM	OCH_3
14	prenyl	OBn	OH	OH	OCH_3
15	isopentyl	OH	OH	OH	OCH_3
16	H	OBn	O-prenyl	OH	OCH_3
17	H	OBn	dihydrofuro	OMOM	OCH_3
18	prenyl	*	OH	*	OCH_3

* = O-(tetraacetylglucose)

FIGURE 1 | Effect of the icariin analogs on estrogen biosynthesis in osteoblast cells. **(A)** The chemical structure of icariin analogs. **(B)** UMR 106 cells seeded in 24-well plates were pretreated with the Dex (100 nM) and icariin analogs (25 μM) for 24 h. Subsequently, the cells were supplemented with testosterone (10 nM) for an additional 24 h and the 17β-estradiol (E_2) concentration in the culture medium was quantified using a 17β-estradiol (E_2) magnetic particle-based ELISA. **(C)** The concentration-response curve of compounds **13**, **14**, and **15** for the promotion of estrogen biosynthesis in UMR 106 cells. **(D)** Viability of UMR106 cells. UMR 106 cells grown in 96 well plates were pretreated with compounds **13**, **14**, and **15** (1-100 μM) for 24 h. Cell were then incubated with Alamar Blue reagent for an additional 4 h, and the fluorescence intensities were measured. Cont., DMSO-treated control; Dex, 100 nM dexamethasone. Error bars represent the standard deviation of the measurement. (*) $p < 0.05$, (**) $p < 0.01$, (***) $p < 0.001$ and (****) $p < 0.0001$ compared to the DMSO control.

the intracellular cGMP level. As shown in **Figure 3D**, similar to sildenafil, **14** significantly stimulated the intracellular cGMP level in UMR106 cells. These findings suggest that **14** directly interacts with PDE5 and inhibits its activity in cells.

Computer docking analysis was conducted to assess the binding sites in PDE5. Based on our results, **14** fitted well within the active site of PDE5 (**Figure 3E**). The formation of hydrogen-bond (H-bond) and the hydrophobic interactions between **14** and PDE5 were evaluated. Two polar hydrogens in **14** are involved in its H-bonding with the amino acid Gln817, Ala767, Leu765, Tyr612 and His613, of PDE5 with a high glide energy of -11 kcal/mol^{-1}. **14** also formed hydrophobic interactions with the residues Ile768, Phe820, Met816, Leu804, Val782, Phe786 and Asn661 (**Figures 3F, G**), which may contribute to its inhibition of PDE5. The binding sites of sildenafil (site A) and **14** (site B) were very close with binding sites near the zinc ions and magnesium ions. Sildenafil formed a hydrogen bond with the amino acid Gln817 (**Figure 3H**), thereby aligning with previous reports (25). These results suggest that **14** might be subjected to a nucleophilic attack in the PDE5 to inhibit its activity.

Effect of 14 on Osteoblastic Cell Differentiation

To demonstrate that increased estrogen biosynthesis by **14** may promote osteoblastic cell differentiation, we examined the

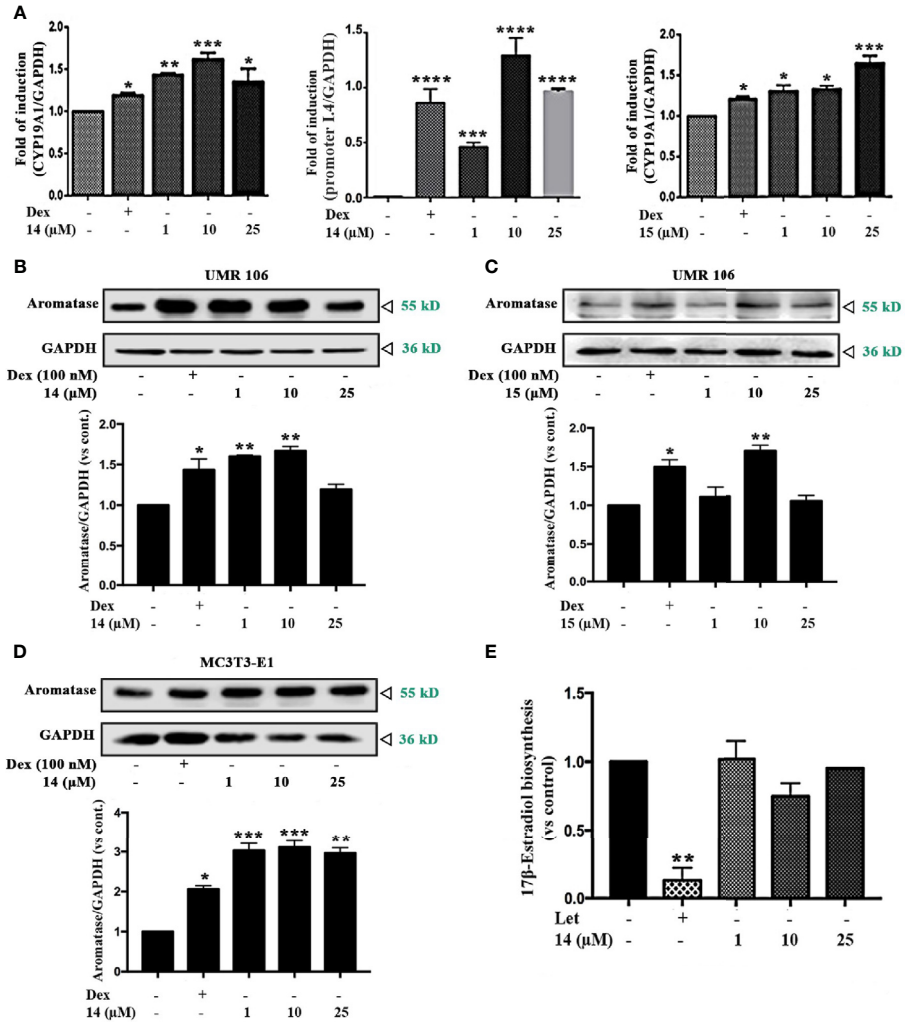

FIGURE 2 | Effect of the icariin analogs on aromatase expression. **(A)** The mRNA expression of *aromatase* in UMR106 cells. UMR 106 cells were incubated with the indicated concentrations of **14** and **15** and Dex (100 nM) for 24 h. *Aromatase* mRNA was measured in total cellular RNA by real-time qPCR. The results are expressed as fold increase relative to levels in untreated cells. *GAPDH* was used as an internal control. **(B, C)** UMR106 cells were treated with the indicated concentrations of **14** and **15** for 24 h. The cell lysates were immunoblotted with aromatase and GAPDH antibodies. **(D)** MC3T3-E1 cells were treated with the indicated concentrations of **14** for 24 h. The cell lysates were immunoblotted with aromatase and GAPDH antibodies. **(E)** Let (10 μM) and 14 at the indicated concentrations treated aromatase-overexpressing HEK293A cells seeded in 24 well plates for 24 h, and then supplemented with tesoterone (10 nM) for a further 24. The culture medium was quantified using a 17β-estradiol ELISA. Cont., DMSO control; Dex, 100 nM dexamethasone; Let, 10 μM letrozole. (*) $p < 0.05$, (**) $p < 0.01$, (***) $p < 0.001$ and (****) $p < 0.0001$ compared to the control.

mRNA expression of osteoblastic cell differentiation markers in UMR106 cells. 17β-Estradiol significantly increased mRNA levels of *osteocalcin* (*OCN*), *osterix* (*Osx*), *alkaline phosphatase* (*ALP*), and *Runt-related transcription factor 2* (*Runx2*) (**Figures 4A–D**), aligning with the findings of previous reports (26, 27). Similar to sildenafil, **14** significantly increased the mRNA levels of *OCN*, *Osx*, *ALP*, and *Runx2* (**Figures 4A–D**). The bone formation/resorption balance can be observed from the ratio of *OPG*/*RANKL* expression, which is stimulated by 17β-estradiol (28). Similar to 17β-estradiol, both **14** and sildenafil increased the ratio of *OPG*/*RANKL* (**Figure 4E**). Compared with the control, calcium deposition was increased after treatment with **14** in a dose dependent manner (**Figure S7**). While **14** had no effect on BMP2 protein expression (**Figure S8**). These results indicate that **14** can promote osteoblast formation and differentiation.

Effect of 14 on cGMP/PKG/Src/ERK Signaling

The stimulation of intracellular cGMP by the 14-induced PDE5 inhibition may activate PKG to increase aromatase expression. Therefore, we examined the role of PKG in the regulation of estrogen biosynthesis. PKG inhibition by the PKG inhibitor, KT5823 or Rp-8-pCPT-cGMPS, abolished the stimulatory effect

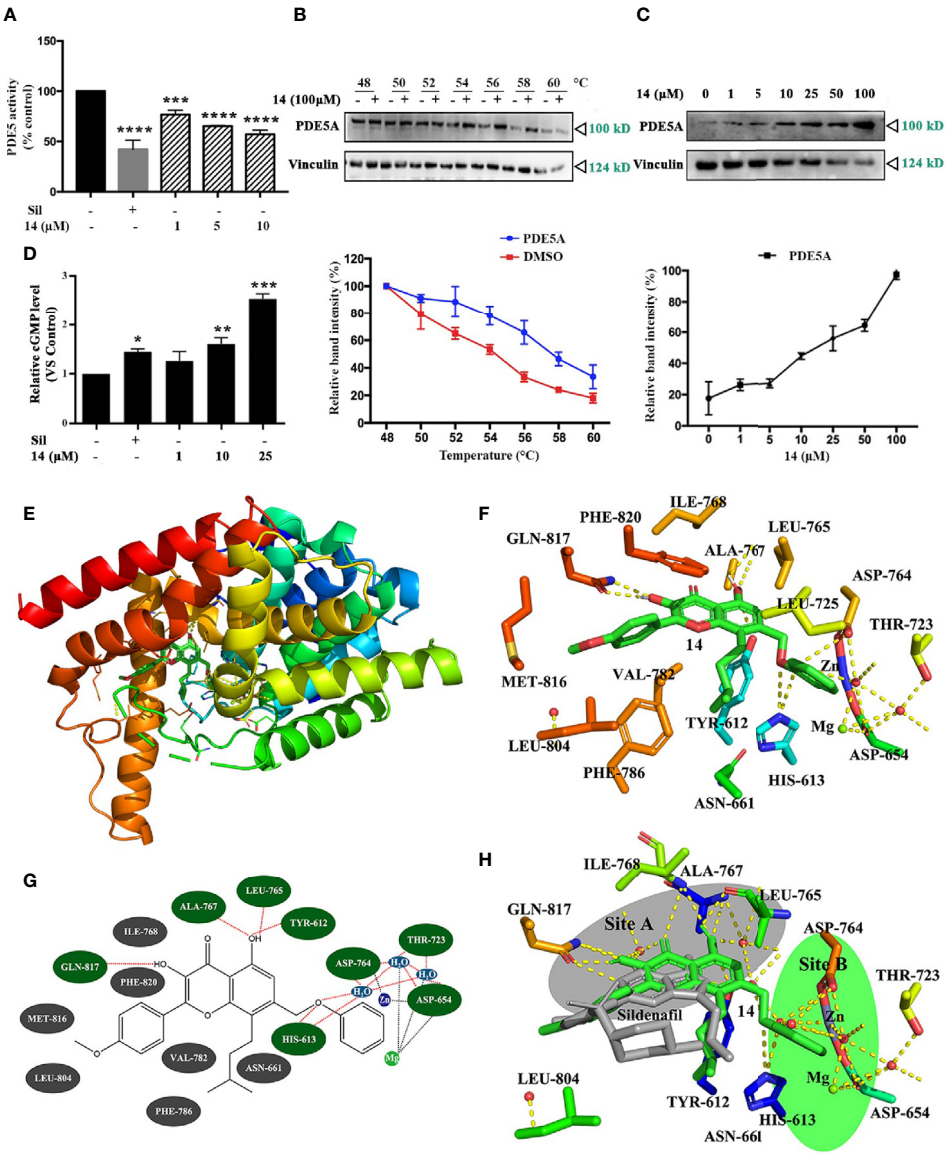

FIGURE 3 | Inhibitory effect of **14** on PDE5. **(A)** The intracellular PDE5 level was detected. Basal PDE5 activity is normalized to a control. Cont., DMSO control; Sil, 10 μM sildenafil. (***) p <0.001 and (****) p <0.0001 compared to the DMSO control. **(B, C)** The cellular thermal shift assay was performed on HEK293T cells as described in Materials and Methods. The stabilization effect of **14** on PDE5A and vinculin at different temperatures **(B)** and different concentrations **(C)** was evaluated by western blot. Each experiment was repeated at least three times. **(D)** UMR106 cells were seeded in 6-well plates overnight were treated with the indicated concentration of 14 or 10 μM sildenafil for 24 h. The concentrations of intracellular cGMP were determined by ELISA as described in the materials and methods section. (*) $p < 0.05$, (**) $p < 0.01$, (***) $p < 0.001$ compared to the DMSO control. **(E)** Molecular docking model of PDE5 complexed with **14**. **(F)** Stereo view of the active site of the PDE5-**14** complex. **14** showed interaction with Gln817, Ala767, Leu765, Tyr612 and His613. The yellow dotted lines represent hydrogen bonds and coordination interaction, excluding the coordination bonds interaction with Asp654 and the water molecule are connected to the $Zn^{2+}$and Mg^{2+}. **(G)** Simplified structure showing interaction between **14** and amino acid residues at binding site. Hydrogen bond and hydrophobic interactions are colored in green and gray with red dotted line, respectively. **(H)** Comparison of sildenafil and **14** active sites in PDE5. Binding sites of sildenafil (colored gray) is site A and **14** (colored green) is site B.

of 14 and sildenafil on 17β-estradiol production (**Figure 5A** and **Figure S9**). PKG inhibition also abolished the stimulatory effect of **14** and sildenafil on ALP activity, a well-known marker of osteoblast differentiation (**Figure 5B**). These results suggest that PKG mediates the promotive effect of **14** on estrogen biosynthesis and differentiation in osteoblastic cells. As the cGMP-PKG signaling pathway activates Src and ERK in mechanically stimulated osteoblasts (8), we further examined the effect of **14** on Src and ERK in both UMR106 and MC3T3-E1 cells. Src activity is regulated by phosphorylation, where Tyr^{529} phosphorylation at the C-terminal retains Src in an inactive conformation. Dephosphorylation of Tyr^{529} is a key event in Src

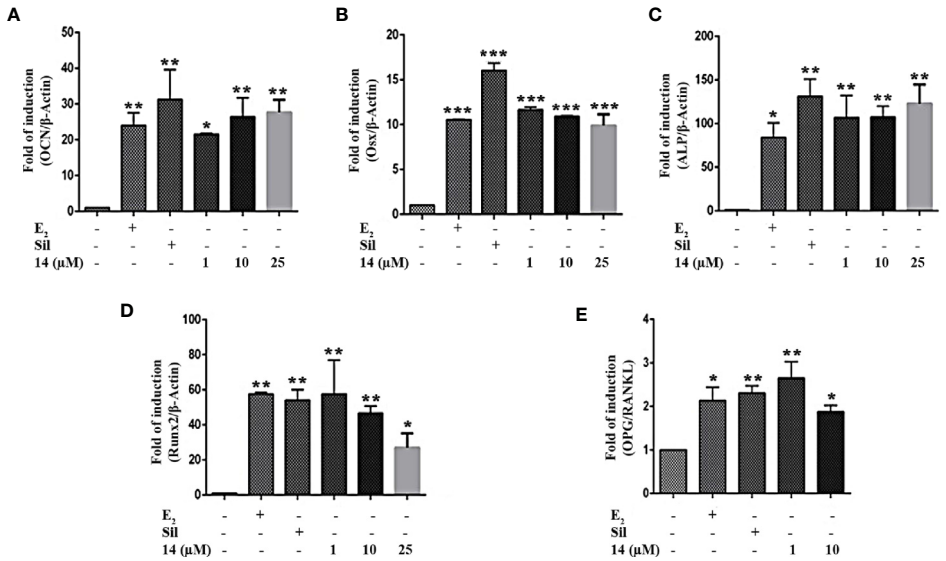

FIGURE 4 | Effect of **14** on osteoblastic cell differentiation. The mRNA expression of **(A)** *OCN*, **(B)** *Osx*, **(C)** *ALP*, **(D)** *Runx2*, and **(E)** *OPG/RANKL* in UMR106 cells treated for 24 h. mRNA expression levels were quantified by qRT-PCR. The results are expressed as a fold increase relative to levels in untreated cells. *β-Actin* was used as the internal control. Quantitative results are depicted. Cont., DMSO-treated control; β-Actin control; OCN, osteocalcin; Osx, osterix; ALP, alkaline phosphatase; Runx2, Runt-related transcription factor 2; OPG, osteoprotegerin; RANKL, Receptor activator of nuclear factor-κB ligand; E_2, 10 nM 17β-estradiol; Sil, 10 μM Sildenafil. (*) $p < 0.05$, (**) $p < 0.01$, (***) $p < 0.001$ and compared to the DMSO control.

activation as it changes the protein to an active conformation and enables autophosphorylation of Tyr^{418} in the kinase domain activation loop (29). As shown in **Figure 5C**, **14** significantly promoted the Src phosphorylation on Tyr^{529} and decreased the phosphorylation on Tyr^{418}, indicating Src activation. Similarly, **14** also promoted phosphorylation of ERK in both UMR106 and MC3T3-E1 cells. We treated the cells with a ERK inhibitor and found that it completely abolished the stimulatory effect of **14** on aromatase expression compared with **14** alone (**Figure 5D**), indicating that **14** enhances activation of ERK pathway signaling, thereby supporting the finding that inhibition of PKG abolished the stimulatory effect of **14** on estrogen biosynthesis (**Figure 5A**). These results suggest that **14** promotes osteoblast differentiation by activating the PKG/Src/ERK pathway.

Effect of 14 on SHP2 Activation

In osteoblasts, cGMP/PKG-induced Src activation is mediated by SHP-2 (8). Compared to the DMSO control, **14** significantly promoted SHP2 activity in the treated cells in a concentration-dependent manner, similar to sildenafil (**Figure 6A**). SHP2 activity was also stimulated by **14** in a time-dependent manner (**Figure 6B**). To further confirm the role of SHP2 in the **14**-enhanced Src/ERK pathway signaling, we examined the effect of **14** alone or in combination with the SHP2 inhibitor (NSC87877). Based on our findings, SHP2 inhibitor treatment completely eliminated the promotive effect of **14** on the phosphorylation of Src-pTy^{418} and phosphorylation of ERK (**Figure 6C**). Furthermore, SHP2 inhibitor treatment significantly decreased the stimulatory effect of **14** on aromatase expression in both UMR106 and MC3T3-E1 cells (**Figure 6D**). These results indicate that **14** stimulates aromatase expression by activating SHP2.

DISCUSSION

Icariin is the most abundant bioactive flavonoid contained in *E. brevicornum* (30, 31). Both icariin and *E. brevicornum* exhibit anti-osteoporotic effects *in vitro* and *in vivo* by stimulating osteoblast proliferation; these findings support the wide use of *E. brevicornum* in many Traditional Chinese Medicine formulas for the treat bone fracture and prevent osteoporosis (32–34). Of the 18 icariin analogs examined in the present study, 11 could increase estrogen biosynthesis in rat osteoblast-like UMR106 cells. This was consistent with a previous report where structure-activity relationship analysis suggested that prenylation at the C-8 and C-6 position was essential for promoting the differentiation of primary osteoblasts (35). In this study, we found that the prenyl group at the C-8 position was more potent than the prenyl group at the C-6 position for promoting estrogen biosynthesis. In the adipose tissue and bone, aromatase expression is stimulated primarily by class I cytokines through promoter I.4 (5). Consistently, we found that **14** potently promoted estrogen biosynthesis by increasing promoter I.4-driven aromatase mRNA and protein expression in osteoblastic UMR-106 and MC3T3-1 cells. Previously, we found that 2-phenylbenzo[b]furans might enhance estrogen biosynthesis *via* direct allosteric regulation of aromatase enzymatic activity (18, 19). However, in this study, we found that **14** had no effect on

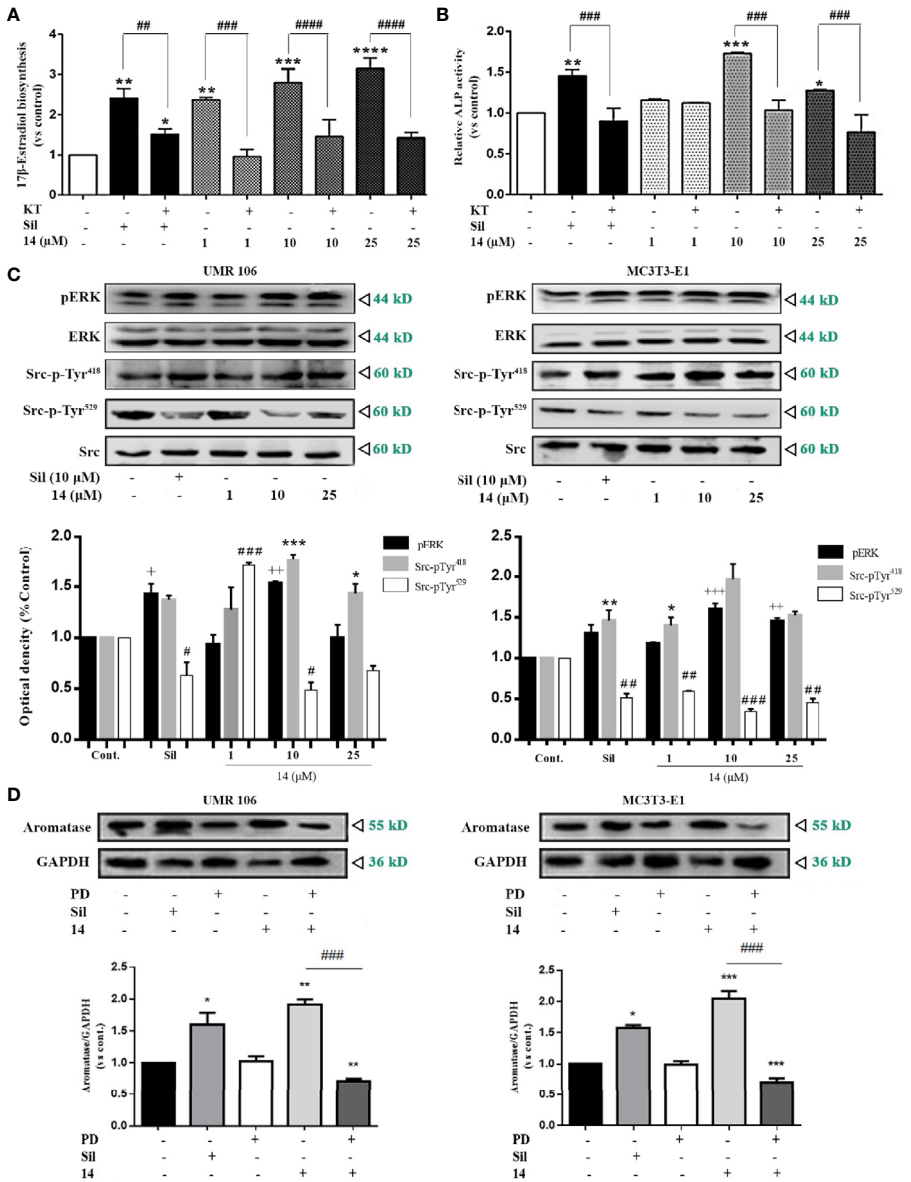

FIGURE 5 | **14** activates PKG/Src/ERK pathway signaling. **(A)** UMR106 cells seeded in 24-well plates overnight were treated with compounds for 2 h. Subsequently, the cells were supplemented with testosterone (10 nM) for an additional 48 h. 17β-estradiol concentration in the culture medium was quantified with an ELISA (E2) detection kit. (*) $p < 0.05$, (**) $p < 0.01$, (***) $p < 0.001$ and (****) $p < 0.0001$ compared to the DMSO control; (##) $p < 0.01$, (###) $p < 0.001$ and (####) $p < 0.0001$ compared to KT5823 (10 μM)-treated cells **(B)** UMR106 cells seeded in 24-well plates overnight were treated with 14 and KT5823 (10 μM) for 2 h. Subsequently, the cells were supplemented with testosterone (10 nM) for an additional 48 h. ALP activity of the cell lysates was quantified with the ALP detection kit. (*) $p < 0.05$, (**) $p < 0.01$ and (***) $p < 0.001$ compared to the DMSO control; (###) $p < 0.001$ compared to KT-treated cells **(C)** UMR 106 and MC3T3-E1 cells were treated with different concentrations of 14 and sildenafil (10 μM) for 1 h. The cell lysates were immunoblotted with antibodies against phospho-ERK, ERK, phospho-Src-pTyr418, phospho-Src-pTyr529, and Src. (+) $p < 0.05$, (++) $p < 0.01$ and (+++) $p < 0.001$ compared to the p-ERK control; (*) $p < 0.05$, (**) $p < 0.01$, (***) $p < 0.001$ compared to the Src-pTyr418 control; (#) $p < 0.05$, (##) $p < 0.01$ and (###) $p < 0.001$ compared to the Src-pTyr529 control. **(D)** UMR 106 and MC3T3-E1 cells were treated with different concentrations of 14 and PD (10 μM) for 1 h. The cell lysates were immunoblotted with antibodies against aromatase. GAPDH was used as the internal control. Cont., DMSO-treated control; E2, 17β-estradiol (10 nM); Sil, sildenafil (10 μM); Rp-pCPT-cGMPS, ERK inhibitor (0.5 mM); KT, PKG inhibitor (KT5823, 10 μM); PD, ERK inhibitor (PD98059, 10 μM). Error bars represent the standard deviation of the measurement. (*) $p < 0.05$ (**) $p < 0.01$, (***) $p < 0.001$ compared to the DMSO control; (###) $p < 0.001$.

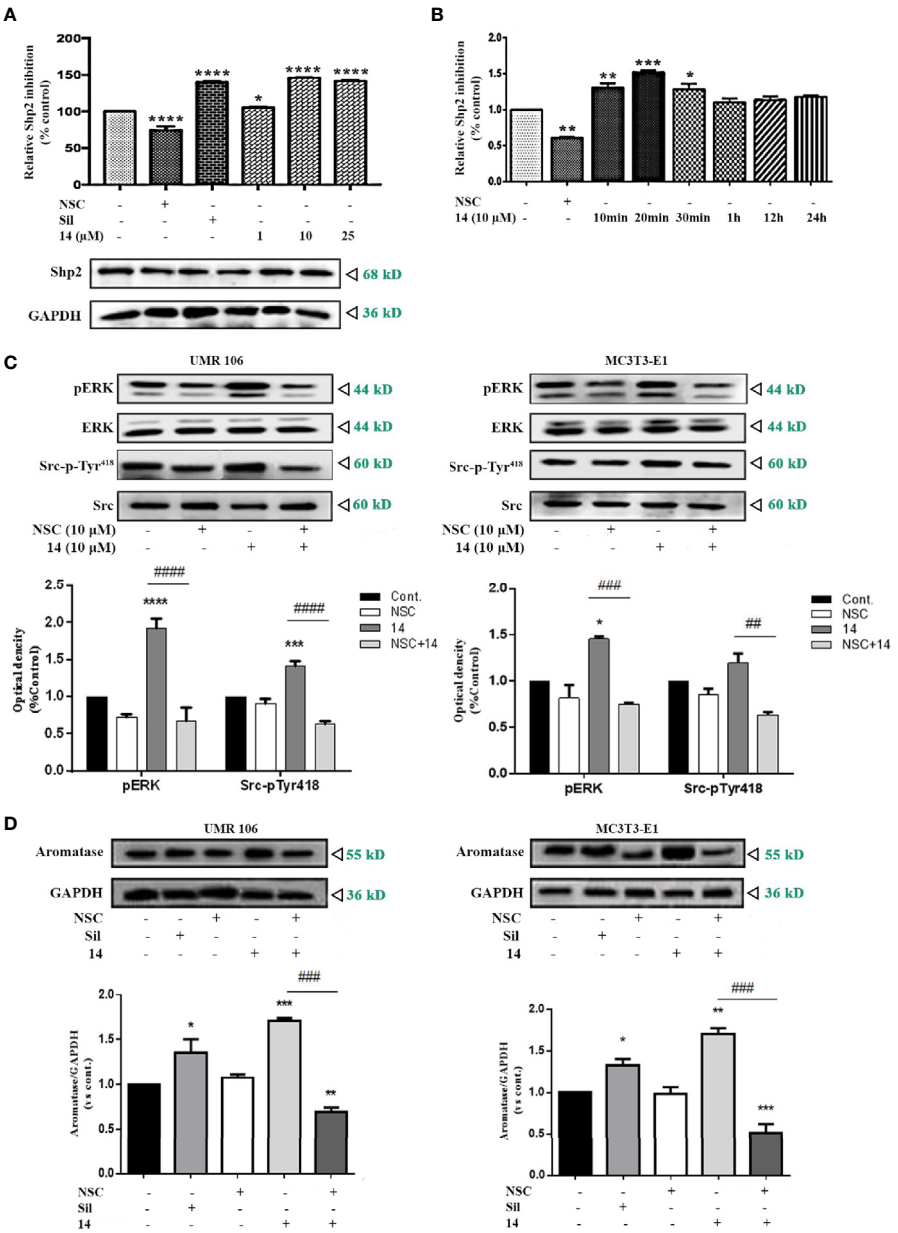

FIGURE 6 | Effect of **14** on SHP2 activation. **(A)** UMR106 cells treated with compounds for 30 min were lysed and immunoprecipitated with the anti-SHP2 antibody. Thereafter, SHP2 activity was determined. GAPDH was used as the input. (*) $p < 0.05$ and (****) $p < 0.0001$ compared to the DMSO control. **(B)** Time-dependent effect of **14** on SHP2 activity. UMR106 cells treated with 10 μM NSC-87877 (30 min) and 10 μM **14** at the indicated time were lysed, immunoprecipitated with anti-SHP2 antibody, and SHP2 activity was determined. (*) $p < 0.05$, (**) $p < 0.01$ and (***) $p < 0.001$ compared to the DMSO control. **(C)** UMR106 and MC3T3-E1 cells were treated with compounds for 1 h. The cell lysates were immunoblotted with antibodies against phospho-ERK, ERK, phospho-Src-pTyr^{418}, and Src. (*) $p < 0.05$, (***) $p < 0.001$ and (****) $p < 0.0001$ compared to the DMSO control; (##) $p < 0.01$, (###) $p < 0.001$, (####) $p < 0.0001$ compared to compared to **14** alone treatment. **(D)** UMR106 and MC3T3-E1 cells were treated with **14** (10 μM) or sildenafil (10 μM) alone for 24 h, or pretreated with NSC-87877 for 1 h, and then **14** (10 μM) was added for additional 24 h. Cell lysates were immunoblotted with antibodies against aromatase. GAPDH was used as the internal control. (*) $p < 0.05$, (**) $p < 0.01$, (***) $p < 0.001$ compared to the DMSO control. (###) $p < 0.001$ compared to **14** alone treatment. Cont., DMSO-treated control; NSC, 10 μM NSC-87877; Sil, 10 μM sildenafil. Error bars represent the standard deviation of the measurement.

the catalytic activity of aromatase protein, excluding the probable role of **14** in the direct modulation of the catalytic activity of the aromatase protein. Local estrogen biosynthesis in bone plays a key role in bone homeostasis in postmenopausal women due to the loss of function of the ovary. As it is rarely reported that small chemical compounds could stimulate estrogen biosynthesis in osteoblasts, further developing **14** and its analogs as new antiosteoporotic therapeutics would be worthwhile.

Currently, several PDE5 inhibitors have been approved by the FDA for the treatment of erectile dysfunction and pulmonary arterial hypertension (36). PDE5 plays a key role in cGMP signaling; however, its role in estrogen biosynthesis in the bone has been rarely evaluated. In the present study, we found that the icariin analog, **14**, a validated PDE5 inhibitor with IC_{50} 9.914 ± 0.3325 μM, promoted estrogen biosynthesis in UMR 106 and MC3T3-E1 cells by enhancing aromatase expression in a similar manner to icariin (14). Earlier studies also revealed the importance of Gln817, Tyr612, Phe786, and Ala783 amino acid in PDE5-inhibitor interaction (25). Here, we found that both sildenafil and compound **14** could bind to these amino acids in PDE5. Additionally, **14** also differently binds to other amino acids in PDE5. Thus, further investigation is required to determine whether these amino acids also regulate PDE5 activity. PDE5 inhibitors, such as tadalafil and sildenafil, have been found to stimulate aromatase expression in human adipocytes (12), further supporting the role of PDE5 in the regulation of promoter I.4-driven aromatase expression. cGMP plays a key role in osteoblast differentiation by activating PKG (37). Icariin analogs, which inhibits PDE5 activity, was found to promote osteoblast differentiation and exhibit antiosteoporotic effect *in vivo* (32–34, 38), thereby aligning with our finding that **14** increased the expression of osteoblast differentiation markers. PDE5 inhibitors were also reported to exert beneficial effects on ovariectomy or glucocorticoid-induced osteoporosis in rats (39, 40). Furthermore, PDE5 inhibition was found to reduce bone mass by suppressing canonical Wnt signaling, indicating that long-term treatment with PDE5 inhibitors at high dosage may cause bone catabolism (41). Therefore, the role of PDE5 in the regulation of bone homeostasis should be further investigated to develop PDE5 inhibitors as new antiosteoporotic therapeutics. Recently it is reported that PDE5 inhibitors could enhance osteoblastic bone formation by targeting PDE5A and reverse osteopenia in ovariectomy mice by an osteogenic mechanism (42, 43). Therefore, our findings that PDE5 inhibitors promote estrogen biosynthesis provide new insights for the clinical benefits of PDE5 inhibitors in the treatment of osteoporosis. Moreover, the prenyl group contributes to higher osteogenic activity than do flavonoids possibly by modulating estrogen receptors (44, 45). Thus, whether **14** exhibits its osteogenic activity by a dual-functional modulator of PDE5 and estrogen receptor needs further investigation.

Mechanical stimulation, such as exercise, can strengthen bones and reduce the risk of fractures (46). Compressive forces generated by weight bearing and locomotion induce small bone deformations and increase interstitial fluid flow, thereby promoting anabolic responses in osteoblasts through different signal transduction pathways, including calcium channels, Raf-MEK-ERK cascade, and nitric oxide (NO) (47). Recently, the NO-cGMP-PKG pathway was reported to regulate osteoblast proliferation and differentiation through the formation of an Src-containing mechanosome (8). Consistent with this result, we found that **14** or sildenafil increased intracellular cGMP level and activated ERK and Src *via* PKG in osteoblasts. More interestingly, we found that PKG inhibition suppressed **14** or sildenafil-induced estrogen production in osteoblasts, which

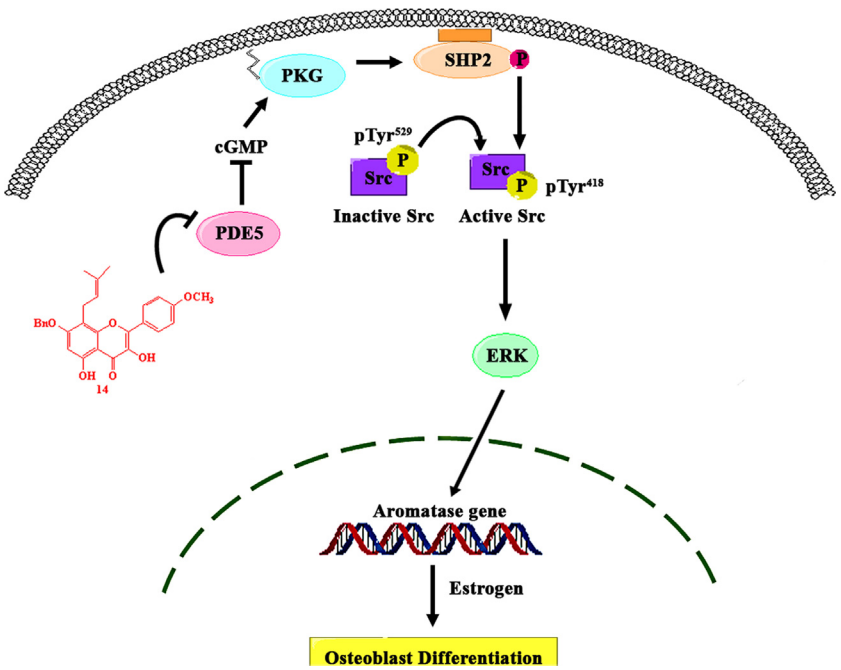

FIGURE 7 | Proposed model of the role of PDE5 in the regulation of aromatase in osteoblasts. **14** inhibits the activity of PDE5, thereby stimulating the intracellular cGMP level, which causes PKG activation. PKG activation by **14** stimulated the activity of SHP2, which subsequently activated Src and ERK signaling and increased ERK-dependent gene expression, including that of aromatase, in osteoblasts.

could be justified by our finding that **14** or sildenafil stimulated the activity of SHP2 that was directly phosphorylated by PKG and was required to activate Src (8). ERK has been implied to promote osteoblast differentiation by regulating ALP activity, integrin synthesis, focal adhesion kinase, Runx2 phosphorylation, and transcriptional activity (48–50). In this study, we found that the inhibition of ERK also attenuated the stimulatory effect of **14** on aromatase expression, providing new insight into mechanical stimulation in osteoblast differentiation. ERK could phosphorylate the glucocorticoid receptor and modulate its transcriptional activity (51). Therefore, it will be of interest to further investigate whether ERK modulates the glucocorticoid receptor or other transcriptional factors to stimulate promoter I.4-driven aromatase expression in osteoblasts. 17β-Estradiol can rapidly enhance aromatase enzymatic activity by increasing aromatase protein phosphorylation in breast cancer cell lines, which is mediated by Src (10). Thus, **14**-induced Src activation may also stimulate aromatase enzymatic activity to promote estrogen production, which should be further investigated. SHP-2 regulates cell survival and proliferation by the activation of the RAS-ERK signaling pathway (52). SHP2 is found to physically interact with the estrogen receptor, which is necessary for the synergistic and persistent activation of ERK by leptin and estrogen (53). cGMP/PKG-mediated SHP2 activation may also regulate the function of the estrogen receptor to exert its anabolic effect in osteoblasts. Therefore, a further investigation to determine whether mechanical stimulation also modulates local estrogen biosynthesis or estrogen receptor to exert its antiosteoporotic effect is warranted.

CONCLUSIONS

In summary, we found that the prenylated flavonoid **14** promotes osteoblast differentiation by activating the cGMP/PKG/SHP2/Src/ERK cascade *via* PDE5 inhibition, thereby leading to the localized production of estrogen by stimulating aromatase expression (**Figure 7**). These data not only provide new insights into the role of estrogen biosynthesis in mechanical stimulation-induced osteoblast differentiation but also support the use of PDE5-inhibiting drugs to mimic the anabolic effects of mechanical bone stimulation in the treatment of osteoporosis.

DATA AVAILABILITY STATEMENT

The original contributions presented in the study are included in the article/**Supplementary Material**. Further inquiries can be directed to the corresponding authors.

AUTHOR CONTRIBUTIONS

WW, D-yC, and FW wrote the manuscript. WW, KW, D-yC, X-kS, and Z-yZ conducted the biological experiments. Z-hZ conducted the molecular docking analysis. FL, Q-gM, and CW synthesized the compounds. AS, G-lZ, and FW supervised the study, designed the experiments, and revised the manuscript. All authors contributed to the article and approved the submitted version.

FUNDING

This work was supported by the National Natural Science Foundation of China (No. 21861142007, 21977092, 21550110193), Science & Technology Department of Sichuan Province (No. 2019YSF0106), CAS-TWAS President's PhD Fellowship Program, Chinese Academy of Sciences President's International Fellowship Initiative (No. 2016CTF092), Biological Resources Programme, Chinese Academy of Sciences (KFJ-BRP-008), and the National New Drug Innovation Major Project of China (2018ZX09711001-001-006). Support from The Thailand Research Fund (No. DBG6180030) is gratefully acknowledged.

SUPPLEMENTARY MATERIAL

The Supplementary Material for this article can be found online at: https://www.frontiersin.org/articles/10.3389/fendo.2021.636784/full#supplementary-material

REFERENCES

1. Riggs BL, Khosla S, Melton LJ. A unitary model for involutional osteoporosis: estrogen deficiency causes both type I and type II osteoporosis in postmenopausal women and contributes to bone loss in aging men. *J Bone Miner Res* (1998) 13(5):763–73. doi: 10.1359/jbmr.1998.13.5.763
2. Simpson ER, Clyne C, Rubin G, Boon WE, Robertson KB, Speed CM, et al. Aromatase-a brief overview. *Annu Rev Physiol* (2002) 64:93–127. doi: 10.1146/annurev.physiol.64.081601.142703
3. Simpson ER. Aromatase: biologic relevance of tissue-specific expression. *Semin Reprod Med* (2004) 22(1):11–23. doi: 10.1055/s-2004-823023
4. Enjuanes A, Garcia-Giralt N, Supervía A, Nogués X, Ruiz-Gaspà S, Bustamante M, et al. Functional analysis of the I.3, I.6, pII and I.4 promoters of CYP19 (aromatase) gene in human osteoblasts and their role in vitamin D and dexamethasone stimulation. *Eur J Endocrinol* (2005) 153(6):981–8. doi: 10.1530/eje.1.02032
5. Ribot C, Tremollieres F, Pouilles JM. Aromatase and regulation of bone remodeling. *Joint Bone Spine* (2006) 73:37–42. doi: 10.1016/j.jbspin.2005.02.005
6. Horstman AM, Dillon EL, Urban RJ, Sheffield-Moore M. The Role of androgens and estrogens on healthy aging and longevity. *J Gerontol A Biol Sci* (2012) 67(11):1140–52. doi: 10.1093/gerona/gls068
7. Cui J, Shen Y, Li R. Estrogen synthesis and signaling pathways during aging: from periphery to brain. *Trends Mol Med* (2013) 19(3):197–209. doi: 10.1016/j.molmed.2012.12.007
8. Rangaswami H, Schwappacher R, Marathe N, Zhuang S, Casteel DE, Haas B, et al. Cyclic GMP and protein kinase G control a Src-containing mechanosome in osteoblasts. *Sci Signal* (2010) 3(153):ra91. doi: 10.1126/scisignal.2001423
9. O'Shaughnessy MC, Polak JM, Afzal F, Hukkanen MV, Huang P, Maclntyre I, et al. Nitric oxide mediates 17β-estradiol-stimulated human and rodent osteoblast proliferation and differentiation. *Biochem Biophys Res Commun* (2000) 277(3):604–10. doi: 10.1006/bbrc.2000.3714

10. Catalano S, Baron I, Giordano C, Rizza P, Qi H, Gu G, et al. Rapid estradiol/ERα signaling enhances aromatase enzymatic activity in breast cancer cells. *Mol Endocrinol* (2009) 23(10):1634–45. doi: 10.1210/me.2009-0039
11. Marathe N, Rangaswami H, Zhuang S, Boss GR, Pilz RB. Pro-survival effects of 17β-estradiol on osteocytes are mediated by nitric oxide/cgmp via differential actions of cgmp-dependent protein kinases i and ii. *J Biol Chem* (2012) 287(2):978–88. doi: 10.1074/jbc.M111.294959
12. Aversa A, Caprio M, Antelmi A, Armani A, Brama M, Greco EA, et al. Exposure to phosphodiesterase type 5 inhibitors stimulates aromatase expression in human adipocytes in vitro. *J Sex Med* (2011) 8(3):696–704. doi: 10.1111/j.1743-6109.2010.02152.x
13. Li F, Du BW, Lu DF, Wu WX, Wongkrajiang K, Wang L, et al. Flavonoid glycosides isolated from *Epimedium brevicornum* and their estrogen biosynthesis-promoting effects. *Sci Rep* (2017) 7(1):7760–72. doi: 10.1038/s41598-017-08203-7
14. Yang L, Lu D, Guo J, Meng X, Zhang G-L, Wang F. Icariin from *Epimedium brevicornum* Maxim promotes the biosynthesis of estrogen by aromatase (CYP19). *J Ethnopharmacol* (2013) 145(3):715–21. doi: 10.1016/j.jep.2012.11.031
15. Dell'Agli M, Galli GV, Cero ED, Belluti F, Matera R, Zironi E, et al. Potent inhibition of human phosphodiesterase-5 by icariin derivatives. *J Nat Prod* (2008) 71(9):1513–7. doi: 10.1021/np800049y
16. Mei G, Wang C, Zhao Z, Yuan W, Zhang G-L. Synthesis of icariin from kaempferol through regioselective methylation and *para*-Claisen–Cope rearrangement. *Beilstein J Org Chem* (2015a) 11:1220–5. doi: 10.3762/bjoc.11.135
17. Mei G, Wang C, Yuan W, Zhang G-L. Selective methylation of kaempferol via benzylation and deacetylation of kaempferol acetates. *Beilstein J Org Chem* (2015b) 11:288–93. doi: 10.3762/bjoc.11.33
18. Pu WC, Yuan Y, Lu DF, Wang X, Liu H, Wang C, et al. 2-Phenylbenzo[b]furans: synthesis and promoting activity on estrogen biosynthesis. *Bioorg Med Chem Lett* (2016) 26(22):5497–500. doi: 10.1016/j.bmcl.2016.10.013
19. Lu DF, Yang LJ, Li QL, Gao XP, Wang F, Zhang GL. Egonol gentiobioside and egonol gentiotrioside from *Styrax perkinsiae* promote the biosynthesis of estrogen by aromatase. *Eur J Pharmacol* (2012) 691(1-3):275–82. doi: 10.1016/j.ejphar.2012.07.005
20. Yang L, Chen Q, Wang F, Zhang G. Antiosteoporotic compounds from seeds of *Cuscuta chinensis*. *J Ethnopharmacol* (2011) 135(2):553–60. doi: 10.1016/j.jep.2011.03.056
21. Igbe I, Shen X-F, Jiao W, Qiang Z, Deng T, Li S, et al. Dietary quercetin potentiates the antiproliferative effect of interferon-α in hepatocellular carcinoma cells through activation of JAK/STAT pathway signaling by inhibition of SHP2 phosphatase. *Oncotarget* (2017) 8(69):113734–48. doi: 10.18632/oncotarget.22556
22. Eyre LJ, Bland R, Bujalska IJ, Sheppard MC, Stewart PM, Hewison M. Characterization of aromatase and 17β-hydroxysteroid dehydrogenase expression in rat osteoblastic cells. *J Bone Miner Res* (1998) 13:998–1004. doi: 10.1359/jbmr.1998.13.6.996
23. Shozu M, Simpson ER. Aromatase expression of human osteoblast-like cells. *Mol Cell Endocrinol* (1998) 139(1-2):117–29. doi: 10.1016/S0303-7207(98)00069-0
24. Jafari R, Almqvist H, Axelsson H, Ignatushchenko M, Lundback T, Nordlund P, et al. The cellular thermal shift assay for evaluating drug target interactions in cells. *Nat Protoc* (2014) 9(9):2100–22. doi: 10.1038/nprot.2014.138
25. Sung B-J, Hwang KY, Jeon YH, Lee JL, Heo Y-S, Kim JH, et al. Structure of the catalytic domain of human phosphodiesterase 5 with bound drug molecules. *Nature* (2003) 425(6953):98–102. doi: 10.1038/nature01914
26. Qu Q, Perälä-Heape M, Kapanen A, Dahllund J, Salo J, Väänänen HK, et al. Estrogen enhances differentiation of osteoblasts in mouse bone marrow culture. *Bone* (1998) 22(3):201–9. doi: 10.1016/s8756-3282(97)00276-7
27. Guo AJ, Choi RC, Zheng KY, Chen VP, Dong TT, Wang ZT, et al. Kaempferol as a flavonoid induces osteoblastic differentiation via estrogen receptor signaling. *Chin Med* (2012) 7:10. doi: 10.1186/1749-8546-7-10
28. Mok SK, Chen WF, Lai WP, Leung PC, Wang XL, Yao XS, et al. Icariin protects against bone loss induced by oestrogen deficiency and activates oestrogen receptor-dependent osteoblastic functionsin UMR 106 cells. *Br J Pharmacol* (2010) 159(4):939–49. doi: 10.1111/j.1476-5381.2009.00593.x
29. Harrison SC. Variation on an Src-like theme. *Cell* (2003) 112(6):737–40. doi: 10.1016/s0092-8674(03)00196-x
30. Meng FH, Li YB, Xiong ZL, Jiang ZM, Li FM. Osteoblastic proliferative activity of *Epimedium brevicornum* Maxim. *Phytomedicine* (2005) 12(3):189–93. doi: 10.1016/j.phymed.2004.03.007
31. Ma H, He X, Yang Y, Li M, Hao D, Jia Z. The genus Epimedium: an ethnopharmacological and phytochemical review. *J Ethnopharmacol* (2011) 134(3):519–41. doi: 10.1016/j.jep.2011.01.001
32. Mok S-K, Chen W-F, Lai W-P, Leung P-C, Wang X-L, Yao X-S, et al. Icariin protects against bone loss induced by oestrogen deficiency and activates oestrogen receptor-dependent osteoblastic functions in UMR 106 cells[J]. *Br J Pharmacol* (2010) 159(4):939–49. doi: 10.1111/j.1476-5381.2009.00593.x
33. Nian H, Ma MH, Nian SS, Xu LL. Antiosteoporotic activity of icariin in ovariectomized rats. *Phytomedicine* (2009) 16(4):320–6. doi: 10.1016/j.phymed.2008.12.006
34. Hsieh TP, Sheu SY, Sun JS, Chen MH, Liu MH. Icariin isolated from *Epimedium pubescens* regulates osteoblasts anabolism through BMP-2, SMAD4, and Cbfa1 expression. *Phytomedicine* (2010) 17(6):414–23. doi: 10.1016/j.phymed.2009.08.007
35. Zhang DW, Cheng Y, Wang NL, Zhang JC, Yang MS, Yao XS. Effects of total flavonoids and flavonol glycosides from *Epimedium koreanum* Nakai on the proliferation and differentiation of primary osteoblasts. *Phytomedicine* (2008a) 15(1-2):55–61. doi: 10.1016/j.phymed.2007.04.002
36. Rabal O, Sanchez-Arias JA, Cuadrado-Tejedor M, Miguel ID, Perez-Gonzalez M, Garcia-Barroso C, et al. Design, synthesis, and biological evaluation of first-in-class dual acting histone deacetylases (HDACs) and phosphodiesterase 5 (PDE5) inhibitors for the treatment of Alzheimer's disease. *J Med Chem* (2016) 59(19):8967–9004. doi: 10.1021/acs.jmedchem.6b00908
37. Kalyanaraman H, Schall N, Pilz RB. Nitric oxide and cyclic GMP functions in bone. *Nitric Oxide* (2018) 76:62–70. doi: 10.1016/j.niox.2018.03.007
38. Zhang Y, Li XL, Yao XS, Wong MS. Osteogenic activities of genistein derivatives were influenced by the presence of prenyl group at ring A. *Arch Pharm Res* (2008b) 31(12):1534–9. doi: 10.1007/s12272-001-2147-5
39. Alp HH, Huyut Z, Yildirim S, Basbugan Y, Ediz L, Sekeroglu MR. The effect of PDE5 inhibitors on bone and oxidative damage in ovariectomy-induced osteoporosis. *Exp Biol Med* (2017) 242(10):1051–61. doi: 10.1177/1535370217703352
40. Huyut Z, Bakan N, Yildirim S, Alp HH. Effects of the phosphodiesterase-5 (PDE-5) inhibitors, avanafil and zaprinast, on bone remodeling and oxidative damage in a rat model of glucocorticoid-induced osteoporosis. *Med Sci Monit Basic Res* (2018) 24:47–58. doi: 10.12659/MSMBR.908504
41. Gong Y, Xu CY, Wang JR, Hu XH, Hong D, Ji X, et al. Inhibition of phosphodiesterase 5 reduces bone mass by suppression of canonical Wnt signaling. *Cell Death Dis* (2014) 5:e1544. doi: 10.1038/cddis.2014.510
42. Kim SM, Taneja C, Perez-Pena H, Ryu V, Zaidi M. Repurposing erectile dysfunction drugs tadalafil and vardenafil to increase bone mass. *Proc Natl Acad Sci* (2020) 117(25):14386–94. doi: 10.1073/pnas.2000950117
43. Pal S, Rashid M, Singh SK, Porwal K, Chattopadhyay N. Skeletal restoration by phosphodiesterase 5 inhibitors in osteopenic mice: evidence of osteoanabolic and osteoangiogenic effects of the drugs. *Bone* (2020) 135:115305. doi: 10.1016/j.bone.2020.115305
44. Ming LG, Lv X, Ma XN, Ge BF, Zhen P, Song P, et al. The prenyl group contributes to activities of phytoestrogen 8-prenynaringenin in enhancing bone formation and inhibiting bone resorption in vitro. *Endocrinology* (2013) 154(3):1202–14. doi: 10.1210/en.2012-2086
45. Yang X, Jiang Y, Yang J, He J, Sun J, Chen F, et al. Prenylated flavonoids, promising nutraceuticals with impressive biological activities. *Trends Food Sci Tech* (2015) 44(1):93–104. doi: 10.1016/j.tifs.2015.03.007
46. Ozcivici E, Luu YK, Adler B, Qin Y-X, Rubin J, Judex S, et al. Mechanical signals as anabolic agents in bone. *Nat Rev Rheumatol* (2010) 6(1):50–9. doi: 10.1038/nrrheum.2009.239
47. Shaywitz AJ, Greenberg ME. CREB: a stimulus-induced transcription factor activated by a diverse array of extracellular signals. *Annu Rev Biochem* (1999) 68:821–61. doi: 10.1146/annurev.biochem.68.1.821
48. Lai CF, Chaudhary L, Fausto A, Halstead LR, Ory DS, Avioli LV, et al. Erk is essential for growth, differentiation, integrin expression, and cell function in human osteoblastic cells. *J Biol Chem* (2001) 276(17):14443–50. doi: 10.1074/jbc.M010021200
49. Young SR, Gerard-O'Riley R, Kim JB, Pavalko FM. Focal adhesion kinase is important for fluid shear stress induced mechanotransduction in osteoblasts. *J Bone Miner Res* (2009) 24(3):411–24. doi: 10.1359/jbmr.081102
50. Ge C, Xiao G, Jiang D, Franceschi RT. Critical role of the extracellular signal–regulated kinase–MAPK pathway in osteoblast differentiation and skeletal development. *J Cell Biol* (2007) 176(5):709–18. doi: 10.1083/jcb.200610046

51. Galliher-Beckley AJ, Cidlowski JA. Emerging roles of glucocorticoid receptor phosphorylation in modulating glucocorticoid hormone action in health and disease. *IUBMB Life* (2009) 61(10):979–86. doi: 10.1002/iub.245
52. Matozaki T, Murata Y, Saito Y, Okazawa H, Ohnishi H. Protein tyrosine phosphatase SHP-2: a proto-oncogene product that promotes Ras activation. *Cancer Sci* (2009) 100(10):1786–93. doi: 10.1111/j.1349-7006.2009.01257.x
53. He Z, Zhang SS, Meng Q, Li S, Zhu HH, Raquil MA, et al. Shp2 controls female body weight and energy balance by integrating leptin and estrogen signals. *Mol Cell Biol* (2012) 32(10):1867–78. doi: 10.1128/MCB.06712-11

Conflict of Interest: The authors declare that the research was conducted in the absence of any commercial or financial relationships that could be construed as a potential conflict of interest.

frontiers in Endocrinology

ORIGINAL RESEARCH
published: 23 June 2021
doi: 10.3389/fendo.2021.683226

Sex Steroids and Osteoarthritis: A Mendelian Randomization Study

Yi-Shang Yan[1†], Zihao Qu[2,3†], Dan-Qing Yu[1,4], Wei Wang[2,3], Shigui Yan[2,3] and He-Feng Huang[1*]*

[1] The Key Laboratory of Reproductive Genetics (Zhejiang University), Ministry of Education, Zhejiang University School of Medicine, Hangzhou, China, [2] Department of Orthopedic Surgery, The Second Affiliated Hospital, Zhejiang University School of Medicine, Hangzhou, China, [3] Department of Osteology, Orthopedic Research Institute of Zhejiang University, Hangzhou, China, [4] The Second Affiliated Hospital, School of Medicine, Zhejiang University, Hangzhou, China

Objective: Sex steroids are thought to contribute to the pathogenesis of osteoarthritis (OA). This study investigated the causal role of sex steroids in site- and sex-specific OA and risk of joint replacement surgery using the Mendelian randomization (MR) method.

Methods: Instrumental variables for estradiol, dehydroepiandrosterone sulfate, testosterone (T), and dihydrotestosterone (DHT) were selected. We used the inverse variance weighting (IVW) approach as the main MR method to estimate causal effects based on the summary-level data for OA and joint replacement surgery from genome-wide association studies (GWAS).

Results: A positive causal association was observed between serum T level and risks of hip OA (odds ratio [OR]=1.558, 95% confidence interval [CI]: 1.193–2.034; P=0.001) and hip replacement (OR=1.013, 95% CI: 1.008–1.018; $P=2.15\times10^{-8}$). Serum DHT level was also positively associated with the risk of hip replacement (OR=1.011, 95% CI: 1.006–1.015; $P=4.03\times10^{-7}$) and had potential causality with hip OA (OR=1.398, 95% CI: 1.054–1.855; P=0.020).

Conclusions: Serum T and DHT levels may play causal roles in the development of hip OA and contribute to the risk of hip replacement, although the underlying mechanisms require further investigation.

Keywords: Mendelian randomization, osteoarthritis, dehydroepiandrosterone sulfate, estradiol, testosterone, dihydrotestosterone

OPEN ACCESS

Edited by:
Melissa Orlandin Premaor, Federal University of Minas Gerais, Brazil

Reviewed by:
Felipe Santana, Universidade de São Paulo, Brazil
Fabio V. Comim, Federal University of Minas Gerais, Brazil

***Correspondence:**
Shigui Yan
zrjwsj@zju.edu.cn
He-Feng Huang
hhf57@zju.edu.cn

[†]These authors have contributed equally to this work

Specialty section:
This article was submitted to Bone Research, a section of the journal Frontiers in Endocrinology

Received: *20 March 2021*
Accepted: *02 June 2021*
Published: *23 June 2021*

Citation:
Yan Y-S, Qu Z, Yu D-Q, Wang W, Yan S and Huang H-F (2021) Sex Steroids and Osteoarthritis: A Mendelian Randomization Study. Front. Endocrinol. 12:683226. doi: 10.3389/fendo.2021.683226

INTRODUCTION

Osteoarthritis (OA) is the most common degenerative joint disorder worldwide (1) and one of the main causes of years lived with disability according to the 2010 World Health Organization Global Burden of Disease study (2, 3). OA is clinically characterized by chronic pain, morning stiffness, and crepitus along with radiographic findings in diarthrodial joints such as the knee and hip. The pathogenesis of OA is not fully understood, but excessive physiologic activity and an overload of pathologic factors such as inflammatory cytokines (4) and matrix degradation (5) are known to contribute. Standard treatment for OA includes early prevention and pharmacotherapy, while joint replacement surgery (6) is effective for end-stage disease (7). Additionally, hormone replacement

therapy (HRT) was shown to reduce the revision rate after total knee or hip arthroplasty by almost 40% (8). Middle-aged women are more likely than men to be affected by OA, especially in the hip or knee (9). Low plasma androstenedione concentration was shown to be associated with an increased risk of knee and hip arthroplasty in overweight men (10). The evidence to date indicates that sex steroids play an important role in the development of OA. However, a causal relationship between sex steroids and OA risk has not been established.

We recently reported a positive causal relationship between circulating sex hormone-binding globulin (SHBG) concentration (11) and calcium level (12) and risk of OA. Testosterone (T) and estradiol (E2) are active forms of sex steroids in males and females that are derived from inactive precursors such as dehydroepiandrosterone sulfate (DHEAS) and androstenedione in the circulation. E2 can also be formed from the aromatization of T, which can be converted to the more potent hormone dihydrotestosterone (DHT).

Genome-wide association studies (GWASs) have identified multiple genetic loci represented by single nucleotide polymorphisms (SNPs) that are closely associated with sex steroid concentrations (13). The Mendelian randomization (MR) (14) approach is widely used to evaluate the causal relationship between exposures and clinical outcomes based on summary data from GWASs with SNPs as instrumental variables. The fundamental principle of MR analysis is that genetic variants are randomly inherited at conception; because their distribution in a population is natural, it is presumed that the results of MR analyses are less susceptible to environmental influence and confounds. In the present study, we used validated SNPs and summary statistics from publicly available GWAS datasets to investigate the causal association between sex steroids and OA development with the MR method.

METHODS

Selection of Instrumental Variables

E2, DHEAS, T, and DHT were selected as exposures. SNPs associated with each sex steroid were identified from GWAS datasets of European cohorts of the following sizes: E2, number (N)=11,907 (15); DHEAS, N=14,846 (16); T, N=3239 (17); and DHT, N=3239 (17). All SNPs selected as instrumental variables were correlated with the corresponding exposure at a genome-wide significance level ($P<5\times10^{-8}$). A linkage disequilibrium (LD) test (**Supplementary Table 1**) was performed on the LD-link website (https://ldlink.nci.nih.gov/; European, $r^2<0.2$). Detailed information of the association between the selected SNPs and exposures is shown in **Table 1**. The potential confounders associated with the selected SNPs were analyzed in the PhenoScanner database(http://www.phenoscanner.medschl.cam.ac.uk/) (**Supplementary Table 2**).

Genetic Associations With Outcomes

Because both knee and hip are common sites of OA (3), summary data for overall OA and hip and knee OA were derived from a GWAS meta-analysis of UK Biobank and Arthritis Research UK Osteoarthritis Genetics datasets (18) that included 455,221; 393,873; and 403,124 European individuals. Given that sex is a risk factor of OA, summary-level data for OA in each sex was extracted from the UK Biobank (http://www.nealelab.is/uk-biobank), which included 30,046 cases of OA (19,397 women and 10,649 men) among 361,141 European subjects (194,153 women and 166,988 men). Summary data for hip and knee replacement surgery were also obtained from UK Medical Research Council Integrative Epidemiology Unit OpenGWAS Project (https://gwas.mrcieu.ac.uk/), which included 7322 cases of hip and 5657 cases of knee replacement among 462,933 European individuals. The association

TABLE 1 | Characteristics of SNPs for exposures from GWAS.

Exposure	Gene	SNP	Chromosome: Position	EA	Association with exposure	
					β (SE)	P value
E_2	CYP19A1	rs727479	15:51534547	A	1.39 (0.12)	8.2×10^{-30}
E_2	CYP19A1	rs16964258	15:51605408	G	2.13 (0.25)	8.2×10^{-15}
E_2	FAM9B	rs5934505	X:8913826	C	0.67 (0.12)	3.4×10^{-8}
E_2	MIR	rs5951794	X:146432188	G	0.68 (0.11)	3.1×10^{-10}
DHEAS	BCL2L11	rs6738028	2:111949327	G	-0.04 (0.01)	1.72×10^{-8}
DHEAS	ARPC1A	rs740160	7:98957880	T	0.15 (0.02)	1.56×10^{-16}
DHEAS	TRIM4	rs17277546	7:99489571	A	-0.11 (0.02)	4.50×10^{-11}
DHEAS	HHEX	rs2497306	10:94485211	C	-0.04 (0.01)	4.64×10^{-9}
DHEAS	CYP2C9	rs2185570	10:96751270	C	-0.06 (0.01)	2.29×10^{-8}
DHEAS	BMF	rs7181230	15:40360741	G	0.05 (0.01)	5.44×10^{-11}
DHEAS	SULT2A1	rs2637125	19:48401893	A	-0.09 (0.01)	2.61×10^{-19}
T	JMJD1C	rs10822186	10:65350383	A	-0.06 (0.01)	1.20×10^{-8}
T	SHBG	rs4239258	17:7397043	A	-0.16 (0.03)	4.47×10^{-8}
T	SHBG	rs34790908	17:7451110	T	0.07 (0.01)	1.66×10^{-9}
T	SHBG	rs727428	17:7537792	T	-0.07 (0.01)	1.26×10^{-12}
DHT	SHBG	rs4151121	17:7342294	G	0.10 (0.02)	7.96×10^{-10}
DHT	SHBG	rs4265880	17:7396267	T	-0.24 (0.04)	1.89×10^{-8}
DHT	SHBG	rs4227	17:7491177	G	0.09 (0.02)	3.68×10^{-8}

Gene, nearest gene to the SNP; EA, effect allele; β, per allele effect on the exposure; SE, standard error; P value, p-value for the genetic association.

data of the selected instrumental variables and sex steroids along with outcomes are provided in **Supplementary Tables 3–5**. All studies contributing data to our analyses were approved by the relevant ethics committees, and all study participants provided written, informed consent (**Supplementary Table 6**).

Statistical Analysis

A 2-sample MR approach was adopted in our study. Causal associations between sex steroids and risks of OA and joint replacement were estimated based on the random-effects inverse variance weighting (IVW) model (19). Since four separate outcomes are being tested in our study, the threshold for adjusted p-value was 0.0125. The analytical results with a p-value between 0.125 and 0.05 are considered nominally significant results.

A weighted median (WM) analysis, which involved calculating the median value of ratio instrumental variable estimates, was also performed as sensitivity analysis. The MR-Egger and MR pleiotropy residual sum and outlier (MR-PRESSO) (20) methods were used to account for pleiotropic effects (21) to exclude bias observed in the sensitivity analysis. Outlying genetic variants were identified by MR-PRESSO and used to correct the results. Moreover, SNPs associated with included outcomes ($P<1\times10^{-4}$) were removed from IVW in the sensitivity analysis. The estimated effects are reported as odds ratios (ORs) with 95% confidence intervals (CIs). We used R v3.6.1 and the R MendelianRandomization package (22) for all statistical analyses.

RESULTS

Causal Associations Between Sex Steroid Levels and Overall and Site-Specific OA

The primary IVW analyses provide no evidence for the causal relationship between the included sex steroids and overall OA (**Figure 1**). Nevertheless, the risk of hip OA was causally influenced by serum T levels (OR=1.558, 95% CI: 1.193–2.034; P=0.001). And the nominally significant results suggested a positive association between serum DHT levels (OR=1.398, 95% CI: 1.054–1.855; P=0.020) and hip OA. However, there was no evidence for associations between the levels of other sex steroids and hip and knee OA (**Figure 2**).

Causal Association Between Sex Steroid Levels and OA by Sex

The nominally significant results of IVW analyses showed that serum DHT level tended to have a causal effect on the risk of OA in women (OR=1.012, 95% CI: 1.000–1.025; P=0.046), while no relationship was observed between sex steroid levels and OA risk in men (**Figure 3**).

Causal Association Between Sex Steroid Levels and Joint Arthroplasty

Because of a lack of corresponding outcome data for E2-associated SNPs, the association between serum E2 level and joint replacement was not estimated by IVW analysis in our study. The results of the analysis showed that the risk of hip replacement was causally influenced by serum T (OR=1.013, 95% CI: 1.008–1.018; $P=2.15\times10^{-8}$) and DHT (OR=1.011, 95% CI: 1.006–1.015; $P=4.03\times10^{-7}$) levels. However, we found no evidence of an association between the exposures and knee replacement (**Figure 4**).

Sensitivity Analysis

First, the WM method was used for sensitivity analysis. Similar with the results of main IVW analyses, the WM analyses suggested a positive causal relationship between serum DHT (P=0.006) and T ($P=4.97\times10^{-4}$) levels and hip OA and the causal effects of serum DHEAS (P=0.017) and T ($P=4.10\times10^{-5}$) levels on the risk of hip replacement were statistically significant (**Supplementary Tables 7–9**). However, positive associations

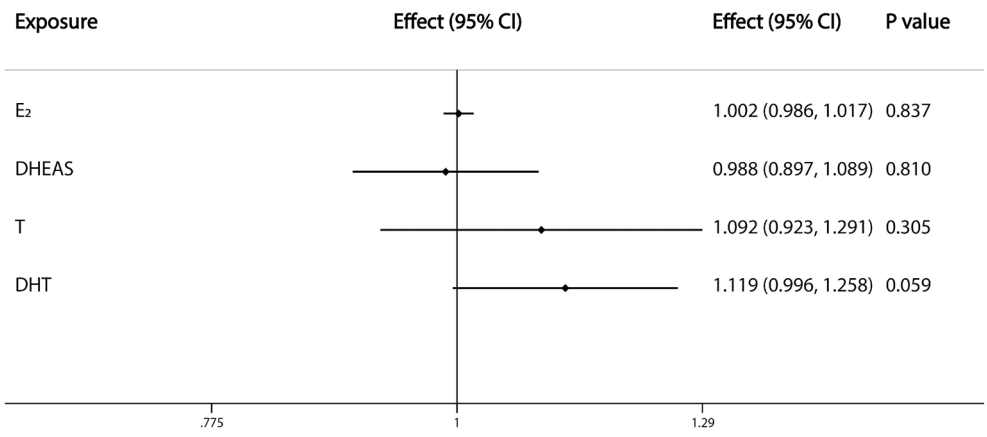

FIGURE 1 | Causal effects of sex steroids on the risk of overall OA. The estimated effects, 95% confidence intervals and p-values of associations were contained. Effect, the combined causal effect; CI, confidence interval; P value, p-value of the causal estimate.

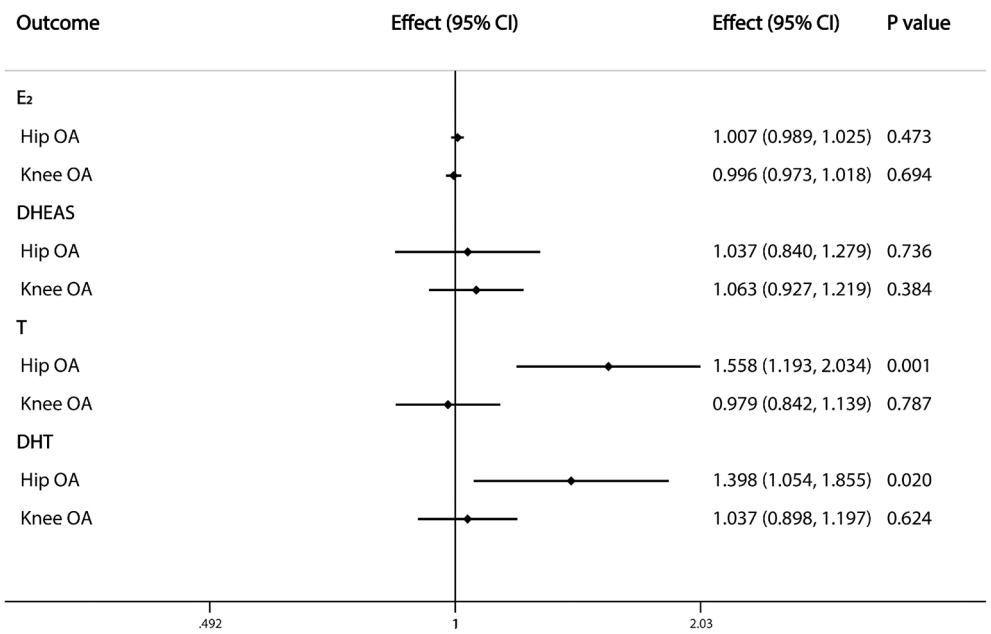

FIGURE 2 | Causal effects of sex steroids on the risk of OA of hip and knee. The estimated effects, 95% confidence intervals and p-values of associations were contained. Effect, the combined causal effect; CI, confidence interval; P value, p-value of the causal estimate.

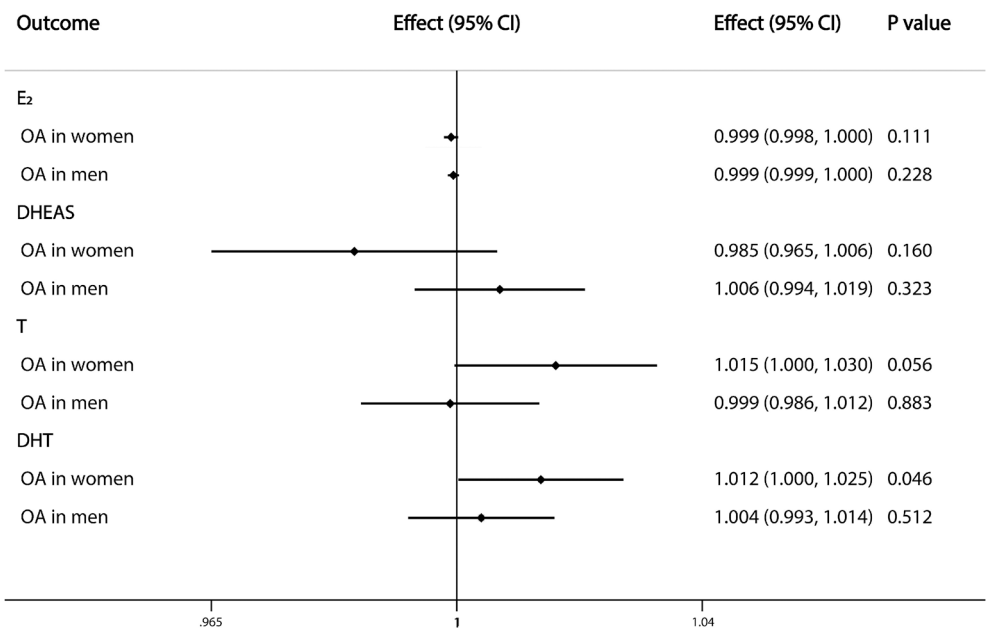

FIGURE 3 | Causal effects of sex steroids on the risk of OA in single sex. The estimated effects, 95% confidence intervals and p-values of associations were contained. Effect, the combined causal effect; CI, confidence interval; P value, p-value of the causal estimate.

were found between serum DHT level and overall OA and between serum T level and OA in women, which were inconsistent with our primary findings. Second, in the MR-Egger analysis, nearly all of the intercept terms were centered around the origin, suggesting that there was no horizontal pleiotropy (**Supplementary Tables 7–9**). Nevertheless, there

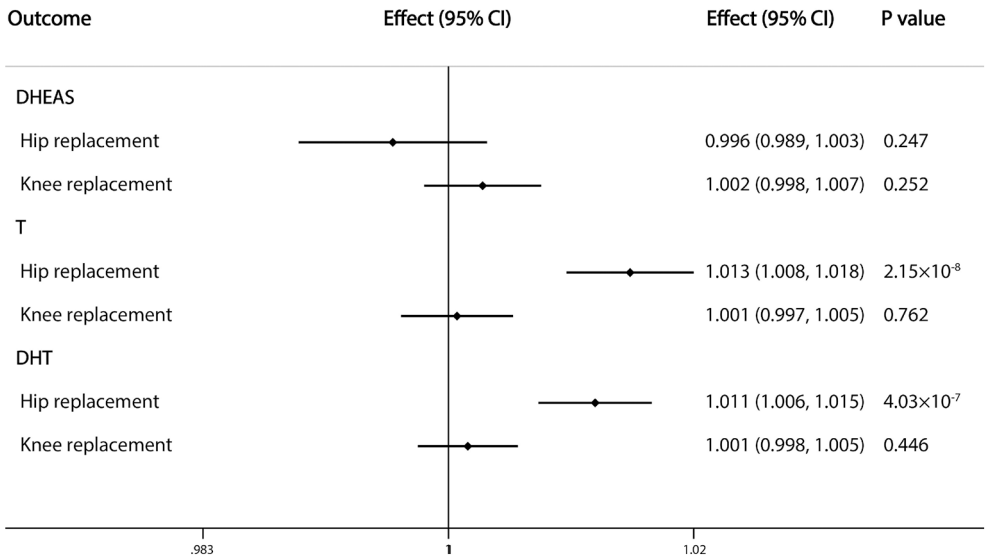

FIGURE 4 | Causal effects of sex steroids on the risk of joint replacement of hip and knee. The estimated effects, 95% confidence intervals and p-values of associations were contained. Effect, the combined causal effect; CI, confidence interval; P value, p-value of the causal estimate.

were some exceptions such as the P value of the pleiotropy estimate of the relationships between E2 and overall OA and between DHT and overall or hip OA.

The MR-PRESSO analysis was performed to identify outlying SNPs when the number of genetic variants for specific exposure was >3. In the association between serum E_2 level and overall OA, rs5934505 was identified as an outlier and removed; rs747279 and rs5934505 were also identified as outliers and were excluded from the MR-PRESSO analysis of the association between serum E2 level and knee OA. Rs34790908 was another outlying SNP in the association between serum T level and overall OA. After removing these outliers, the causal association between serum T level and hip OA was still observed in the MR-PRESSO analysis (OR=1.558, 95% CI: 1.193–2.034; P=0.047). Additionally, after removing genetic variants that were directly associated with the outcome measures (rs5934505 for overall OA; rs34790908 for hip OA and hip replacement; and rs4227 for hip OA and hip replacement), the positive causal effects of serum T (hip OA: P=0.001; hip replacement: $P=4.52\times10^{-5}$) and DHT (hip OA: P=0.011; hip replacement: P=0.002) levels on risk of hip OA and hip replacement remained significant in the IVW analyses (**Supplementary Table 10**).

DISCUSSION

This MR study was conducted to investigate the causal relationship between sex steroids levels and OA risk. Our results revealed positive causal effects of serum concentrations of T on the risk of hip OA. There was potential positive association between DHT and hip OA as well while little evidence of the association between sex steroids levels and overall OA was found. Interestingly, males were reported to have higher scores for cartilage damage than age-matched females in a murine OA model induced by destabilization of the medial meniscus (23). Orchiectomized males had less severe damage than their intact counterparts whereas the opposite was true for ovariectomized females, indicating that sex hormones play varied roles in the progression of OA. In fact, the steroid hormones 17β-estradiol, DHEA, and T were shown to promote articular cartilage integration (24).

In a cohort of healthy middle-aged men with no symptoms of knee OA or risk factors, serum free T level was associated with the rate of tibial cartilage loss leading to the development of arthritis 2 years later (25). In a cross-sectional study, a higher concentration of serum T was associated with higher cartilage volume (26), possibly due to greater physical activity and stress on the articular cartilage. Thus, chronic stress and damage to weight-bearing joints—especially the hip and knee—can contribute to OA. However, the protective effects of E2 and DHEAS on OA occurrence are unclear. In a cohort of community-dwelling older subjects, a lower DHEAS was associated with OA irrespective of site and sex (27); and histomorphometric studies in a rabbit model of progressive OA showed that DHEAS treatment reduced cartilage lesions and delayed cartilage degeneration (28, 29). DHEAS was shown to modulate the imbalance between matrix metalloproteinases (MMPs) and its inhibitors (30–33); and intra-articular administration of DHEA reduced aggrecanase expression *in vivo* (34).

In our study, a nominally significant result for the relationship between serum DHT levels and risk of OA in women was found, while little evidence of the sex-specific association between serum T levels and OA was provided. However, a 2-year double-blind cross-sectional analysis of 273 seniors with severe knee OA at an average

age of 70.3 years found that a higher T level was associated with less knee disability in non-operated women and less pain (as determined by the Western Ontario and McMaster Universities Osteoarthritis Index) in normal-weight men (35). In another longitudinal investigation on the association between endogenous sex hormone levels and knee OA features and pain, T level was inversely associated with effusion-synovitis volume and pain score in female OA patients (36). However, these findings can only explain the relationship between T level and severity of knee OA symptoms because all of the subjects were OA patients. Besides, our results were based on a non–age-stratified population. A clinical study reported that middle-aged menopausal women with generalized OA had a slightly higher T level and lower circulating SHBG level than control subjects (37).

Unexpectedly, we did not observe any causal association between E2 level and OA risk in women, which may be caused by the male-specific GWAS from which the SNPs for E2 were selected. The marked increase in OA incidence during or soon after menopause is well established. Moreover, estradiol is a known protective factor against OA. The use of oral estrogen was found to be associated with a decreased incidence of radiographic hip OA in elderly Caucasian women (38). A case–control study of women aged ≥45 years found that short-term HRT (up to 5 years) was associated with an increased risk of hip OA, while long-term treatment had a nonsignificant protective effect (39). In premenopausal Caucasian women with knee grade ≥2, a clinical diagnosis of OA was positively correlated with serum estradiol level (40). These findings indicate that the effects of reproductive hormones vary according to age and concentration.

E2 level was shown to be negatively correlated with OA severity and positively correlated with interleukin (IL)-1, IL-6, and tumor necrosis factor (TNF)-α concentrations in the synovial fluid of postmenopausal women (41). In vitro studies have demonstrated that 17β-estradiol treatment enhanced proliferation and viability in chondrocytes by inhibiting mitophagy *via* the G protein-coupled estrogen receptor (GPER/GPR30) and phosphatidylinositol 3-kinase (PI3K)/protein kinase B (AKT) signaling pathways (42, 43), and induced chondrocyte redifferentiation *via* the estrogen receptor (ER)α66/specificity protein (Sp)1/Sp3/SRY-box (SOX)9/p300 protein complex (44). In experiments with mice, a reduction in serum E2 caused by ovariectomy induced severe OA, while supplementary administration of β-estradiol rescued bone turnover and tissue degradation (45). Lower levels of endogenous estrogen and its metabolites were significantly associated with the development of knee OA (46, 47). E2 was shown to inhibit activation of the NOD-, LRR-, and pyrin domain-containing protein (NLRP)3 inflammasome, IL-1β and IL-18 expression, and the catabolic activity of MMPs *via* estrogen receptor or miR-140 (48–52). Our findings suggested that women are more susceptible to OA than men because of differences in sex steroid profiles.

Our results showed a positive causal association between serum T and DHT levels and risk of hip replacement while no relationship was found between E_2 and arthroplasty due to data deficiencies. A long-term study with a mean follow-up of 12.7 years reported that oral contraceptive use, current HRT use, and longer duration of HRT were associated with increased risk of total knee arthroplasty for OA in women aged 40–69 years (53). However, in another prospective cohort study, the association between incidence of total knee replacement for OA and lower E2 concentration was independent of established risk factors for knee OA, and there was no relationship between E2 and total hip replacement (54). In spite of the exclusion of LD-linkage, rs5934505 for E_2 and rs727428 for DHT were found to be confounded with T, and rs4227 for T was found to be confounded with DHT by the analysis in PhenoScanner database. Both of them are all located in the same chromosome locus named SHBG. Previous studies suggested that SHBG was significantly associated with T and DHT levels in European ancestry (17) but was not associated with T in Japanese men (55). Moreover, a mutant allele of rs727428 was found to be positively correlated with PCOS in Mediterranean women (56). rs4227 was found to be positively associated with IgA nephropathy in Han Chinese which located in 17p13 7431901 coding MPDU1 gene (57).

Compared to traditional retrospective analyses and case–control prospective studies, MR is less likely to introduce artificial errors and bias. Sex steroid levels fluctuate over time and measurements are often imprecise and experiment design cannot always be perfect. The cost of data collection and analysis can be high, and the MR method can to some extent mitigate data migration; moreover, sequential application of different algorithms in the sensitivity analysis can increase the accuracy and reliability of the results. Nonetheless, our study had several limitations. First, the outcome datasets and representative SNPs were sometimes too limited for us to carry out sensitivity analyses. Second, age-adjusted IVW analyses are necessary to exclude the influence of aging on OA and sex steroid levels, but we did not find any age-stratified OA datasets to perform adjusted IVW analyses. Third, since the GWASs on E2, T and DHT included only male participants in this study, the results of sex-stratified analyses may be influenced by the exposure data. Forth, there might be some dependencies between T and DHT. Finally, our study focused on the causal role of sex steroids in the pathogenesis of OA, but the underlying mechanisms remain to be elucidated.

In conclusion, serum T and DHT levels were causally related to the risk of hip replacement surgery and T was positively associated with risk of hip OA. Further, a nominally significant relationship was found between serum DHT levels and OA in women as well as hip OA. Thus, these sex steroids may contribute to the development of OA. Our findings can guide the development of effective clinical management strategies to maintain joint health and prevent OA, especially in women.

DATA AVAILABILITY STATEMENT

Summary data used in our study was downloaded from GWAS Catalog (https://www.ebi.ac.uk/gwas/), Neale's lab (http://www.

nealelab.is/uk-biobank) and IEU OpenGWAS project (https://gwas.mrcieu.ac.uk/).

ETHICS STATEMENT

Ethical review and approval was not required for the study on human participants in accordance with the local legislation and institutional requirements. Written informed consent for participation was not required for this study in accordance with the national legislation and the institutional requirements.

AUTHOR CONTRIBUTIONS

Y-SY, ZQ, D-QY, WW, SY, H-FH desinged the study. ZQ analyzed the data. Y-SY wrote the manuscript. All authors contributed to the article and approved the submitted version.

FUNDING

This work was supported by the National Natural Science Foundation of China (grant no. 81772360).

ACKNOWLEDGMENTS

All cited projects and datasets were approved by the relevant ethics committees. We thank the authors of the cited studies for making their datasets available for download.

SUPPLEMENTARY MATERIAL

The Supplementary Material for this article can be found online at: https://www.frontiersin.org/articles/10.3389/fendo.2021.683226/full#supplementary-material

REFERENCES

1. Glyn-JonesS, Palmer AJR, Agricola R, Price AJ, Vincent TL, Weinans H, et al. Osteoarthritis. *Lancet* (2015) 386:376–87. doi: 10.1016/S0140-6736(14)60802-3
2. Vos T, Flaxman AD, Naghavi M, Lozano R, Michaud C, Ezzati M, et al. Years Lived With Disability (Ylds) for 1160 Sequelae of 289 Diseases and Injuries 1990-2010: A Systematic Analysis for the Global Burden of Disease Study 2010. *Lancet* (2012) 380:2163–96. doi: 10.1016/S0140-6736(12)61729-2
3. Cross M, Smith E, Hoy D, Nolte S, Ackerman I, Fransen M, et al. The Global Burden of Hip and Knee Osteoarthritis: Estimates From the Global Burden of Disease 2010 Study. *Ann Rheum Dis* (2014) 73:1323–30. doi: 10.1136/annrheumdis-2013-204763
4. Wang T, He C. Pro-Inflammatory Cytokines: The Link Between Obesity and Osteoarthritis. *Cytokine Growth Factor Rev* (2018) 44:38–50. doi: 10.1016/j.cytogfr.2018.10.002
5. Rahmati M, Nalesso G, Mobasheri A, Mozafari M. Aging and Osteoarthritis: Central Role of the Extracellular Matrix. *Ageing Res Rev* (2017) 40:20–30. doi: 10.1016/j.arr.2017.07.004
6. Harris WH, Sledge CB. Total Hip and Total Knee Replacement (2). *N Engl J Med* (1990) 323:801–7. doi: 10.1056/NEJM199009203231206
7. Hunter DJ, Bierma-Zeinstra S. Osteoarthritis. *Lancet* (2019) 393:1745–59. doi: 10.1016/S0140-6736(19)30417-9
8. Prieto-Alhambra D, Javaid MK, Judge A, Maskell J, Cooper C, Arden NK. Hormone Replacement Therapy and Mid-Term Implant Survival Following Knee or Hip Arthroplasty for Osteoarthritis: A Population-Based Cohort Study. *Ann Rheum Dis* (2015) 74:557–63. doi: 10.1136/annrheumdis-2013-204043
9. Ding C, Cicuttini F, Blizzard L, Scott F, Jones G. A Longitudinal Study of the Effect of Sex and Age on Rate of Change in Knee Cartilage Volume in Adults. *Rheumatol (Oxford)* (2007) 46:273–9. doi: 10.1093/rheumatology/kel243
10. Hussain SM, Cicuttini FM, Giles GG, Graves SE, Wang Y. Relationship Between Circulating Sex Steroid Hormone Concentrations and Incidence of Total Knee and Hip Arthroplasty Due to Osteoarthritis in Men. *Osteoarthr Cartil* (2016) 24:1408–12. doi: 10.1016/j.joca.2016.04.008
11. Qu Z, Huang J, Yang F, Hong J, Wang W, Yan S. Sex Hormone-Binding Globulin and Arthritis: A Mendelian Randomization Study. *Arthritis Res Ther* (2020) 22:118. doi: 10.1186/s13075-020-02202-2
12. Qu Z, Yang F, Hong J, Wang W, Li S, Jiang G, et al. Causal Relationship of Serum Nutritional Factors With Osteoarthritis: A Mendelian Randomization Study. *Rheumatol (Oxford)* (2020) 60(5):2383–90. doi: 10.1093/rheumatology/keaa622
13. Harroud A, Richards JB. Mendelian Randomization in Multiple Sclerosis: A Causal Role for Vitamin D and Obesity? *Multiple Sclerosis J* (2018) 24:80–5. doi: 10.1177/1352458517737373
14. Emdin CA, Khera AV, Kathiresan S. Mendelian Randomization. *JAMA* (2017) 318:1925–6. doi: 10.1001/jama.2017.17219
15. Eriksson AL, Perry JRB, Coviello AD, Delgado GE, Ferrucci L, Hoffman AR, et al. Genetic Determinants of Circulating Estrogen Levels and Evidence of a Causal Effect of Estradiol on Bone Density in Men. *J Clin Endocrinol Metab* (2018) 103:991–1004. doi: 10.1210/jc.2017-02060
16. Zhai G, Teumer A, Stolk L, Perry JRB, Vandenput L, Coviello AD, et al. Eight Common Genetic Variants Associated With Serum DHEAS Levels Suggest a Key Role in Ageing Mechanisms. *PloS Genet* (2011) 7:e1002025. doi: 10.1371/journal.pgen.1002025
17. Jin G, Sun J, Kim S-T, Feng J, Wang Z, Tao S, et al. Genome-Wide Association Study Identifies a New Locus JMJD1C at 10q21 That may Influence Serum Androgen Levels in Men. *Hum Mol Genet* (2012) 21:5222–8. doi: 10.1093/hmg/dds361
18. Tachmazidou I, Hatzikotoulas K, Southam L, Esparza-Gordillo J, Haberland V, Zheng J, et al. Identification of New Therapeutic Targets for Osteoarthritis Through Genome-Wide Analyses of UK Biobank Data. *Nat Genet* (2019) 51:230–6. doi: 10.1038/s41588-018-0327-1
19. Pierce BL, Burgess S. Efficient Design for Mendelian Randomization Studies: Subsample and 2-Sample Instrumental Variable Estimators. *Am J Epidemiol* (2013) 178:1177–84. doi: 10.1093/aje/kwt084
20. Verbanck M, Chen C-Y, Neale B, Do R. Detection of Widespread Horizontal Pleiotropy in Causal Relationships Inferred From Mendelian Randomization Between Complex Traits and Diseases. *Nat Genet* (2018) 50:693–8. doi: 10.1038/s41588-018-0099-7
21. Stearns FW. One Hundred Years of Pleiotropy: A Retrospective. *Genetics* (2010) 186:767–73. doi: 10.1534/genetics.110.122549
22. Yavorska OO, Burgess S. MendelianRandomization: An R Package for Performing Mendelian Randomization Analyses Using Summarized Data. *Int J Epidemiol* (2017) 46:1734–9. doi: 10.1093/ije/dyx034
23. Ma HL, Blanchet TJ, Peluso D, Hopkins B, Morris EA, Glasson SS. Osteoarthritis Severity is Sex Dependent in a Surgical Mouse Model. *Osteoarthr Cartil* (2007) 15:695–700. doi: 10.1016/j.joca.2006.11.005
24. Englert C, Blunk T, Fierlbeck J, Kaiser J, Stosiek W, Angele P, et al. Steroid Hormones Strongly Support Bovine Articular Cartilage Integration in the Absence of Interleukin-1beta. *Arthritis Rheumatism* (2006) 54:3890–7. doi: 10.1002/art.22250
25. Hanna F, Ebeling PR, Wang Y, O'Sullivan R, Davis S, Wluka AE, et al. Factors Influencing Longitudinal Change in Knee Cartilage Volume Measured From Magnetic Resonance Imaging in Healthy Men. *Ann Rheum Dis* (2005) 64:1038–42. doi: 10.1136/ard.2004.029355
26. Cicuttini FM, Wluka A, Bailey M, O'Sullivan R, Poon C, Yeung S, et al. Factors Affecting Knee Cartilage Volume in Healthy Men. *Rheumatol (Oxford)* (2003) 42:258–62. doi: 10.1093/rheumatology/keg073
27. Veronese N, Maggi S, Noale M, Trevisan C, De Rui M, Bolzetta F, et al. Serum Dehydroepiandrosterone Sulfate and Osteoarthritis in Older People: The Pro.V.A. Study. *Clin Rheumatol* (2016) 35:2609–14. doi: 10.1007/s10067-016-3213-1

28. Huang K, Bao J-p, Jennings GJ, Wu L-d. The Disease-Modifying Effect of Dehydroepiandrosterone in Different Stages of Experimentally Induced Osteoarthritis: A Histomorphometric Study. *BMC Musculoskelet Disord* (2015) 16:178. doi: 10.1186/s12891-015-0595-1
29. Wu LD, Yu HC, Xiong Y, Feng J. Effect of Dehydroepiandrosterone on Cartilage and Synovium of Knee Joints With Osteoarthritis in Rabbits. *Rheumatol Int* (2006) 27:79–85. doi: 10.1007/s00296-006-0238-9
30. Jo H, Park JS, Kim EM, Jung MY, Lee SH, Seong SC, et al. The In Vitro Effects of Dehydroepiandrosterone on Human Osteoarthritic Chondrocytes. *Osteoarthr Cartil* (2003) 11:585–94. doi: 10.1016/S1063-4584(03)00094-3
31. Sun JS, Wu CX, Tsuang YH, Chen LT, Sheu SY. The In Vitro Effects of Dehydroepiandrosterone on Chondrocyte Metabolism. *Osteoarthr Cartil* (2006) 14:238–49. doi: 10.1016/j.joca.2005.09.012
32. Jo H, Ahn HJ, Kim EM, Kim HJ, Seong SC, Lee I, et al. Effects of Dehydroepiandrosterone on Articular Cartilage During the Development of Osteoarthritis. *Arthritis Rheumatism* (2004) 50:2531–8. doi: 10.1002/art.20368
33. . Bao J-p, . Chen W-p, Feng J, Zhao J, . Shi Z-l, Huang K, et al. Variation Patterns of Two Degradation Enzyme Systems in Articular Cartilage in Different Stages of Osteoarthritis: Regulation by Dehydroepiandrosterone. *Clin Chim Acta; Int J Clin Chem* (2009) 408:1–7. doi: 10.1016/j.cca.2009.06.040
34. Huang K, Zhang C, Zhang X-W, Bao J-P, Wu L-D. Effect of Dehydroepiandrosterone on Aggrecanase Expression in Articular Cartilage in a Rabbit Model of Osteoarthritis. *Mol Biol Rep* (2011) 38:3569–72. doi: 10.1007/s11033-010-0467-6
35. Freystaetter G, Fischer K, Orav EJ, Egli A, Theiler R, Münzer T, et al. Total Serum Testosterone and WOMAC Pain and Function Among Older Men and Women With Severe Knee OA. *Arthritis Care Res (Hoboken)* (2019) 72 (11):1511–8. doi: 10.1002/acr.24074
36. Jin X, Wang BH, Wang X, Antony B, Zhu Z, Han W, et al. Associations Between Endogenous Sex Hormones and MRI Structural Changes in Patients With Symptomatic Knee Osteoarthritis. *Osteoarthr Cartil* (2017) 25:1100–6. doi: 10.1016/j.joca.2017.01.015
37. Spector TD, Perry LA, Jubb RW. Endogenous Sex Steroid Levels in Women With Generalised Osteoarthritis. *Clin Rheumatol* (1991) 10:316–9. doi: 10.1007/BF02208698
38. Nevitt MC, Cummings SR, Lane NE, Hochberg MC, Scott JC, Pressman AR, et al. Association of Estrogen Replacement Therapy With the Risk of Osteoarthritis of the Hip in Elderly White Women. *Study Osteoporotic Fractures Res Group Arch Intern Med* (1996) 156:2073–80. doi: 10.1001/archinte.156.18.2073
39. Dennison EM, Arden NK, Kellingray S, Croft P, Coggon D, Cooper C. Hormone Replacement Therapy, Other Reproductive Variables and Symptomatic Hip Osteoarthritis in Elderly White Women: A Case-Control Study. *Br J Rheumatol* (1998) 37:1198–202. doi: 10.1093/rheumatology/37.11.1198
40. Sowers MF, Hochberg M, Crabbe JP, Muhich A, Crutchfield M, Updike S. Association of Bone Mineral Density and Sex Hormone Levels With Osteoarthritis of the Hand and Knee in Premenopausal Women. *Am J Epidemiol* (1996) 143:38–47. doi: 10.1093/oxfordjournals.aje.a008655
41. Liu YP, Li J, Xin SB, JX. Study the Relevance Between Inflammatory Factors and Estradiol and Their Association With Knee Osteoarthritis in Postmenopausal Women. *Eur Rev Med Pharmacol Sci* (2018) 22:472–8. doi: 10.26355/eurrev_201801_14197
42. Fan D-X, Yang X-H, Li Y-N, Guo L. 17β-Estradiol on the Expression of G-Protein Coupled Estrogen Receptor (Gper/Gpr30) Mitophagy, and the PI3K/Akt Signaling Pathway in ATDC5 Chondrocytes In Vitro. *Med Sci monit Int Med J Exp Clin Res* (2018) 24:1936–47. doi: 10.12659/MSM.909365
43. Huang JG, Xia C, Zheng XP, Yi TT, Wang XY, Song G, et al. 17β-Estradiol Promotes Cell Proliferation in Rat Osteoarthritis Model Chondrocytes Via PI3K/Akt Pathway. *Cell Mol Biol Lett* (2011) 16:564–75. doi: 10.2478/s11658-011-0023-y
44. Maneix L, Servent A, Porée B, Ollitrault D, Branly T, Bigot N, et al. Up-Regulation of Type II Collagen Gene by 17β-Estradiol in Articular Chondrocytes Involves Sp1/3, Sox-9, and Estrogen Receptor α. *J Mol Med (Berlin Germany)* (2014) 92:1179–200. doi: 10.1007/s00109-014-1195-5
45. Yang J-H, Kim J-H, Lim D-S, Oh K-J. Effect of Combined Sex Hormone Replacement on Bone/Cartilage Turnover in a Murine Model of Osteoarthritis. *Clin Orthop Surg* (2012) 4:234–41. doi: 10.4055/cios.2012.4.3.234
46. Sowers MR, McConnell D, Jannausch M, Buyuktur AG, Hochberg M, Jamadar DA. Estradiol and its Metabolites and Their Association With Knee Osteoarthritis. *Arthritis Rheumatism* (2006) 54:2481–7. doi: 10.1002/art.22005
47. Gao W, Zeng C, Cai D, Liu B, Li Y, Wen X, et al. Serum Concentrations of Selected Endogenous Estrogen and Estrogen Metabolites in Pre- and Post-Menopausal Chinese Women With Osteoarthritis. *J Endocrinological Invest* (2010) 33:644–9. doi: 10.1007/BF03346664
48. Shi J, Zhao W, Ying H, Zhang Y, Du J, Chen S, et al. Estradiol Inhibits NLRP3 Inflammasome in Fibroblast-Like Synoviocytes Activated by Lipopolysaccharide and Adenosine Triphosphate. *Int J Rheumatic Dis* (2018) 21:2002–10. doi: 10.1111/1756-185X.13198
49. Liang Y, Duan L, Xiong J, Zhu W, Liu Q, Wang D, et al. E2 Regulates MMP-13 Via Targeting miR-140 in IL-1β-Induced Extracellular Matrix Degradation in Human Chondrocytes. *Arthritis Res Ther* (2016) 18:105. doi: 10.1186/s13075-016-0997-y
50. Claassen H, Steffen R, Hassenpflug J, Varoga D, Wruck CJ, Brandenburg LO, et al. 17β-Estradiol Reduces Expression of MMP-1, -3, and -13 in Human Primary Articular Chondrocytes From Female Patients Cultured in a Three Dimensional Alginate System. *Cell Tissue Res* (2010) 342:283–93. doi: 10.1007/s00441-010-1062-9
51. Lee YJ, Lee EB, Kwon YE, Lee JJ, Cho WS, Kim HA, et al. Effect of Estrogen on the Expression of Matrix Metalloproteinase (MMP)-1, MMP-3, and MMP-13 and Tissue Inhibitor of Metalloproternase-1 in Osteoarthritis Chondrocytes. *Rheumatol Int* (2003) 23:282–8. doi: 10.1007/s00296-003-0312-5
52. Tsai CL, Liu TK, Chen TJ. Estrogen and Osteoarthritis: A Study of Synovial Estradiol and Estradiol Receptor Binding in Human Osteoarthritic Knees. *Biochem Biophys Res Commun* (1992) 183:1287–91. doi: 10.1016/S0006-291X(05)80330-4
53. Hussain SM, Wang Y, Giles GG, Graves S, Wluka AE, Cicuttini FM. Female Reproductive and Hormonal Factors and Incidence of Primary Total Knee Arthroplasty Due to Osteoarthritis. *Arthritis Rheumatol (Hoboken N.J.)* (2018) 70:1022–9. doi: 10.1002/art.40483
54. Hussain SM, Cicuttini FM, Bell RJ, Robinson PJ, Davis SR, Giles GG, et al. Incidence of Total Knee and Hip Replacement for Osteoarthritis in Relation to Circulating Sex Steroid Hormone Concentrations in Women. *Arthritis Rheumatol (Hoboken N.J.)* (2014) 66:2144–51. doi: 10.1002/art.38651
55. Sato Y, Tajima A, Katsurayama M, Nozawa S, Yoshiike M, Koh E, et al. An Independent Validation Study of Three Single Nucleotide Polymorphisms at the Sex Hormone-Binding Globulin Locus for Testosterone Levels Identified by Genome-Wide Association Studies. *Hum Reprod Open* (2017) 2017(1): hox002. doi: 10.1093/hropen/hox002
56. Martinez-Garcia MA, Gambineri A, Alpanes M, Sanchon R, Pasquali R, Escobar-Morreale HF. Common Variants in the Sex Hormone-Binding Globulin Gene (SHBG) and Polycystic Ovary Syndrome (PCOS) in Mediterranean Women. *Hum Reprod* (2012) 27(12):3569–76. doi: 10.1093/humrep/des335
57. Yu XQ, Li M, Zhang H, Low HQ, Wei X, Wang JQ, et al. A Genome-Wide Association Study in Han Chinese Identifies Multiple Susceptibility Loci for IgA Nephropathy. *Nat Genet* (2011) 44(2):178–82. doi: 10.1038/ng.1047

Conflict of Interest: The authors declare that the research was conducted in the absence of any commercial or financial relationships that could be construed as a potential conflict of interest.

frontiers in Endocrinology

ORIGINAL RESEARCH
published: 20 July 2021
doi: 10.3389/fendo.2021.706504

Inhibition of Lipoxygenases Showed No Benefit for the Musculoskeletal System in Estrogen Deficient Rats

Dominik Saul[1,2*†], *Friederike Eva Hohl*[1], *Max Konrad Franz*[1], *Ilka Meyer*[1], *Stefan Taudien*[3], *Paul Jonathan Roch*[1], *Stephan Sehmisch*[1] *and Marina Komrakova*[1†]

[1] Department of Trauma Surgery, Orthopaedics and Plastic Surgery, University Medical Center Goettingen, Goettingen, Germany, [2] Kogod Center on Aging and Division of Endocrinology, Mayo Clinic, Rochester, MN, United States, [3] Division of Infection Control and Infectious Diseases, Georg-August-University of Goettingen, Goettingen, Germany

OPEN ACCESS

Edited by:
Melissa Orlandin Premaor, Federal University of Minas Gerais, Brazil

Reviewed by:
Astrid Kamilla Stunes, Norwegian University of Science and Technology, Norway
Hitoshi Saito, Chugai Pharmaceutical Co., Ltd, Japan

***Correspondence:**
Dominik Saul
Dominik.Saul@med.uni-goettingen.de

†ORCID:
Dominik Saul
orcid.org/0000-0002-0673-3710
Marina Komrakova
orcid.org/0000-0002-6225-4378

Specialty section:
This article was submitted to Bone Research, a section of the journal Frontiers in Endocrinology

Received: 07 May 2021
Accepted: 29 June 2021
Published: 20 July 2021

Citation:
Saul D, Hohl FE, Franz MK, Meyer I, Taudien S, Roch PJ, Sehmisch S and Komrakova M (2021) Inhibition of Lipoxygenases Showed No Benefit for the Musculoskeletal System in Estrogen Deficient Rats. Front. Endocrinol. 12:706504. doi: 10.3389/fendo.2021.706504

Background: In previous studies, we reported the beneficial impact of two lipoxygenase-inhibitors, Baicalein and Zileuton, on osteoporotic bone in a postmenopausal rat model. Whereas subcutaneous Baicalein predominantly improved cortical bone, Zileuton enhanced vertebral and femoral trabecular bone. In this study, we aimed to reveal whether the oral administration of Baicalein caused similar effects on bone and whether a combined administration of Baicalein and Zileuton could act synergistically to ameliorate the formerly reported effects in the musculoskeletal system.

Methods: We treated ovariectomized (OVX) female Sprague-Dawley rats either with Baicalein (10mg/kg BW), Zileuton (10mg/kg BW) or a combination of both (each 10mg/kg BW) for 13 weeks and compared with untreated OVX and NON-OVX groups (n=12-16 rats per group). Lumbar vertebral bodies and femora were analyzed. Tibiae were osteotomized, plate-stabilized (at week 8 after OVX) and likewise analyzed by biomechanical, histological, micro-computed tomographical and ashing tests. The skeletal muscle structure was analyzed.

Results: Oral administration of Baicalein did not confirm the reported favorable cortical effects in neither vertebra nor femur. Zileuton showed a beneficial effect on trabecular vertebra, while the femur was negatively affected. Callus formation was enhanced by all treatments; however, its density and biomechanical properties were unaltered. Lipoxygenase inhibition did not show a beneficial effect on skeletal muscle. The combination therapy did not ameliorate OVX-induced osteoporosis but induced even more bone loss.

Conclusions: The preventive anti-osteoporotic treatments with two lipoxygenase inhibitors applied either alone or in combination showed no benefit for the musculoskeletal system in estrogen deficient rats.

Keywords: baicalein, bone healing, lipoxygenase-inhibitor, muscle tissue, osteoporosis, zileuton

INTRODUCTION

With a prevalence of 200 million people worldwide, mostly postmenopausal women are affected by osteopenia or osteoporosis. In line with that, the annual amount of osteoporotic fractures among Medicare beneficiaries in the United States is estimated to be over 2.3 million (1–3). The "silent disease" loses covertness more and more due to extended guidelines and better prevention, but yet the long-term use of established medicamentous therapies causes several new dilemmas (4). Consequently and with a better understanding of underlying mechanisms that control bone turnover, new targets of therapy have been discovered and addressed (5). On this way, Receptor Activator of NF-κB Ligand (RANKL)- and Sclerostin-antibodies have found their way into the clinic (6, 7). However, advanced search for novel therapeutic approaches is ongoing.

Lipoxygenase (LOX) inhibitors have been found to suppress osteoclast formation and enhance bone formation *in vivo* (8, 9). A LOX inhibitor, Baicalein, which is extracted from the plant *Scutellaria baicalensis* inhibits 12- and 15-Lipoxygenase (*12- and 15-LOX*). Another lipoxygenase inhibitor, Zileuton, inhibits *5-LOX* and has been FDA-approved (Zyflo®) for the treatment of asthma. Both lipoxygenase-inhibitors exert an antioxidative effect providing protection for cellular components and inhibiting apoptosis both in *in vitro* and *in vivo* studies (10–12).

In our previous studies we reported beneficial effects of these two LOX inhibitors applied as a mono-therapy for 4 to 5 weeks on bone parameters in the postmenopausal rat model. Baicalein was able to improve cortical bone, while Zileuton enhanced the trabecular structure in lumbar vertebrae and femora (13, 14). In addition to that, we demonstrated a beneficial effect of these treatments on the capillarization of the skeletal muscle (15). The bone healing process was also favorably affected by these LOX inhibitors (14, 16). Zileuton therapy improved cortical, callus and total bone volume at the osteotomy site in the tibia in ovariectomized rats (14), while a Baicalein monotherapy enhanced callus density without improving callus formation rate (16).

In the present study, we subsequently aimed to examine whether a combined therapy of Zileuton and Baicalein had an additional or interfering effect on cortical and trabecular bone in the lumbar spine and femur in an estrogen-deficient rat model. Furthermore, we elucidated the bone healing process in the tibia amongst these treatments and investigated their effects on skeletal muscle tissue. The LOX-inhibitors were applied orally to overcome the negative side effects of subcutaneous Baicalein administration (15) for a prolonged period of thirteen weeks, after the pharmacokinetics of Baicalein, orally administered in a concentration of 10 and 20 mg/kg, have been demonstrated to be reliably stable in rats by Kim et al. (17).

MATERIAL AND METHODS

Animals and Treatment

Seventy virgin female Sprague-Dawley rats (Janvier, Le Genest-Saint-Isle, France) were housed at 20°C and with a humidity of 55% in Makrolon® IV cages (Techniplast Germany GmbH, Hohenpeissenberg, Germany). The experiments were conducted after approval of the local district government and in compliance with the ethical standards of animal care (no. 14/1530).

The rats were ovariectomized at the age of 3 months, one group (n=12) was left non-ovariectomized (NON-OVX). OVX rats were randomly divided into 4 groups and treated orally according to the group assignment for up to 13 weeks. One group was ovariectomized and left untreated (OVX, n=12), while another group was ovariectomized and received oral Baicalein therapy (10 mg/kg body weight [BW], Baicalein, n=15). The Zileuton-group was ovariectomized and received 10 mg/kg BW of Zileuton (Zileuton, n=15) and the other ovariectomized group received both Baicalein and Zileuton (each 10 mg/kg BW, Baicalein+Zileuton, n=16, **Figure 1A**).

A bilateral ovariectomy was performed as described earlier (13). Briefly, the surgical procedure was carried out under isoflurane anesthesia. Accordingly, anesthesia, shaving and disinfection were followed by incision on the abdomen bilaterally and dissection of adnexa before wound closure. Immediately after OVX, treatments with Baicalein and/or Zileuton were started. A soy-free diet [ssniff® special diet; GmbH, Soest, Germany, ingredients listed in (13)] was supplemented either with Zileuton (Zyflo®; Cornerstone Therapeutics Inc., Cary, NC, USA) and/or Baicalein (98%; Sigma-Aldrich Chemie GmbH, Munich, Germany) at a concentration of 175 mg/kg food to achieve the dose of 10 mg/kg BW, respectively. This dose of Baicalein and Zileuton was shown to have an effect on bone tissue in previous studies (13–15, 18). During the experiment, all rats received soy-free diet either supplemented with Baicalein and/or Zileuton or without supplementation and demineralized water *ad libitum*.

Body weight and food intake were recorded on a weekly basis, with calculation of average daily food intake. The resulting effective dose averaged 10.35 ± 0.24 mg/kg BW in Baicalein group, 10.43 ± 0.22 mg/kg BW in Zileuton group and 10.48 ± 0.26 mg/kg BW (both) in Baicalein+Zileuton group. To ensure comparable amounts of food uptake, the individual rat weight was measured on a weekly basis (**Figures 1B, C**).

Eight weeks after OVX, a bilateral 0.5 mm osteotomy of the tibia metaphysis with consecutive 5-hole T-shaped titanium plate osteosynthesis (57-05140; Stryker Trauma, Selzach, Switzerland) was performed as described earlier (19) (**Figure 2F**). The osteotomy operation was performed under intraperitoneal anesthesia with 38 mg ketamine (Ketamin Inresa, Inresa Arzneimittel GmbH, Freiburg, Germany) and 2.5 mg midazolam (Rotexmedica GmbH, Trittau, Germany) per kg BW, respectively, along with isoflurane inhalation anesthesia (14, 19). Four rats died during osteotomy operation due to an anaesthesia side effect. After the osteotomy, rats were treated with 5 mg/kg BW Carprieve (Carprieve® 50 mgl/ml Injekt, Norbrook Labs Ltd, Newry, Northern Ireland) twice a day for 5 days. Thereafter, 16 rats died due to the perforation of the intestine and the pain therapy was interrupted. No further losses were observed. Thus, precautions should be taken by applying

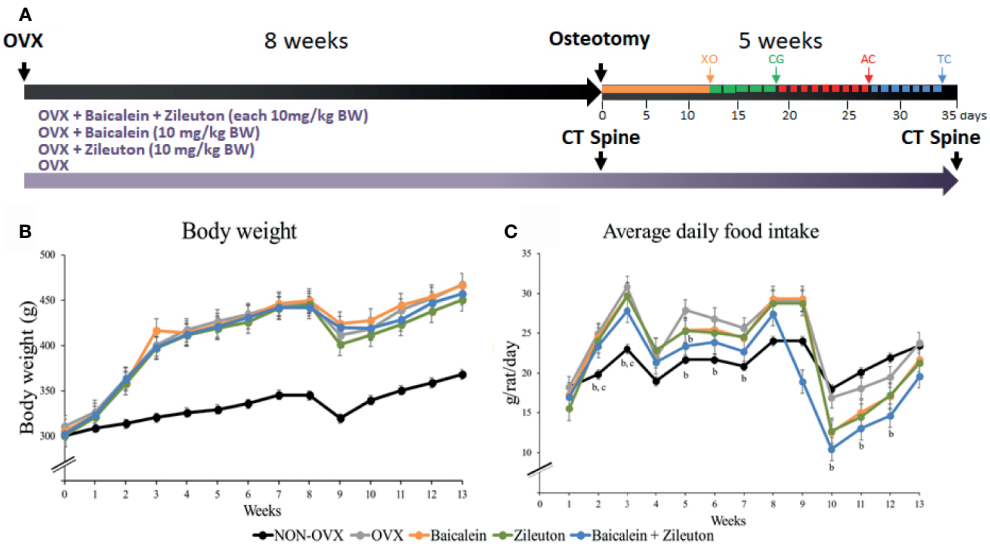

FIGURE 1 | Graphical abstract of experimental setup. **(A)** After ovariectomy, 13 weeks-treatments with either Baicalein, Zileuton or their combination were conducted. Bilateral tibia osteotomy was performed 8 weeks after OVX. *In vivo* CT of the spine was executed after 8 and 13 weeks. On day 12, xylenol orange was administered, on day 19 calcein green, on day 27 alizarin complexone, followed by tetracycline on day 33. **(B)** The body weight of rats (g). **(C)** The average daily food intake (g/rat/day). [b]Differs from OVX. [c]Differs from Baicalein.

analgesic treatments, since one of the side effects of NSAIDs is gastrointestinal damage (20). The administration of Carprieve once per day proved to be sufficient and had no severe side effects (19, 21, 22).

At the end of the experiment, the following numbers of animals were analyzed in NON-OVX group: 8, in OVX: 10, in Baicalein: 11, in Zileuton: 11 and in Baicalein+Zileuton 10.

Thirteen weeks after OVX, the rats were weighed, and decapitated after CO_2-anesthesia. The uterus weight was recorded. Forth lumbar vertebral body (L4) was isolated, stored at -20°C for micro-computed tomography (micro-CT), ashing and compression test as described earlier (13). Right femora and right osteotomized tibiae were stored at -20°C for biomechanical, ashing and micro-CT analyses (23).

In Vivo Quantitative Computed Tomography

Eight and thirteen weeks after OVX, *in vivo* pQCT of L4 was performed in isoflurane-anesthetized rats (n=5/group) using a pQCT device XCT Research SA (Stratec Medizintechnik GmbH, Pforzheim, Germany). The scans were performed in the same rats at both time points, with an exception in groups NON-OVX, OVX and Baicalein + Zileuton, where one rat in each group was replaced because of losses occurred after osteotomy. Bone mineral density (BMD, mg/cm³), total bone area (mm²) and stress-strain index (SSI) of L4 (central slice) and cross-sectional abdominal area (CSA, mm²) were measured as described in detail earlier (21). Three digital sections were analyzed for each animal. Analysis was performed using XCT-6.20C software (Stratec Medizintechnik GmbH, Pforzheim, Germany) as described earlier (13).

Biomechanical Test

Biomechanical parameters of L4, right femora and right tibiae were assessed with a Zwick machine (145,660 Z020/TND; Ulm, Germany) (22–24). The L4 was fixed at the aluminum base and the stamp was loaded to the vertebral body (compression test). The femoral head was located in a 4 mm well on the end of the plate and loaded to the trochanteric region (breaking test). The tibia was placed on the aluminum base and loaded 2-3 mm distally to the osteotomy at tuberositas tibiae (bending test). A stamp mechanically dropped with 5 mm/min onto the bone with an initial force of 1 N. After this fixing procedure, measurements were performed with an accuracy of 0.2-0.4% within 2 and 500N and recorded with the aid of testXpert software (Zwick GmbH & Co. KG, Ulm, Germany) (13). The test was finalized after the initial linear curve increase declined more than 10N in L4 and femur and more than 2N in tibia. In femur, the test was performed until fracture occurred, whereas in tibia until plastic deformation of the bone. Reported values were the highest force, that the bone could withstand (Fmax, N) and slope of linear increment of the curve (Stiffness, N/mm), calculated using Microsoft Excel (Microsoft Corporation, Redmond, WA) (13).

Micro-CT Analysis

To analyze cortical and trabecular parameters, L4, right femora and right tibiae were scanned using Quantum FX micro-CT (Caliper Sciences, Hopkinton, MA, USA). The scan protocol was as follows: 70 kVp, 200 µA, 30 Hz detector frame rate, 360° rotation, 3600 projections, 20x20 mm² field of view, 512-pixel matrix and a 40 µm resolution. A phantom block with 5 defined hydroxyapatite elements (0.2, 0.4, 0.6, 0.8 and 1.0 g/cm³) accompanied every scan to convert grey values into bone

mineral density (BMD) (16). 3D OsteoAnalyze software was used to calculate density and volume (16). Femoral region-of-interest was the head, which was cut in the transition zone from the *collum femoris* to the *trochanter major*. BV/TV, total BMD, cortical BMD (Ct.BMD), trabecular BMD (Tb.BMD), total and soft tissue volumes were measured (13, 25). Vertebral region-of-interest was the *corpus vertebra* as described earlier. Herein, we analyzed trabecular BMD (Tb.BMD), trabecular volume (Tb.V), total BMD and BV/TV (13). Tibial region-of-interest extended 1.5 mm proximally and distally from the osteotomy line (14). Analyzed values were cortical BMD (Ct.BMD), cortical volume (Ct.V), total bone BMD, total callus BMD (Cl.BMD) and osseous callus volume fraction (osseous Cl.V/total Cl.V) according to Bouxsein et al. (26). An exemplarily representation of the used thresholds with a NON-OVX rat for femur, tibia and lumbar vertebral body is shown in **Supplementary Figure 1**.

Further detailed structural analyses were performed on transformed 2D images. Three images of sagittal cut vertebral bodies, femora and tibiae were analyzed using MetaMorph Basic Acquisition Software (Leica Mikrosysteme Vertrieb GmbH, Wetzlar, Germany). Collected cortical data were thickness (Ct.Th, mm), area (Ct.Ar, mm^2) and density (Ct. Dn, %). Trabecular parameters were density (Tb.Dn, %), number of nodes (N.Nd), density of trabecular nodes (N/mm^2), trabecular thickness (Tb.Th, mm) and trabecular area (Tb.Ar, mm^2). Callus parameters were density (Cl. Dn, %) and thickness (Cl. Th, mm) (13, 14, 16).

Bone Healing Analysis

Dynamic callus formation was monitored using histological sections of right tibia stained in-vivo with fluorescent dyes: Xylenol orange (XO, 90 mg/kg BW), calcein green (CG, 10 mg/kg BW), alizarin complexone (AC, 30mg/kg BW) and tetracycline (TC, 25 mg/kg BW) were injected subcutaneously on days 12, 19, 27 and 33 after osteotomy, respectively (16) (**Figure 1A**). Briefly, tibia samples embedded in methyl methacrylate (Merck, Darmstadt, Germany) were cut longitudinally (150 µm thickness) using a diamond saw microtome (Leica SP1600, Leica Instruments GmbH, Nussloch, Germany). Subsequently, the 3 representative central sections were digitalized using a digital camera (Leica DC300F) and a zoom stereo microscope (Leica MZ75, Bensheim, Germany). The measurement area extended 2.5 mm from the osteotomy line and was divided into a ventral (plate side), dorsal (opposite side) and endosteal part. In each of these, the total callus area and labeling-specific callus areas were determined using the MetaMorph Basic Acquisition Software (Leica Mikrosysteme). XO and CG labeled callus areas were measured concurrently (XO+CG) (22).

Ashing

For analysis of mineral content, L4 and right femur were ashed at 750°C for one hour in a muffle oven. Weight before ashing (organic) and after ashing (anorganic) were recorded (13, 27).

Muscle Analysis

After sacrifice, Musculus gastrocnemius, soleus and longissimus were extracted and weighed. All muscles were frozen in liquid nitrogen and stored at -80°C for further histological analyses. Muscle from the right side were used for histological analyses. Samples were cut with a cryotome (12 µm sections,CM1900, Leica Microsystems). In Periodic acid-Schiff (PAS) stained sections, capillaries and fibers were counted manually within two 0.25 mm^2 squares at 10x resolution. The ratio of capillaries to muscle fibers was analyzed (15). In ATPase stained sections, the diameter and area of single fibers in a 0.25mm^2 square were edged (n = 90 per fiber type) and determined using the NIS-Elements AR 4.0 program (Nikon Instruments Europe, Amsterdam, Netherlands). Type I and type IIb fibers were analyzed in combination (shown as type I fibers).

Serum Analyses

After decapitation, serum samples were collected to detect levels of calcium, magnesium, phosphorus, alkaline phosphatase (Alp) activity, osteocalcin (OC) and RatLaps. The analyses were conducted at the Department of Clinical Chemistry, University of Goettingen using an Architect c16000 analyzer (Abbott, Wiesbaden, Germany) according to the manufacturer´s instructions.

OC was assessed with Rat-MID Osteocalcin EIA (Immunodiagnostic Systems [IDS], Frankfurt am Main, Germany). RatLaps was measured with RatLaps (CTX-I) EIA (IDS).

Statistics

Statistical analysis was performed with GraphPad Prism 9.0 (GraphPad Software, San Diego, CA, USA) and R 4.0.2 (The R Foundation for Statistical Computing, Vienna, Austria). Normal distribution was assessed with Anderson-Darling test. One-way analysis of variance (ANOVA, $p<0.05$) was applied to detect the impact of the treatments. Differences between the groups were estimated by Tukey's *post hoc* test with a significance level of 0.05 (95% confidence interval) ($p<0.05$). Data are presented as means and standard errors of the mean.

RESULTS

LOX Inhibition Had No Effect on Body Weight, Uterus Weight, and Food Intake

While the body weight in the beginning was equally distributed among groups, all OVX groups had higher final weight compared to NON-OVX (**Table 1** and **Figures 1B, C**). Weight of uteri was significantly lower in all OVX groups compared to NON-OVX rats (**Table 1** and **Figures 1B, C**). The treatments with LOX inhibitors affected neither body weight nor uterus weight. The daily food intake was similarly distributed among the groups at the respective week (**Figure 1C**).

Combination Therapy Increased Serum OC Levels

The serum electrolytes calcium, magnesium and phosphorus did not differ significantly between the experimental groups (**Table 1**), whereas Alp was higher in OVX compared to NON-OVX group. RatLaps showed no differences, while OC was upregulated in combination therapy compared to NON-OVX control group, indicating a higher bone formation rate.

TABLE 1 | Body weight, uterus weight, serum analyses, biomechanical and ashing analyses of bone.

	NON-OVX		OVX		Baicalein		Zileuton		Baicalein+Zileuton	
	Mean	SEM	Mean	SEM	Mean	SEM	Mean	SEM	Mean	SEM
Weight	n=8		n=10		n=11		n=11		n=10	
Body weight beginning (g)	300	4.0	310	4.5	306	3.3	300	4.6	302	4.2
Body weight end (g)	368[b-e]	7.5	467	11.8	467	7.0	451	7.9	458	15.3
Uterus weight (g)	0.57[b-e]	0.04	0.10	0.01	0.11	0.01	0.09	0.01	0.09	0.01
Biomechanics - L4	n=7		n=9		n=9		n=11		n=10	
Stiffness [N/mm]	351	28.2	298	22.5	282	18.2	339	16.6	327	19.7
Fmax [N]	326[b-e]	23.4	228	15.4	240	20.6	253	13.8	238	11.6
Femur	n=8		n=9		n=11		n=11		n=10	
Stiffness [N/mm]	387	30.3	334	19.1	324	25.8	343	24.5	299	19.9
Fmax [N]	194[b,e]	9.6	146	7.3	163	9.0	163	8.2	147	10.8
Tibia	n=7		n=10		n=11		n=11		n=9	
Stiffness [N/mm]	80	14.81	78	15.16	73	8.77	70	11.81	90	18.20
Fmax [N]	48	13.40	42	7.00	58	10.19	49	5.89	62	7.82
Serum analysis	n=8		n=10		n=11		n=11		n=10	
Calcium [mmol/l]	2.01	0.05	2.09	0.02	1.99	0.05	2.12	0.06	2.09	0.04
Magnesium [mmol/l	0.70	0.02	0.73	0.02	0.70	0.02	0.75	0.03	0.73	0.01
Phosphorus [mmol/l]	1.76	0.04	1.90	0.06	1.74	0.07	1.89	0.07	1.96	0.07
Alkaline phosphatase (Alp; U/l)	114	7.5	189[a]	15.1	154	11.8	176	22.7	157	13.7
Osteocalcin (OC; ng/ml)	116	5.0	147	11.5	177	18.0	170	19.3	211[a]	31.4
RatLaps (ng/ml)	5.47	1.22	9.48	0.91	9.69	1.64	9.70	1.84	10.67	1.77
Ashing – L4	n=8		n=10		n=11		n=11		n=10	
% organic content	67[c,d]	0.9	70	0.8	71	0.8	71	0.6	70	0.9
% anorganic content	33[c,d]	0.9	30	0.8	29	0.8	29	0.6	30	0.9
Femur	n=8		n=10		n=11		n=11		n=10	
% organic content	55[b-e]	0.7	59	0.8	58	0.8	59	0.7	61	1.3
% anorganic content	45[b-e]	0.7	41	0.8	42	0.8	41	0.7	39	1.3

[a]*Differs from NON-OVX.* [b]*Differs from OVX.* [c]*Differs from Baicalein.* [d]*Differs from Zileuton.* [e]*Differs from Baicalein+Zileuton ($p < 0.05$).*

The combination therapy increased serum OC levels but did not affect other serum parameters (**Table 1**).

The Osteoporotic Phenotype Overweighs the Effect of LOX Inhibitors In In Vivo pQCT and Biomechanical Measurements

At both time points, before osteotomy (8 weeks after OVX) and at the end of the experiment, CSA was significantly higher in all OVX rats compared to NON-OVX irrespective of the treatments (**Table 2**). BMD of L4 was significantly lower in Baicalein- and Zileuton-treated groups after 8 weeks compared to NON-OVX (**Table 2**), whereas, at the end, all OVX groups showed lower BMD than NON-OVX rats (**Table 2**). The SSI was significantly higher in Zileuton compared to the OVX group (**Table 2**), while in other 3 OVX groups SSI was lower than in NON-OVX group at week 8 after OVX. At the end of the study, only the Baicalein group did not differ from NON-OVX, whereas SSI in the other OVX groups was significantly lower than in NON-OVX (**Table 2**).

The biomechanical analysis showed a reduction of Fmax in all OVX groups in vertebra and femur, but not of Fmax or stiffness in tibia, where no differences occurred (**Table 1**).

Zileuton Ameliorated Trabecular Bone in L4, While Zileuton and Combined Therapies Deteriorated Trabecular Properties in the Femur

In L4, trabecular BMD, total BMD and BV/TV were reduced in all OVX groups irrespectively of the treatment (**Table 3**). In the femur, BV/TV was reduced in all OVX groups compared with the NON-OVX group (**Table 3**), whereas trabecular BMD was impaired in Baicalein and Baicalein+Zileuton groups and total BMD in OVX and Zileuton groups (**Table 3**). Summarizing, the micro-CT 3D analysis demonstrated a consistent effect of the ovariectomy in all treatment groups.

Micro-CT 2D analysis revealed an improvement in L4 Tb.Dn, N.Nd and Tb.Th as well as Tb.Ar in Zileuton group compared to the OVX group in which an overall reduction of these parameters were observed compared to NON-OVX (**Table 3**). The cortical density was impaired in Zileuton and combination therapy in L4 (**Table 3**). In the femur, Zileuton and combination therapy led to reduced Tb.Dn and N.Nd compared to NON-OVX and OVX groups (**Table 3**), while the combination therapy significantly reduced Tb.Th, Tb.Ar and Ct.Dn (**Table 3**).

Taken together, sole treatment with Baicalein, did not change trabecular or cortical parameters compared to OVX (**Table 3**). The ovariectomy-induced negative effect on trabecular parameters could be rescued by Zileuton only therapy in L4, but in the femur the effect was contrary. The combination therapy had no effect on bone in L4, while in the femur, the diminishing effect of Zileuton remained after the addition of Baicalein.

Organic Content Is Raised by Baicalein and Zileuton Therapies in L4

The organic content of L4 was significantly higher and, correspondingly, the anorganic content lower in Baicalein- and

TABLE 2 | L4, *in vivo* pQCT.

	NON-OVX (n=5)		OVX (n=5)		Baicalein (n=5)		Zileuton (n=5)		Baicalein+Zileuton (n=5)	
	Mean	**SEM**	**Mean**	**SEM**	**Mean**	**SEM**	**Mean**	**SEM**	**Mean**	**SEM**
CSA (mm²)										
8 w after OVX	1886[b-e]	39.73	2306	39.91	2381	78.71	2380	32.38	2321	50.23
13 w after OVX	1866 [b-e]	25.63	2284	58.66	2256	22.47	2438	41.57	2424	47.05
BMD L4 (mg/cm³)										
8 w after OVX	585.0[c,d]	6.9	551.2	10.3	531.5	9.1	536.1	12.4	547.5	9.1
13 w after OVX	554.8[b-e]	7.8	511.9	7.8	505.2	5.6	502.2	7.7	506.5	8.4
SSI L4										
8w after OVX	19.91[b,c,e]	0.75	15.59[d]	0.32	15.84	0.38	18.43	0.82	16.79	0.58
13w after OVX	18.21[b,d,e]	0.73	14.94	0.74	16.91	1.06	14.71	0.47	14.61	0.55

[b]Differs from OVX. [c]Differs from Baicalein. [d]Differs from Zileuton. [e]Differs from Baicalein+Zileuton ($p < 0.05$).

Zileuton only treated groups than in the NON-OVX group (**Table 1**). Organic content of femora was detected to be lower in the NON-OVX group than in all other groups, while the anorganic weight showed the opposite results (**Table 1**).

Baicalein Accelerated Mid-Stage Callus Formation, While Zileuton and Combination Therapies Improved Cortical Parameters in the Tibia

Analyses of fluorochrome stained sections of the tibia (**Figure 2E**) revealed no differences in the time of the first osseous bridging of osteotomized bone ends (mean: 24 ± 1 day after osteotomy). The late ventral callus area (28-33d after osteotomy, TC staining) was significantly larger in NON-OVX animals compared to all other treatment groups (**Figure 2A**). Moreover, the late dorsal callus area was larger in NON-OVX compared to Zileuton and combination therapy groups (**Figure 2B**). Baicalein led to a larger midtime area (20-27d after osteotomy, AC staining) of dorsal callus area compared to the OVX group. Midtime endosteal callus area (AC, **Figure 2C**) and total callus area (**Figure 2D**) were larger in the Baicalein group than in the combination therapy group. The late total callus area (TC staining) in the NON-OVX group exceeded the OVX group (**Figure 2D**).

TABLE 3 | micro-CT of L4, femora and tibiae, 3D and 2D analyses.

	NON-OVX		OVX		Baicalein		Zileuton		Baicalein+Zileuton	
	Mean	**SEM**	**Mean**	**SEM**	**Mean**	**SEM**	**Mean**	**SEM**	**Mean**	**SEM**
L4, 3D	n=8		n=10		n=10		n=11		n=10	
Tb. BMD (g/cm³)	0.634[b-e]	0.004	0.611	0.002	0.609	0.003	0.614	0.002	0.607	0.001
Total BMD (g/cm³)	0.606[b-e]	0.013	0.509	0.011	0.496	0.013	0.519	0.011	0.481	0.007
BV/TV (%)	70.67[b-e]	1.02	59.40	1.09	59.15	1.24	62.02	1.11	58.27	0.85
L4,2D	n=8		n=10		n=10		n=11		n=10	
Tb.Dn (%)	44.18[b-e]	1.126	26.37	0.6563	26.66	0.8595	31.44[b,c,e]	0.9328	27.86	0.7008
N.Nd (n)	40.63[b-e]	1.508	31.53	0.8033	29.70	1.387	34.79[b,c]	0.9342	32.52	0.9605
Tb.Th (mm)	0.25[b-e]	0.01	0.13[d]	0.01	0.14	0.01	0.17	0.01	0.15	0.01
Tb.Ar (mm²)	7.45[b-e]	0.23	4.84	0.11	4.80	0.17	5.85[b,c,e]	0.21	5.12	0.13
Ct.Dn (%)	94.43[d,e]	0.77	90.99	0.49	91.62	0.60	87.48	2.70	86.86	0.65
Femur, 3D	n=8		n=10		n=11		n=11		n=10	
Tb. BMD (g/cm³)	0.871[c,e]	0.006	0.854	0.003	0.848	0.007	0.852	0.004	0.849	0.004
Total BMD (g/cm³)	0.822[b,d]	0.021	0.663	0.017	0.726	0.029	0.695	0.026	0.690	0.014
BV/TV (%)	76.46[b-e]	1.68	60.65	2.46	65.27	2.49	65.53	2.38	64.09	1.22
Femur, 2D	n=8		n=10		n=11		n=11		n=10	
Tb.Dn (%)	49.18[b-e]	2.323	32.30[d,e]	1.995	29.96[e]	1.616	23.79	1.372	21.63	1.177
N.Nd (n)	73.54[b-e]	2.44	38.40[d,e]	2.71	32.87	2.32	30.18	1.55	20.52[c,d]	0.92
Tb.Th (µm)	121[b-e]	5.8	89	2.4	86	2.4	81	1.5	74[b,c]	1.4
Tb.Ar (mm²)	5.75[b-e]	0.18	3.67[c-e]	0.20	2.97	0.15	2.95	0.11	2.27[c,d]	0.09
Ct.Dn (%)	97.49	0.24	97.20	0.26	96.51	0.43	96.71	0.30	95.19[a,b,d]	0.52
Tibia, 3D	n=7		n=10		n=10		n=10		n=10	
Ct. BMD (g/cm³)	1.116[d,e]	0.034	1.083[d,e]	0.030	1.158	0.025	1.210	0.008	1.214	0.007
Ct.V (mm³)	20.40	5.158	14.43[d,e]	4.243	27.52	4.168	34.84	1.550	29.03	1.680
Total bone BMD (g/cm³)	0.585	0.025	0.519	0.024	0.522	0.018	0.532	0.021	0.496	0.019
Cl. BMD (g/cm³)	0.392[b-e]	0.012	0.326	0.017	0.333	0.005	0.331	0.007	0.327	0.012
Osseous Cl.V/Total Cl.V BV/TV	66.30[b,e]	2.19	57.67	2.534	59.18	1.09	59.16	1.50	55.98	1.77

[a]Differs from NON-OVX. [b]Differs from OVX. [c]Differs from Baicalein. [d]Differs from Zileuton. [e]Differs from Baicalein+Zileuton ($p < 0.05$).

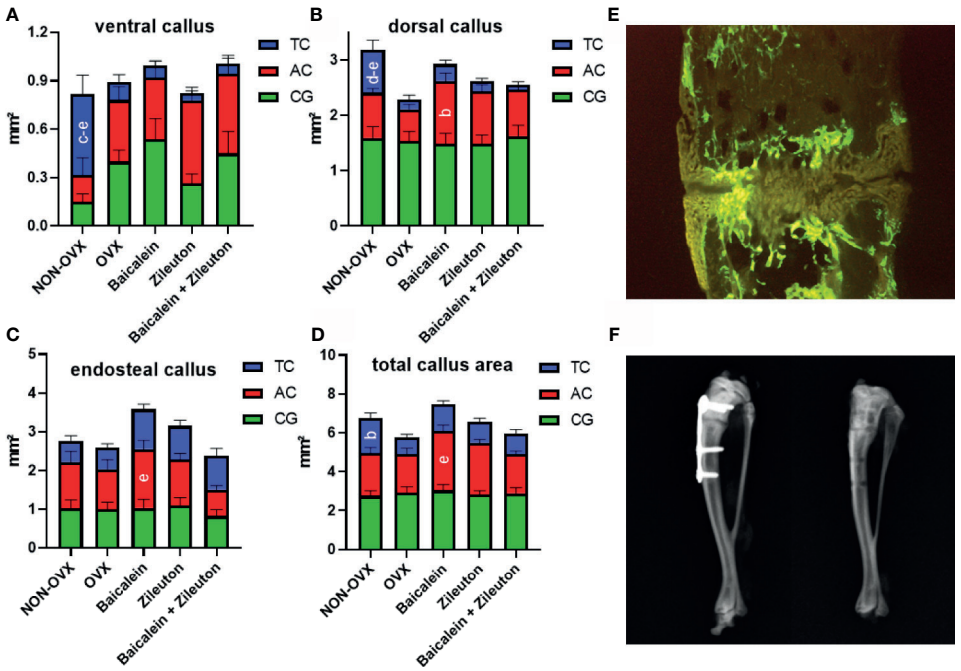

FIGURE 2 | Tibia healing analysis. Ventral callus area **(A)**, dorsal callus area **(B)**, endosteal callus area **(C)** and total callus area **(D)** stained with fluorochromes XO+CG (0-19d after osteotomy), AC (20-27d after osteotomy) and TC (28-33d after osteotomy) and measured on histological sections **(E)**. X-rays prove the correct positioning of the plate after tibial osteotomy and healing is confirmed after plate removal **(F)**. [NON-OVX: n=8; OVX: n=10; Baicalein: n=9; Zileuton: n=11; Baicalein + Zileuton: n=11 (3 histological sections per animal)]. [b]Differs from OVX. [c]Differs from Baicalein. [d]Differs from Zileuton. [e]Differs from Baicalein+Zileuton ($p < 0.05$).

Micro-CT 3D analysis showed enhanced Ct. BMD and Ct.V in the tibia in both Zileuton and combination therapy groups (**Table 3**), while total Cl. BMD was reduced in all OVX groups (**Table 3**). The osseous callus volume fraction, however, was lowest in the combination therapy group (**Table 3**), while total bone BMD did not differ among the groups (**Table 3**).

Summarizing, Baicalein treatment resulted in enhanced endosteal and total callus area compared to combination therapy and increased dorsal callus area compared to the OVX group. The cortical parameters in the tibia were enhanced by Zileuton and combination therapy compared to OVX.

Combination Therapy Enhanced Capillary Ratio in M. Gastrocnemius

In Musculus gastrocnemius, soleus and longissimus neither diameter nor area of muscle fibers differed significantly among treatment groups (**Table 4**). The combination therapy in M. gastrocnemius led to a higher capillary ratio compared to NON-OVX and OVX groups, which was not noticeable in M. longissimus and M. soleus (**Table 4**).

DISCUSSION

Osteoporosis as a systemic disease is manifested on both cortical and trabecular bone. The detection of osteoporosis as well as the therapeutic success are closely connected to the structural changes in spine and proximal femur (28, 29). Due to an aging society, an increasing socioeconomic relevance is attributed to this "silent disease" and the need for new therapeutic approaches is evident (5, 30, 31). Recently, we have reported promising results of sole Baicalein and Zileuton treatments on osteoporotic bone tissue (13, 14, 16), though some undesirable side-effects resulted from subcutaneous administration of the former. We subsequently decided on an oral administration of both LOX inhibitors. A oral administration of Baicalein in a dose of 10mg/kg per day exhibited inhibitory effects in a xenograft experiment in mice (32), while in a rat experiment, an oral dose of 10 and 20mg/kg Baicalein led to a stable concentration of its active metabolite, Baicalin, in the rat plasma (17).

In the present study, we investigated the effect of a combined treatment of Baicalein and Zileuton as well as single treatments of these substances on lumbar vertebral body and femur, and on bone healing in the osteotomized tibia as well as on the skeletal muscle in an ovariectomized rat model of postmenopausal osteoporosis (13, 22). Effects of the LOX inhibitors on body weight, uterus weight or food intake were ruled out since the treatments did not lead to differences in these compared to the OVX group. We did not detect effects of these substances on the whole body composition in our previous studies either (13, 16, 19).

TABLE 4 | Histological analyses of M. Gastrocnemius (MG), M. Longissimus (ML) and M. Soleus (MS).

	NON-OVX (n=8)		OVX (n=10)		Baicalein (n=10)		Zileuton (n=11)		Baicalein+Zileuton (n=10)	
	Mean	SEM	Mean	SEM	Mean	SEM	Mean	SEM	Mean	SEM
MG, type I										
Diameter (µm)	48.91	2.76	50.91	1.79	51.42	1.22	50.25	1.75	50.01	1.72
Area (µm²)	1939	222	2094	135	2094	101	2048	148	2034	135
MG, type IIa										
Diameter (µm)	71.84	2.54	76.42	2.25	77.17	2.38	73.29	1.28	72.78	2.44
Area (µm²)	4153	309	4699	277	4790	289	4285	154	4098	319
MG, capillarization										
Capillary/Fiber	1.22	0.05	1.27	0.04	1.45	0.075	1.39	0.077	1.67[a,b]	0.10
ML, type I										
Diameter (µm)	56.64	1.83	56.84	1.16	54.46	1.94	57.16	1.25	54.55	2.21
Area (µm²)	2619	168	2606	109	2390	176	2610	117	2372	183
ML, type IIa										
Diameter (µm)	82.81	0.84	88.71	1.86	81.90	3.18	84.99	1.62	83.32	3.09
Area (µm²)	5442	115	6248	317	5387	412	5725	230	5551	407
ML, capillarization										
Capillary/Fiber	1.15	0.09	1.38	0.07	1.46	0.08	1.42	0.07	1.38	0.08
MS, type I										
Diameter (µm)	68.39	1.33	66.93	2.48	67.50	1.34	67.73	1.50	66.90	0.73
Area (µm²)	3733	145.9	3604	287.5	3628	146.9	3665	168.5	3554	76.18
MS, capillarization										
Capillary/Fiber	1.57	0.06	1.81	0.08	1.57	0.06	1.59	0.07	1.71	0.11

[a]*Differs from NON-OVX.* [b]*Differs from OVX.*

Previously, we detected favorable effects on the capillarization of muscle after subcutaneous injection of Baicalein (15) and oral administration of Zileuton (unpublished data) for up to 4-5 weeks. In the present study, the effect was less pronounced. Solely the combination therapy increased capillarization in M. gastrocnemius. One reason might be that the muscular effect is short-lasting, leading to detectable effects after short-term treatments [as in our previous study (15)], but diminishing due to adaption after 13 weeks. Another possible reason might root in the time of administration. In this study, the LOX inhibitors were applied as preventive treatments, immediately after OVX, whereas previously they were applied 8 weeks after OVX when changes in the musculoskeletal system due to hormone deficiency had already manifested (33).

In our *in vivo* pQCT, no effect of LOX inhibitors was observed on CSA. The combination therapy did not change SSI of L4, whereas Zileuton-treatment showed higher SSI than that in the OVX group after an 8 week treatment, which is comparable to our previous 5 week treatment (13). The oral route of administration for Baicalein was demonstrated to be safe, however it showed no effect on BMD and SSI in the *in vivo* pQCT analyses. The micro-CT 3D analysis revealed no effect of either therapy on bone parameters, whereas the 2D analysis illustrated a beneficial effect of Zileuton on trabecular bone parameters in the lumbar spine. Thus, the previously reported trabecular accentuated effects of Zileuton on the vertebra (13) could again be confirmed after the longer treatment regimen for 13 weeks in this study. In contrast to these findings in L4, the trabecular bone was impaired in femur after Zileuton and combination treatments. Furthermore, the cortical bone lost its density after these treatments in L4, too. After a short-term application, the Zileuton treatment caused an increase of bone volume in the femur, whereas femoral density was reduced (14). An oral Baicalein treatment did not change parameters measured by micro-CT in the present study. Hence, we supported our previous findings of Zileuton being favorable in trabecular bone in spine and unfavorable in femur (13), while Baicalein did not show any effect on bone and did not reduce the negative effect of Zileuton in the combination therapy in femur.

Proximal femur fractures, which occur commonly in the aged people, constitute a devastating diagnosis with 1-year mortality rates of up to 36%, regularly indicating missed anti-osteoporotic therapy (34). The previously reported effects of Baicalein were sparse (16), while cortical volume in the distal femur was significantly ameliorated after Zileuton-therapy in a dose of 10mg/kg BW (14). Three-dimensional analysis of femoral head confirmed weak effects of Baicalein. The advantage of Zileuton on cortical volume was not consistent after prolonged therapy in our study. The combination therapy, however, reduced Tb.Th and Ct.Dn substantially. All of these findings put the combination therapy in an unfavorable light.

In our bone healing analysis, a favorable effect of sole Baicalein therapy was detected in the dorsal callus area, mostly in the midterm healing period. Indeed, the main effect of both Baicalein and Zileuton as their combination therapy on ventral and dorsal callus formation was observed within 20 and 33 days after osteotomy. In a former study, we could detect an impairment of early callus formation after subcutaneous Baicalein administration (16). The oral treatment with either Baicalein, Zileuton or both in the current study showed a reduction in these groups in the late ventral callus formation, whereas the cortical parameters were improved after Zileuton

und combination therapies at the osteotomy site. Contrary to our descriptions of a partial deterioration of fracture healing *via* pharmacological lipoxygenase-inhibition, the positive effect of a lipoxygenase knockout on fracture healing was demonstrated in a *5-LO*(KO) mouse model by Manigrasso et al. (29). In their knockout model, the authors observed enhanced healing with substantially better mechanical properties of the newly formed bone compared to wild type mice (35).

However, the exact underlying molecular mechanism of Baicalein's mode of action is not understood in detail. Several key enzymes like *5-*, *12-* and *15-LOX* are inhibited next to cyclooxygenases (*COX 1* and *2*), resulting in reduced synthesis of prostaglandins (36, 37). Intriguingly, both Zileuton and Baicalein have been demonstrated to inhibit stress-mediated 5-LOX metabolite (cysteinyl leukotrienes) production, which may be a reason for the lack of synergistic effects in our study (36). Besides, Baicalein was demonstrated to inhibit parathormone (PTH)-induced DNA synthesis and cytokines like *IL-6* and *TNF-α* (38, 39). Further stimulating osteoblast differentiation, the induction of *NF-κB* and *nuclear factor of activated T-cells, cytoplasmic 1* (*NFATc1*) as well as the induction of osteoclast apoptosis have been described, resulting in an overall osteogenic effect (40, 41). In our previous study, we speculated that Baicalein had an antioxidative effect next to osteoclast apoptosis (via Wnt/β-catenin pathway) and radical-scavenging effect (16). The main effect of Zileuton is created *via 5-LOX* inhibition. While *in vivo* data show modulation of cytokine release and reduced osteoclast differentiation (42), additionally giving rise to osteoanabolic reactions, our own analysis showed an upregulation of *osteocalcin* and *Alp* in the serum (14, 42). Despite the bone healing analyses showed no sweeping effects of Zileuton and combination therapy on callus density, callus area and cortical bone (Ct.BMD and Ct.V), the healed cortical tibia (Ct.BMD, Ct.V) was favorably affected by these treatments. A connecting role may be attributed to the raised serum levels of *osteocalcin* which we measured in combination therapy. These have been similarly described after 5-LOX inhibition elsewhere (16, 43).

CONCLUSION

Summarizing, the spinal trabecular bone was improved by Zileuton, but not by combination therapy, which is even in disfavor for Tb.BMD, BV/TV and Ct.Dn. The analysis of the clinically crucial proximal femur could not show the expected ameliorative influence of LOX inhibitors, but instead clarified plain negative consequences of combined therapy of Baicalein and Zileuton on cortical and trabecular bone. The oral administration of Baicalein - despite a longer therapy period – did not lead to the same beneficial cortical effects as described earlier (16). Though the dynamic bone healing process was favorably affected by all LOX inhibitor treatments, their overall effect on bone healing was minor. Furthermore, inhibition of LOX did not have a profound benefit on the skeletal muscle.

Taken together, our data showed no perspective of both lipoxygenase inhibitors neither alone or in combination for the musculoskeletal system in estrogen deficient rats and particularly not as a preventive treatment of osteoporosis.

Limitations

The oral administration of Baicalein instead of the previously reported subcutaneous administration - due to reported negative side effects - might have affected the results (15). The lack of assessment of metabolic parameters in our rat model yet limits the mechanistic insights of Baicalein and Zileuton action.

DATA AVAILABILITY STATEMENT

The raw data supporting the conclusions of this article will be made available by the authors, without undue reservation.

ETHICS STATEMENT

The animal study was reviewed and approved by the the local district government (Oldenburg, Germany) and in compliance with the ethical standards of animal care.

AUTHOR CONTRIBUTIONS

MK and SS designed the study. FH, MF, IM, and ST performed all experimental procedures. Data analysis was carried out by DS and MK. DS wrote the manuscript with the help of MK. DS, FH, MF, IM, ST, PR, SS, and MK critically revised it for important intellectual content. All authors contributed to the article and approved the submitted version.

FUNDING

DS was funded by the Deutsche Forschungsgemeinschaft (DFG, German Research Foundation) – 413501650. We thank the Elsbeth Bonhoff Stiftung for financial support (Grant N114).

ACKNOWLEDGMENTS

The authors thank R. Castro-Machguth,A. Witt and R. Wigger for technical support.

SUPPLEMENTARY MATERIAL

The Supplementary Material for this article can be found online at: https://www.frontiersin.org/articles/10.3389/fendo.2021.706504/full#supplementary-material

REFERENCES

1. Reginster J-Y, Burlet N. Osteoporosis: A Still Increasing Prevalence. *Bone* (2006) 38:S4–9. doi: 10.1016/j.bone.2005.11.024
2. Watts NB, Bilezikian JP, Camacho PM, Greenspan SL, Harris ST, Hodgson SF, et al. American Association of Clinical Endocrinologists Medical Guidelines for Clinical Practice for the Diagnosis and Treatment of Postmenopausal Osteoporosis. *Endocr Pract* (2010) 16(Suppl 3):1–37. doi: 10.4158/EP.16.S3.1
3. Hansen D, Bazell C, Pelizzari P, Pyenson B. Medicare Cost of Osteoporotic Fractures: The Clinical and Cost Burden of an Important Consequence of Osteoporosis (2020). Available at: https://static1.squarespace.com/static/5c0860aff793924efe2230f3/t/5d76b949deb7e9086ee3d7dd/1568061771769/Medicare+Cost+of+Osteoporotic+Fractures+20190827.pdf. (Accessed March 08, 2021).
4. Brown C. Osteoporosis: Staying Strong. *Nature* (2017) 550:S15–7. doi: 10.1038/550S15a
5. Makras P, Delaroudis S, Anastasilakis AD. Novel Therapies for Osteoporosis. *Metabolism* (2015) 64:1199–214. doi: 10.1016/j.metabol.2015.07.011
6. Cosman F, Crittenden DB, Adachi JD, Binkley N, Czerwinski E, Ferrari S, et al. Romosozumab Treatment in Postmenopausal Women With Osteoporosis. *N Engl J Med* (2016) 375:1532–43. doi: 10.1056/NEJMoa1607948
7. Cummings SR, San Martin J, McClung MR, Siris ES, Eastell R, Reid IR, et al. Denosumab for Prevention of Fractures in Postmenopausal Women With Osteoporosis. *N Engl J Med* (2009) 361:756–65. doi: 10.1056/NEJMoa0809493
8. Kang J-H, Ting Z, Moon M, Sim J-S, Lee J-M, Doh K-E, et al. 5-Lipoxygenase Inhibitors Suppress RANKL-Induced Osteoclast Formation *Via* NFATc1 Expression. *Bioorg Med Chem* (2015) 23:7069–78. doi: 10.1016/j.bmc.2015.09.025
9. Cottrell JA, Keshav V, Mitchell A, O'Connor JP. Local Inhibition of 5-Lipoxygenase Enhances Bone Formation in a Rat Model. *Bone Joint Res* (2013) 2:41–50. doi: 10.1302/2046-3758.22.2000066
10. Kang KA, Zhang R, Piao MJ, Chae S, Kim HS, Park JH, et al. Baicalein Inhibits Oxidative Stress-Induced Cellular Damage *Via* Antioxidant Effects. *Toxicol Ind Health* (2012) 28:412–21. doi: 10.1177/0748233711413799
11. Wu Q-Q, Deng W, Xiao Y, Chen J-J, Liu C, Wang J, et al. The 5-Lipoxygenase Inhibitor Zileuton Protects Pressure Overload-Induced Cardiac Remodeling *Via* Activating PPARα. *Oxid Med Cell Longev* (2019) 2019:7536803. doi: 10.1155/2019/7536803
12. Shi L, Hao Z, Zhang S, Wei M, Lu B, Wang Z, et al. Baicalein and Baicalin Alleviate Acetaminophen-Induced Liver Injury by Activating Nrf2 Antioxidative Pathway: The Involvement of ERK1/2 and PKC. *Biochem Pharmacol* (2018) 150:9–23. doi: 10.1016/j.bcp.2018.01.026
13. Saul D, Gleitz S, Nguyen HH, Kosinsky RL, Sehmisch S, Hoffmann DB, et al. Effect of the Lipoxygenase-Inhibitors Baicalein and Zileuton on the Vertebra in Ovariectomized Rats. *Bone* (2017) 101:134–44. doi: 10.1016/j.bone.2017.04.011
14. Saul D, Ninkovic M, Komrakova M, Wolff L, Simka P, Gasimov T, et al. Effect of Zileuton on Osteoporotic Bone and its Healing, Expression of Bone, and Brain Genes in Rats. *J Appl Physiol (Bethesda Md 1985)* (2018) 124:118–30. doi: 10.1152/japplphysiol.01126.2016
15. Saul D, Kling JH, Kosinsky RL, Hoffmann DB, Komrakova M, Wicke M, et al. Effect of the Lipoxygenase Inhibitor Baicalein on Muscles in Ovariectomized Rats. *J Nutr Metab* (2016) 2016:3703216. doi: 10.1155/2016/3703216
16. Saul D, Weber M, Zimmermann MH, Kosinsky RL, Hoffmann DB, Menger B, et al. Effect of the Lipoxygenase Inhibitor Baicalein on Bone Tissue and Bone Healing in Ovariectomized Rats. *Nutr Metab* (2019) 16:4. doi: 10.1186/s12986-018-0327-2
17. Kim YH, Jeong DW, Kim Y-C, Sohn DH, Park E-S, Lee HS. Pharmacokinetics of Baicalein, Baicalin and Wogonin After Oral Administration of a Standardized Extract of Scutellaria Baicalensis, PF-2405 in Rats. *Arch Pharm Res* (2007) 30:260–5. doi: 10.1007/BF02977703
18. Kim DH, Hossain MA, Kang YJ, Jang JY, Lee YJ, Im E, et al. Baicalein, an Active Component of Scutellaria Baicalensis Georgi, Induces Apoptosis in Human Colon Cancer Cells and Prevents AOM/DSS-induced Colon Cancer in Mice. *Int J Oncol* (2013) 43:1652–8. doi: 10.3892/ijo.2013.2086
19. Komrakova M, Fiebig J, Hoffmann DB, Krischek C, Lehmann W, Stuermer KM, et al. The Advantages of Bilateral Osteotomy Over Unilateral Osteotomy for Osteoporotic Bone Healing. *Calcif Tissue Int* (2018) 103:80–94. doi: 10.1007/s00223-018-0392-6
20. Smolinske SC, Hall AH, Vandenberg SA, Spoerke DG, McBride PV. Toxic Effects of Nonsteroidal Anti-Inflammatory Drugs in Overdose. An Overview of Recent Evidence on Clinical Effects and Dose-Response Relationships. *Drug Saf* (1990) 5:252–74. doi: 10.2165/00002018-199005040-00003
21. Komrakova M, Hoffmann DB, Nuehnen V, Stueber H, Wassmann M, Wicke M, et al. The Effect of Vibration Treatments Combined With Teriparatide or Strontium Ranelate on Bone Healing and Muscle in Ovariectomized Rats. *Calcif Tissue Int* (2016) 99:408–22. doi: 10.1007/s00223-016-0156-0
22. Komrakova M, Weidemann A, Dullin C, Ebert J, Tezval M, Stuermer KM, et al. The Impact of Strontium Ranelate on Metaphyseal Bone Healing in Ovariectomized Rats. *Calcif Tissue Int* (2015) 97:391–401. doi: 10.1007/s00223-015-0019-0
23. Tezval M, Stuermer EK, Sehmisch S, Rack T, Stary A, Stebener M, et al. Improvement of Trochanteric Bone Quality in an Osteoporosis Model After Short-Term Treatment With Parathyroid Hormone: A New Mechanical Test for Trochanteric Region of Rat Femur. *Osteoporos Int* (2010) 21:251–61. doi: 10.1007/s00198-009-0941-y
24. Sehmisch S, Erren M, Rack T, Tezval M, Seidlova-Wuttke D, Richter J, et al. Short-Term Effects of Parathyroid Hormone on Rat Lumbar Vertebrae. *Spine* (2009) 34:2014–21. doi: 10.1097/BRS.0b013e3181afe846
25. Parfitt AM, Drezner MK, Glorieux FH, Kanis JA, Malluche H, Meunier PJ, et al. Bone Histomorphometry: Standardization of Nomenclature, Symbols, and Units. Report of the ASBMR Histomorphometry Nomenclature Committee. *J Bone Miner Res* (1987) 2:595–610. doi: 10.1002/jbmr.5650020617
26. Bouxsein ML, Boyd SK, Christiansen BA, Guldberg RE, Jepsen KJ, Müller R. Guidelines for Assessment of Bone Microstructure in Rodents Using Micro-Computed Tomography. *J Bone Miner Res* (2010) 25:1468–86. doi: 10.1002/jbmr.141
27. Komrakova M, Stuermer EK, Sturm A, Schmelz U, Tezval M, Stuermer KM, et al. Efficiency of 48h vs. 24h Injection of Parathyroid Hormone for Amelioration of Osteopenic Spine Properties in Male Rats. *Open Bone J* (2012) 4:20–6. doi: 10.2174/1876525401204010020
28. Siris ES, Adler R, Bilezikian J, Bolognese M, Dawson-Hughes B, Favus MJ, et al. The Clinical Diagnosis of Osteoporosis: A Position Statement From the National Bone Health Alliance Working Group. *Osteoporos Int* (2014) 25:1439–43. doi: 10.1007/s00198-014-2655-z
29. Wright NC, Saag KG, Dawson-Hughes B, Khosla S, Siris ES. The Impact of the New National Bone Health Alliance (NBHA) Diagnostic Criteria on the Prevalence of Osteoporosis in the USA. *Osteoporos Int* (2017) 28:1225–32. doi: 10.1007/s00198-016-3865-3
30. Rachner TD, Khosla S, Hofbauer LC. Osteoporosis: Now and the Future. *Lancet (London England)* (2011) 377:1276–87. doi: 10.1016/S0140-6736(10)62349-5
31. Watts NB, Bilezikian JP. Advances in Target-Specific Therapy for Osteoporosis. *J Clin Endocrinol Metab* (2014) 99:1149–51. doi: 10.1210/jc.2014-1065
32. Miocinovic R, McCabe N, Keck RW, Jankun J, Hampton JA, Selman SH. *In Vivo* and *In Vitro* Effect of Baicalein on Human Prostate Cancer Cells. *Int J Oncol* (2005) 26(1):241–6. doi: 10.3892/ijo.26.1.241
33. Yousefzadeh N, Kashfi K, Jeddi S, Ghasemi A. Ovariectomized Rat Model of Osteoporosis: A Practical Guide. *EXCLI J* (2020) 19:89–107. doi: 10.17179/excli2019-1990
34. Bhandari M, Swiontkowski M. Management of Acute Hip Fracture. *N Engl J Med* (2017) 377:2053–62. doi: 10.1056/NEJMcp1611090
35. Manigrasso MB, O'Connor JP. Accelerated Fracture Healing in Mice Lacking the 5-Lipoxygenase Gene. *Acta Orthop* (2010) 81:748–55. doi: 10.3109/17453674.2010.533931
36. Li C, Zhang W, Fang S, Lu Y, Zhang L, Qi L, et al. Baicalin Attenuates Oxygen-Glucose Deprivation-Induced Injury by Inhibiting Oxidative Stress-Mediated 5-Lipoxygenase Activation in PC12 Cells. *Acta Pharmacol Sin* (2010) 31:137–44. doi: 10.1038/aps.2009.196
37. Chen S. Natural Products Triggering Biological Targets–a Review of the Anti-Inflammatory Phytochemicals Targeting the Arachidonic Acid Pathway in Allergy Asthma and Rheumatoid Arthritis. *Curr Drug Targets* (2011) 12:288–301. doi: 10.2174/138945011794815347

38. Somjen D, Tordjman K, Katzburg S, Knoll E, Sharon O, Limor R, et al. Lipoxygenase Metabolites are Mediators of PTH-Dependent Human Osteoblast Growth. *Bone* (2008) 42:491–7. doi: 10.1016/j.bone.2007.11.005
39. Hu S, Chen Y, Wang Z-F, Mao-Ying Q-L, Mi W-L, Jiang J-W, et al. The Analgesic and Antineuroinflammatory Effect of Baicalein in Cancer-Induced Bone Pain. *Evid Based Complement Altern Med* (2015) 2015:973524. doi: 10.1155/2015/973524
40. Kim JM, Lee S-U, Kim YS, Min YK, Kim SH. Baicalein Stimulates Osteoblast Differentiation *Via* Coordinating Activation of MAP Kinases and Transcription Factors. *J Cell Biochem* (2008) 104:1906–17. doi: 10.1002/jcb.21760
41. Kim MH, Ryu SY, Bae MA, Choi J-S, Min YK, Kim SH. Baicalein Inhibits Osteoclast Differentiation and Induces Mature Osteoclast Apoptosis. *Food Chem Toxicol* (2008) 46:3375–82. doi: 10.1016/j.fct.2008.08.016
42. Moura AP, Taddei SR, Queiroz-Junior CM, Madeira MF, Rodrigues LF, Garlet GP, et al. The Relevance of Leukotrienes for Bone Resorption Induced by Mechanical Loading. *Bone* (2014) 69:133–8. doi: 10.1016/j.bone.2014.09.019
43. Cottrell JA, O'Connor JP. Pharmacological Inhibition of 5-Lipoxygenase Accelerates and Enhances Fracture-Healing. *J Bone Joint Surg Am* (2009) 91:2653–65. doi: 10.2106/JBJS.H.01844

Conflict of Interest: The authors declare that the research was conducted in the absence of any commercial or financial relationships that could be construed as a potential conflict of interest.

frontiers in Endocrinology

REVIEW
published: 06 August 2021
doi: 10.3389/fendo.2021.705499

Update on the Role of Neuropeptide Y and Other Related Factors in Breast Cancer and Osteoporosis

Shu-ting Lin[1], Yi-zhong Li[2], Xiao-qi Sun[1], Qian-qian Chen[1], Shun-fa Huang[1], Shu Lin[3,4] and Si-qing Cai[1]**

[1] Department of Radiology, The Second Affiliated Hospital of Fujian Medical University, Quanzhou, China, [2] Department of Bone, The Second Affiliated Hospital of Fujian Medical University, Quanzhou, China, [3] Centre of Neurological and Metabolic Research, The Second Affiliated Hospital of Fujian Medical University, Quanzhou, China, [4] Diabetes and Metabolism Division, Garvan Institute of Medical Research, Sydney, NSW, Australia

Breast cancer and osteoporosis are common diseases that affect the survival and quality of life in postmenopausal women. Women with breast cancer are more likely to develop osteoporosis than women without breast cancer due to certain factors that can affect both diseases simultaneously. For instance, estrogen and the receptor activator of nuclear factor-κB ligand (RANKL) play important roles in the occurrence and development of these two diseases. Moreover, chemotherapy and hormone therapy administered to breast cancer patients also increase the incidence of osteoporosis, and in recent years, neuropeptide Y (NPY) has also been found to impact breast cancer and osteoporosis.Y1 and Y5 receptors are highly expressed in breast cancer, and Y1 and Y2 receptors affect osteogenic response, thus potentially highlighting a potential new direction for treatment strategies. In this paper, the relationship between breast cancer and osteoporosis, the influence of NPY on both diseases, and the recent progress in the research and treatment of these diseases are reviewed.

Keywords: breast cancer, osteoporosis, neuropeptide Y, estrogen, receptor activator of nuclear factor-κB ligand

OPEN ACCESS

Edited by:
Melissa Orlandin Premaor, Federal University of Minas Gerais, Brazil

Reviewed by:
Alberto Falchetti, Istituto Auxologico Italiano (IRCCS), Italy
Subhashis Pal, Emory University, United States

***Correspondence:**
Si-qing Cai
1920455696@qq.com
Shu Lin
shulin1956@126.com

Specialty section:
This article was submitted to Bone Research, a section of the journal Frontiers in Endocrinology

Received: *05 May 2021*
Accepted: *19 July 2021*
Published: *06 August 2021*

Citation:
Lin S-t, Li Y-z, Sun X-q, Chen Q-q, Huang S-f, Lin S and Cai S-q (2021) Update on the Role of Neuropeptide Y and Other Related Factors in Breast Cancer and Osteoporosis. Front. Endocrinol. 12:705499. doi: 10.3389/fendo.2021.705499

INTRODUCTION

Breast cancer is the most common cancer among women, with 1.6 million cases each year worldwide, making it the second leading cause of cancer-related deaths in women (1). Sex, age, estrogen levels, family history, specific gene mutations, and an unhealthy lifestyle are risk factors for breast cancer (2). The main focus of clinicians and researchers has been how to effectively diagnose, treat, and improve the prognosis of breast cancer.

Abbreviations: RANKL, Receptor activator of nuclear factor-κB ligand; NPY, Neuropeptide Y; GnRH, Gonadotropin hormone-releasing; NPYRs, NPY receptors; SERMs, Selective estrogen receptor modulators; HRT, Hormone replacement therapy; TNF, Tumor necrosis factor; AIs, Aromatase inhibitors; GnRHa, Gonadotropin hormone-releasing agonists; Y1R, NPY Y1 receptor; Y2R, NPY Y2 receptor; Y5R, NPY Y5 receptor; MMTV, Mouse mammary tumor virus; MPA, Medroxyprogesterone acetate; DMBA, 7,12-dimethylbenzanthracene; POI, Possibility of ovarian insufficiency; BMD, Bone mineral density; VIP, Vasoactive intestinal peptide; GRP, Gastrin-releasing peptide; BMSCs, Bone marrow mesenchymal stem cells; HSCs, Hematopoietic stem cells; ADSCs, Adipose stem cells; DEXA, Dual Energy X-ray Absorptiometry.

Osteoporosis is another common disease that affects more than 200 million postmenopausal women worldwide (3). Meanwhile, breast cancer survivors were found to have a 68% higher risk of osteopenia and osteoporosis than women without breast cancer (4). Osteopenia and osteoporosis are more likely to lead to fractures; therefore, breast cancer combined with these conditions can significantly impact the quality of life of breast cancer patients (5). Several factors can simultaneously affect breast and bone tissues, in part because breasts and bones are both estrogen-dependent. However, estrogen plays different roles in the development of breast cancer and osteoporosis; that is, an increase in estrogen increases the risk of breast cancer while reducing the risk of osteoporosis. Certain breast cancer treatments, such as aromatase inhibitors (AIs) (6, 7), chemotherapies (3, 8), and gonadotropin hormone-releasing (GnRH) agonists (8), reduce estrogen levels, which can, subsequently, increase the risk of osteoporosis. Additionally, the receptor activator of nuclear factor-κB (RANKL) also affects breast and bone tissue. In fact, the overexpression of RANKL has been shown to promote the occurrence of breast cancer and boost the activity of osteoclasts (9), leading to bone loss (10). Since breast cancer, and its treatment, increases the risk of osteoporosis, it is important that current and post-treatment breast cancer patients be monitored and treated for osteoporosis.

Neuropeptide Y (NPY) is a polypeptide consisting of 36 amino acid residues and is widely expressed throughout the body. NPY acts through NPY receptors (NPYRs), including Y1, Y2, Y4, Y5, and Y6 receptors that have been cloned in mammals (11, 12). NPY plays an important role in the nervous, immune, and endocrine systems (11, 13–15) and can affect the proliferation, apoptosis, differentiation, migration, mobilization, and cytokine secretion of different cell types (16). Additionally, NPY has recently been found to play a role in the progression of breast cancer (17–19) and osteoporosis (20, 21). Specifically, elevated expression of the NPY Y1 receptor (Y1R) and NPY Y5 receptor (Y5R) promotes the occurrence and migration of breast cancer cells (22). As such, several new treatment methods have been developed that aim to improve the targeting effect of drugs to breast cancer and reduce the damage to other surrounding tissues. In the skeletal system, Y1R and NPY Y2 receptor (Y2R) play a key role in bone homeostasis, while Y1R inhibits bone formation through non-hypothalamic and Y2R through hypothalamic pathways (23, 24), respectively. By applying the principle that Y1R and Y2R function in bone homeostasis, this review provides a comprehensive assessment of the current state of osteoporosis prevention and treatment strategies. We further discuss the relationship between breast cancer and osteoporosis, particularly regarding the influence of NPY on both diseases and how it applies their treatment.

BREAST CANCER AND OSTEOPOROSIS

Links Between Breast Cancer and Postmenopausal Osteoporosis

Breast cancer and osteoporosis are common diseases that affect the survival and quality of life of postmenopausal women. Some studies suggest that these two diseases may occur concurrently. For instance, a recent study found that women newly diagnosed with breast cancer are five times more likely to develop a vertebral fracture within 3 years than healthy women in the general population (25). Additionally, a study of 1,692 breast cancer survivors found that 312 developed osteoporosis during a median follow-up period of 5 years (26). Other studies have found that women with higher bone density have a higher risk of breast cancer (4, 5, 27). Therefore, it is increasingly important to explore the factors that link these two diseases (**Table 1**).

Estrogen

Estrogen increases the risk of breast cancer and inhibits bone loss (34, 35). *In vitro* and *in vivo* studies (36–38) have shown that estrogen is a risk factor for breast cancer and that serum estrogen levels in breast cancer patients are higher than those in healthy individuals. Estrogen may participate in cancer development or progression by stimulating normal breast epithelium and breast cancer cell proliferation (28, 39, 40). Specifically, it may impact proliferation and apoptosis of breast tissue cells through binding to estrogen receptors (40) or stimulating Y1R upregulation (36, 38). Since estrogen is involved in the carcinogenic effects of breast cancer, it is, theoretically, possible to prevent breast cancer *via* bilateral removal of the ovaries, while treatment with tamoxifen and other selective estrogen receptor modulators (SERMs) can also regulate estrogen levels (1, 40).

In addition to its role in breast cancer, 17β-estradiol (E2) is closely related to the regulation of osteohomeostasis *in vivo*. E2 can reduce the release of osteoclasts and promote anti-apoptotic behavior in osteoblasts. Moreover, E2 activates the Fas ligand on osteoblasts through ERα, thus inducing apoptosis of osteoclasts, indicating a protective effect of E2 on bone tissue. ERα and ERβ are two estrogen receptors involved in the regulation of bone homeostasis. However, the distribution of these receptors differs with ERα expressed more in cortical bone, while ERβ is found in bone trabeculae. In addition to the difference in location, the two receptors have also been found to antagonize the skeletal system.

TABLE 1 | Links between breast cancer and osteoporosis.

Factor	Breast cancer	Osteoporosis	Reference
Estrogen	Involved in the carcinogenesis of breast cancer	Reduces bone loss	(28, 29)
RANKL	Accelerate the occurrence of breast cancer	Increases osteoclasts activity	(9, 10, 30)
AIs	A first-line treatment for ER-positive breast cancer	Reduce estrogen and increase the occurrence of osteoporosis	(6, 31)
Chemotherapy	Widely used in early breast cancer and local advanced breast cancer	Leads to ovarian failure and osteoporosis	(3, 8, 28)
GnRHa	Widely used in the treatment of premenopausal breast cancer	Leads to osteoporosis	(8, 32)
NPY1	Promotes the occurrence and migration of breast cancer	Reduces bone formation	(17, 33)

For example, compared with WT mice, K/G-ER-β KO mice exhibit enlarged femurs, while those of K/G-ER-α KO mice are shortened. Moreover, femur width in male C-ER-β KO mice has been shown to increase, while that in C-ERα-KO mice decreases compared to WT mice. These results indicate that the estrogen receptors have opposite effects on femur length and width (29).

The primary cause of postmenopausal osteoporosis is the loss of the protective effect offered by estrogen on bone density together with an increase in osteoclast activity, thus disrupting the balance between bone destruction and resorption, ultimately leading to a rapid reduction in bone density (21, 41). Thus, hormone replacement therapy (HRT) is commonly used to prevent postmenopausal osteoporosis; however, long-term use of HRT is associated with a significantly increased risk of breast cancer. Therefore, SERMs have recently garnered increasing attention as a new treatment option. SERMs bind to estrogen receptors in certain tissues that produce either estrogen antagonists or agonists to reduce the risk of invasive breast cancer in postmenopausal women, while also preventing and treating postmenopausal osteoporosis (42, 43).

Receptor Activator of Nuclear Factor-κB Ligand

RANKL is a member of the tumor necrosis factor (TNF) family and plays an important role in regulating bone homeostasis (44). The main role of RANKL is to control the differentiation and activation of osteoclasts. Specifically, upregulation of RANKL can promote the differentiation and activity of osteoclasts, lead to excessive bone resorption, and cause osteoporosis (30, 45). In the bone tumor microenvironment, cancer cells stimulate osteoblasts and release RANKL receptor activators. RANKL binds to its receptors on pre- and mature osteoclasts to increase bone resorption and cause bone loss (10).

In addition, the RANKL/RANK pathway is related to the occurrence and development of breast cancer. Gonzalez-Suarez et al. (9) found that RANKL and RANK were expressed in both premalignant epithelium and tumor tissue in WT and mouse mammary tumor virus (MMTV)-RANK mice, which were implanted subcutaneously with medroxyprogesterone acetate (MPA), a strong progestin, and 7,12-dimethylbenzanthracene (DMBA), a carcinogen. Compared with WT mice, MMTV-RANK mice were more likely to be induced breast cancer by MPA/DMBA with more extensive and numerous lesions (9). This may be caused by RANKL driving cells into the cell cycle by binding to RANK in breast epithelial cells, while also protecting small breast epithelial cells from apoptosis caused by DNA damage, thereby promoting breast epithelial hyperplasia and increasing the incidence of precancerous lesions and cancers. Additionally, progesterone can promote the proliferation of mammary epithelial cells and increase the incidence of breast cancer. A study found that mice lacking RANK and RANKL receptors exhibit reduced progesterone-induced epithelial cell proliferation, which subsequently reduces the incidence of, or delays the onset of, breast cancer (7). Moreover, hormone- and carcinogen-treated MMTV-RANK and wild-type mice treated subcutaneously with the RANK inhibitor, RANK FC, have reduced epithelial proliferation, precancerous lesions, and reduced incidence of breast cancer (9). Clinically, denosumab, an anti-RANKL monoclonal antibody, is used to treat bone loss caused by osteoporosis and breast cancer (46). A clinical follow-up of 100,368 postmenopausal women with a history of bisphosphonates showed that one-third of these patients had a history of using denosumab, while two-thirds had no history of denosumab treatment. The trial found that patients administered denosumab had a lower incidence of breast cancer compared to those not administered denosumab (46). Although denosumab reduced the risk of breast cancer, a second team followed breast cancer patients treated with denosumab adjuvant therapy and found no significant improvement in bone metastasis-free survival or relapse-free survival (47). So, bisphosphonates are still the drug of choice for the prevention and treatment of osteoporosis in breast cancer patients.

Links Between Breast Cancer Treatment and Osteoporosis

Common treatments for breast cancer include surgery, radiation therapy, and adjuvant chemotherapy, some of which reduce estrogen levels. However, due to the different effects of estrogen on bone and breast tissue, treatments that reduce estrogen can lead to osteoporosis.

Aromatase Inhibitors

ER-positive breast cancer accounts for 70% of breast cancers in postmenopausal women (48). AIs are the first-line treatment for ER-positive breast cancer and are believed to reduce the risk of local, distant, and contralateral breast recurrence, which ultimately improves overall patient survival (31). However, in recent years, AIs were found to increase the risk of bone breakage and fractures. A study found that the incidence of lumbar osteoporosis in patients treated with anastrozole increased to 25% after 3 years of treatment (6).The increased incidence of osteoporosis after AI treatment is likely due to aromatase inhibition. Postmenopausal women convert androgens to estrogen through aromatase; therefore, inhibition of aromatase by AIs results in reduced estrogen synthesis (7). The decrease in estrogen induces an imbalance between bone resorption and bone destruction, which increases the incidence of osteoporosis (25). A study showed that estrogen levels of breast cancer patients dropped significantly within 3 weeks after AIs treatment, and the bone loss rate of those patients was twice that of normal postmenopausal women (49). Although AIs increased the incidence of osteoporosis in breast cancer patients, the risk of osteoporosis caused by AIs did not continue in the follow-up period following withdrawal from the drug, indicating that the severity of osteoporosis is not exacerbated by AIs withdrawal (3, 26).

Chemotherapy

Currently, adjuvant chemotherapy is widely used to treat early breast cancer and locally advanced breast cancer cases as it can prolong the disease-free survival and overall survival of women. Adjuvant chemotherapy can also improve the effectiveness of surgical treatment by reducing the size and grading of tumors (28, 50, 51). However, previous studies have found that nearly 80% of premenopausal women experience menopause and ovarian

failure after chemotherapy (8). Ovarian failure leads to a rapid drop in estrogen levels and accelerated bone loss, particularly in the lumbar spine. In fact, a study that monitored the bone mineral density (BMD) of breast cancer patients undergoing chemotherapy found that BMD was significantly decreased (up to −7.7% in the first year) (3). A prospective study further demonstrated that women who experienced ovarian failure within 6 months due to chemotherapy exhibited a rapid and significant decrease in BMD in their spines and femurs (52). Therefore, it is recommended that bone density be monitored during chemotherapy in breast cancer patients to ensure proper treatments are implemented.

Gonadotropin Hormone-Releasing Agonists

Although ovarian failure following chemotherapy represents a risk for premenopausal breast cancer patients of childbearing age, GnRHa has been shown to reduce the risk of chemotherapy-induced ovarian insufficiency (POI) and improve fertility. Hence, it is currently widely used in the treatment of premenopausal breast cancer patients (32, 53, 54). In addition, GnRHa can reduce breast density and prevent breast cancer in high-risk groups (54). However, the side effects of GnRHa have recently attracted attention as GnRHa-induced low estrogen levels are associated with bone loss in premenopausal breast cancer. A study showed that goserelin (a GnRH agonist) reduced hip BMD by 6.4% and spinal BMD by 10.5% (8) in the first 2 years of treatment. Similarly, compared to patients not administered leuprolide acetate (a GnRH agonist), BMD was significantly reduced after 24 weeks of leuprolide acetate treatment (55). Meanwhile, oestriol [OE(3)] therapy has proven effective for countering GnRHa-induced bone loss (56).

Prevention of Osteoporosis in Breast Cancer Patients

The risk of bone loss and fracture is higher in breast cancer patients than in healthy women; therefore, steps should be taken in both breast cancer and post-treatment patients to prevent and treat bone loss. First, a healthy lifestyle, such as quitting smoking, reducing alcohol consumption, and increasing physical activity, is essential for promoting overall health and reducing bone loss (57). Second, regular monitoring of BMD is necessary. Most guidelines suggest that the BMD should be monitored in patients with the following features: (1) BMD T-score < −2; (2) AIs treatment, especially in older patients (e.g., ≥ 65 years old); (3) premenopausal POI patients; (4) oral glucocorticoids for more than 6 months; (5) low body mass index (BMI < 20 kg/m^2); and (6) patients with a personal or family history of hip fracture and smoking. BMD is commonly used to diagnose osteoporosis and assess the risk of fracture. Therefore, premenopausal women with a Z-value < −2.5 (the diagnostic index for premenopausal women) (58–60), and postmenopausal women with a T-value < −2.5 should be diagnosed with osteoporosis. Thus, women with a T-score < −2 or with two or more clinical fracture risk factors should be recommended for treatment (5, 25). Third, bisphosphonate can be used to prevent bone loss in patients with breast cancer and in those prescribed AIs. Nitrogen-containing bisphosphonates promote osteoclast apoptosis by inhibiting farnesyl pyrophosphate synthase through its conversion to cytotoxic adenosine triphosphate analogs. Bisphosphonates can be administered orally or intravenously, depending on the patient's preference and dosage requirements (61). Coleman et al. (62) compared the effects of immediate and delayed zoledronic acid treatment on patients with early-stage breast cancer and reported that the change in lumbar BMD in the immediate treatment group was +4.3% and −5.4% in the delayed treatment group. Another study showed that the proportion of patients with particularly severe lumbar bone loss (i.e., patients meeting the criteria for significant osteoporosis) dropped from 22% to 1% after 3 years of treatment with zoledronic acid (49). Bisphosphonates cannot only reduce bone loss but also reduce bone metastasis, bone pain, and refractory hypercalcemia caused by breast cancer (61). In addition, bisphosphonates have been found to improve the efficacy of endocrine therapy and reduce the mortality and recurrence rates of early breast cancer. However, significant results can only be achieved in the early stages of treatment (10, 63, 64). In addition, calcium (1000 mg/day) and vitamin D supplementation (8,001,000 IU/day) are also considered necessary for breast cancer patients (31, 49, 65).

NPY AND BREAST CANCER

An increasing number of peptide receptors are overexpressed in tumors; hence, the corresponding peptide hormones can specifically bind to these receptors, affecting tumor cell proliferation, hormone release, and angiogenesis (66). Therefore, it is of great significance to understand what peptide receptors are overexpressed in tumors to effectively target them for treatment.

High Expression of NPY Y1 Receptor in Breast Cancer

Breast cancer has been reported to express different types of peptide receptors, such as somatostatin, vasoactive intestinal peptide (VIP), gastrin-releasing peptide (GRP), and Y1R. GRP and Y1R are the most highly expressed peptide receptors in primary breast cancer, where they appear alone or in combination in more than 82% of resectable primary breast cancers. Tumors with lymph node metastasis also have peptide receptors similar to those in the corresponding primary tumors (67). Overexpression of the NPY receptor was found in 85% of breast cancer patients, with Y1R expressed in most breast cancers and Y2R in only 24% (17). Moreover, Y1R is overexpressed in 90% of human breast tumors and 100% of detected metastatic tumors (18, 68). Meanwhile, Y2R is highly expressed in normal mammary glands; however, when the expression of the NPY receptor subtype is converted from the Y2 to Y1 subtype, normal breast tissue becomes cancerous (69).

High Expression of NPY5 Receptor in Breast Cancer

Recently, researchers have discovered that in addition to Y1R, Y5R also affects the occurrence of breast cancer. Y5R and Y1R were found to be highly expressed in mouse 4T1 breast cancer cells and breast cancer lesions in BALB/c mice (19, 70). NPY receptor (Y1R, Y2R, and Y5R) agonists were used to stimulate mouse 4T1 breast

cancer cell line models. The Y5R agonist was found to promote breast cancer cell proliferation and migration. Additionally, Y1R, Y2R, and Y5R are required for angiogenesis in breast tissue with Y5R playing a major role in vascular proliferation (19, 69). Y5R can promote the growth of vascular endothelial cells by regulating the kinase signaling pathway and inhibiting cAMP (12). In addition, Y5R stimulates the expression and secretion of vascular endothelial growth factor by activating the paracrine system, thus promoting angiogenesis (12, 19, 70). Therefore, Y5R is important for the growth and migration of cancer cells.

NPY SYSTEM AND OSTEOPOROSIS

The brain affects bone mass *via* three main pathways: regulation of the sympathetic nervous system, secretion or regulation of hormones that directly act on bone cells, and neuropeptides (71). Neuropeptides are neurotransmitters commonly found in the brain, spinal cord, and other parts of the body that regulate physiological functions. In recent years, studies have reported that neuropeptide Y and its receptors, which regulate bone metabolism, may be potential regulatory pathways in the pathogenesis of postmenopausal osteoporosis.

NPY System Regulates Bone Metabolism

In the clinical setting, micro-CT and NPY optical density (MOD) of subchondral cancellous bone were compared between osteoporosis and osteoarthritis patients and showed that the bone volume fraction (BV/TV;%), trabecular thickness (Tb. Th; μm), and trabecular number (Tb. N; mm^{-1}) were lower in osteoporosis patients than osteoarthritis patients; however, the NPY MOD value of subchondral cancellous bone was higher in the osteoporosis patients (20). This suggested that NPY was inversely correlated with low bone mass. NPY is thought to coordinate with estrogen in the control and regulation of the osteoblast–adipogenic balance. In ovariectomized rat models, a decrease in NPY and Y2R in the brain was observed in addition to development of osteoporosis (21). Moreover, increased NPY, Y1R, and Y2R were detected in the bones of ovariectomized rat models (72).

The bones receive an abundant supply of NPY from nerve fibers. The neuropeptides regulating bone metabolism primarily originate from the central nervous system, while some originate from the skeletal system; previous studies have confirmed the expression of NPY in osteoblasts and osteocytes (73, 74).Current studies (23, 33, 75) have shown that NPY effects on bone balance are primarily *via* NPY1 and NPY2. NPY2 is only expressed in the central nervous system, while NPY1 is often expressed in the skeletal system. Thus, NPY regulates bone homeostasis mainly through Y2 receptors expressed in the hypothalamus or Y1 receptors expressed in osteoblasts (69, 76, 77). (**Figure 1**).

The Role of NPY Y1 Receptor in Regulating Bone Metabolism

Y1 receptors are expressed in the central nervous system, lower thalamus, and skeletal system. A study of adult-specific hypothalamus Y1R excised ($Y1^{Hyp}$) mice and $Y1^{-/-}$ mice found that $Y1^{Hyp}$ BMD and other osteogenic markers were not significantly altered compared with WT mice, while $Y1^{-/-}$ mice had significantly increased BMD and other osteogenic markers (23). Therefore, Y1R expressed in the hypothalamus does not participate in the regulation of bone homeostasis; however, Y1R in the skeletal system participates in the regulation of bone homeostasis. This has been further demonstrated in recent studies examining the effect of NPY on bone balance using either the Y receptor knockout model or the receptor antagonist model. These studies have reported increased bone mass in both $Y1^{-/-}$ mice (33) and WT rats treated with an oral Y1 receptor antagonist (78, 79). Reduction or inhibition of Y1R can increase osteogenesis in several ways; for example, downregulation of Y1R promotes osteogenesis in bone marrow mesenchymal stem cells (BMSCs) through the cAMP/PKA/CREB pathway and ultimately increases bone mass (78). Studies have shown that the reduction or inhibition of Y1 receptors can also increase osteoblast activity as well as their osteogenic capacity (78). In addition, Y1R antagonists increase lactic acid bacteria probiotics in the intestine, thus strengthening the intestinal epithelial barrier, promoting intestinal calcium absorption and estrogen-like metabolite production, and reducing bone loss (80, 81). With the advanced understanding of the regulatory roles of Y1R in bone metabolism, researchers have begun to explore its application in the treatment of osteoporosis.

The Role of NPY Y2 Receptor in Regulating Bone Metabolism

Unlike Y1R, Y2R is expressed exclusively in the central nervous system. A high bone mass was observed in multiple experiments conducted in $Y2^{-/-}$ mice (24, 82, 83). Hypothalamic Y2R deletion has different effects on osteoblasts and osteoclasts; Y2R increases osteoblastic activity, increases expression of the osteogenic transcription factors Runx2 and Osterix, and reduces the number of osteoclasts, thereby reducing bone loss (72, 75). In addition, Baldock et al. (24) compared mouse models with double ($Y1^{-/-}$ $Y2^{-/-}$) and single ($Y1^{-/-}$ and $Y2^{-/-}$) knockout mice and found no significant difference in the effect of the double and single knockout models on osteogenesis. These results indicate that the double knockout model had no superposition effect on bone. Furthermore, in this study, Y1R downregulation was observed in bone tissue of $Y2^{-/-}$ mice, suggesting that the central Y2R signaling pathway plays a regulatory role in bone homeostasis by regulating the Y1R expression of osteoblasts. The rapid increase in bone mass in adult mice after central Y2R deletion suggests that Y2R may represent a promising new target for the prevention and treatment of osteoporosis.

NPY RECEPTOR IN THE TREATMENT OF BREAST CANCER AND OSTEOPOROSIS

In recent years, with an improved understanding of the role played by NPY in breast tissue and bone tissue (**Figure 2**), people have begun to use NPY in the treatment and diagnosis of breast

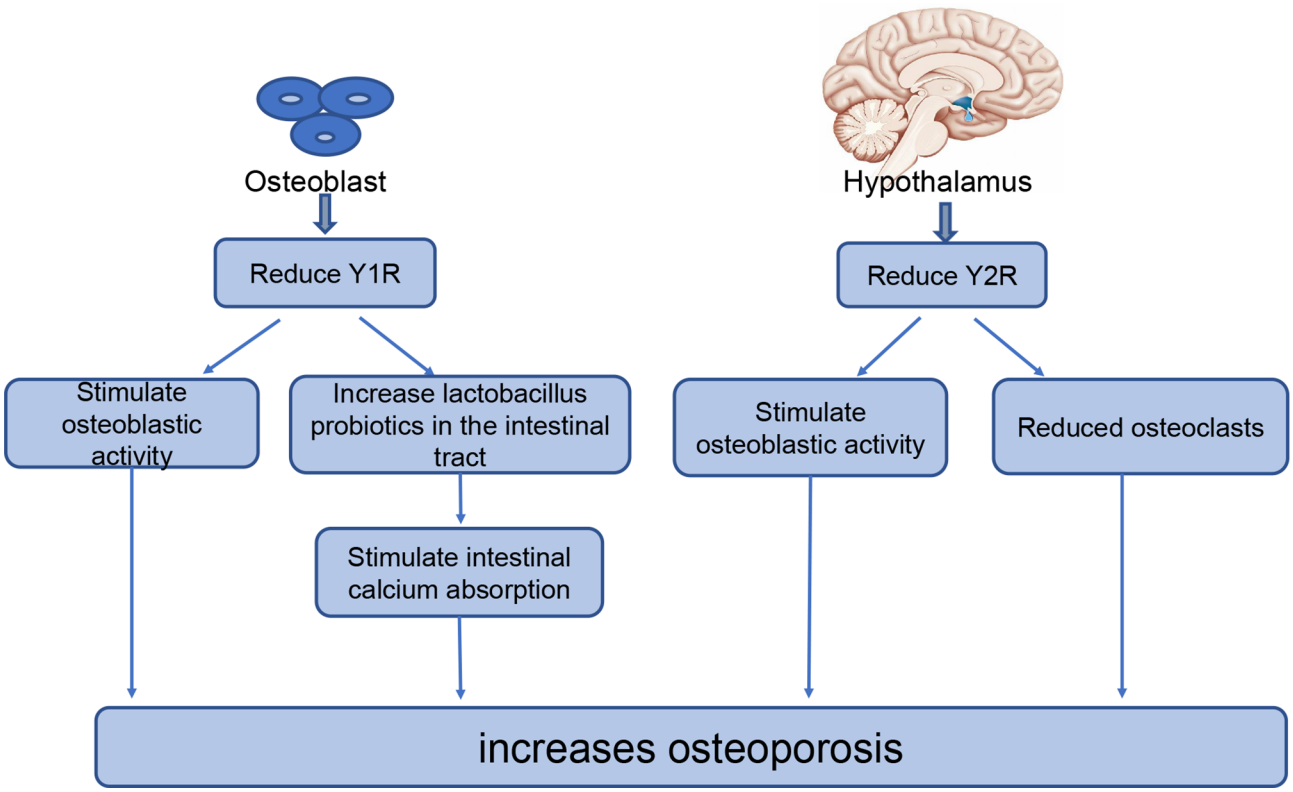

FIGURE 1 | The role of NPY in bone homeostasis. NPYR1 is expressed in osteoblasts and NPYR2 is expressed in the hypothalamus, where they play key roles in bone homeostasis. Reducing NPYR1 increases osteogenesis by increasing the activity of osteoblasts and the level of lactobacillus probiotics in the intestinal tract. Reducing NPYR2 increases osteogenesis by promoting osteoblastic activity and reducing the number of osteoclasts.

cancer and osteoporosis. Specifically, high expression of NPY and its receptor in breast cancer can be used to improve diagnostic and therapeutic efficacy (**Table 2**). Considering that most drugs currently used for osteoporosis, such as HRT, SERMs, and bisphosphonate regulation, have varying degrees of side effects (42, 90), it is important to clarify whether the role of Y1R and Y2R in osteohomeostasis can be exploited for development of new therapies.

Application of NPY Receptor in Breast Cancer Treatment

The characteristics of NPY1 overexpression in breast cancer can be used in imaging diagnosis of breast cancer. A study that intravenously injected an NPY analog-modified radioactive chelate into MCF-7 breast tumor mice found that it selectively bound to Y1, which was beneficial for breast cancer lesion display and diagnosis by positron emission tomography (PET) examination (84). Another study injected NPY nanocomposites into mice with MCF-7 breast tumors and found that it benefited MR and CT imaging for breast cancer evaluation (85).

Chemotherapy is now widely used in the treatment of breast cancer; however, chemotherapeutic drugs can lead to bone marrow suppression, cardiotoxicity, and nephrotoxicity (89). Therefore, improving the therapeutic effect of chemotherapy drugs while reducing their associated side effects has become a focus in breast cancer treatment strategies. Highly expressed peptide receptors in human cancers are now being used for targeted peptide radiotherapy. Among them, the most commonly used peptide receptors are somatostatin and somatostatin receptors; however, many breast cancers do not have a high density of somatostatin receptors. Due to the insufficient and uneven distribution of somatostatin receptors in breast cancer, somatostatin receptor imaging *in vivo* has not yet become a routine diagnostic method and somatostatin receptor-targeted radiotherapy is not widely used in the treatment of breast cancer (67). Conversely, several different treatment methods have been proposed based on the high NPY expression in breast cancer. Studies of NPY peptide–drug conjugates found that these biological conjugates effectively deliver toxic substances to breast cancer cells overexpressing the human Y1R (86, 87). It was also reported that the Y1R ligand combined with a P-GP inhibitor can be used to target drug delivery for breast cancer chemotherapy (88). Additionally, as nanotechnology develops, researchers have begun to use it in combination with NPY for the treatment of breast cancer. For example, an ultra-small, low-toxicity MnP (MC540)/DSPE-PEG-NPY nanocomposite intravenously injected into MCF-7 breast tumor mice was shown to be a high targeting and low-toxicity photodynamic therapy for breast cancer (85).

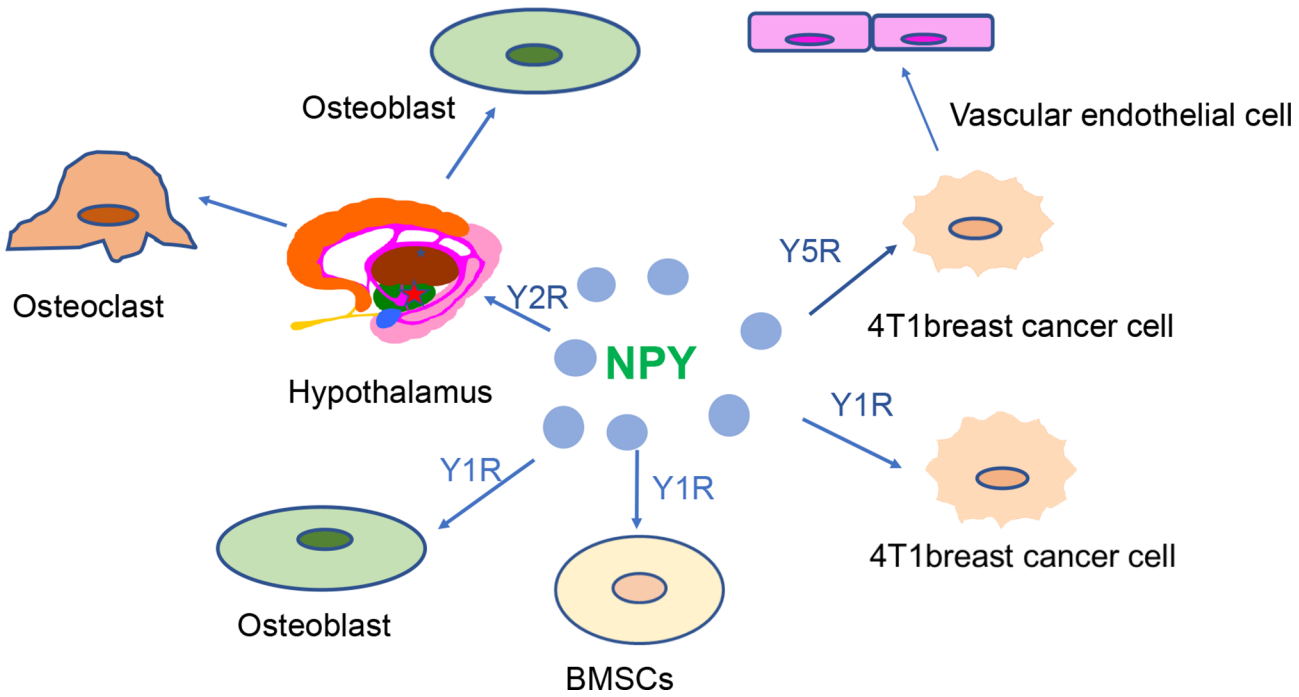

FIGURE 2 | NPY receptors are closely involved in the regulation of breast cancer and bone homeostasis. High expression of Y1R and Y5R is observed in 4T1 breast cancer cells. Y5R can promote the development of breast cancer by promoting the proliferation of vascular endothelial cells. The hypothalamic Y2R regulates bone balance by altering osteoblast and osteoclast proliferation. Alteration of Y1R may affect bone mass by regulating osteoblastic activity and bone marrow stem cell function.

TABLE 2 | Several applications of NPY in the treatment of breast cancer.

Model	Methods	Technology	Outcomes	Application	Reference
MCF-7 breast tumor mice	Injected NPY analog-modified radioactive chelate	PET	Be beneficial for lesion PET imaging	Diagnosis	(84)
MCF-7 breast tumor mice	Injected NPY nanocomposite	Nanotechnology	(1) Be beneficial for lesion MR and CT imaging (2) Targeted drug delivery and reduce the toxicity	Diagnosis Treatment	(85)
Breast cancer cells	Double methotrexate-modified NPY analogs	NPY peptide–drug conjugates	Targeted drug delivery and increase drug resistance	Treatment	(86)
Breast cancer cells overexpressing the Y1R subtype	Tubugi-1–NPY peptide–toxin conjugate	NPY peptide–drug conjugates	Targeted drug delivery	Treatment	(87)
MCF-7 breast tumor mice	Injected Y1R ligand combined with P-GP inhibitor	NPY peptide–drug conjugates	Improve drug targeting and reduce side effects	Treatment	(88)
4T1cell mice	Injected microbubbles modified with Y1 receptor ligand	Ultrasound chemotherapy	Enhanced tumor suppression and prolonged survival	Treatment	(89)

Another novel therapeutic strategy is the combination of ultrasound chemotherapy with administration of chemotherapy drugs embedded into microvesicles. That is, when the microvesicles receive ultrasonic stimulation, they vibrate and expand facilitating drug penetration into the tumor cells. In fact, a study reported that Y1R ligand modified chemotherapy-embedded microvesicles had better anticancer effects in 4T1 tumor cell mice compared with intravenous chemotherapy alone (89). Taking advantage of the high expression of NPY in breast cancer and improving the targeting effect of drugs to the tumor region reduce damage to the surrounding tissues and increase the efficiency of drugs in the diseased region, indicating that this technique is a good supplement to existing breast cancer treatments.

Application of NPY Receptor in the Treatment of Osteoporosis

Most drugs currently used for osteoporosis have varying degrees of side effects. For example, SERMs increase the risk of venous thrombosis, and bisphosphonates increase the incidence of

mandibular osteonecrosis (90). Y1R and Y2R function in bone balancing and provide a new direction for the treatment of osteoporosis. An increase in bone mass was found in both C57/BL6 mice treated with an oral Y1R receptor antagonist (79) and ovariectomized mice treated with a cerebral permeable Y2R antagonist when compared to the blank control group (83). Additionally, the traditional Chinese medicine Epimedium has recently become widely used for the treatment of bone diseases and has been suggested to function by increasing brain NPY and bone NPY1R (73). NPY can affect bone homeostasis through the hypothalamus Y2R; a Y2R-related drug can enter the arched region of the hypothalamus where Y2R is localized and does not need to cross the blood–brain barrier, which could enhance the effectiveness of the drug treatment (21, 41). As such, Y2R can also be used as a target for the treatment or prevention of osteoporosis.

In recent years, the effects of NPY on BMSCs and hematopoietic stem cells (HSCs) have been studied. Studies have shown that NPY treatment can promote the proliferation of bone marrow stem cells, promote their migration to the lesion area, and participate in the osteogenic differentiation of bone marrow stem cells (16). In addition, NPY and its receptor can regulate the proliferation of HSCs, promote their entry into peripheral blood, and increase the abundance of osteoblasts (16, 91, 92). Collectively, these studies suggest that NPY can be used in the treatment of osteoporosis with stem cells.

DISCUSSION

Previous studies (7, 9, 21, 37) have shown that breast cancer and osteoporosis are related to estrogen and RANKL. Additionally, patients with breast cancer are often at risk of osteoporosis after treatment. This is likely to be related to the reduction of estrogen levels in patients from several commonly used breast cancer treatments, such as AIs, chemotherapy, and GnRHa. Therefore, patients with breast cancer and those receiving breast cancer treatment are recommended to also take measures to prevent or treat osteoporosis. Patients can change their habits, measure BMD regularly, and take bisphosphonate, calcium, and vitamin D. NPY has also been found to affect breast and bone tissue, with the overexpression of Y1R and Y5R found in breast cancer patients, both of which promote the growth and migration of breast cancer cells. NPY acts with central Y2R and peripheral Y1R, where it participates in the regulation of bone metabolism. Due to the recent advances in NPY research related to breast cancer and osteoporosis, many researchers have begun to ask whether NPY can be used as a potential new strategy for the diagnosis or treatment of breast cancer or osteoporosis.

Although the application of NPY in breast and bone tissues have yielded positive results in animal models, they remain primarily in the research phase of animal testing. Most existing studies (85, 89) have focused on the high expression of Y1R in breast cancer and have proposed several diagnostic and research methods based on NPY Y1 targets. However, Y5R also plays an important role in the growth and migration of cancer cells, yet only limited studies on NPYY5 targeted therapies have been reported. Future work should, therefore, consider Y5R as a target to determine whether new treatment methods or diagnostic protocols can be proposed based on the high expression of Y5R in breast cancer.

Since Y2R can regulate bone balance through the hypothalamic system, and drugs entering the hypothalamic region do not need to cross the blood–brain barrier, there is a clear opportunity for drug delivery. Therefore, Y2R can be used as an important target for further study of osteoporosis therapeutic methods. In addition, the current diagnosis of osteoporosis is primarily achieved by measuring bone density with Dual Energy X-ray Absorptiometry (DEXA); however, this method can expose the patient to radiation damage. NPY receptor regulation of bone balance may provide insights that could improve the diagnosis of osteoporosis. Specifically, it will be of interest to determine whether Y1R or Y2R levels in plasma or other body fluids are related to BMD, and whether quantitation of NPY receptors can be effectively applied for osteoporosis diagnosis or evaluation of its severity. If we can use these alternative methods instead of DEXA to measure BMD, it will help to protect the patients from unnecessary radiation exposure.

Finally, BMSCs and adipose stem cells are considered to have multidirectional differentiation and sustained proliferation capabilities in the treatment of bone loss in osteoporosis (93). BMSCs and breast cancer stem cells have also been reported for breast cancer (94). NPY can also be applied to patients with osteoporosis caused by breast cancer as Y1R is highly expressed not only in breast cancer but is also positively correlated with osteoporosis. Therefore, Y1R has potential as a therapeutic target in the treatment of breast cancer and may also play a role in the treatment and prevention of cancer-induced osteoporosis. In the future, the combination of Y1R stem cell therapy may offer a unique therapeutic effect for breast cancer and cancer-induced osteoporosis.

In conclusion, neuropeptide Y and its related factors play important roles in breast cancer and osteoporosis development; as such, they may be useful candidates for novel diagnostic and therapeutic strategies for breast cancer and osteoporosis.

AUTHOR CONTRIBUTIONS

S-tL is the first author and involved in the review design, execution, manuscript drafting, and critical discussion of the manuscript. Y-zL, X-qS, Q-qC, and S-fH collected the various studies. S-qC and SL critically revised the manuscript. All authors contributed to the manuscript and approved the submitted version.

FUNDING

This work was funded by the Science and Technology Bureau of Quanzhou (grant numbers 2020CT003 and 2018C054R).

REFERENCES

1. Thorat MA, Balasubramanian R. Breast Cancer Prevention in High-Risk Women. *Best Pract Res Clin Obstet Gynaecol* (2020) 65:18–31. doi: 10.1016/j.bpobgyn.2019.11.006
2. Sun YS, Zhao Z, Yang ZN, Xu F, Lu HJ, Zhu ZY, et al. Risk Factors and Preventions of Breast Cancer. *Int J Biol Sci* (2017) 13(11):1387–97. doi: 10.7150/ijbs.21635
3. van Hellemond IEG, Smorenburg CH, Peer PGM, Swinkels ACP, Seynaeve CM, van der Sangen MJC, et al. Assessment and Management of Bone Health in Women With Early Breast Cancer Receiving Endocrine Treatment in the DATA Study. *Int J Cancer* (2019) 145(5):1325–33. doi: 10.1002/ijc.32205
4. Ramin C, May BJ, Roden RBS, Orellana MM, Hogan BC, McCullough MS, et al. Evaluation of Osteopenia and Osteoporosis in Younger Breast Cancer Survivors Compared With Cancer-Free Women: A Prospective Cohort Study. *Breast Cancer Res* (2018) 20(1):134. doi: 10.1186/s13058-018-1061-4
5. Trémollieres FA. Screening for Osteoporosis After Breast Cancer: For Whom, Why and When. *Maturitas* (2014) 79(3):343–8. doi: 10.1016/j.maturitas.2014.08.001
6. Gnant MF, Mlineritsch B, Luschin-Ebengreuth G, Grampp S, Kaessmann H, Schmid M, et al. Zoledronic Acid Prevents Cancer Treatment-Induced Bone Loss in Premenopausal Women Receiving Adjuvant Endocrine Therapy for Hormone-Responsive Breast Cancer: A Report From the Austrian Breast and Colorectal Cancer Study Group. *J Clin Oncol* (2007) 25(7):820–8. doi: 10.1200/JCO.2005.02.7102
7. Schramek D, Leibbrandt A, Sigl V, Kenner L, Pospisilik JA, Lee HJ, et al. Osteoclast Differentiation Factor RANKL Controls Development of Progestin-Driven Mammary Cancer. *Nature* (2010) 468(7320):98–102. doi: 10.1038/nature09387
8. Milat F, Vincent AJ. Management of Bone Disease in Women After Breast Cancer. *Climacteric* (2015) 18(Suppl 2):47–55. doi: 10.3109/13697137.2015.1100383
9. Gonzalez-Suarez E, Jacob AP, Jones J, Miller R, Roudier-Meyer MP, Erwert R, et al. RANK Ligand Mediates Progestin-Induced Mammary Epithelial Proliferation and Carcinogenesis. *Nature* (2010) 468(7320):103–7. doi: 10.1038/nature09495
10. Coleman RE, Marshall H, Cameron D, Dodwell D, Burkinshaw R, Keane M, et al. Breast-Cancer Adjuvant Therapy With Zoledronic Acid. *N Engl J Med* (2011) 365(15):1396–405. doi: 10.1056/NEJMoa1105195
11. Chen WC, Liu YB, Liu WF, Zhou YY, He HF, Lin S. Neuropeptide Y Is an Immunomodulatory Factor: Direct and Indirect. *Front Immunol* (2020) 11:580378. doi: 10.3389/fimmu.2020.580378
12. Sheriff S, Ali M, Yahya A, Haider KH, Balasubramaniam A, Amlal H. Neuropeptide Y Y5 Receptor Promotes Cell Growth Through Extracellular Signal-Regulated Kinase Signaling and Cyclic AMP Inhibition in a Human Breast Cancer Cell Line. *Mol Cancer Res* (2010) 8(4):604–14. doi: 10.1158/1541-7786.MCR-09-0301
13. Raghanti MA, Conley T, Sudduth J, Erwin JM, Stimpson CD, Hof PR, et al. Neuropeptide Y-Immunoreactive Neurons in the Cerebral Cortex of Humans and Other Haplorrhine Primates. *Am J Primatol* (2013) 75(5):415–24. doi: 10.1002/ajp.22082
14. Yulyaningsih E, Loh K, Lin S, Lau J, Zhang L, Shi Y, et al. Pancreatic Polypeptide Controls Energy Homeostasis *Via* Npy6r Signaling in the Suprachiasmatic Nucleus in Mice. *Cell Metab* (2014) 19(1):58–72. doi: 10.1016/j.cmet.2013.11.019
15. Eva C, Oberto A, Longo A, Palanza P, Bertocchi I. Sex Differences in Behavioral and Metabolic Effects of Gene Inactivation: The Neuropeptide Y and Y Receptors in the Brain. *Neurosci Biobehav Rev* (2020) 119:333–47. doi: 10.1016/j.neubiorev.2020.09.020
16. Wu JQ, Jiang N, Yu B. Mechanisms of Action of Neuropeptide Y on Stem Cells and its Potential Applications in Orthopaedic Disorders. *World J Stem Cells* (2020) 12(9):986–1000. doi: 10.4252/wjsc.v12.i9.986
17. Reubi JC, Gugger M, Waser B, Schaer JC. Y(1)-Mediated Effect of Neuropeptide Y in Cancer: Breast Carcinomas as Targets. *Cancer Res* (2001) 61(11):4636–41. doi: 10.1097/00002820-200106000-00013
18. Li J, Shen Z, Ma X, Ren W, Xiang L, Gong A, et al. Neuropeptide Y Y1 Receptors Mediate [Corrected] Targeted Delivery of Anticancer Drug With Encapsulated Nanoparticles to Breast Cancer Cells With High Selectivity and Its Potential for Breast Cancer Therapy. *ACS Appl Mater Interfaces* (2015) 7(9):5574–82. doi: 10.1021/acsami.5b00270
19. Medeiros PJ, Jackson DN. Neuropeptide Y Y5-Receptor Activation on Breast Cancer Cells Acts as a Paracrine System That Stimulates VEGF Expression and Secretion to Promote Angiogenesis. *Peptides* (2013) 48:106–13. doi: 10.1016/j.peptides.2013.07.029
20. Xiao J, Yu W, Wang X, Wang B, Chen J, Liu Y, et al. Correlation Between Neuropeptide Distribution, Cancellous Bone Microstructure and Joint Pain in Postmenopausal Women With Osteoarthritis and Osteoporosis. *Neuropeptides* (2016) 56:97–104. doi: 10.1016/j.npep.2015.12.006
21. Liu X, Liu H, Xiong Y, Yang L, Wang C, Zhang R, et al. Postmenopausal Osteoporosis Is Associated With the Regulation of SP, CGRP, VIP, and NPY. *BioMed Pharmacother* (2018) 104:742–50. doi: 10.1016/j.biopha.2018.04.044
22. Movafagh S, Hobson JP, Spiegel S, Kleinman HK, Zukowska Z. Neuropeptide Y Induces Migration, Proliferation, and Tube Formation of Endothelial Cells Bimodally *Via* Y1, Y2, and Y5 Receptors. *FASEB J* (2006) 20(11):1924–6. doi: 10.1096/fj.05-4770fje
23. Baldock PA, Allison SJ, Lundberg P, Lee NJ, Slack K, Lin EJ, et al. Novel Role of Y1 Receptors in the Coordinated Regulation of Bone and Energy Homeostasis. *J Biol Chem* (2007) 282(26):19092–102. doi: 10.1074/jbc.M700644200
24. Lundberg P, Allison SJ, Lee NJ, Baldock PA, Brouard N, Rost S, et al. Greater Bone Formation of Y2 Knockout Mice Is Associated With Increased Osteoprogenitor Numbers and Altered Y1 Receptor Expression. *J Biol Chem* (2007) 282(26):19082–91. doi: 10.1074/jbc.M609629200
25. Paschou SA, Augoulea A, Lambrinoudaki I. Bone Health Care in Women With Breast Cancer. *Hormones (Athens)* (2020) 19(2):171–8. doi: 10.1007/s42000-019-00164-y
26. Hamood R, Hamood H, Merhasin I, Keinan-Boker L. Hormone Therapy and Osteoporosis in Breast Cancer Survivors: Assessment of Risk and Adherence to Screening Recommendations. *Osteoporos Int* (2019) 30(1):187–200. doi: 10.1007/s00198-018-4758-4
27. Chowdhury R, Sinha B, Sankar MJ, Taneja S, Bhandari N, Rollins N, et al. Breastfeeding and Maternal Health Outcomes: A Systematic Review and Meta-Analysis. *Acta Paediatr* (2015) 104(467):96–113. doi: 10.1111/apa.13102
28. Ramaswamy B, Shapiro CL. Osteopenia and Osteoporosis in Women With Breast Cancer. *Semin Oncol* (2003) 30(6):763–75. doi: 10.1053/j.seminoncol.2003.08.028
29. Khalid AB, Krum SA. Estrogen Receptors Alpha and Beta in Bone. *Bone* (2016) 87:130–5. doi: 10.1016/j.bone.2016.03.016
30. Boyle WJ, Simonet WS, Lacey DL. Osteoclast Differentiation and Activation. *Nature* (2003) 423(6937):337–42. doi: 10.1038/nature01658
31. Suskin J, Shapiro CL. Osteoporosis and Musculoskeletal Complications Related to Therapy of Breast Cancer. *Gland Surg* (2018) 7(4):411–23. doi: 10.21037/gs.2018.07.05
32. Lambertini M, Moore HCF, Leonard RCF, Loibl S, Munster P, Bruzzone M, et al. Gonadotropin-Releasing Hormone Agonists During Chemotherapy for Preservation of Ovarian Function and Fertility in Premenopausal Patients With Early Breast Cancer: A Systematic Review and Meta-Analysis of Individual Patient-Level Data. *J Clin Oncol* (2018) 36(19):1981–90. doi: 10.1200/JCO.2018.78.0858
33. Lee NJ, Nguyen AD, Enriquez RF, Doyle KL, Sainsbury A, Baldock PA, et al. Osteoblast Specific Y1 Receptor Deletion Enhances Bone Mass. *Bone* (2011) 48(3):461–7. doi: 10.1016/j.bone.2010.10.174
34. Fontanges E, Fontana A, Delmas P. Osteoporosis and Breast Cancer. *Joint Bone Spine* (2004) 71(2):102–10. doi: 10.1016/j.jbspin.2003.02.001
35. Muhammad A, Mada SB, Malami I, Forcados GE, Erukainure OL, Sani H, et al. Postmenopausal Osteoporosis and Breast Cancer: The Biochemical Links and Beneficial Effects of Functional Foods. *BioMed Pharmacother* (2018) 107:571–82. doi: 10.1016/j.biopha.2018.08.018
36. Amlal H, Faroqui S, Balasubramaniam A, Sheriff S. Estrogen Up-Regulates Neuropeptide Y Y1 Receptor Expression in a Human Breast Cancer Cell Line. *Cancer Res* (2006) 66(7):3706–14. doi: 10.1158/0008-5472.CAN-05-2744
37. Hulka BS, Moorman PG. Breast Cancer: Hormones and Other Risk Factors. *Maturitas* (2008) 61(1-2):203–213; discussion 13. doi: 10.1016/j.maturitas.2008.11.016
38. Memminger M, Keller M, Lopuch M, Pop N, Bernhardt G, von Angerer E, et al. The Neuropeptide Y Y(1) Receptor: A Diagnostic Marker? Expression in

Mcf-7 Breast Cancer Cells is Down-Regulated by Antiestrogens *In Vitro* and in Xenografts. *PloS One* (2012) 7(12):e51032. doi: 10.1371/journal.pone.0051032
39. Hulka BS, Moorman PG. Breast Cancer: Hormones and Other Risk Factors. *Maturitas* (2001) 38(1):103–113; discussion 13–16. doi: 10.1016/S0378-5122(00)00196-1
40. Samavat H, Kurzer MS. Estrogen Metabolism and Breast Cancer. *Cancer Lett* (2015) 356(2 Pt A):231–43. doi: 10.1016/j.canlet.2014.04.018
41. Allison SJ, Herzog H. NPY and Bone. *EXS* (2006) 95(95):171–82. doi: 10.1007/3-7643-7417-9_13
42. Ko SS, Jordan VC. Treatment of Osteoporosis and Reduction in Risk of Invasive Breast Cancer in Postmenopausal Women With Raloxifene. *Expert Opin Pharmacother* (2011) 12(4):657–74. doi: 10.1517/14656566.2011.557360
43. Lee WL, Chao HT, Cheng MH, Wang PH. Rationale for Using Raloxifene to Prevent Both Osteoporosis and Breast Cancer in Postmenopausal Women. *Maturitas* (2008) 60(2):92–107. doi: 10.1016/j.maturitas.2008.04.009
44. Hofbauer LC, Rachner TD, Hamann C. From Bone to Breast and Back - the Bone Cytokine RANKL and Breast Cancer. *Breast Cancer Res* (2011) 13(3):107. doi: 10.1186/bcr2842
45. Sigl V, Penninger JM. RANKL/RANK - From Bone Physiology to Breast Cancer. *Cytokine Growth Factor Rev* (2014) 25(2):205–14. doi: 10.1016/j.cytogfr.2014.01.002
46. Giannakeas V, Cadarette SM, Ban JK, Lipscombe L, Narod SA, Kotsopoulos J. Denosumab and Breast Cancer Risk in Postmenopausal Women: A Population-Based Cohort Study. *Br J Cancer* (2018) 119(11):1421–7. doi: 10.1038/s41416-018-0225-4
47. Coleman R, Finkelstein DM, Barrios C, Martin M, Iwata H, Hegg R, et al. Adjuvant Denosumab in Early Breast Cancer (D-CARE): An International, Multicentre, Randomised, Controlled, Phase 3 Trial. *Lancet Oncol* (2020) 21(1):60–72. doi: 10.1016/S1470-2045(19)30687-4
48. Lu Y, Liu W. Selective Estrogen Receptor Degraders (SERDs): A Promising Strategy for Estrogen Receptor Positive Endocrine-Resistant Breast Cancer. *J Med Chem* (2020) 63(24):15094–114. doi: 10.1021/acs.jmedchem.0c00913
49. Hadji P. Aromatase Inhibitor-Associated Bone Loss in Breast Cancer Patients is Distinct From Postmenopausal Osteoporosis. *Crit Rev Oncol Hematol* (2009) 69(1):73–82. doi: 10.1016/j.critrevonc.2008.07.013
50. Fisusi FA, Akala EO. Drug Combinations in Breast Cancer Therapy. *Pharm Nanotechnol* (2019) 7(1):3–23. doi: 10.2174/2211738507666190122111224
51. Kümmel S, Holtschmidt J, Loibl S. Surgical Treatment of Primary Breast Cancer in the Neoadjuvant Setting. *Br J Surg* (2014) 101(8):912–24. doi: 10.1002/bjs.9545
52. Shapiro CL, Manola J, Leboff M. Ovarian Failure After Adjuvant Chemotherapy Is Associated With Rapid Bone Loss in Women With Early-Stage Breast Cancer. *J Clin Oncol* (2001) 19(14):3306–11. doi: 10.1200/JCO.2001.19.14.3306
53. Zhong Y, Lin Y, Cheng X, Huang X, Zhou Y, Mao F, et al. GnRHa for Ovarian Protection and the Association Between AMH and Ovarian Function During Adjuvant Chemotherapy for Breast Cancer. *J Cancer* (2019) 10(18):4278–85. doi: 10.7150/jca.31859
54. Li XL, Yu Y, Zong XY. [Summary and Expectation of the Role of GnRHa in the Treatment of Breast Cancer]. *Zhonghua Zhong Liu Za Zhi* (2019) 41(4):246–50. doi: 10.3760/cma.j.issn.0253-3766.2019.04.002
55. Matsuo H. [Bone Loss Induced by GnRHa Treatment in Women]. *Nihon Rinsho* (2003) 61(2):314–8.
56. Wang Y, Yano T, Kikuchi A, Yano N, Matsumi H, Ando K, et al. Comparison of the Effects of Add-Back Therapy With Various Natural Oestrogens on Bone Metabolism in Rats Administered a Long-Acting Gonadotrophin-Releasing Hormone Agonist. *J Endocrinol* (2000) 165(2):467–73. doi: 10.1677/joe.0.1650467
57. Shapiro CL. Osteoporosis: A Long-Term and Late-Effect of Breast Cancer Treatments. *Cancers (Basel)* (2020) 12(11):3094. doi: 10.3390/cancers12113094
58. Hadji P, Coleman RE, Wilson C, Powles TJ, Clézardin P, Aapro M, et al. Adjuvant Bisphosphonates in Early Breast Cancer: Consensus Guidance for Clinical Practice From a European Panel. *Ann Oncol* (2016) 27(3):379–90. doi: 10.1093/annonc/mdv617
59. Leslie WD, Brennan-Olsen SL, Morin SN, Lix LM. Fracture Prediction From Repeat BMD Measurements in Clinical Practice. *Osteoporos Int* (2016) 27(1):203–10. doi: 10.1007/s00198-015-3259-y
60. Jain RK, Vokes T. Dual-Energy X-Ray Absorptiometry. *J Clin Densitom* (2017) 20(3):291–303. doi: 10.1016/j.jocd.2017.06.014
61. D'Oronzo S, Wood S, Brown JE. The Use of Bisphosphonates to Treat Skeletal Complications in Solid Tumours. *Bone* (2021) 147:115907. doi: 10.1016/j.bone.2021.115907
62. Coleman R, de Boer R, Eidtmann H, Llombart A, Davidson N, Neven P, et al. Zoledronic Acid (Zoledronate) for Postmenopausal Women With Early Breast Cancer Receiving Adjuvant Letrozole (ZO-FAST Study): Final 60-Month Results. *Ann Oncol* (2013) 24(2):398–405. doi: 10.1093/annonc/mds277
63. Gnant M, Mlineritsch B, Stoeger H, Luschin-Ebengreuth G, Knauer M, Moik M, et al. Zoledronic Acid Combined With Adjuvant Endocrine Therapy of Tamoxifen Versus Anastrozol Plus Ovarian Function Suppression in Premenopausal Early Breast Cancer: Final Analysis of the Austrian Breast and Colorectal Cancer Study Group Trial 12. *Ann Oncol* (2015) 26(2):313–20. doi: 10.1093/annonc/mdu544
64. Early Breast Cancer Trialists' Collaborative Group (EBCTCG). Adjuvant Bisphosphonate Treatment in Early Breast Cancer: Meta-Analyses of Individual Patient Data From Randomised Trials. *Lancet* (2015) 386(10001):1353–61. doi: 10.1016/S0140-6736(15)60908-4
65. Trémollieres FA, Ceausu I, Depypere H, Lambrinoudaki I, Mueck A, Pérez-López FR, et al. Osteoporosis Management in Patients With Breast Cancer: EMAS Position Statement. *Maturitas* (2017) 95:65–71. doi: 10.1016/j.maturitas.2016.10.007
66. Körner M, Reubi JC. NPY Receptors in Human Cancer: A Review of Current Knowledge. *Peptides* (2007) 28(2):419–25. doi: 10.1016/j.peptides.2006.08.037
67. Reubi C, Gugger M, Waser B. Co-Expressed Peptide Receptors in Breast Cancer as a Molecular Basis for *In Vivo* Multireceptor Tumour Targeting. *Eur J Nucl Med Mol Imaging* (2002) 29(7):855–62. doi: 10.1007/s00259-002-0794-5
68. Ruscica M, Dozio E, Motta M, Magni P. Role of Neuropeptide Y and its Receptors in the Progression of Endocrine-Related Cancer. *Peptides* (2007) 28(2):426–34. doi: 10.1016/j.peptides.2006.08.045
69. Houweling P, Kulkarni RN, Baldock PA. Neuronal Control of Bone and Muscle. *Bone* (2015) 80:95–100. doi: 10.1016/j.bone.2015.05.006
70. Medeiros PJ, Al-Khazraji BK, Novielli NM, Postovit LM, Chambers AF, Jackson DN. Neuropeptide Y Stimulates Proliferation and Migration in the 4T1 Breast Cancer Cell Line. *Int J Cancer* (2012) 131(2):276–86. doi: 10.1002/ijc.26350
71. Xu Y, Liu X, Li H, Liu H, Pan Z, Chen G. Brain Neural Effects of the 'Tonifying Kidney and Benefiting Marrow' Method in the Treatment of Osteoporosis. *J Tradit Chin Med* (2019) 39(6):902–9. doi: 10.19852/j.cnki.jtcm.2019.06.018
72. Xie W, Li F, Han Y, Li Z, Xiao J. Neuropeptides are Associated With Pain Threshold and Bone Microstructure in Ovariectomized Rats. *Neuropeptides* (2020) 81:101995. doi: 10.1016/j.npep.2019.101995
73. Liu H, Xiong Y, Wang H, Yang L, Wang C, Liu X, et al. Effects of Water Extract From Epimedium on Neuropeptide Signaling in an Ovariectomized Osteoporosis Rat Model. *J Ethnopharmacol* (2018) 221:126–36. doi: 10.1016/j.jep.2018.04.035
74. Baldock PA, Lee NJ, Driessler F, Lin S, Allison S, Stehrer B, et al. Neuropeptide Y Knockout Mice Reveal a Central Role of NPY in the Coordination of Bone Mass to Body Weight. *PloS One* (2009) 4(12):e8415. doi: 10.1371/journal.pone.0008415
75. Baldock PA, Sainsbury A, Couzens M, Enriquez RF, Thomas GP, Gardiner EM, et al. Hypothalamic Y2 Receptors Regulate Bone Formation. *J Clin Invest* (2002) 109(7):915–21. doi: 10.1172/JCI14588
76. Sousa DM, McDonald MM, Mikulec K, Peacock L, Herzog H, Lamghari M, et al. Neuropeptide Y Modulates Fracture Healing Through Y1 Receptor Signaling. *J Orthop Res* (2013) 31(10):1570–8. doi: 10.1002/jor.22400
77. Horsnell H, Baldock PA. Osteoblastic Actions of the Neuropeptide Y System to Regulate Bone and Energy Homeostasis. *Curr Osteoporos Rep* (2016) 14(1):26–31. doi: 10.1007/s11914-016-0300-9
78. Xie W, Li F, Han Y, Qin Y, Wang Y, Chi X, et al. Neuropeptide Y1 Receptor Antagonist Promotes Osteoporosis and Microdamage Repair and Enhances Osteogenic Differentiation of Bone Marrow Stem Cells *Via* cAMP/PKA/CREB Pathway. *Aging (Albany NY)* (2020) 12(9):8120–36. doi: 10.18632/aging.103129
79. Sousa DM, Baldock PA, Enriquez RF, Zhang L, Sainsbury A, Lamghari M, et al. Neuropeptide Y Y1 Receptor Antagonism Increases Bone Mass in Mice. *Bone* (2012) 51(1):8–16. doi: 10.1016/j.bone.2012.03.020

80. Xie W, Han Y, Li F, Gu X, Su D, Yu W, et al. Neuropeptide Y1 Receptor Antagonist Alters Gut Microbiota and Alleviates the Ovariectomy-Induced Osteoporosis in Rats. *Calcif Tissue Int* (2020) 106(4):444–54. doi: 10.1007/s00223-019-00647-5
81. Xu X, Jia X, Mo L, Liu C, Zheng L, Yuan Q, et al. Intestinal Microbiota: A Potential Target for the Treatment of Postmenopausal Osteoporosis. *Bone Res* (2017) 5:17046. doi: 10.1038/boneres.2017.46
82. Baldock PA, Sainsbury A, Allison S, Lin EJ, Couzens M, Boey D, et al. Hypothalamic Control of Bone Formation: Distinct Actions of Leptin and Y2 Receptor Pathways. *J Bone Miner Res* (2005) 20(10):1851–7. doi: 10.1359/JBMR.050523
83. Seldeen KL, Halley PG, Volmar CH, Rodríguez MA, Hernandez M, Pang M, et al. Neuropeptide Y Y2 Antagonist Treated Ovariectomized Mice Exhibit Greater Bone Mineral Density. *Neuropeptides* (2018) 67:45–55. doi: 10.1016/j.npep.2017.11.005
84. Vall-Sagarra A, Litau S, Decristoforo C, Wängler B, Schirrmacher R, Fricker G, et al. Design, Synthesis, *In Vitro*, and Initial *In Vivo* Evaluation of Heterobivalent Peptidic Ligands Targeting Both NPY(Y(1))- and GRP-Receptors-an Improvement for Breast Cancer Imaging? *Pharmaceuticals* (2018) 11(3):65. doi: 10.3390/ph11030065
85. Yu Z, Xia Y, Xing J, Li Z, Zhen J, Jin Y, et al. Y1-Receptor-Ligand-Functionalized Ultrasmall Upconversion Nanoparticles for Tumor-Targeted Trimodality Imaging and Photodynamic Therapy With Low Toxicity. *Nanoscale* (2018) 10(36):17038–52. doi: 10.1039/c8nr02387e
86. Böhme D, Krieghoff J, Beck-Sickinger AG. Double Methotrexate-Modified Neuropeptide Y Analogues Express Increased Toxicity and Overcome Drug Resistance in Breast Cancer Cells. *J Med Chem* (2016) 59(7):3409–17. doi: 10.1021/acs.jmedchem.6b00043
87. Kufka R, Rennert R, Kaluđerović GN, Weber L, Richter W, Wessjohann LA. Synthesis of a Tubugi-1-Toxin Conjugate by a Modulizable Disulfide Linker System With a Neuropeptide Y Analogue Showing Selectivity for Hy1r-Overexpressing Tumor Cells. *Beilstein J Org Chem* (2019) 15:96–105. doi: 10.3762/bjoc.15.11
88. Wang Y, Jiang Z, Yuan B, Tian Y, Xiang L, Li Y, et al. A Y1 Receptor Ligand Synergized With a P-Glycoprotein Inhibitor Improves the Therapeutic Efficacy of Multidrug Resistant Breast Cancer. *Biomater Sci* (2019) 7(11):4748–57. doi: 10.1039/c9bm00337a
89. Qian X, Wang Y, Xu Y, Ma L, Xue N, Jiang Z, et al. Active Targeting Nano-Scale Bubbles Enhanced Ultrasound Cavitation Chemotherapy in Y1 Receptor-Overexpressed Breast Cancer. *J Mater Chem B* (2020) 8(31):6837–44. doi: 10.1039/d0tb00556h
90. Khosla S, Hofbauer LC. Osteoporosis Treatment: Recent Developments and Ongoing Challenges. *Lancet Diabetes Endocrinol* (2017) 5(11):898–907. doi: 10.1016/S2213-8587(17)30188-2
91. Park MH, Kim N, Jin HK, Bae JS. Neuropeptide Y-Based Recombinant Peptides Ameliorate Bone Loss in Mice by Regulating Hematopoietic Stem/Progenitor Cell Mobilization. *BMB Rep* (2017) 50(3):138–43. doi: 10.5483/bmbrep.2017.50.3.191
92. Park MH, Lee JK, Kim N, Min WK, Lee JE, Kim KT, et al. Neuropeptide Y Induces Hematopoietic Stem/Progenitor Cell Mobilization by Regulating Matrix Metalloproteinase-9 Activity Through Y1 Receptor in Osteoblasts. *Stem Cells* (2016) 34(8):2145–56. doi: 10.1002/stem.2383
93. Jiang Y, Zhang P, Zhang X, Lv L, Zhou Y. Advances in Mesenchymal Stem Cell Transplantation for the Treatment of Osteoporosis. *Cell Prolif* (2021) 54(1):e12956. doi: 10.1111/cpr.12956
94. Ono M, Kosaka N, Tominaga N, Yoshioka Y, Takeshita F, Takahashi RU, et al. Exosomes From Bone Marrow Mesenchymal Stem Cells Contain a microRNA That Promotes Dormancy in Metastatic Breast Cancer Cells. *Sci Signal* (2014) 7(332):ra63. doi: 10.1126/scisignal.2005231

Conflict of Interest: The authors declare that the research was conducted in the absence of any commercial or financial relationships that could be construed as a potential conflict of interest.

Publisher's Note: All claims expressed in this article are solely those of the authors and do not necessarily represent those of their affiliated organizations, or those of the publisher, the editors and the reviewers. Any product that may be evaluated in this article, or claim that may be made by its manufacturer, is not guaranteed or endorsed by the publisher.

frontiers in Endocrinology

ORIGINAL RESEARCH
published: 13 January 2022
doi: 10.3389/fendo.2021.815245

Analysis and Validation of Hub Genes in Blood Monocytes of Postmenopausal Osteoporosis Patients

Yi-Xuan Deng[1,2†], Wen-Ge He[2,3,4†], Hai-Jun Cai[1,2], Jin-Hai Jiang[1,2], Yuan-Yuan Yang[1,2], Yan-Rong Dan[1,2], Hong-Hong Luo[1,2], Yu Du[3], Liang Chen[3,4] and Bai-Cheng He[1,2*]*

[1] Department of Pharmacology, School of Pharmacy, Chongqing Medical University, Chongqing, China, [2] Key Laboratory of Biochemistry and Molecular Pharmacology of Chongqing, Chongqing Medical University, Chongqing, China, [3] Department of Orthopaedics, The Second Affiliated Hospital, Chongqing Medical University, Chongqing, China, [4] Department of Bone and Soft Tissue Oncology, Chongqing University Cancer Hospital, Chongqing, China

OPEN ACCESS

Edited by:
Sadiq Umar,
University of Illinois at Chicago,
United States

Reviewed by:
Md Zahid Akhter,
University of Illinois at Chicago,
United States
Farhath Sultana,
Mount Sinai Hospital, United States

***Correspondence:**
Liang Chen
Chen.liang.1979@cqu.edu.cn
Bai-Cheng He
bche@cqmu.edu.cn

[†]These authors have contributed equally to this work

Specialty section:
This article was submitted to Bone Research, a section of the journal Frontiers in Endocrinology

Received: 15 November 2021
Accepted: 13 December 2021
Published: 13 January 2022

Citation:
Deng Y-X, He W-G, Cai H-J, Jiang J-H, Yang Y-Y, Dan Y-R, Luo H-H, Du Y, Chen L and He B-C (2022) Analysis and Validation of Hub Genes in Blood Monocytes of Postmenopausal Osteoporosis Patients. Front. Endocrinol. 12:815245. doi: 10.3389/fendo.2021.815245

Osteoporosis is a common systemic bone disease caused by the imbalance between osteogenic activity and osteoclastic activity. Aged women are at higher risk of osteoporosis, partly because of estrogen deficiency. However, the underlying mechanism of how estrogen deficiency affects osteoclast activity has not yet been well elucidated. In this study, GSE2208 and GSE56815 datasets were downloaded from GEO database with 25 PreH BMD women and 25 PostL BMD women in total. The RRA algorithm determined 38 downregulated DEGs and 30 upregulated DEGs. Through GO analysis, we found that downregulated DEGs were mainly enriched in myeloid cell differentiation, cytokine-related functions while upregulated DEGs enriched in immune-related biological processes; pathways like Notch signaling and MAPK activation were found in KEGG/Rectome pathway database; a PPI network which contains 66 nodes and 91 edges was constructed and three Modules were obtained by Mcode; Correlation analysis helped us to find highly correlated genes in each module. Moreover, three hub genes FOS, PTPN6, and CTSD were captured by Cytohubba. Finally, the hub genes were further confirmed in blood monocytes of ovariectomy (OVX) rats by real-time PCR assay. In conclusion, the integrative bioinformatics analysis and real-time PCR analysis were utilized to offer fresh light into the role of monocytes in premenopausal osteoporosis and identified FOS, PTPN6, and CTSD as potential biomarkers for postmenopausal osteoporosis.

Keywords: postmenopausal osteoporosis, microarray, enrichment analysis, hub genes, OVX

INTRODUCTION

Osteoporosis is a common systemic bone disease caused by the decrease of bone density and bone mass, the destruction of bone microstructure, the increase of bone fragility and the easy occurrence of fracture due to a variety of reasons (1). One in three women and one in five men over the age of 50 are at risk of osteoporotic fractures. The prevalence of osteoporosis in people over 50 years of age

was 19.2%, 6.0% for men and 32.1% for women in China. The prevalence of osteoporosis in people over 65 years of age was as high as 32.0%, with 10.7% in men and 51.6% in women (2). According to the pathogenetic factors of osteoporosis, it can be divided into primary osteoporosis and secondary osteoporosis. The former includes postmenopausal osteoporosis and senile osteoporosis, of which postmenopausal osteoporosis is one of the most common types of osteoporosis (3).

Postmenopausal osteoporosis (PMOP) is a metabolic disease that is caused by the reduction of ovarian function and decreasing estrogen levels in postmenopausal women (4). The etiology of PMOP is complex, and the precise mechanism is yet unknown. A variety of signaling pathways and immune factors, such as receptor activator of nuclear factor-κB/receptor activator of nuclear factor-κB ligand/osteoprotegerin, Wnt/β-catenin, Semaphorin3A/neuropilin-1, peroxisome proliferator-activated receptor, and others, may be involved in the regulation of PMOP, which form a regulatory network in the body and cause an imbalance in the process of bone remodeling, and when the bone destruction is greater than the bone formation, PMOP ultimately manifests (5–8).

It is well known that osteoporosis is closely related to bone formation, remodeling, and resorption, which mainly depends on the activity of osteoblasts and osteoclasts (9). Osteoblasts are the major cellular components of bone, derived from mesenchymal stem cells, and abundant in periosteum, the thin connective tissue layer on the outer surface of bone and the intima (10). They deposit new bone minerals through a mechanism that has not yet been fully described. Osteoclasts are multinucleated cells derived from bone marrow hematopoietic progenitor cells. They have highly active ion channels on the membrane and can pump protons into the extracellular space, thereby reducing the pH of their own microenvironment to promote bone resorption (11). Although there has been significant progress in pathogenesis for osteoporosis, effects of blood monocytes on osteoporosis, especially postmenopausal osteoporosis, need to be further elucidated.

In recent years, with the continuous development and maturity of gene detection technology, microarray and high-throughput sequencing technology are increasingly widely used to search for potential biomarkers related to diagnosis, treatment, and prognosis. It is well known that public databases such as the Gene Expression Omnibus (GEO) are widely used to explore diagnostic and prognostic biomarkers for many diseases. Meanwhile, in order to overcome the limited or inconsistent results caused by different technology platforms and small sample sizes, robust rank aggregation (RRA) was used to obtain robust difference expressed genes (DEGs) (12). This method is widely used in the comprehensive analysis of multiple data sets and is robust to errors and noise (13–15). However, there have been no reports of RRA in postmenopausal osteoporosis.

Animal models of osteoporosis can be used to investigate new techniques of prevention and therapy of osteoporosis. The ovariectomy rat model (OVX) is the first alternative, and it is the most commonly utilized approach in such investigations (16). The ovariectomy rat model is an excellent preclinical model for postmenopausal osteoporosis, according to FDA recommendations (17). The de-ovulatory rat osteoporosis model replicates estrogen deficiency-induced bone loss and shows postmenopausal osteoporosis clinical symptoms (18). Furthermore, it was reported that six months is the optimal time to induce OVX. The success of OVX can be verified 1–3 weeks after surgery, when the normal estrous cycle is stopped, estradiol, progesterone, and uterine weight are decreased, and LH and FSH levels are increased (19). Therefore, it is a suitable tool for the OVX model to study postmenopausal osteoporosis.

In this study, the mRNA expression data of blood monocytes of PMOP from the GEO databases were analyzed by RRA, and we further explored the development of PMOP through functional enrichment and protein-protein interaction (PPI) analysis. Then, the hub genes we got were subjected to real-time PCR analysis for further validation in the OVX model. This study provides a possible basis for understanding the etiology and potential molecular events of PMOP by analyzing the differentially expressed genes.

MATERIALS AND METHODS

Sample Collection

Samples of monocytes were isolated from whole blood of aged women which were obtained from the Gene Expression Omnibus (GEO) database (20). Searching terms as "BMD", "Osteoporosis", "postmenopausal", "Gene expression", "Microarray", and the datasets which are according to the following criteria will be adopted: (1) at least 10 samples each are included; (2) at least 5 cases of PMOP and 5 controls are included; and (3) raw data or series matrix file is available in GEO datasets. We finally found two datasets, GSE56815 and GSE2208 (21,22), which are completely in conformity with our criteria. Five cases of PMOP and 5 controls in GSE2208 while 20 cases of PMOP and 20 controls in GSE56815 are collected from the corresponding datasets. More information is shown on **Table 1**.

Datasets Analyses

The annotated R package was downloaded through Bioconductor and the microarray probes were converted to symbols in R. The Limma package of R software was used to identify the differentially expressed genes (DEGs) associated with the PreH group and the PostL group. P-Value <0.05 and |log2 fold change (FC)| >0 were regarded as the threshold to determine the DEGs (23).

RRA Analysis

"Robust Rank Aggregation" package (24), which could effectively reduce the errors by integrating the DEGs of these two microarray datasets and correcting for multiple times, was used to screen the robust DEGs. Genes with P-Value <0.05 and |log2 fold change (FC)| >0.5 in the ranking list were selected

TABLE 1 | Information for selected microarray datasets.

Sr. No	GEO Accession Total samples	Selected samples Platform	Source tissue
	19 samples	10 samples	blood monocytes
1	GSE2208 Sample types:	GPL96 Sample types:	
	10 high BMD	5 PreH BMD	
	9 low BMD	5 postL BMD	
	80 samples	40 samples	
2	GSE56815 Sample types:	GPL96 Sample types:	blood monocytes
	40 high BMD	20 PreH BMD	
	40 low BMD	20 postL BMD	

as upregulated/downregulated DEGs respectively for further study.

Enrichment Analysis

Gene Ontology (GO) enrichment and the Kyoto Encyclopedia of Genes and Genomes (KEGG)/Reactome Pathway Database were used to figure out the functional roles of the Robust DEGs. The GO enrichment results, namely, biological process (BP), cellular component (CC), and molecular function (MF) were performed by using R package "clusterprofiler" with the criteria of P-Value <0.05 and P-Value <0.05. Cytoscape software plug-in ClueGO was used for pathway analysis. The criterion was that a node contained at least 3 genes and the medium Kappa score was used for pathway network connectivity (P <0.05 was considered statistically significant) (25,26). GO enrichment of Robust DEGs used the cut off criteria of P-Value <0.05. The bubble color represents P-Value in enriched pathways, and the size of the bubble represents the gene number. In the pathway enrichment analysis, each node represents a pathway, the connection between the nodes reflects the correlation between the pathways, and the size of the nodes indicates the degree of gene enrichment. All nodes contain at least three genes, and each node has a P-value <0.05.

PPI Network Construction and its Sub-Module Analysis

By uploading the whole robust DEGs to the STRING online database (27), the PPI network which contains 66 nodes and 91 edges with confidence >0.4, was established. Pulling the results into Cytoscape (28), we visualized the PPI network and screened three key modules by using MCODE plugin.

Correlation Analysis

After finding the key modules, we used Pearson's correlation coefficient as an analysis method to visualize statistically significant (P-Value <0.05) and highly correlated genes in the modules by correlation analysis. Also, genes that are not statistically different are indicated by a cross. In this analysis, Package "corrplot" was used to visualize the results (29,30).

Hub Gene Identification

To obtain as much of exact hub genes, 10 different algorithms including MCC, DMNC, MNC, Degree, EPC, BottleNeck, EcCentricity, Closeness, Radiality, and Betweenness (each approach could predict the hub genes) in Cytohubba was used (31). The first ten top ranked genes of each algorithm were regarded as the hub genes of the algorithm. After calculating, we took the one that intersects most of these algorithms and finally 3 downregulated genes which appear in nine out of ten were regarded as the most likely hub genes. Our outcome was visualized by using the R package "UpSetR" and the hub genes were represented in the red bar (32).

OVX Model Construction

Twelve healthy female Sprague Dawley (SD) rats aged 8 weeks were purchased from the Animal Experiment Center of Chongqing Medical University. SD Rats were randomly divided into two groups: the sham operation group and the ovariectomy (OVX) group, and after 1 week of maintenance in a pathogen-free facility, bilateral ovariectomy and sham operation were performed as previously reported (33,34). Twelve weeks after surgery, the rats were sacrificed and femur and blood samples were collected and stored for further testing. This experiment was approved by the institutional animal care and use committee of Chongqing Medical University (Chongqing, China).

Microcomputed Tomography (μ-CT) Analysis of the Proximal Femur

All the femurs were dissected, cleaned, and fixed in 4% paraformaldehyde. Then, they were scanned by a microcomputed tomography 100 (μ-CT100) system (SCANCO MicroCT). Proximal femurs were scanned by using a 20 μm voxel size, 70 kV, 200 μA and 0.6° rotation steps (180° angular range). For the trabecular bone, an area of 1.5 mm thick downward from the proximal femur growth plate was evaluated by μ-CT. This area is located 1.5 mm below the growth plate. μ-CT 516.1 software was used for 3D reconstruction and quantitative analysis. After 3D reconstruction, the bone mineral density (BMD), bone volume fraction (BV/TV), trabecular thickness (Tb.th), trabecular number (TB.n), and trabecular spacing (TB.sp) were calculated or directly measured by using μCT100 system (SCANCO MicroCT).

Quantitative Real Time PCR Assay

Monocytes were isolated from whole blood by rat peripheral blood mononuclear cell Isolation kit. Total RNA was extracted from monocytes using SteadyPure Quick RNA Extraction Kit (AG21023-S AG). Real time PCR was performed using SYBER green mixture kit with gene specific primers (**Table 2**). The RT-PCR amplification reactions were performed using

QuantStudio™ 3(Thermo Fisher SCIENTIFIC). The RT-PCR program was programmed to perform 42 cycles in total. The mean value and standard error of three independent experiments were calculated, and each experiment was repeated 3 times. The relative mRNA expression level was calculated using β-actin as internal reference.

Statistical Analysis

The quantitative data was presented as the mean ± SD. The two-tailed Student's t-test was used to analyze the differences between the two groups. Each assay condition was performed in triplicate for all quantitative assays. All data collected were statistically analyzed. A P-value of less than 0.05 was defined as statistically significant.

RESULTS

Identification of Robust DEGs Between Premenopausal High BMD and Postmenopausal Low BMD

According to the previous criteria, samples from two microarray datasets, GSE2208 and GSE56815, were downloaded from the GEO database. The two datasets contain 50 samples in total, one half were from premenopausal high BMD women, the other half were from postmenopausal low BMD women. The details of each dataset are shown in **Table 1**. To explore the most valuable differential genes, we first analyzed the DEGs by using R software through "Limma" package and presented it in the form of Volcano plot (**Figures 1A, B**). Then the "Robust Rank Aggregation" package (RRA) was used to screen Robust genes with P-Value <0.05 and |logFC| >0.5. Finally, 38 DEGs that were downregulated and 30 DEGs that were upregulated were found. The top 20 downregulated DEGs and top 20 upregulated DEGs were presented in a heatmap (**Figure 1C**).

Functional Enrichment Analysis of Robust DEGs

To figure out the functions of Robust DEGs, "clusterprofiler", an R package, was used for GO enrichment (biological process, molecular function, and cellular component) (**Figure 2**) and CLUEGO was used to find out the statistically significant pathways through the KEGG/Reactome database (**Figure 3**). To make sure the outcomes are clear and intuitive, the upregulated DEGs and downregulated DEGs were analyzed separately in GO enrichment. The downregulated genes, the results revealed that myeloid cell differentiation which is significantly enriched in GO analysis, are highly associated with the emergence of monocytes and granulocytes. Additionally the complicated biological processes, namely, regulation of cytokine biosynthetic process, cytokine biosynthetic process, and cytokine metabolic process, have all been linked to osteoporosis. In the upregulated genes, immune-related processes, namely, neutrophil degranulation, neutrophil activation involved in immune response, neutrophil activation, neutrophil mediated immunity, and immunoglobulin binding, have long been recognized to have a relationship with the skeletal systems.

There were fourteen pathways significantly enriched in robust DEGs. Notch signaling pathway is of great importance in Human Skeletal Diseases, and collagen degradation, to a large extent, affecting the balance of bone formation and bone resorption. Moreover, the immune system mediated by PD-1 signaling and the activation of MAPK signaling pathway are also involved in bone regulation. The genes contained in each node and the number of genes, and the P-value of the node are detailed in the **Supplementary Material** (**Data Sheet 1**).

PPI Network Construction and Its Sub-Module Analysis

The robust DEGs were used to construct the PPI network for further study. The results show that with confidence >0.4, a PPI network which contains 66 nodes and 91 edges was constructed (**Figure 4**). MCODE plugin was used to explore those highly connected modules, and three of them were found (**Figures 5A–C**). The genes in Module one were connected with TNF signaling pathway and osteoclast differentiation while genes in Module two were associated with antigen processing, presentation, and antigen receptor-mediated signaling pathway. Besides, the BP of genes in Module three was particularly related to extracellular matrix disassembly.

Correlation Analysis of Highly Connected Genes in Each Module

Pearson's correlation coefficient, as an analysis method, and package "correplot" were used to calculate and visualize statistically significant (P-Value <0.05) and highly correlated genes in the modules by correlation analysis. Also, genes that are not statistically different are indicated by a cross. By this

TABLE 2 | The primers used for PCR.

Gene	Primer	Sequence (5'-3')
β-actin	F	GGAGATTACTGCCCTGGCTCCTA
	R	GACTCATCGTACTCCTGCTTGCTG
FOS	F	TGCAGACCGAGATTGCCAAT
	R	CCTCAGACTCTGGGGTGGTA
CTSD	F	GGTCCCCTCCATTCATTGCA
	R	ATGGAACCGACACAGTGTCC
PTPN6	F	TGCAGGGACGTGACAGTAAC
	R	TGACACGAGTGTTCTCCTGC

F, Forward; R, Reverse.

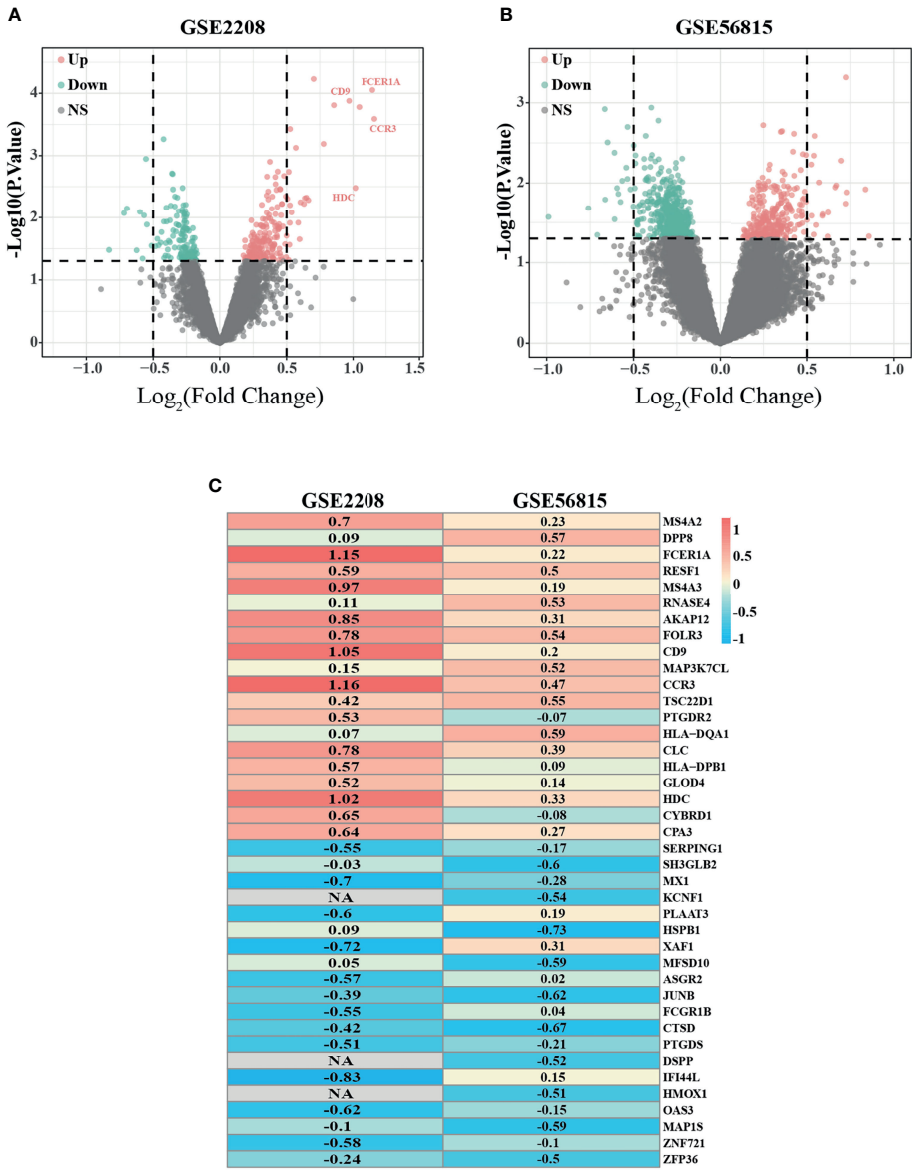

FIGURE 1 | Identification of differentially expressed genes (DEGs) with the cut off criteria of P-Value <0.05. **(A)** Volcano plot of DEGs for GSE2208 datasets. **(B)** Volcano plot of DEGs for GSE56815 datasets. **(C)** The heatmap of top 40 (20 upregulated DEGs and 20 downregulated DEGs) DEGs according to RRA algorithm. As the color goes from red to blue, indicating the changing from up to downregulation. NA represents genes with no statistical significance in GSE2208, but it can be reflected in RRA algorithm because of its high ranking and small P value in GSE56815. Similar results can be referenced in https://doi.org/10.3389/fonc.2019.00996.

method, we identified genes with significant positive correlations, such as PTPN6 vs CTSD and JUNB vs ZFP36. We also found many genes with significant negative correlations, such as CTSD vs HLA-DPB1 and ADAM10 vs ITGAL. These findings provide us new insight for finding potential biomarkers (**Figures 5D–F**).

Identification of Hub Genes and Their Expression in Different Dataset

Cytohubba, as a Cytoscape plugin, is applied to search for the hub genes, and was used to obtain as many of exact hub genes (**Figure 6A**). We picked up the most intersection genes by calculating ten different algorithms, and then we explored the description of those three hub genes, namely, their full names, synonyms and functions (**Table 3**). Subsequently, we presented the consistent expression of these three hub genes of different datasets by violin plots (**Figures 6B–G**).

Validation of the Hub Genes *In Vivo*

In order to verify the hub genes *in vivo*, OVX rats were used to replace the PMOP patients for the validation. A diagram exhibited how we validate our results of hub genes (**Figure 7A**). We confirmed that the OVX model was

TABLE 3 | Description of the Hub genes.

Gene	Full name	Synonyms	Function
FOS	proto-oncogene c-fos	G0S7	On TGF-beta activation, forms a multimeric SMAD3/SMAD4/JUN/FOS complex at the AP1/SMAD-binding site to regulate TGF-beta-mediated signaling. Has a critical function in regulating the development of cells destined to form and maintain the skeleton. It is thought to have an important role in signal transduction, cell proliferation and differentiation.
CTSD	Cathepsin D	CPSD	Acid protease active in intracellular protein breakdown. Plays a role in APP processing following cleavage and activation by ADAM30 which leads to APP degradation
PTPN6	Tyrosine-protein phosphatase non-receptor type 6	HCP, PTP1C	Modulates signaling by tyrosine phosphorylated cell surface receptors such as KIT and the EGF receptor/EGFR. The SH2 regions may interact with other cellular components to modulate its own phosphatase activity against interacting substrates. Together with MTUS1, induces UBE2V2 expression upon angiotensin II stimulation. Plays a key role in hematopoiesis.

successfully established through the μ-CT analysis femur of the SD rat three months later after surgery, and the femur 1.5 mm thick below the growth plate was used for analysis of bone cortex and cancellous bone. The μ-CT analysis results showed that the OVX group had fewer trabeculae than the sham group, whereas there was little difference in bone cortex (**Figure 7B**). Meanwhile, the mRNA of monocytes isolated from whole blood was used to detect the expression of those three hub genes (FOS, CTSD, and

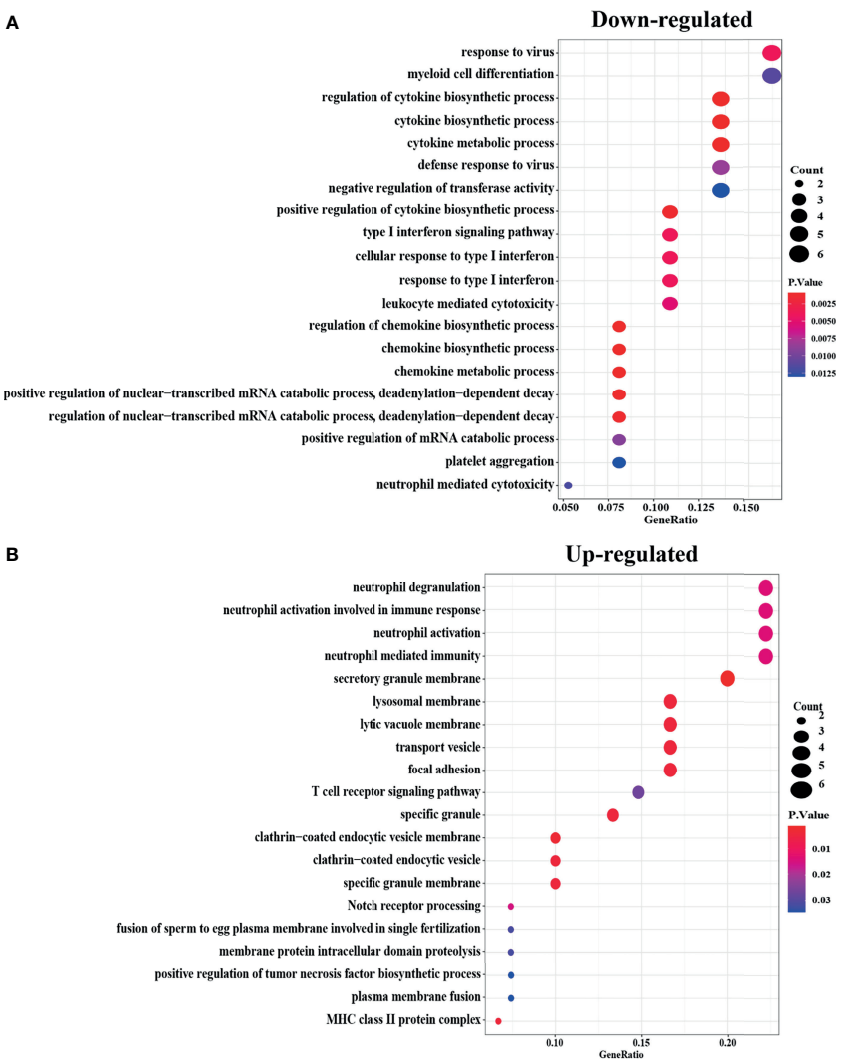

FIGURE 2 | GO enrichment of Robust DEGs with the cut off criteria of P-Value <0.05. The bubble color represents P-Value in enriched pathways, and the size of the bubble represents the gene number. **(A)** Downregulated Robust DEGs in three parts of GO enrichment (BP, CC, and MF). **(B)** Upregulated Robust DEGs in three parts of GO enrichment (BP, CC, and MF). DEG, differentially expressed gene; GO, Gene Ontology; BP, biological process; CC, cellular component; MF, molecular function.

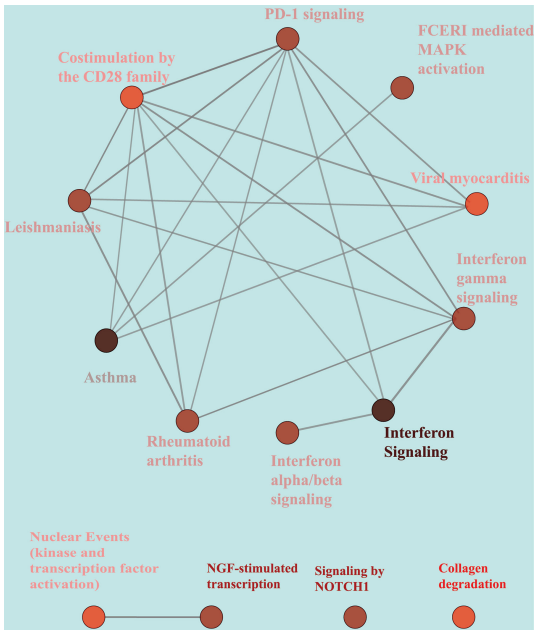

FIGURE 3 | KEGG/Rectome pathways enrichment analysis of Robust DEGs. KEGG, Kyoto Encyclopedia of Genes and Genomes. Rectome, Rectome pathway database.

PTPN6) that we found by bioinformatics analysis, and the real-time PCR results showed that the mRNA expression level of the three hub genes in OVX group was lower than that in the sham group (**Figures 7C–E**). These results are consistent with the bioinformatics analysis results, indicating that the hub genes may be used as biomarkers of PMOP. However, the exact mechanism needs to be further elucidated.

DISCUSSION

Postmenopausal osteoporosis (PMOP) is a complex bone metabolism disorder characterized by the loss of bone minerals and an increased risk of bone fracture. PMOP is recognized as a metabolism disease which is caused by the imbalance between bone formation and bone resorption after estrogen deficiency. In

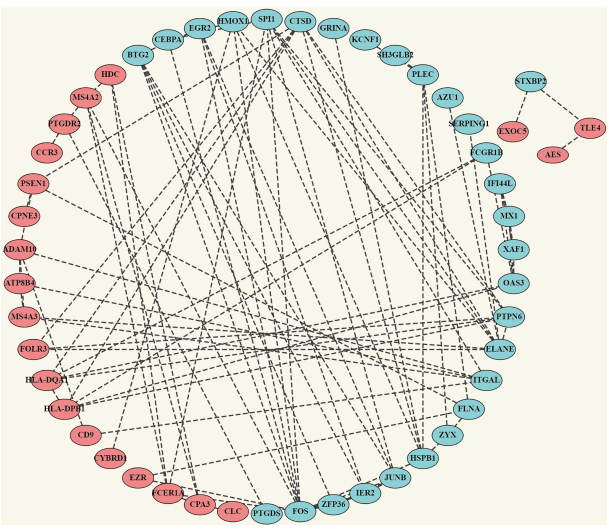

FIGURE 4 | Construction of PPI network. Complete PPI network diagram which contains 66 nodes and 91 edges with the confidence >0.4. Upregulated Robust DEGs are marked in red while Downregulated Robust DEGs are marked in blue. PPI, Protein–Protein Interaction Network.

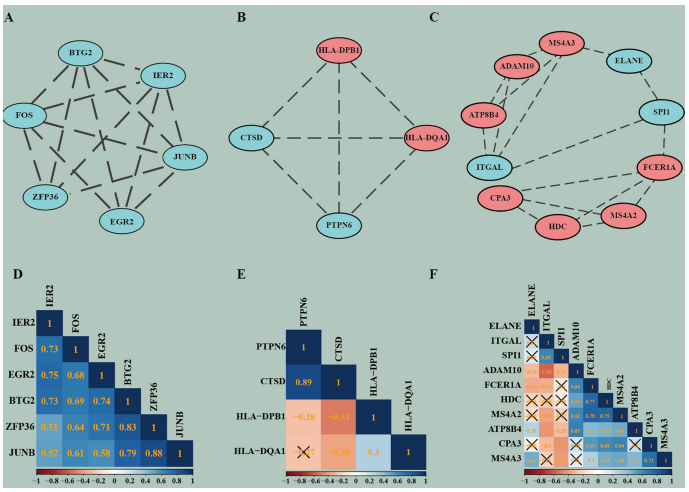

FIGURE 5 | The highly connected modules of PPI and the correlation matrix corresponding to each module. **(A–C)** Modules of PPI network. **(D–F)** Correlation matrixes of highly connected genes in each module. In the modules, red represents genes that are upregulated and blue represents genes that are downregulated. In the correlation analysis, blue indicates positive correlations, red indicates negative correlations, and higher values indicate higher correlations. Squares marked with a cross indicate that the correlation analysis between genes is not statistically significant ($P > 0.05$).

previous studies, many susceptibility genes for PMOP (35,36), especially cytokines and osteoprotegerin, which are involved in bone remodeling balance, have been identified. It is well known that TNF-α has been shown to affect bone metabolisms by promoting osteoclast differentiation and inhibiting osteoblast differentiation (37). Spon1 may play an important role in the etiology of PMOP (20). However, the use of RRA to detect DEGS in PMOP has not been reported. Therefore, it is very important to investigate the cause of this disease and to find potential treatments by identifying the susceptibility gene of PMOP. This study was the first to search and combine microarrays on PMOP in GEO, in particular, the detection and analysis of blood monocytes, which has not been studied in previous research. It is well known that blood monocytes are precursors of osteoclasts (38), and blood monocytes can secrete a number of potent cytokines important for osteoclast differentiation, activation, and apoptosis (39). The aim of our research was to identify key genes and pathways involved in the pathogenesis of PMOP. Therefore, two microarrays were included in our studies, gene expression profiles of PMOP were compared with controls, and the RRA analysis was adopted to integrate results with more statistical power. Furthermore, PPI network construction and Gene Ontology (GO) enrichment were performed to understand the potential biological function of the DEGs. Meanwhile, hub genes were calculated for further study.

There were 68 DEGs filtered out from two datasets with 38 downregulated genes and 30 upregulated. FOS, PTPN6, and CTSD were the most significant genes among these DEGs, which were identified as hub genes by PPI network analysis. As we all know, FOS is a member of the AP-1 transcription factor complex, which is a central regulator for many physiological functions. In osteoimmunology, Fos/AP-1, as osteoclastogenic transcription factor, plays a critical role in inflammatory bone loss by regulating genes like NFATc1 and also the interferon system (40–42). In the previous study, Sugatani found a positive feedback loop of c-Fos/miR-21/PDCD4, which regulates osteoclastogenesis (43). Besides, the FOS-related protein Fra-2 controls osteoclast size and survival (44).

PTPN6, a cytoplasmic phosphatase, functions to prevent autoimmune and interleukin 1 receptor (IL-1R)-dependent caspase-1-independent inflammatory disease. It has dual function in negative regulation of p38 mitogen-activated protein kinase activation to control tumor necrosis factor and IL-1α/β expression, thereby inhibiting caspase-8-and Ripk3/Mlkl-dependent inflammation (45). Moreover, PTPN6 can regulate the activity of over 50 cytoplasmic signaling proteins and cell surface receptors. It has been reported that PTPN6 mediated autophagy contributes to the inhibition of macrophage foam cell formation by the D3-VDR-PTPN6 axis (46), and participates in the epigenetic regulation mechanism of advanced chronic myeloid leukemia (47). Besides, PTPN6 was upregulated in the coculture system which consists of primary myeloma and healthy donor hematopoietic bone marrow, indicating that PTPN6 plays an important role in microenvironment interactions (48). Another hub gene, CTSD, which is one of the major lysosomal proteases indispensable for the maintenance of cellular proteostasis by turning over substrates of endocytosis, phagocytosis, and autophagy. Consequently, CTSD deficiency leads to a strong impairment of the lysosomal-autophagy machinery (49). However, there were few studies about the definite function and mechanisms of PTPN6 and CTSD in PMOP.

In our GO enrichment analysis, we divided DEGs into two groups. In the downregulated genes, results revealed that myeloid cell differentiation is highly associated with the emergence of monocytes and granulocytes, and the regulation

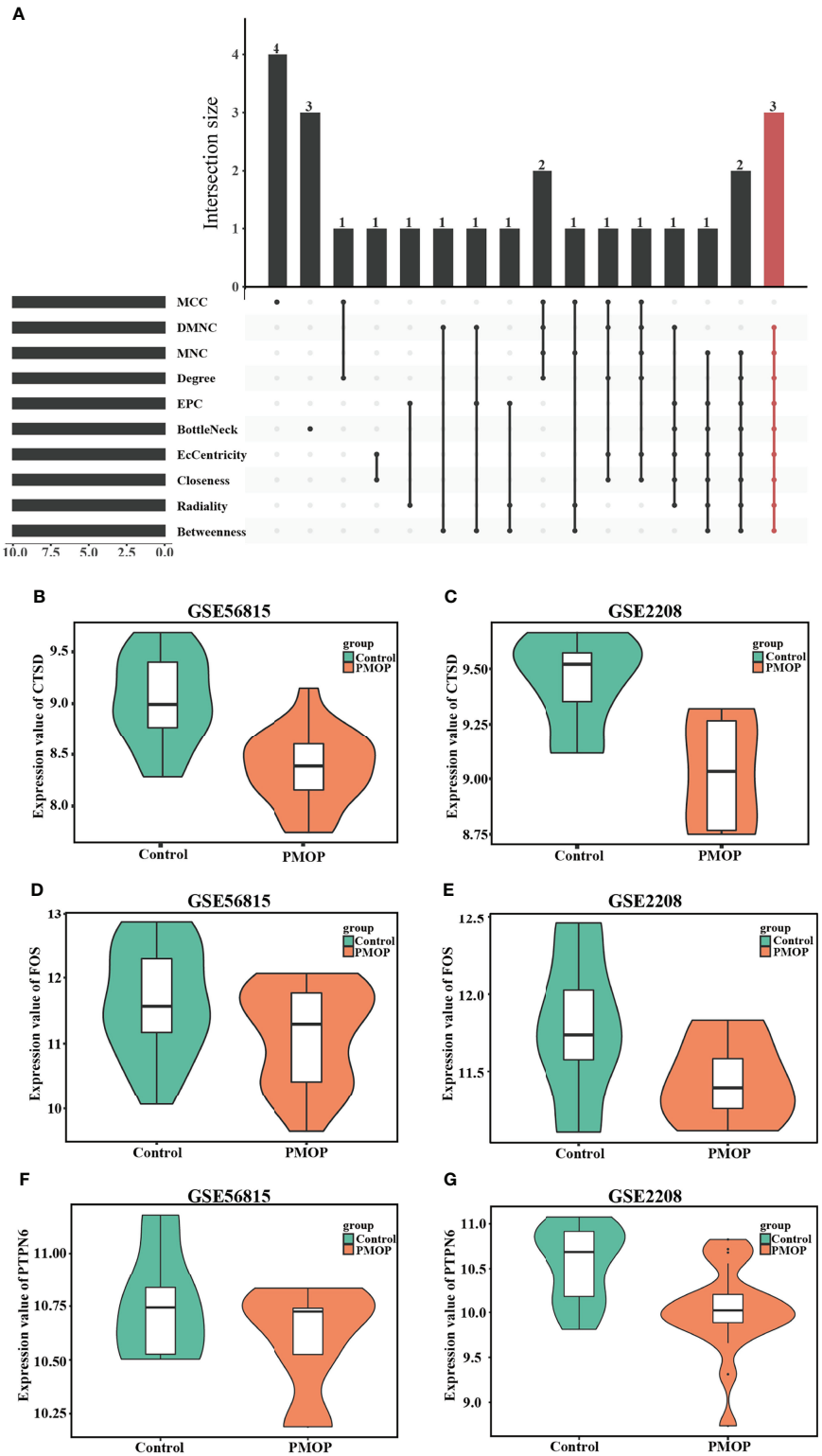

FIGURE 6 | Identification of hub genes and Boxplot of hub genes that expressed consistently across two datasets. **(A)** Hub genes were identified by intersection of 50 genes from 10 algorithms, namely, MCC, DMNC, MNC, Degree, EPC, BottleNeck, EcCentricity, Closeness, Radiality, and Betweenness. The consistent expression of CTSD in **(B)** GSE56815 and **(C)** GSE2208. The consistent expression of FOS in **(D)** GSE56815 and **(E)** GSE2208. The consistent expression of PTPN6 in **(F)** GSE56815 and **(G)** GSE2208.

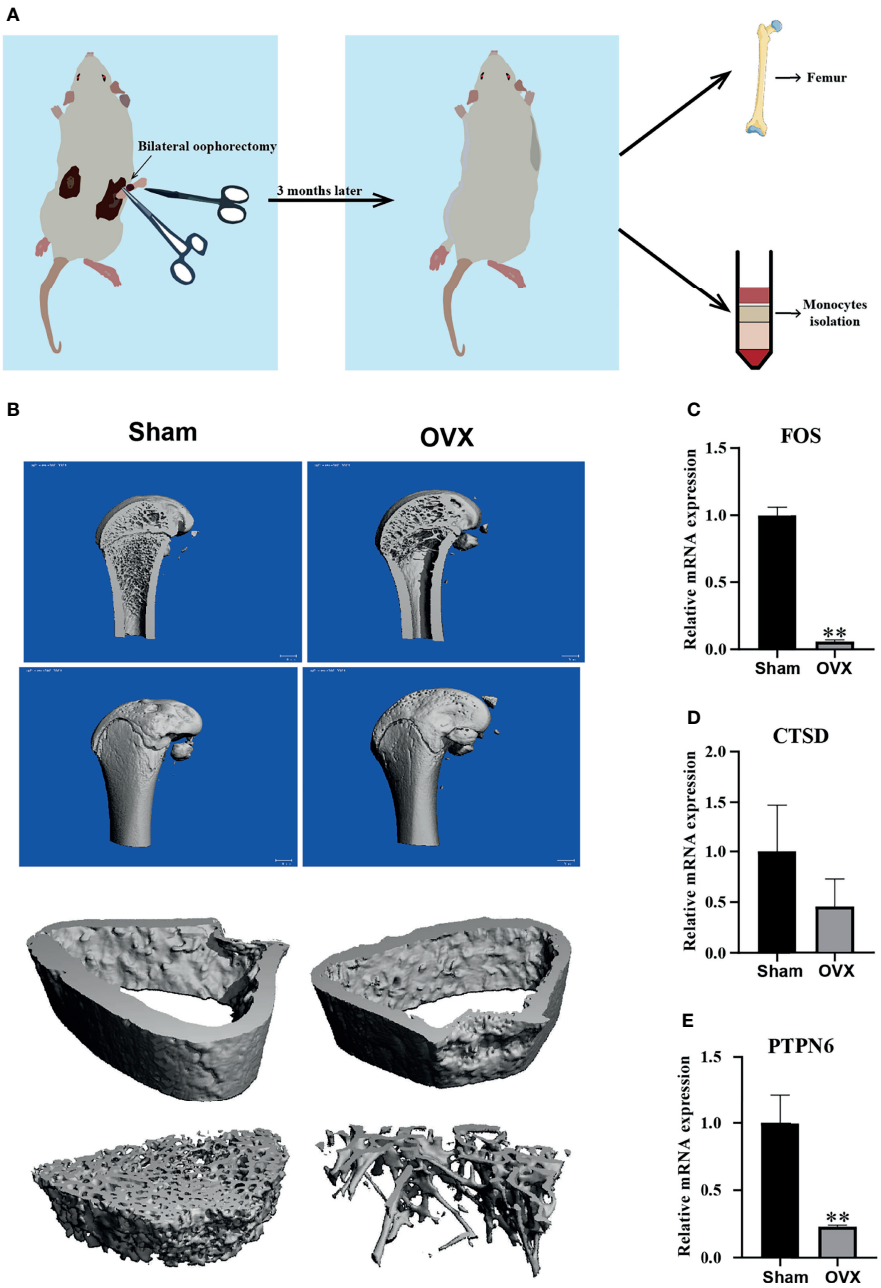

FIGURE 7 | Validation of the hub genes *in vivo*. **(A)** A diagram exhibited how we validate our results of hub genes. **(B)** Representative μ-CT analysis image of SD rat femur in sham and OVX group, and femur 1.5 mm thick below the growth plate was used for analysis of bone cortex and cancellous bone. **(C–E)** The mRNA expression level of three hub genes (FOS, CTSD, and PTPN6) in sham group and OVX group. Compared with the Sham group, $^{**}p < 0.01$.

of cytokine metabolic process and cytokine biosynthetic process. These complicated biological processes have all been linked to osteoporosis (11,50,51). While in the upregulated genes, immune-related processes such as neutrophil activation, neutrophil degranulation involved in immune response, neutrophil activation, neutrophil mediated immunity and immunoglobulin binding have long been recognized to have a relationship with the skeletal systems (52).

In the current study, we established a postmenopausal osteoporosis model in rats by bilateral oophorectomy. We found that PTPN6, CTSD, and FOS from blood monocytes in the OVX group were lower than that in the control group, which is consistent with our bioinformatic analysis results. However, monocytes isolated from the whole blood of older women may yield different sequencing data than OVX rats. It is a pity that we cannot get sequencing data from monocytes of humans because

of strict social rules and ethical requirements during the COVID-19 pandemic. These findings provide a new target for further research on the role of blood monocytes in the development of postmenopausal osteoporosis. However, the occurrence of postmenopausal osteoporosis involves estrogen level, immune factors, osteoblast activity, and many other factors. It will be worthwhile to further study the roles of PTPN6, CTSD, and FOS in other cells or biological processes except osteoclasts, and explore their significance in the occurrence and development of osteoporosis from the perspective of proteomics and protein modification omics. At last, we believe our results from the GEO data and animal experiment validation may provide a fresh light into the role of monocytes in premenopausal osteoporosis and identified FOS, PTPN6, and CTSD as potential biomarkers for premenopausal osteoporosis.

In conclusion, by using the RRA approach, our study successfully provided a deeper understanding of the overall molecular changes in the pathogenesis of PMOP and identified several potential therapeutic candidates, namely, FOS, PNPT6, and CTSD, as central genes. Besides, through GO and KEGG pathway analysis, we found that these differential genes were mainly enriched in cytokine metabolic process and cytokine biosynthetic process, and may be involved in Notch signaling pathway and immune system. Collectively, this study may provide reliable molecular biomarkers for diagnosis, screening and prognosis of PMOP. It also lays a foundation for exploring new therapeutic targets of PMOP. However, the underlying molecular mechanisms have not yet been fully elucidated. In the future, more experiments are needed to verify the changes of gene expression and it is necessary to collect a large number of bone marrow tissues from patients with PMOP and bone tissues from normal controls for further research.

DATA AVAILABILITY STATEMENT

The datasets presented in this study can be found in online repositories. The names of the repository/repositories and accession number(s) can be found in the article/**Supplementary Material**.

ETHICS STATEMENT

The animal study was reviewed and approved by The Ethics Committee of Chongqing Medical University.

AUTHOR CONTRIBUTIONS

Funding acquisition, YD and LC. Investigation, H-JC, J-HJ, Y-YY, and H-HL. Software, Y-RD. Supervision, CH. Validation, Y-XD and W-GH. Writing—Original draft, Y-XD and W-GH.

FUNDING

This work was supported by the National Natural Science Foundation of China (NSFC, 81572226 to B-CH) and the youth project (Grant No. 82000836 to YD).

SUPPLEMENTARY MATERIAL

The Supplementary Material for this article can be found online at: https://www.frontiersin.org/articles/10.3389/fendo.2021.815245/full#supplementary-material

REFERENCES

1. Ohta H, Solanki J. Incorporating Bazedoxifene Into the Treatment Paradigm for Postmenopausal Osteoporosis in Japan. *Osteoporos Int* (2015) 26(3):849–63. doi: 10.1007/s00198-014-2940-x
2. Compston JE, McClung MR, Leslie WD. Osteoporosis. *Lancet* (2019) 393 (10169):364–76. doi: 10.1016/S0140-6736(18)32112-3
3. Khosla S, Melton LJ3rd, Riggs BL. The Unitary Model for Estrogen Deficiency and the Pathogenesis of Osteoporosis: Is a Revision Needed? *J Bone Miner Res* (2011) 26(3):441–51. doi: 10.1002/jbmr.262
4. Selby P. Postmenopausal Osteoporosis. *Curr Osteoporos Rep* (2004) 2(3):101–6. doi: 10.1007/s11914-004-0018-y
5. Shen G, Ren H, Shang Q, Zhao W, Zhang Z, Yu X, et al. Foxf1 Knockdown Promotes BMSC Osteogenesis in Part by Activating the Wnt/β-Catenin Signalling Pathway and Prevents Ovariectomy-Induced Bone Loss. *EBioMedicine* (2020) 52:102626. doi: 10.1016/j.ebiom.2020.102626
6. Liu YQ, Han XF, Bo JX, Ma HP. Wedelolactone Enhances Osteoblastogenesis But Inhibits Osteoclastogenesis Through Sema3A/NRP1/PlexinA1 Pathway. *Front Pharmacol* (2016) 7:375. doi: 10.3389/fphar.2016.00375
7. Catalano A, Loddo S, Bellone F, Pecora C, Lasco A, Morabito N. Pulsed Electromagnetic Fields Modulate Bone Metabolism *via* RANKL/OPG and Wnt/β-Catenin Pathways in Women With Postmenopausal Osteoporosis: A Pilot Study. *Bone* (2018) 116:42–6. doi: 10.1016/j.bone.2018.07.010
8. Wang Y, Pan Z, Chen F. Inhibition of Pparγ by Bisphenol A Diglycidyl Ether Ameliorates Dexamethasone-Induced Osteoporosis in a Mouse Model. *J Int Med Res* (2019) 47(12):6268–77. doi: 10.1177/0300060519870723
9. Kassel KM, Owens AP 3rd, Rockwell CE, Sullivan BP, Wang R, Tawfik O, et al. Protease-Activated Receptor 1 and Hematopoietic Cell Tissue Factor are Required for Hepatic Steatosis in Mice Fed a Western Diet. *Am J Pathol* (2011) 179(5):2278–89. doi: 10.1016/j.ajpath.2011.07.015
10. Wang T, Zhang X, Bikle DD. Osteogenic Differentiation of Periosteal Cells During Fracture Healing. *J Cell Physiol* (2017) 232(5):913–21. doi: 10.1002/jcp.25641
11. Boyle WJ, Simonet WS, Lacey DL. Osteoclast Differentiation and Activation. *Nature* (2003) 423(6937):337–42. doi: 10.1038/nature01658
12. Yang X, Zhu S, Li L, Zhang L, Xian S, Wang Y, et al. Identification of Differentially Expressed Genes and Signaling Pathways in Ovarian Cancer by Integrated Bioinformatics Analysis. *Onco Targets Ther* (2018) 11:1457–74. doi: 10.2147/OTT.S152238
13. Ni M, Liu X, Wu J, Zhang D, Tian J, Wang T, et al. Identification of Candidate Biomarkers Correlated With the Pathogenesis and Prognosis of Non-Small Cell Lung Cancer *via* Integrated Bioinformatics Analysis. *Front Genet* (2018) 9:469. doi: 10.3389/fgene.2018.00469
14. Gan X, Luo Y, Dai G, Lin J, Liu X, Zhang X, et al. Identification of Gene Signatures for Diagnosis and Prognosis of Hepatocellular Carcinomas Patients at Early Stage. *Front Genet* (2020) 11:857. doi: 10.3389/fgene.2020.00857
15. Chen DQ, Kong XS, Shen XB, Huang MZ, Zheng JP, Sun J, et al. Identification of Differentially Expressed Genes and Signaling Pathways in Acute Myocardial Infarction Based on Integrated Bioinformatics Analysis. *Cardiovasc Ther* (2019) 2019:8490707. doi: 10.1155/2019/8490707

16. Turner AS. Animal Models of Osteoporosis–Necessity and Limitations. *Eur Cell Mater* (2001) 1:66–81. doi: 10.22203/eCM.v001a08
17. Food, D.A.J.D.o. Metabolism and R. Endocrine Drug Products, Md. In: *Guidelines for Preclinical and Clinical Evaluation of Agents Used in the Prevention or Treatment of Postmenopausal Osteoporosis*. Mary Land, United States: FDA (1994).
18. Jee WS, Yao W. Overview: Animal Models of Osteopenia and Osteoporosis. *J Musculoskelet Neuronal Interact* (2001) 1(3):193–207.
19. Yousefzadeh N, Kashfi K, Jeddi S, Ghasemi A. Ovariectomized Rat Model of Osteoporosis: A Practical Guide. *Excli J* (2020) 19:89–107. doi: 110.17179/excli2019-1990
20. Patra BG, Maroufy V, Soltanalizadeh B, Deng N, Zheng WJ, Roberts K, et al. A Content-Based Literature Recommendation System for Datasets to Improve Data Reusability - A Case Study on Gene Expression Omnibus (GEO) Datasets. *J BioMed Inform* (2020) 104:103399. doi: 10.1016/j.jbi.2020.103399
21. Zhou Y, Gao Y, Xu C, Shen H, Tian Q, Deng HW. A Novel Approach for Correction of Crosstalk Effects in Pathway Analysis and Its Application in Osteoporosis Research. *Sci Rep* (2018) 8(1):668. doi: 10.1038/s41598-018-19196-2
22. Liu YZ, Dvornyk V, Lu Y, Shen H, Lappe JM, Recker RR, et al. A Novel Pathophysiological Mechanism for Osteoporosis Suggested by an *In Vivo* Gene Expression Study of Circulating Monocytes. *J Biol Chem* (2005) 280 (32):29011–6. doi: 10.1074/jbc.M501164200
23. Ritchie ME, Phipson B, Wu D, Hu Y, Law CW, Shi W, et al. Limma Powers Differential Expression Analyses for RNA-Sequencing and Microarray Studies. *Nucleic Acids Res* (2015) 43(7):e47. doi: 10.1093/nar/gkv007
24. Kolde R, Laur S, Adler P, Vilo J. Robust Rank Aggregation for Gene List Integration and Meta-Analysis. *Bioinformatics* (2012) 28(4):573–80. doi: 10.1093/bioinformatics/btr709
25. Yu G, Wang LG, Han Y, He QY. Clusterprofiler: An R Package for Comparing Biological Themes Among Gene Clusters. *Omics* (2012) 16(5):284–7. doi: 10.1089/omi.2011.0118
26. Mlecnik B, Galon J, Bindea G. Automated Exploration of Gene Ontology Term and Pathway Networks With ClueGO-REST. *Bioinformatics* (2019) 35 (19):3864–6. doi: 10.1093/bioinformatics/btz163
27. Szklarczyk D, Gable AL, Lyon D, Junge A, Wyder S, Huerta-Cepas J, et al. STRING V11: Protein-Protein Association Networks With Increased Coverage, Supporting Functional Discovery in Genome-Wide Experimental Datasets. *Nucleic Acids Res* (2019) 47(D1):D607–d613. doi: 10.1093/nar/gky1131
28. Doncheva NT, Morris JH, Gorodkin J, Jensen LJ. Cytoscape StringApp: Network Analysis and Visualization of Proteomics Data. *J Proteome Res* (2019) 18(2):623–32. doi: 10.1021/acs.jproteome.8b00702
29. Ito K, Murphy D. Application of Ggplot2 to Pharmacometric Graphics. *CPT Pharmacometrics Syst Pharmacol* (2013) 2(10):e79. doi: 10.1038/psp.2013.56
30. Yang D, Lyu W, Hu Z, Gao J, Zheng Z, Wang W, et al. Probiotic Effects of Lactobacillus Fermentum ZJUIDS06 and Lactobacillus Plantarum ZY08 on Hypercholesteremic Golden Hamsters. *Front Nutr* (2021) 8:705763. doi: 10.3389/fnut.2021.705763
31. Chin CH, Chen SH, Wu HH, Ho CW, Ko MT, Lin CY. Cytohubba: Identifying Hub Objects and Sub-Networks From Complex Interactome. *BMC Syst Biol* (2014) 8(Suppl 4)(Suppl 4):S11. doi: 10.1186/1752-0509-8-S4-S11
32. Lex A, Gehlenborg N, Strobelt H, Vuillemot R, Pfister H. UpSet: Visualization of Intersecting Sets. *IEEE Trans Vis Comput Graph* (2014) 20(12):1983–92. doi: 10.1109/TVCG.2014.2346248
33. Squadrito F, Altavilla D, Squadrito G, Saitta A, Cucinotta D, Minutoli L, et al. Genistein Supplementation and Estrogen Replacement Therapy Improve Endothelial Dysfunction Induced by Ovariectomy in Rats. *Cardiovasc Res* (2000) 45(2):454–62. doi: 10.1016/S0008-6363(99)00359-4
34. Mawatari T, Miura H, Higaki H, Moro-Oka T, Kurata K, Murakami T, et al. Effect of Vitamin K2 on Three-Dimensional Trabecular Microarchitecture in Ovariectomized Rats. *J Bone Miner Res* (2000) 15(9):1810–7. doi: 10.1359/jbmr.2000.15.9.1810
35. Tural S, Alayli G, Kara N, Tander B, Bilgici A, Kuru O. Association Between Osteoporosis and Polymorphisms of the IL-10 and TGF-Beta Genes in Turkish Postmenopausal Women. *Hum Immunol* (2013) 74(9):1179–83. doi: 10.1016/j.humimm.2013.03.005
36. Wolski H, Drews K, Bogacz A, Kamiński A, Barlik M, Bartkowiak-Wieczorek J, et al. The RANKL/RANK/OPG Signal Trail: Significance of Genetic Polymorphisms in the Etiology of Postmenopausal Osteoporosis. *Ginekol Pol* (2016) 87(5):347–52. doi: 10.5603/GP.2016.0014
37. Zhao B. TNF and Bone Remodeling. *Curr Osteoporos Rep* (2017) 15(3):126–34. doi: 10.1007/s11914-017-0358-z
38. Fujikawa Y, Quinn JM, Sabokbar A, McGee JO, Athanasou NA. The Human Osteoclast Precursor Circulates in the Monocyte Fraction. *Endocrinology* (1996) 137(9):4058–60. doi: 10.1210/endo.137.9.8756585
39. Horton MA, Spragg JH, Bodary SC, Helfrich MH. Recognition of Cryptic Sites in Human and Mouse Laminins by Rat Osteoclasts Is Mediated by Beta 3 and Beta 1 Integrins. *Bone* (1994) 15(6):639–46. doi: 10.1016/8756-3282(94)90312-3
40. Wagner EF, Eferl R. Fos/AP-1 Proteins in Bone and the Immune System. *Immunol Rev* (2005) 208:126–40. doi: 10.1111/j.0105-2896.2005.00332.x
41. Lu SH, Chen TH, Chou TC. Magnolol Inhibits RANKL-Induced Osteoclast Differentiation of Raw 264.7 Macrophages Through Heme Oxygenase-1-Dependent Inhibition of NFATc1 Expression. *J Nat Prod* (2015) 78(1):61–8. doi: 10.1021/np500663y
42. Wagner EF. Bone Development and Inflammatory Disease Is Regulated by AP-1 (Fos/Jun). *Ann Rheum Dis* (2010) 69(Suppl 1):i86–88. doi: 10.1136/ard.2009.119396
43. Sugatani T, Vacher J, Hruska KA. A microRNA Expression Signature of Osteoclastogenesis. *Blood* (2011) 117(13):3648–57. doi: 10.1182/blood-2010-10-311415
44. Bozec A, Bakiri L, Hoebertz A, Eferl R, Schilling AF, Komnenovic V, et al. Osteoclast Size Is Controlled by Fra-2 Through LIF/LIF-Receptor Signalling and Hypoxia. *Nature* (2008) 454(7201):221–5. doi: 10.1038/nature07019
45. Speir M, Nowell CJ, Chen AA, O'Donnell JA, Shamie IS, Lakin PR, et al. Ptpn6 Inhibits Caspase-8- and Ripk3/Mlkl-Dependent Inflammation. *Nat Immunol* (2020) 21(1):54–64. doi: 10.1038/s41590-019-0550-7
46. Kumar S, Nanduri R, Bhagyaraj E, Kalra R, Ahuja N, Chacko AP, et al. Vitamin D3-VDR-PTPN6 Axis Mediated Autophagy Contributes to the Inhibition of Macrophage Foam Cell Formation. *Autophagy* (2020) 17 (9):2273–89. doi: 10.1080/15548627.2020.1822088
47. Zhang X, Yang L, Liu X, Nie Z, Wang X, Pan Y, et al. Research on the Epigenetic Regulation Mechanism of the PTPN6 Gene in Advanced Chronic Myeloid Leukaemia. *Br J Haematol* (2017) 178(5):728–38. doi: 10.1111/bjh.14739
48. Bam R, Khan S, Ling W, Randal SS, Li X, Barlogie B, et al. Primary Myeloma Interaction and Growth in Coculture With Healthy Donor Hematopoietic Bone Marrow. *BMC Cancer* (2015) 15:864. doi: 10.1186/s12885-015-1892-7
49. Marques ARA, Di Spiezio A, Thießen N, Schmidt L, Grötzinger J, Lüllmann-Rauch R, et al. Enzyme Replacement Therapy With Recombinant Pro-CTSD (Cathepsin D) Corrects Defective Proteolysis and Autophagy in Neuronal Ceroid Lipofuscinosis. *Autophagy* (2020) 16(5):811–25. doi: 10.1080/15548627.2019.1637200
50. Bassler K, Schulte-Schrepping J, Warnat-Herresthal S, Aschenbrenner AC, Schultze JL. The Myeloid Cell Compartment-Cell by Cell. *Annu Rev Immunol* (2019) 37:269–93. doi: 10.1146/annurev-immunol-042718-041728
51. Rachner TD, Khosla S, Hofbauer LC. Osteoporosis: Now and the Future. *Lancet* (2011) 377(9773):1276–87. doi: 10.1016/S0140-6736(10)62349-5
52. Okamoto K, Nakashima T, Shinohara M, Negishi-Koga T, Komatsu N, Terashima A, et al. Osteoimmunology: The Conceptual Framework Unifying the Immune and Skeletal Systems. *Physiol Rev* (2017) 97(4):1295–349. doi: 10.1152/physrev.00036.2016

Conflict of Interest: The authors declare that the research was conducted in the absence of any commercial or financial relationships that could be construed as a potential conflict of interest.

Publisher's Note: All claims expressed in this article are solely those of the authors and do not necessarily represent those of their affiliated organizations, or those of the publisher, the editors and the reviewers. Any product that may be evaluated in this article, or claim that may be made by its manufacturer, is not guaranteed or endorsed by the publisher.

frontiers in Endocrinology

SYSTEMATIC REVIEW
published: 04 February 2022
doi: 10.3389/fendo.2022.827512

Do Relaxin Levels Impact Hip Injury Incidence in Women? A Scoping Review

Emily A. Parker[1*†], *Alex M. Meyer*[1†], *Jessica E. Goetz*[1,2†], *Michael C. Willey*[1†] *and Robert W. Westermann*[1†]

[1] *Department of Orthopedics and Rehabilitation, University of Iowa Hospitals and Clinics, Iowa City, IA, United States,* [2] *Orthopedic Biomechanics Laboratories, Department of Orthopedics and Rehabilitation, University of Iowa Hospitals and Clinics, Iowa City, IA, United States*

OPEN ACCESS

Edited by:
Sadiq Umar,
University of Illinois at Chicago, United States

Reviewed by:
Liping Zhou,
Capital Medical University, China
Yixuan Deng,
Chongqing Medical University, China

***Correspondence:**
Emily A. Parker
Emily-A-Parker@uiowa.edu

[†]*These authors have contributed equally to this work*

Specialty section:
This article was submitted to Bone Research, a section of the journal Frontiers in Endocrinology

Received: *02 December 2021*
Accepted: *05 January 2022*
Published: *04 February 2022*

Citation:
Parker EA, Meyer AM, Goetz JE, Willey MC and Westermann RW (2022) Do Relaxin Levels Impact Hip Injury Incidence in Women? A Scoping Review. Front. Endocrinol. 13:827512. doi: 10.3389/fendo.2022.827512

Purpose: The aim of this review is to assess the current evidence regarding the impact of relaxin on incidence of soft tissue hip injuries in women.

Methods: A trained research librarian assisted with searches of PubMed, Embase, CINAHL, and SPORTDiscus, with a preset English language filter. The review was completed per the Joanna Briggs Institute (JBI) Manual for Evidence Synthesis methodology. Included studies required assessment of relaxin effects on musculoskeletal health, pelvic girdle stability, or hip joint structures in human subjects. Letters, texts, and opinion papers were excluded.

Results: Our screen yielded 82 studies. Molecularly, relaxin activates matrix metalloproteinases (MMPs) including collagenases MMP-1/-13 and gelatinases MMP-2/-9 to loosen pelvic ligaments for parturition. However, relaxin receptors have also been detected in female periarticular tissues, such as the anterior cruciate ligament, which tears significantly more often during the menstrual cycle peak of relaxin. Recently, high concentrations of relaxin-activated MMP-9 receptors have been found on the acetabular labrum; their expression upregulated by estrogen.

Conclusions: Menstrual cycle peaks of relaxin activate MMPs, which locally degrade collagen and gelatine. Women have relaxin receptors in multiple joints including the hip and knee, and increased relaxin correlates with increased musculoskeletal injuries. Relaxin has paracrine effects in the female pelvis on ligaments adjacent to hip structures, such as acetabular labral cells which express high levels of relaxin-targeted MMPs. Therefore, it is imperative to investigate the effect of relaxin on the hip to determine if increased levels of relaxin are associated with an increased risk of acetabular labral tears.

Keywords: hip preservation, sex differences, female reproductive cycle, relaxin, sex-based, menstrual cycle hormones, hormonal contraceptives

INTRODUCTION

Female athletes still face sex-based disparity in sports-related injury with significantly lower likelihood of a healthy career. One in five female collegiate athletes will suffer an anterior cruciate ligament (ACL) injury in college (1–3). ACL ruptures are a more evident, more thoroughly researched female-predominant injury (4–6); females in this age group are also more likely to undergo surgical treatment for athletic hip injuries. Multiple factors contribute to the female predominance of ACL injuries, including neuromuscular discrepancies and fluctuating levels of reproductive hormones (7). Hormonal research has recently identified a promising target: relaxin (1, 7–10). This has not been investigated in relation to young athletic hip conditions.

Relaxin cycles with other menstrual hormones and weakens collagen in target tissues such as the pubic symphysis (1, 9–14). While necessary for parturition, this can be detrimental outside of the reproductive system (15–17). Multiple studies correlate relaxin peaks with female ACL tears (1, 9). However, despite large-scale relaxin synthesis in the pelvis, and a known paracrine activity profile, there is a paucity of literature assessing if relaxin levels correlate with another female-predominant lower extremity injury impacting athletes such as acetabular labral tears (18–21). If relaxin does significantly contribute to the elevated rates of both knee and hip injuries in women, further research into preventive strategies is critical.

The absence of literature regarding relaxin vs. hip injuries necessitated a scoping review to appraise available information on factors related to relaxin versus hip injury, and to identify conceptual gaps (22). This review assessed relevant literature on nanoscale, microscale, and macroscale actions of relaxin. The objective of this scoping review is to show that it is scientifically logical and medically important to further explore the potential correlation between relaxin levels and female hip injuries.

METHODS

A preliminary search of MEDLINE, the Cochrane Database of Systematic Reviews and JBI Evidence Synthesis (Joanna Briggs Institute, Adelaide, Australia) was conducted and no current or underway systematic reviews or scoping reviews on the topic were identified. The scoping review was conducted in accordance with the JBI methodology for scoping reviews (JBI Manual for Evidence Synthesis) and the Preferred Reporting Items for Systematic reviews and Meta-Analyses for Scoping Reviews (PRISMA-ScR) Checklist (**Supplementary Material: Appendix 1**).

Types of Sources

This scoping review considered all traditional types of papers, with the exclusion of commentaries, editorials, and opinion papers.

Search Strategy

The search strategy was developed by the authors with the assistance of a Health Sciences librarian specializing in development of database queries. The search strategy aimed to locate both published and unpublished studies ("gray literature"). An initial limited search of MEDLINE and EMBASE was undertaken to identify articles on the topic. The index terms used to describe the articles were used to develop the full search strategy, along with text words derived from the titles and abstracts of relevant articles.

The initial search strategy was developed for MEDLINE. The first search concept focused on female hormonal variations, with MeSH terms such as estrogens, progesterone, relaxin, and contraceptives. Text words and phrases included "cyclic hormonal variation" and "female athlete hormonal variation". The second search concept focused on non-arthritic hip pain, with MeSH terms such as hip dysplasia and femoroacetabular impingement. Text words and phrases included "acetabular labral tear" and "pelvic floor disorder". The full search strategy for MEDLINE can be found in the Appendix (**Supplementary Material: Appendix 2**).

The search strategy was then adapted for EMBASE and CINAHL. Full search strategies for these databases are available upon request. The reference list of all included sources of evidence was screened for additional source materials *via* SCOPUS. A filter for English language studies was used. During the screening process, the decision was made to exclude animal-only studies.

Source of Evidence Selection and Data Extraction

All identified citations were uploaded to EndNote (EndNote X9.2, Clarivate Analytics, PA, USA) and duplicates removed by a combination of software screening and manual review. Titles and abstracts were then screened by two authors independently against the inclusion criteria (**Table 1**). A full-text assessment was then performed to identify final inclusions. We elected to exclude animal-only studies, and include studies of pregnant women only for the pelvis and hip subsections. Any disagreements during the selection process were resolved by the senior authors.

Data was extracted by two authors, independently, with oversight from the senior authors. The data included subject demographics, concept/context, study methods, and key findings relevant to the present review questions. The data extraction approach was modified and revised as necessary. The data was documented in one or more analytical categories of relaxin effect level: cellular/molecular, systemic-musculoskeletal, pelvic structure-specific, and hip-specific.

Per scoping review protocol, critical appraisal of individual sources was not completed. The current review will not individually discuss all included studies. Discussion will address studies with novel information and/or critical concepts, which will be recorded in subject-specific tables (**Tables 2**–**4**). However, all included references are listed in **Supplementary Material: Appendix 3**.

DATA ANALYSIS RESULTS

Of the initial library screened, 82 articles were included for scoping review (1, 4, 5, 7–21, 23–86). There was overlap between analysis categories for numerous papers; most prevalent with the subjects are of cellular/molecular and systemic-musculoskeletal effects. The effects of relaxin were discussed at the cellular/molecular level by 24

TABLE 1 | Scoping review screening, inclusion and exclusion criteria.

Inclusion	Exclusion

• Adults and children
• Level I-V, unpublished ("gray") literature
• Systematic Reviews/Meta-Analyses
• All publication dates
• Mixed studies with animal and human subjects
  • Ex) Molecular analysis of porcine and human ligaments
• Human cadaver studies
• Must address a scoping review question:
  • Relaxin and musculoskeletal health
  • Relaxin and pelvic girdle stability
  • Relaxin and hip structures
	• Non-English
	• Animal only
	• Commentary, editorial, letters, opinion statements, technical descriptions
	• Studies addressing a key scoping review area (musculoskeletal health, pelvic girdle stability, and/or hip structures) which address relaxin in a manner with negligible extractable information
	  • Ex) Analysis of hormone levels versus pelvic instability which only mentions relaxin briefly ("relaxin may also play a role in pelvic instability")

studies (10, 13, 16, 17, 23–33, 58, 62, 68, 71, 76, 77, 80, 83, 84), and at the systemic-musculoskeletal level by 25 studies (1, 4, 7–9, 11, 12, 14, 15, 34–39, 57, 60, 61, 63, 64, 67, 75, 81, 82, 85). The pelvic structure-specific effects of relaxin were discussed by 17 studies (21, 40–51, 59, 73, 74, 86), and 9 studies focused on hip joint-specific relaxin effects (18–21, 45, 52–55).

DATA PRESENTATION AND DISCUSSION

The present review identified conceptual gaps regarding the intersection of relaxin levels and female hip injuries, and appraised available information on factors related to the topic, with review of 82 studies. Literature data was documented in conceptual categories of relaxin effects. Important/main concepts from the data assessed for each category are reported in the following sub-sections.

CELLULAR/MOLECULAR EFFECTS OF RELAXIN

Basic Properties of Relaxin

Relaxin is a peptide hormone present in both sexes, with known paracrine, autocrine, and endocrine actions. The corpus luteum synthesizes the bulk of relaxin, but the endometrium, placenta, breast tissue, and prostate have also been detected as synthesis sites. Average serum relaxin concentration (SRC) is similar between non-pregnant women and men; although women's levels peak at menstrual cycle day 21-24. As relaxin often acts in a paracrine fashion, SRC does not consistently reflect the extent of hormone activity (**Table 2**). The menstrual cycle peaks and corresponding molecular changes in the body for the three essential menstrual hormones—estrogen, progesterone, and relaxin—are depicted in **Figure 1**.

Properties of Relaxin Receptors

The location of relaxin family peptide receptors (RXFPs) is a sensitive indicator of physiological roles. Thus, the curiosity regarding sex-specific musculoskeletal roles of relaxin, as RXFPs are uniformly present—only in women—in the synovial lining of ACL remnants, and present in high concentrations in women undergoing first carpometacarpal arthroplasty. Additionally, RXFP expression is primed by estrogen and progesterone (**Table 2**).

General Functional and Physiologic Properties of Relaxin

Relaxin is a controller of ECM turnover, upregulating MMP-1/-13 (collagenases) and MMP-2/-9 (gelatinases) to degrade existing collagen while suppressing synthesis of new collagen. Poor collagen quality in the target tissues, along with a lesser amount of proximate total collagen, are the result of these complementary actions of relaxin; illustrated in **Figure 2**.

KEY REFERENCE ONE: ROLES OF MATRIX METALLOPROTEINASES

Relaxin modulates many of its effects *via* MMPs, whose roles were detailed in a 2011 review article by Klein et al. (31) MMP-1 uniquely degrades triple-helical (fibrillar) collagen, leaving it susceptible to gelatinases. Dysregulation causes insufficient or excessive tissue regeneration. MMP-13, activated by MMP-3, cleaves type II collagen during bone remodeling. Dysfunction has been linked to cartilage destruction in osteoarthritis and rheumatoid arthritis. MMP-2 degrades gelatine (denatured collagen) and is constitutively expressed. It has roles in angiogenesis and basement membrane structure. MMP-9 also degrades gelatine and is highly inducible by other MMPs. It signals immune cells and is crucial for endometrial tissue remodeling during the menstrual cycle. MMP-3 degrades numerous ECM proteins and is involved in activation of gelatinases and MMP-13 (31).

SYSTEMIC-MUSCULOSKELETAL EFFECTS OF RELAXIN

Anterior Cruciate Ligament

The bulk of literature directly addressing relaxin and sex-specific disparities in musculoskeletal health focuses on incidence of ACL rupture. It has been cited that a combination of neuromuscular/biomechanical differences and sex-specific hormonal variations

TABLE 2 | Cellular/molecular effects of relaxin- relevant literature findings.

Subcategory	Author, Year	Findings
Basic Properties of Relaxin	Goldsmith et al. (23) Grossman et al. (24) Lubahn et al. (25) MacLennan et al. (26) Powell et al. (27) Wolf et al. (17) Wolf et al. (28)	• Relaxin (RLX*) is a peptide hormone in the insulin-like growth factor (IGF†) family • Men and women have similar serum levels (400-500 pg/mL and 360-495 pg/mL), with luteal phase peaks in women • Oral contraceptives decrease relaxin below a detectable serum level • The major gene for relaxin in humans is H2; H2 relaxin binds relaxin family peptide receptor 1 and 2 • The corpus luteum produces most relaxin, but synthesis occurs in the endometrium, placenta, breast tissue, and prostate • Relaxin is biologically and immunologically active during pregnancy • The capacity of relaxin to act locally means that serum levels do not always reflect activity
Properties of Relaxin Receptors	Bryant-Greenwood et al. (29) Dragoo et al. (10) Kapila et al. (30) Kleine et al. (31) MacLennan et al. (26) Powell et al. (27)	• In humans, relaxin family peptide receptor-1 (RXFP‡) is most common, and has the highest affinity for H2 relaxin • Relaxin binds receptors in a time-, temperature-, and pH-dependent manner • RXFP‡ expression is primed by estrogen/progesterone in chondroblasts, fibrochondroblasts, myofibroblasts, and ligaments • Estrogen-primed receptors can show maximum response at RLX* levels 10-100 times lower than normal • Estrogen, progesterone, and relaxin receptors modulate MMP§ transcription and post-translational modification • Radioreceptor location detection is a sensitive indicator of the physiological roles of RLX* • Relaxin receptors are detectable in anterior cruciate ligament (ACL¶) remnants of female, but not male, surgical patients • RLX* binding was uniform, saturable, and specific to the synovial lining, stromal fibroblasts, and intima. • Relaxin receptors have been detected in the carpometacarpal joint of the thumb (1st CMC#) in arthroplasty patients • The synovial lining, dorsoradial ligament, volar oblique ligament, and articular cartilage cells had receptors • Concentration of RLX* receptors was significantly higher in women compared to men • Relaxin receptors have been detected in the temporomandibular joint (TMJ**), on fibrochondrocytes and ligaments
Functional, Physiologic Properties of Relaxin	Ando et al. (32) Dragoo et al. (10) Galey et al. (33) Goldsmith et al. (23) Grossman et al. (24) Nose-Ogura et al. (13) Powell et al. (27)	• Relaxin controls extracellular matrix (ECM††) turnover by stimulating collagen degradation, and suppressing synthesis • Relaxin upregulates MMP¥ production, specifically collagenases (MMP-1/-13) and gelatinases (MMP§-2/-9) • Active collagenases cleave tropocollagen, making it susceptible to subsequent denaturation by gelatinases • The density and organization of collagen bundles, and total local collagen content decrease • MMP§s induced by relaxin degrade collagen at a nanoscale level, and macro-level effects are not always appreciable • Relaxin has dose-dependent and differential functioning; its effects depend on location and presence of other hormones • There is a significant correlation between peak serum relaxin and peak serum progesterone levels • Intracellular relaxin activates MAPK‡‡ and PI3K§§, increasing cAMP¶¶ and triggering vasodilation *via* MMP§-2/-9 • Estrogen, progesterone, and relaxin binding synovial receptors upregulates inflammatory MMP§s, increasing OA## risk • Relaxin upregulates production of collagenases and gelatinases in ligaments and fibrocartilage • During parturition, relaxin binding pubic ligaments dissociates collagen, increases water uptake, and decreases viscosity

*RLX, relaxin.
†IGF, insulin-like growth factor.
‡RXFP1 or 2, relaxin family peptide receptor 1 or 2.
§MMP, matrix metalloproteinase.
¶ACL, anterior cruciate ligament.
#1st CMC, first/thumb carpometacarpal joint.
**TMJ,temporomandibular joint.
††ECM, extra-cellular matrix.
‡‡MAPK, mitogen-activated phosphate kinase.
§§PI3K, phosphoinositide-3-kinase.
¶¶cAMP, cyclic adenosine monophosphate.
##OA, osteoarthritis.

are responsible for the high rate of female ACL injuries. Current injury prevention programs to correct biomechanics have had some success decreasing ACL rupture rates, but a systematic review of prevention program studies concluded that neuromuscular differences alone could not account for the disparity. The female ACL contains receptors for estrogen, progesterone, relaxin, and testosterone, and coupled with the complexity of the hormonal cycle, the authors also noted that single-timepoint hormonal analyses were not depictive (**Table 4**). Additionally, two studies found that in males, their naturally higher testosterone levels have a protective effect on the ACL, by downregulating collagenolytic activity (87, 88).

TABLE 3 | Musculoskeletal effects of relaxin- relevant literature findings.

Subcategory	Author, Year	Findings
Relaxin and Tendons, Ligaments of the Leg	Arnold et al. (8) Brophy et al. (7) Clifton et al. (34) Dragoo et al. (1) Dragoo et al. (9) Pearson et al. (35)	• 4-year careers of 128 Division 1 collegiate female athletes in sports with the highest ACL‡ tear risk—basketball, lacrosse, field hockey, and soccer— tested SRC# during mid-luteal phase, CD** 21-24 • Cumulative career incidence of ACL‡ tears was 21.9%; associated average SRC# was higher (6.0 ± 8.1 vs. 1.8 ± 3.4, p<0.013) • Subgroup: 46/128 athletes with detectable SRC#- ACL‡ tear incidence was 30.4% (14/46) with associated average SRC# 12.1 ± 7.7 (vs. 5.7 ± 3.6, p<0.002) • Trial of ACL‡ injury risk screening at SRC# 6.0 pg/mL: Screen was 71% sensitive, 69% specific; PPV‡‡ 52%, NPV†† 88% • Conclusion: Elite female athletes with SRC#>6.0 pg/mL had 4 times more ACL‡ tears (RR*** 4.4, χ^2 p=0.003, ROC§§ 0.002) • A separate analysis of the same 128 D1 female athletes assessed SRC# vs. menstrual cycle status • With OCP## use: SRC# 1.41 (vs. 3.08, p<0.002); significant lower SPC¶¶ was also seen (2.8 vs. 6.99, p<0.0002) • Without OCP## use: No significant SRC# difference in eumenorrheic vs. amenorrheic vs. oligomenorrheic athletes • Sex-specific neuromuscular differences account for some disparity in ACL‡ tear rates, but hormonal differences are also involved • Current biomechanics training has some success, role of fatigue in competition unknown • ACL‡ estrogen/progesterone/relaxin/testosterone receptors; due to the complexity of hormone signaling, single-timepoint analyses are not reliable • 165,748 females ACL‡ reconstruction patients assessed for use of OCPs##: OR*** for ACL‡ tear on OCPs## was 0.82 • Most significant in 15-19 yo age group with OR*** 0.37, a 63% risk reduction, NNT††† of 6 • Eumenorrheic females, no OCPs##: Luteal phase SRC# peaks correlated with laxity of patellar tendon, no change in gastrocnemius
Relaxin and the Thumb CMC§ Joint	Komatsu et al. (36) Wolf et al. (15) Wolf et al. (4)	• CMC§ arthroplasty patients with elevated SRC# expressed increased RXFP1‡ in nearby ligaments • RXFP1‡ upregulates MMP1➔ increases joint laxity, abnormal loading • CMC§ subluxation risk positively correlates with detectable SRC# • Effects of relaxin should be considered during CMC§ ligament repairs in women of childbearing age
Relaxin and the Jaw, Mouth	Deniz et al. (14) Deniz et al. (37) McGorray et al. (38)	• TMJD¶ patients with OA‡‡‡ and joint effusion had higher synovial fluid relaxin levels vs. TMJD¶ patients with OA‡‡‡ alone • Weekly gingival relaxin injections did not impact tooth movement during adjustive treatment
Relaxin and the Shoulder	Owens et al. (39)	• Military cadets with an episode of acute shoulder instability (47M:6F); were compared to age/sex/height/weight matched controls • Those with instability had higher SRC# (3.69 vs. 2.20, p=0.02) • For every 1 pg/mL increase in SRC# at baseline, cadets were 2.18 times more likely to have an episode (95% CI 1.01-4.76)

**RLX, Relaxin.*
†RXFP1, RXFP2, Relaxin family peptide receptor 1, 2.
‡ACL(R), Anterior cruciate ligament (repair).
§1st CMC, First/thumb carpometacarpal joint.
¶TMJ(D), Temporomandibular joint disorder.
#SRC, Serum relaxin concentration.
***CD, [Menstrual] cycle day.*
††NPV, Negative predictive value.
‡‡PPV, Positive predictive value.
§§ROC, Receiver operator curve.
¶¶SPC, Serum progesterone concentration.
##OCP, Oral contraceptive.
****OR/RR, Odds ratio, risk ratio.*
†††NNT, Number needed to treat.
‡‡‡OA, Osteoarthritis.

ACL tear incidence in elite female athletes is as high as 21.9%, as demonstrated in a study which included nearly 130 Division 1 (D1) female collegiate athletes during their 4-year careers in sports with a high risk of ACL injury: basketball, lacrosse, field hockey, and soccer. The athletes underwent SRC testing during the mid-luteal phase of their menstrual cycle (day 21-24), which showed significantly higher average SRC among athletes who had, or would, suffer ACL tears (6.0 ± 8.1 vs. 1.8 ± 3.4, p<0.013) (**Table 3**).

Given that SRCs are not always detectable, a subgroup of the 46 athletes with detectable mid-luteal SRC were analyzed. The ACL tear incidence of this subgroup was 30.4% (14/46). Average SRC of injured athletes was 12.1 ± 7.7, vs. 5.7 ± 3.6 in those without injury (p<0.002). Among this group, researchers trialed an SRC of 6.0 pg/mL as the cutoff level for ACL injury risk screening. This screen proved to be 71% sensitive and 69% specific, with a PPV of 52% and an NPV of 88%. Researchers

TABLE 4 | Pelvic and hip joint related effects of relaxin- relevant literature findings.

Subcategory	Author, Year	Findings
Relaxin and the Pubic Symphysis	MacLennan et al. (40) MacLennan et al. (41) Schuster et al. (21)	• 135 women with pubic symphysis disorder (SPD*) had SRC† above the 95% percentile for an average female population • Infants with DDH‡ born to mothers with PS§ instability will also have PS§ instability on exam • Pubic symphysis: Fibrocartilaginous joint, supported by symphyseal ligaments, arcuate ligaments between inferior pubic rami, posterior sacral ligaments, and iliolumbar ligaments—outside of pregnancy, takes 2600 lbs of force to separate
Relaxin and Uterine Ligaments	Kieserman-Schmokler et al. (42) Reisenauer et al. (43) Schott et al. (44) Uden et al. (45)	• Uterine prolapse patients have significantly higher SRC†, R2 *in utero*sacral ligaments—modulated by oxytocin and relaxin • Female infants with DDH‡ have an 11.2 times higher inguinal hernia risk in their first 3 months of life; have surgery earlier (1 mo vs. 10 mo) • Of all operations on female infants <3 mo of age for inguinal hernias, 25% have DDH‡
Relaxin Peripartum	Bookhout et al. (46) Kristiansson et al. (47) Ritchie et al. (48) Saugstead et al. (49)	• Pregnant women with pelvic pain and pelvic joint instability (PPPJI¶) were diagnosed earlier if multiparous, prior OCP# use • Severe PPPJI¶ symptoms in the 3rd trimester correlated with higher SRC† • Infants of PPPJI¶ mothers tended to be post-term, higher weight, and female; 25 in 1000 had DDH‡ • 25% of women will have disabling musculoskeletal pain of the pelvis/low back at some point during pregnancy • Primigravid women had a significant positive correlation between SRC† and pelvic/back pain, stratified at 36 weeks • SRC†<420: 20% had lumbosacral and PS§ pain • SRC† 420-890: 45% had lumbosacral and PS§ pain • SRC†>890: 55% had lumbosacral and PS§ pain, 10% had greater trochanteric pain • SPD* occurs in 1/36 pregnancies; worse PS§ pain correlates with more PS§ separation; acute PS§ disruption risk is 1:300-1000
Relaxin Postpartum	Borg-Stein et al. (50) Leadbetter et al. (51)	• Women with higher SRC† during pregnancy take significantly longer to recover • Postpartum relaxin does not return to baseline until 4-12 weeks; injury risk remains elevated; leg and foot pain twice as likely
Relaxin and Maternal Factors Impacting DDH‡	Andren et al. (18) Bracken et al. (52) Forst et al. (53) MacLennan et al. (19) Roof et al. (54)	• If the uterine wall does not put normal pressure on the femoral head/acetabular socket interface, DDH‡ occurs • Two studies found that maternal SPD* increased infant DDH‡ risk five-fold; one postulated a genetic susceptibility to relaxin • A majority of DDH‡ infants had primigravid mothers; risk is also increased in twin births, (monozygotic>dizygotic) • A sibling with DDH‡ increases risk 4.3-14%, while a parent with DDH‡ increases risk 1.6-2.3% • No association between cord blood SRC† and DDH‡ diagnosis; in two studies DDH‡ infant cord blood SRC† was mildly lower • Lower maternal relaxin was theorized to decrease laxity of the birth canal
Relaxin and Fetal Factors Impacting DDH‡	Andren et al. (18) Bracken et al. (52) Forst et al. (53) Morey et al. (20) Rhodes et al. (55) Roof et al. (54) Schuster et al. (21) Uden et al. (45)	• DDH‡ risk factors, research supported: breech, family history, firstborn, oligohydramnios, high birth weight, postmaturity • However, 73-90% of infants with DDH‡ have no identifiable risk factors other than female sex • Female fetuses are more responsive to maternal hormones, but normally metabolizes and excretes them (hepatic metabolism) • DDH‡ could reflect decreased ability to metabolize/increased sensitivity to hormones • Neonates with DDH‡ and abnormal estrogen excretion tend to have PS§ instability • Could be an inborn, possibly hereditary error of estrogen metabolism • DDH‡ risk, female infants: 19/1000 baseline, 44/1000 with family history, 120/1000 with breech birth; 25/1000 in PPPJI¶ moms • 80% of DDH‡ cases are bilateral, unilateral cases are 4 times more likely to be left sided due to intrauterine positioning
Relaxin and Neonatal Findings	Andren et al. (18) Bracken et al. (52) Uden et al. 45)	• In a study of 90 DDH‡ neonates, a majority of infants had concurrent pelvic instability on exam • Abnormalities on neonatal hip ultrasound are significantly more likely to spontaneously resolve in males • Female neonates with DDH‡ have an 11.2 times greater risk of developing an inguinal hernia during their first 3 months of life

**SPD, symphysis pubis dysfunction/pubic symphysis dysfunction.*
†SRC, serum relaxin concentration.
‡DDH, developmental dysplasia of the hip.
§PS, pubic symphysis.
¶PPPJI, pelvic pain and pelvic joint instability.
#OCP, Oral contraceptive.

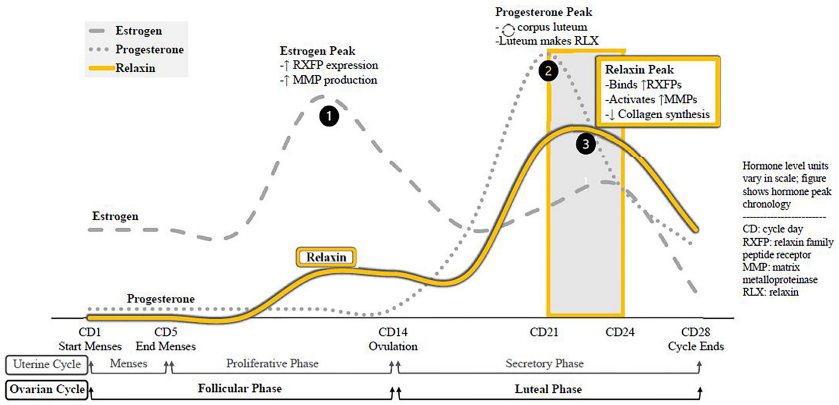

FIGURE 1 | Menstrual cycle hormone peaks, molecular effects. The sequence of hormone peaks for ovulatory cycles. Estrogen levels peak first, increasing expression of relaxin receptors in the body and increasing global synthesis of MMPs. The drop in estrogen triggers ovulation, and the remains of that ovarian follicle from the corpus luteum. As a temporary endocrine body, the corpus luteum secretes progesterone to prepare the endometrium for pregnancy and to sustain itself. It also synthesizes and relaxin, which binds receptors and activates. MMPs recently upregulated by estrogen while suppressing de novo collagen synthesis. Relaxin is active during the luteal phase, chiefly CD21-24.

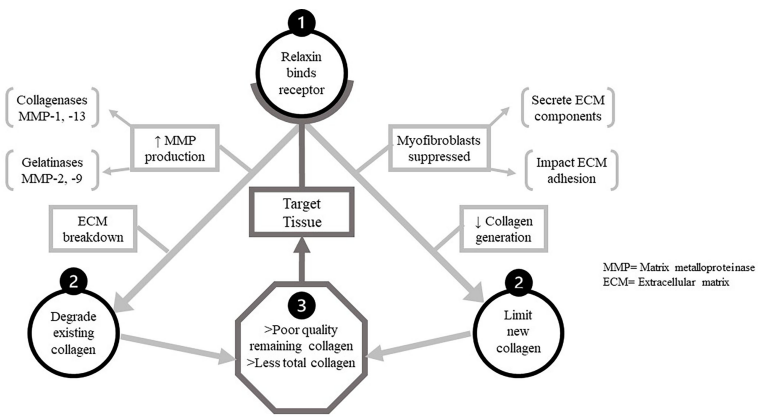

FIGURE 2 | The dual functions of relaxin in target tissues. The two main mechanistic pathways by which relaxin decreases tissue quality and quantity of collagen after binding to its receptor. Upon binding relaxin receptors in target tissue, two processes impacting collagen proceed concurrently. Above, left-relaxin increases production of all MMPs, but particularly the collagenases and gelatinases capable of digesting ECM components. Thus one mechanistic pathway detrimental to target tissue collagen is the degradation of existing collagen by these. MMPs. Above, right-relaxin also suppresses function of/differentiation into myofibroblasts. These cell secrete multiple ECM components and modulate ECM cross-linkage, allowing relaxin to impair de novo collagen synthesis is target tissue.

concluded that elite female athletes with SRC>6.0 pg/mL had a 4-fold increased risk of an ACL tear during their career (RR 4.4, χ^2 p=0.003, ROC =0.002) (**Table 3**).

This group of D1 athletes was also surveyed about oral contraceptive pill (OCP) use, to assess potential effects on SRC and ACL tears. It was found that athletes taking OCPs had significantly lower average SRC (1.41 vs 3.08, p<0.002) and average serum progesterone concentration (SPC) (2.8 vs. 6.99, p<0.0002). Interestingly, SRC was not significantly different between eumenorrheic, amenorrheic, and oligomenorrheic athletes. While this cohort study showed that OCPs significantly reduce SRC, a database review of nearly 170,000 female ACL reconstructions showed that OCP also reduced the likelihood of an ACL tear (0.82). This was most significant among 15-19 year-olds, with likelihood of an ACL tear decreasing by 63% (OR 0.37). Analyzing OCPs as a preventive treatment for ACL tears in this age group yielded an NNT of 6 adolescent athletes (**Table 3**).

First CMC Joint (Trapeziometacarpal Joint)

First CMC arthroplasty is a common procedure among women. Studies of first CMC instability and degeneration found the risk of subluxation to be positively correlated with detectable SRC. Immunohistochemical studies of tissue from arthroplasty patients with elevated average SRC showed increased expression of the relaxin receptor RXFP1 in nearby ligaments

subsequently increasing collagen degradation leading to increased CMC laxity and abnormal weight loading (**Table 3**).

Other Musculoskeletal Tissues

Patients with temporomandibular joint disorder (TMJD), another female-predominant condition, showed higher average synovial fluid relaxin levels in those with TMJ OA plus joint effusion, rather than OA alone. Shoulder instability, an issue common in young female athletes playing overhead sports, was assessed in a cohort study of 53 military cadets (47 male, 6 female) with episodes of acute shoulder instability. Compared to controls matched for age, sex, height, and weight, these 53 cadets had significantly higher SRC (3.69 vs. 2.20, p=0.02). Risk of an acute instability episode vs. SRC had a dose-dependent correlation; every 1 pg/mL increase in baseline SRC making acute instability 2.18 times more likely (95% CI 1.01-4.76) (**Table 3**).

PELVIC STRUCTURE-SPECIFIC EFFECTS OF RELAXIN

Pubic Symphysis

The fibrocartilaginous pubic symphysis joint is stabilized by a combination of symphyseal ligaments, arcuate ligaments between inferior pubic rami, posterior sacral ligaments, and iliolumbar ligaments. Normally, this joint takes 2600 lbs of force to separate; but during late pregnancy and parturition, relaxin triggers enough collagen degradation for separation to occur at much lower forces. In women with the musculoskeletal/genitourinary symptoms of symphysis pubis dysfunction (SPD) their average SRC was above the 95th percentile for average SRC distribution among age and sex matched controls (**Table 4**).

Uterine/Pelvic Ligaments

Relaxin and oxytocin modulate the integrity of uterosacral ligaments, and uterine prolapse patients had significantly higher SRC versus controls, as well as significantly increased RL-2 in ligament samples from prolapse patients vs. control patients undergoing gynecologic surgery. Even prior to puberty relaxin impacts pelvic soft tissues. During the first three months of life, female infants with developmental hip dysplasia (DDH), theorized to have an associated with excess relaxin, have an 11.2 times greater risk of developing an inguinal hernia, and tend to require earlier surgical repairs (1 mo vs. 10 mo). Of all female infants less than 3 months old who require operative intervention for inguinal hernias, 25% have DDH (**Table 4**).

Peripartum Pubic Symphysis, Lumbosacral Joints

A study of pregnant women with pelvic pain and pelvic joint instability (PPPJI) found earlier onset and increased severity in patients with a history of OCP use (exogenously lowered relaxin) and for multiparous women (prior pelvic ligament degradation). Those with severe 3rd trimester symptoms had significantly higher SRC. Their infants tended to be post-term, higher weight, and female; and approximately 25/1000 had DDH. A study of primigravid women at 36 weeks recorded pain incidence and location stratified by mean SRC. Of women with low SRC (<420 pg/mL), 20% had lumbosacral and PS pain. In women with moderate SRC (420-890 pg/mL), 45% had this pain, and which bothered 55% of women with high SRC (>890 pg/mL); 10% of whom also had greater trochanteric pain. Research found that 25% of pregnant women will at some point experience disabling musculoskeletal pain of spine and/or pelvis.

Postpartum Pelvic Recovery

Women with higher peripartum SRC took longer to recover from childbirth. Relaxin does not return to baseline SRC until 4-12 weeks postpartum, and women are 2 times more likely to have leg and foot pain secondary to pelvic instability during this period (**Table 4**).

HIP-SPECIFIC EFFECTS OF RELAXIN

Fetal Factors Related to DDH

DDH has well-defined risk factors, including breech delivery, female sex, family history, firstborn status, high birth weight, and post-maturity. However, 73-90% of infants with DDH have no identifiable risk factor other than female sex; generating the hypothesis that female fetuses are more susceptible to maternal hormones. In normal physiological states, the fetal liver will metabolize these hormones. This is one potential "problem point" leading to DDH; if the fetus has decreased metabolic abilities or increased hormonal sensitivity. Given that neonates with abnormal estrogen excretion and DDH commonly have PS instability on exam, an inborn and possibly hereditary error of estrogen metabolism could be a contributing factor (**Table 4**).

Maternal Factors Related to DDH

In utero, if the maternal uterine wall does not put normal pressure on the fetal femoral head/acetabular socket interface, DDH results. If pregnant women have persistent pelvic/PS pain, their infants have a 5 times increased risk of DDH. The risk of DDH for female infants at baseline was listed at 19:1000 ("normal" risk of DDH varied by source, but generally ranged between 14-20:1000). Per SPD research, women with more pelvic pain during pregnancy likely have significantly increased SRC, and as previously discussed studies of mothers with SSPJI, symptomatic SPD in pregnancy increases DDH risk to approximately 25:1000 (**Table 4**).

Primigravid mothers and those with multiple gestation pregnancies, monozygotic more than dizygotic, have an increased risk of neonate DDH. No significant association has been established between cord blood SRC and incidence of DDH; two studies in this review noted insignificantly lower SRC in cord blood of infants with SRC. It was not known if this could be secondary to inadequate relaxation of the birth canal; or if cord blood SRC was not useful to analyze in this situation given the known local effects of relaxin (**Table 4**).

Physical Findings Indicating Excess Relaxin in Neonates with DDH

A study of 90 neonates with DDH detected concurrent pelvic instability on physical exam in a majority of neonates. Abnormalities detected on neonatal hip ultrasound were significantly more likely to spontaneously resolve in male infants. Additionally, further supporting the theory of pelvic effects of relaxin, female neonates with DDH have an 11.2 times greater risk of developing an inguinal hernia during the first three months of life (**Table 4**).

KEY REFERENCE TWO: METABOLISM OF CELLS OF THE ACETABULAR LABRUM

A critical scientific component linking known actions of relaxin to a potential impact on hip health is research by Dhollander et al (89) exploring the cellular metabolism of human acetabular labral cells. Analysis was performed on articular and capsular side labral cells, articular chondrocytes, and meniscal cells (fibrochondrocytes). Labral cells had a number of properties similar to meniscal fibrochondrocytes, such as high COL1A1 levels and ECM turnover in response to increased IL-1 (89).

In labral cells, IL-1 triggers ECM degradation *via* secretion of IL-6, MMP-1/-2/-3/-9/-13, and ADAMTS-4/-5, while suppressing COL1A1 and COL2A1 expression. The secreted MMPs, ADAMTSs, and IL-6 are known to increase systemic cartilage damage and joint inflammation. Labral cells are unique in their increased MMP-9 expression after exposure to IL-1; MMP-9 is an inducible gelatinase which specifically degrades type IV and V collagen (89).

SUMMARY OF APPRAISED INFORMATION: FACTORS RELATED TO RELAXIN AND HIP INJURIES

One aim of this scoping review is to show that it is scientifically logical that a correlation would exist between relaxin levels and the high incidence of soft tissue hip injuries in women. This review appraised available information on factors related to the issue of interest. To derive an abridged synopsis of the topics covered, it is helpful to revisit the comparatively large pool of literature that is available which addresses relaxin vs. ACL tears at the micro and macro level.

Beginning at the macro level, numerous studies correlate increased SRC with increased incidence of ACL tear. Conversely, decreasing SRC with OCPs decreased incidence of ACL tears. The impact of relaxin on the ACL during the menstrual cycle is facilitated by preceding estrogen and progesterone peaks which prime target tissues. Relaxin impacts only female ACLs, which display relaxin receptors with specific and saturable binding. Conversely, male ACLs display no relaxin receptors. This binding increases the susceptibility of the ACL to macro-physiologic injury, because micro-physiologic collagen degradation is upregulated while *de novo* synthesis is suppressed.

Beginning at the micro level for relaxin vs. hip soft tissue injuries, it is known that pelvic ligaments normally have a uniform distribution of relaxin receptors, and the receptor and hormone levels significantly increase in pathologic states such as uterine prolapse. It is also known that acetabular labral cells can be induced to express collagen-degrading MMPs while suppressing deposition of new collagen. The response is unique in the high expression levels of MMP-9; an inducible gelatinase crucial in the female reproductive system for endometrial remodeling during menstruation and basement membrane degradation capacity. MMP-9 is also well-known among pulmonologist for destroying a serine protease inhibitor, facilitating tissue breakdown at inflammatory sites.

The labral cells are adjacent to the ovaries, where the recurring corpus luteum synthesizes large amounts of the paracrine hormone relaxin during the mid-luteal phase. Relaxin remodels endometrial tissue, acting *via* MMP-9, expression of which also peaks just after ovulation. Relaxin modulates tissue dissolution by stimulating collagenases (MMP-1/-13) and gelatinases (MMP-2/-9); MMPs expressed by labral cells, particularly MMP-9.

Therefore, since relaxin acts in a paracrine fashion, it would be predicted to act throughout the female pelvis during the luteal phase. Due to the presence of relaxin receptors on uterosacral ligaments, ligament laxity would occur. If relaxin has receptors on the neighboring acetabular labral tissue, binding will also trigger collagen turnover *via* MMP-1/-2/-3/-9/-13 and other components. Labral cells have inducible high expression of MMP-9, which is upregulated in luteal phase reproductive tissue, implicating a large potential role for MMP-9 in relaxin-induced degradation of the acetabular labrum. The trio of known molecular components—MMP-9 properties, relaxin properties, and, recently, the metabolism of labral cells—hypothetically working in reciprocal and mutual ways to target the collagen of the acetabular labrum is detailed in **Figure 3**.

As seen in women with SPD, the micro level degradation of ligaments from high relaxin resulted in macro level instability of the pelvis. As hypothesized in recent DDH studies, relaxin-induced laxity of the pelvis vs. hips is interrelated: mothers with elevated relaxin causing pelvic instability are more likely to give birth to infants with DDH, who also display pelvic instability on early exams. In macro level research of the other ball-and-socket joint in humans—the glenohumeral joint—a significant correlation of increased relaxin levels with acute episodes of instability was found.

In addition to appraising available information on factors relevant to a potential hip injury/relaxin relationship, this scoping review also aimed to identify conceptual gaps for future research. The two main gaps in knowledge/research that were identified are as follows:

CONCEPTUAL GAP 1: DO SOFT TISSUES OF THE FEMOROACETABULAR JOINT RESPOND TO RELAXIN?

There is, in essence, a "missing arrow" in the hypothetical cascade starting at cyclic relaxin peaks and ending at an increased risk of soft tissue injuries of the hip. It is known that relaxin is synthesized in the

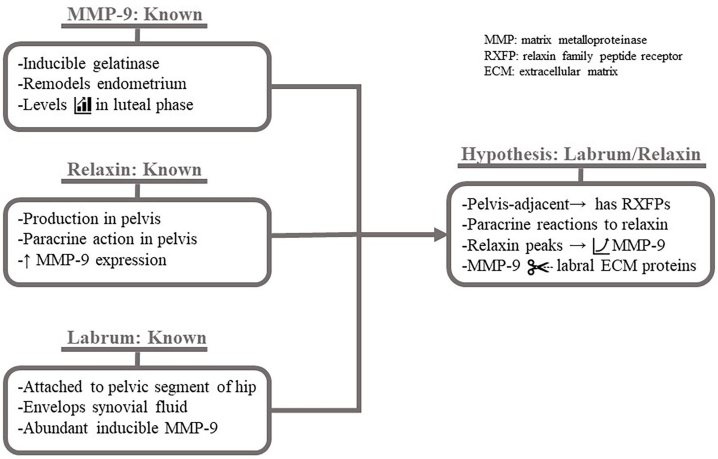

FIGURE 3 | Hypothesized mechanism of relaxin-induced acetabular labrum damage. Known factors giving rise to hypothetical impact of relaxin on the acetabular labrum. It is known that MMP-9 is the inducible gelatinase (MMP-2 is not) which is expressed at high levels during the luteal phase for endometrial. It is known that relaxin, produced in the pelvis and exerting paracrine effects, increases MMP-9 expression. Finally, it is known that the anchored to the pelvis serves as a "seal" enclosing synovial fluid, which may contain hormones, and that the cells express MMP-9 at an unusually high level when induced . Given these known factors: the acetabular labrum likely expresses RXFPs and increases MMP-9 expression in a paracrine to relaxin. MMP-9 degrades ECM proteins, weakening the labrum.

pelvis, has paracrine capabilities, and upregulates expression of the same collagen-degrading MMPs present on the acetabular labrum. What is not known, the "missing link", is whether cells of the acetabular labrum, hip joint synovium, and other soft tissues of the hip joint contain the relaxin receptors necessary to bridge the route from relaxin peaks to increased risk of female hip injuries.

CONCEPTUAL GAP 2: HOW CAN DETRIMENTAL MUSCULOSKELETAL SIDE EFFECTS OF RELAXIN BE COUNTERED?

It is known that relaxin is crucial for correct function/fertility of the female reproductive tract. Therefore, a theoretical broad "anti-relaxin" would prove harmful. However, it is also apparent that many musculoskeletal effects of relaxin are not physiologically necessary nor desirable, such as hip and knee injuries in female athletes. This presents the question of how to decrease detrimental side effects of relaxin peaks on the musculoskeletal system without causing iatrogenic issues. There are likely multiple avenues by which to approach this issue. Studies in the present review highlight problematic effects of relaxin, but also bring up potential mitigating factors, such as OCP use and menstrual cycle tracking.

LIMITATIONS

Due to the veritable absence of any type of literature discussing women's hip injuries in the context of relaxin, the premise of this review is based entirely on inductive reasoning. Additionally, consideration of lower-level of evidence literature and inconclusive literature was necessary.

SUMMARY OF SCOPING REVIEW

The present review showed the scientific logic and medical importance of further researching the potential causative role of relaxin in female hip injuries. Appraisal of available information on related factors, and identification of conceptual gaps for future research was completed.

Collectively, the factors examined in this review support the inference that relaxin impacts the female predominance of soft tissue hip injuries. The steps from relaxin peak to increased ACL injury risk are likely highly analogous to the methodology by which relaxin can precipitate hip damage. Relaxin's synthesis in the pelvis and paracrine profile of action support the potential of relaxin/hip interactions.

This review also highlights why relaxin's sex-specific musculoskeletal effects should be a major orthopedic research focus. The first conceptual gap, bridged simply by assessing male vs. female hip tissue for relaxin receptors, could show a female-specific, predictable susceptibility to devastating lower extremity injuries. Subsequently, multiple considerations for the second conceptual gap, attenuating relaxin-associated musculoskeletal damage in women, would be critical to explore in order to provide quality, equitable orthopedic care to male and female patients.

CONCLUSION

Menstrual cycle peaks of relaxin activate MMPs, which locally degrade collagen and gelatine. Women have relaxin receptors in multiple joints, and increased relaxin correlates with increased musculoskeletal injuries. Relaxin has paracrine effects in the female pelvis on ligaments adjacent to hip structures, such as

acetabular labral cells and hip capsule/synovial cells which express high levels of relaxin-targeted MMPs. Therefore, it is imperative to investigate the effect of relaxin on the hip to determine if increased levels of relaxin are associated with an increased risk of acetabular labral tears.

DATA AVAILABILITY STATEMENT

The original contributions presented in the study are included in the article/**Supplementary Material**. Further inquiries can be directed to the corresponding author.

AUTHOR CONTRIBUTIONS

Per the International Committee of Medical Journal Editors Recommendations for the Conduct, Reporting, Editing, and Publication of Scholarly Work in Medical Journals (ICMJE) Recommendations 2019. EP—author, per ICMJE 2019 recommendations. AM—author, per ICMJE 2019 recommendations. JG—author, per ICMJE 2019 recommendations. MW—author, per ICMJE 2019 recommendations. RW—author, per ICMJE 2019 recommendations. JB—contributor, per ICMJE 2019 recommendations. EP conceived the original review idea, and presented this idea to AM, JG, MW, and RW to direct further topic exploration and refinement of the review focus. JB advised the authors on the design of the work, providing scoping review information. EP ran preliminary PubMed literature searches before EP, AM, and JB met to tailor the search strings for data acquisition. EP and AM performed preliminary data analysis *via* the paper screening process, with oversight and input from JG, MW, and RW with regard to screening directions, such as inclusion or exclusion of animal-only subjects. EP and AM then performed more detailed analysis of included studies and interpretation of the charting results, with guidance from JG, MW, and RW on matters such as appropriate categories into which data could be grouped and assessed (i.e. the musculoskeletal effects of relaxin category). EP and AM drafted the manuscript, with significant changes to manuscript organization implemented by JG, MW, and RW. All authors then continued to revise the manuscript until, by consensus, each gave the current version final approval for publication. All authors agree to be held accountable for accuracy and integrity of the work.

ACKNOWLEDGMENTS

The authors would like to thank Dr. Michael Haugsdal in the Department of Obstetrics and Gynecology for his review of the accuracy of **Figure 1**; depicting the general chronology of menstrual cycle hormone peaks in a eumenorrheic woman. The authors would also like to thank Jennifer DeBerg from the Hardin Library of Health Sciences for her assistance and expertise in refining search strategies. There was no source of funding for this study.

SUPPLEMENTARY MATERIAL

The Supplementary Material for this article can be found online at: https://www.frontiersin.org/articles/10.3389/fendo.2022.827512/full#supplementary-material

REFERENCES

1. Dragoo JL, Castillo TN, Braun HJ, Ridley BA, Kennedy AC, Golish SR. Prospective Correlation Between Serum Relaxin Concentration and Anterior Cruciate Ligament Tears Among Elite Collegiate Female Athletes. *Am J Sports Med* (2011) 39(10):2175–80. doi: 10.1177/0363546511413378
2. Narvani AA, Tsiridis E, Kendall S, Chaudhuri R, Thomas P. A Preliminary Report on Prevalence of Acetabular Labrum Tears in Sports Patients With Groin Pain. *Knee Surg Sports Traumatol Arthrosc* (2003) 11(6):403–8. doi: 10.1007/s00167-003-0390-7
3. Weber AE, Nakata H, Mayer EN, Bolia IK, Philippon MJ, Snibbe J, et al. Return to Sport After Hip Arthroscopy for Femoroacetabular Impingement Syndrome in NCAA Division I Athletes: Experience at a Single Institution. *Orthop J Sports Med* (2020) 8(5):2325967120918383. doi: 10.1177/2325967120918383
4. Wolf JM, Williams AE, Delaronde S, Leger R, Clifton KB, King KB. Relationship of Serum Relaxin to Generalized and Trapezial-Metacarpal Joint Laxity. *J Handb Surg Am* (2013) 38(4):721–8. doi: 10.1016/j.jhsa.2013.01.019
5. Wolf JM. The Influence of Ligamentous Laxity and Gender: Implications for Hand Surgeons. *J Handb Surg Am* (2009) 34(1):161–3. doi: 10.1016/j.jhsa.2008.09.012
6. Sung JK, Akelman E. Thumb Carpometacarpal Arthritis. *Tech Orthop* (2009) 24(1):23–6. doi: 10.1097/BTO.0b013e3181a07f4c
7. Brophy RH, Silvers HJ, Mandelbaum BR. Anterior Cruciate Ligament Injuries: Etiology and Prevention. *Sports Med Arthroscopy Rev* (2010) 18 (1):2–11. doi: 10.1097/JSA.0b013e3181cdd195
8. Arnold C, Van Bell C, Rogers V, Cooney T, Arnold C, Van Bell C, et al. The Relationship Between Serum Relaxin and Knee Joint Laxity in Female Athletes. *Orthopedics* (2002) 25(6):669–73. doi: 10.3928/0147-7447-20020601-18
9. Dragoo JL, Castillo TN, Korotkova TA, Kennedy AC, Kim HJ, Stewart DR. Trends in Serum Relaxin Concentration Among Elite Collegiate Female Athletes. *Int J Womens Health* (2011) 3:19–24.
10. Dragoo JL, Lee RS, Benhaim P, Finerman GA, Hame SL. Relaxin Receptors in the Human Female Anterior Cruciate Ligament. *Am J Sports Med* (2003) 31 (4):577–84. doi: 10.1177/0363546503030310041701
11. DeFroda SF, Bokshan SL, Worobey S, Ready L, Daniels AH, Owens BD. Oral Contraceptives Provide Protection Against Anterior Cruciate Ligament Tears: A National Database Study of 165,748 Female Patients. *Phys Sportsmed* (2019) 47(4):416–20. doi: 10.1080/00913847.2019.1600334
12. Alves de Oliveira J, Marques Simek Vega GonÃ§alves TS, Soares Reis Vilanova L, Maria Bovi Ambrosano G, Rodrigues Garcia RCM. Female Hormones Fluctuation and Chewing Movement of Patients With Disc Displacement. *Rev Odonto Ciencia* (2012) 27(1):20–5. doi: 10.1590/S1980-65232012000100004
13. Nose-Ogura S, Yoshino O, Yamada-Nomoto K, Nakamura M, Harada M, Dohi M, et al. Oral Contraceptive Therapy Reduces Serum Relaxin-2 in Elite Female Athletes. *J Obstet Gynaecol Res* (2017) 43(3):530–5. doi: 10.1111/jog.13226
14. Deniz K, Bascil Tutuncu N, Bayraktar N, Uckan S. Does Hormone Relaxin Have a Potential Role in TMJ Internal Derangements? *J Oral Maxillofacial Surg* (2012) 70(9):e99–100. doi: 10.1016/j.joms.2012.06.150
15. Wolf JM, Williams AE, King KB. Serum Relaxin is Correlated With Relaxin and Mmp-1 in the Anterior Oblique Ligament Level 3 Evidence. *J Hand Surg* (2011) 36(8):28. doi: 10.1016/S0363-5023(11)60032-4

16. Henneman S, Bildt MM, DeGroot J, Kuijpers-Jagtman AM, Von den Hoff JW. Relaxin Stimulates MMP-2 and α-Smooth Muscle Actin Expression by Human Periodontal Ligament Cells. *Arch Oral Biol* (2008) 53(2):161–7. doi: 10.1016/j.archoralbio.2007.08.010
17. Wolf J, Scott F, Etchell E, Williams AE, Delaronde S, King KB. Serum Relaxin is Correlated With Relaxin Receptors and MMP-1 in the Anterior Oblique Ligament. *Osteoarthr Cartil* (2012) 20:S250. doi: 10.1016/j.joca.2012.02.416
18. Andren L. Pelvic Instability in Newborns With Special Reference to Congenital Dislocation of the Hip and Hormonal Factors. *A Roentgenol Study Acta Radiol Suppl* (1962) 212:1–66.
19. Maclennan AH, Maclennan SC. Symptom-Giving Pelvic Girdle Relaxation of Pregnancy, Postnatal Pelvic Joint Syndrome and Developmental Dysplasia of the Hip. *Acta Obstetricia Gynecol Scandinavica* (1997) 76(8):760–4. doi: 10.3109/00016349709024343
20. Morey SS. AAP Develops Guidelines for Early Detection of Dislocated Hips. *Am Family Physician* (2001) 63(3):565–8.
21. Schuster RO, Port M. Abnormal Pronation in Children. An Hormonal Etiology. *J Am Podiatry Assoc* (1977) 67(9):613–5. doi: 10.7547/87507315-67-9-613
22. Munn Z, Peters MDJ, Stern C, Tufanaru C, McArthur A, Aromataris E. Systematic Review or Scoping Review? Guidance for Authors When Choosing Between a Systematic or Scoping Review Approach. *BMC Med Res Methodol* (2018) 18(1):143. doi: 10.1186/s12874-018-0611-x
23. Goldsmith LT, Weiss G, Steinetz BG. Relaxin and Its Role in Pregnancy. *Endocrinol Metab Clin North Am* (1995) 24(1):171–86. doi: 10.1016/S0889-8529(18)30058-6
24. Grossman J, Frishman WH. Relaxin: A New Approach for the Treatment of Acute Congestive Heart Failure. *Cardiol Rev* (2010) 18(6):305–12. doi: 10.1097/CRD.0b013e3181f493e3
25. Lubahn J, Ivance D, Konieczko E, Cooney T. Immunohistochemical Detection of Relaxin Binding to the Volar Oblique Ligament. *J Handb Surg Am* (2006) 31(1):80–4. doi: 10.1016/j.jhsa.2005.09.012
26. MacLennan AH. The Role of Relaxin in Human Reproduction. *Clin Reprod Fertil* (1983) 2(2):77–95.
27. Powell BS, Dhaher YY, Szleifer IG. Review of the Multiscale Effects of Female Sex Hormones on Matrix Metalloproteinase-Mediated Collagen Degradation. *Crit Rev BioMed Eng* (2015) 43(5-6):401–28. doi: 10.1615/CritRevBiomedEng.2016016590
28. Wolf JM, Cameron KL, Clifton KB, Owens BD. Serum Relaxin Levels in Young Athletic Men Are Comparable With Those in Women. *Orthopedics* (2013) 36(2):128–31. doi: 10.3928/01477447-20130122-06
29. Bryant-Greenwood GD, Mercado-Simmen R, Yamamoto SY, Arakaki RF, Uchima FD, Greenwood FC. Relaxin Receptors and a Study of the Physiological Roles of Relaxin. *Adv Exp Med Biol* (1982) 143:289–314. doi: 10.1007/978-1-4613-3368-5_27
30. Kapila S, Xie Y. Targeted Induction of Collagenase and Stromelysin by Relaxin in Unprimed and β-Estradiol-Primed Diarthrodial Joint Fibrocartilaginous Cells But Not in Synoviocytes. *Lab Invest* (1998) 78(8):925–38.
31. Kleine SA, Budsberg SC. Synovial Membrane Receptors as Therapeutic Targets: A Review of Receptor Localization, Structure, and Function. *J Orthop Res* (2017) 35(8):1589–605. doi: 10.1002/jor.23568
32. Ando H, Moriwaki C. Studies on Relaxin Assay With X-Ray Photography. *Endocrine J* (1960) 7:167–70. doi: 10.1507/endocrj1954.7.167
33. Galey S, Konieczko EM, Arnold CA, Cooney TE. Immunohistological Detection of Relaxin Binding to Anterior Cruciate Ligaments. *Orthopedics* (2003) 26(12):1201–4. doi: 10.3928/0147-7447-20031201-08
34. Clifton K, Rodner CM, Drissi H, Wolf JM. Detection of Relaxin Receptor in the Synovium and Dorsoradial Ligament of the Trapeziometacarpal Joint: Not a Clinical Study. *J Handb Surg* (2012) 37(8):7. doi: 10.1016/S0363-5023(12)60010-0
35. Pearson SJ, Burgess KE, Onambélé GL. Serum Relaxin Levels Affect the *In Vivo* Properties of Some But Not All Tendons in Normally Menstruating Young Women. *Exp Physiol* (2011) 96(7):681–8. doi: 10.1113/expphysiol.2011.057877
36. Komatsu I, Lubahn JD. Anatomy and Biomechanics of the Thumb Carpometacarpal Joint. *Operative Techniques Orthopaedics* (2018) 28(1):1–5. doi: 10.1053/j.oto.2017.12.002
37. Deniz K, Guler N, Bascil Tutuncu N, Uckan S. Analysis of Hormone Relaxin in the Synovial Fluid of Patients With Temporomandibular Disorders. *Int J Oral Maxillofacial Surg* (2013) 42(10):1359. doi: 10.1016/j.ijom.2013.07.672
38. McGorray SP, Dolce C, Kramer S, Stewart D, Wheeler TT. A Randomized, Placebo-Controlled Clinical Trial on the Effects of Recombinant Human Relaxin on Tooth Movement and Short-Term Stability. *Am J Orthod Dentofacial Orthop* (2012) 141(2):196–203. doi: 10.1016/j.ajodo.2011.07.024
39. Owens BD, Cameron KL, Clifton KB, Svoboda SJ, Wolf JM. Association Between Serum Relaxin and Subsequent Shoulder Instability. *Orthopedics* (2016) 39(4):e724–8. doi: 10.3928/01477447-20160421-01
40. MacLennan AH, Nicolson R, Green RC, Bath M. Serum Relaxin and Pelvic Pain of Pregnancy. *Lancet* (1986) 2(8501):243–5. doi: 10.1016/S0140-6736(86)92069-6
41. MacLennan AH. The Role of the Hormone Relaxin in Human Reproduction and Pelvic Girdle Relaxation. *Scand J Rheumatol Suppl* (1991) 88:7–15.
42. Kieserman-Shmokler C, Swenson CW, Chen L, Desmond LM, Ashton-Miller JA, DeLancey JO. From Molecular to Macro: The Key Role of the Apical Ligaments *In Utero*vaginal Support. *Am J Obstetrics Gynecol* (2020) 222(5):427–36. doi: 10.1016/j.ajog.2019.10.006
43. Reisenauer C, Renz M, Busch C, Drews U. Smooth Muscle in the Sacrouterine Ligament is Regulated by Oxytocin and Relaxin: Perfusion of Surgical Samples Under the Microscope. *Arch Gynecol Obstetrics* (2010) 282:S57. doi: 10.1007/s00404-010-1632-9
44. Schott S, Reisenauer C, Busch C. Presence of Relaxin-2, Oxytocin and Their Receptors *In Utero*sacral Ligaments of Pre-Menopausal Patients With and Without Pelvic Organ Prolapse. *Acta Obstet Gynecol Scand* (2014) 93(10):991–6. doi: 10.1111/aogs.12462
45. Udén A, Lindhagen T. Inguinal Hernia in Patients With Congenital Dislocation of the Hip. A Sign of General Connective Tissue Disorder. *Acta Orthop Scand* (1988) 59(6):667–8. doi: 10.3109/17453678809149421
46. Bookhout MM, Boissonnault JS. Musculoskeletal Dysfunction in the Female Pelvis. *Orthopaedic Phys Ther Clinics North Am* (1996) 5(1):23–45.
47. Kristiansson P, Svardsudd K, Von Schoultz B. Serum Relaxin, Symphyseal Pain, and Back Pain During Pregnancy. *Am J Obstetrics Gynecol* (1996) 175(5):1342–7. doi: 10.1016/S0002-9378(96)70052-2
48. Ritchie JR. Orthopedic Considerations During Pregnancy. *Clin Obstetrics Gynecol* (2003) 46(2):456–66. doi: 10.1097/00003081-200306000-00024
49. Saugstad LF. Persistent Pelvic Pain and Pelvic Joint Instability. *Eur J Obstet Gynecol Reprod Biol* (1991) 41(3):197–201. doi: 10.1016/0028-2243(91)90024-F
50. Borg-Stein J, Dugan SA. Musculoskeletal Disorders of Pregnancy, Delivery and Postpartum. *Phys Med Rehabil Clinics North America* (2007) 18(3):459–76. doi: 10.1016/j.pmr.2007.05.005
51. Leadbetter RE, Mawer D, Lindow SW. Symphysis Pubis Dysfunction: A Review of the Literature. *J Maternal-Fetal Neonatal Med* (2004) 16(6):349–54. doi: 10.1080/jmf.16.6.349.354
52. Bracken J, Tran T, Ditchfield M. Developmental Dysplasia of the Hip: Controversies and Current Concepts. *J Paediatrics Child Health* (2012) 48(11):963–73. doi: 10.1111/j.1440-1754.2012.02601.x
53. Forst J, Forst C, Forst R, Heller KD. Pathogenetic Relevance of the Pregnancy Hormone Relaxin to Inborn Hip Instability. *Arch Orthop Trauma Surg* (1997) 116(4):209–12. doi: 10.1007/BF00393711
54. Roof AC, Jinguji TM, White KK. Musculoskeletal Screening: Developmental Dysplasia of the Hip. *Pediatr Ann* (2013) 42(11):229–35. doi: 10.3928/00904481-20131022-10
55. Rhodes AM, Clarke NM. A Review of Environmental Factors Implicated in Human Developmental Dysplasia of the Hip. *J Child Orthop* (2014) 8(5):375–9. doi: 10.1007/s11832-014-0615-y
56. Armfield DR, Kim DHM, Towers JD, Bradley JP, Robertson DD. Sports-Related Muscle Injury in the Lower Extremity. *Clinics Sports Med* (2006) 25(4):803–42. doi: 10.1016/j.csm.2006.06.011
57. Arya RK. Low Back Pain - Signs, Symptoms, and Management. *J Indian Acad Clin Med* (2014) 15(1).
58. Braddon SA. The Effects of Relaxin on Cyclic-AMP an Ornithine Decarboxylase Levels in Target Tissues. *Adv Exp Med Biol* (1982) 143:255–72. doi: 10.1007/978-1-4613-3368-5_23
59. Camiel MR. Relaxin and the Radiolucent Fissure in the Symphysis Pubis During Pregnancy: The Gas Phenomenon. *Am J Obstetrics Gynecol* (1986) 154(5):1104–5. doi: 10.1016/0002-9378(86)90763-5

60. Charalambous CP, Morrey BF. Posttraumatic Elbow Stiffness. *J Bone Joint Surg Ser A* (2012) 94(15):1428–37. doi: 10.2106/JBJS.K.00711
61. Em S, Oktayoglu P, Bozkurt M, Caglayan M, Karakoc M, Ucar D, et al. Serum Relaxin Levels in Benign Hypermobility Syndrome. *J Back Musculoskelet Rehabil* (2015) 28(3):473–9. doi: 10.3233/BMR-140543
62. Ferlin A, Pepe A, Facciolli A, Gianesello L, Foresta C. Relaxin Stimulates Osteoclast Differentiation and Activation. *Bone* (2010) 46(2):504–13. doi: 10.1016/j.bone.2009.10.007
63. Gates C, Huard J. Management of Skeletal Muscle Injuries in Military Personnel. *Operative Techniques Sports Med* (2005) 13(4):247–56. doi: 10.1053/j.otsm.2006.01.012
64. Gould S, Hooper J, Strauss E. Anterior Cruciate Ligament Injuries in Females Risk Factors, Prevention, and Outcomes. *Bull Hosp Joint Dis* (2016) 74(1):46–51.
65. Hamilton DAJr., Wright RDJr., Moghadamian ES, Bruce BT. Orthopaedic Considerations in the Pregnant Patient. *Curr Orthopaedic Pract* (2012) 23 (6):601–8. doi: 10.1097/BCO.0b013e318264843e
66. Heckman JD, Sassard R. Musculoskeletal Considerations in Pregnancy. *J Bone Joint Surg Ser A* (1994) 76(11):1720–31. doi: 10.2106/00004623-199411000-00018
67. Huston LJ, Greenfield MLVH, Wojtys EM. Anterior Cruciate Ligament Injuries in the Female Athlete: Potential Risk Factors. *Clin Orthopaedics Related Res* (2000) 372):50–63. doi: 10.1097/00003086-200003000-00007
68. Kapila S, Park Y, Ahmad N, Hosomichi J, Hayami T, Tacon C. Mechanisms for Relaxin's Modulation of MMPs and Matrix Loss in Fibrocartilages. *Ital J Anat Embryol* (2013) 118(1 SUPPL.):62–5.
69. Marshall-Gradisnik S, Nicholson V, Weatherby R, Bryant A. The Relationship Between Relaxin, Tumour Necrosis Factor Alpha and Macrophage Inflammatory Factor and Monophasic Oral Contraception Pill. *J Sci Med Sport* (2004) 7(4 Supplement):28–. doi: 10.1016/S1440-2440(04)80102-6
70. Martin B, Romero G, Salama G. Cardioprotective Actions of Relaxin. *Mol Cell Endocrinol* (2019) 487:45–53. doi: 10.1016/j.mce.2018.12.016
71. Nistri S, Bigazzi M, Bani D. Relaxin as a Cardiovascular Hormone: Physiology, Pathophysiology and Therapeutic Promises. *Cardiovasc Hematol Agents Med Chem* (2007) 5(2):101–8. doi: 10.2174/187152507780363179
72. Noon ML, Hoch AZ. Challenges of the Pregnant Athlete and Low Back Pain. *Curr Sports Med Rep* (2012) 11(1):43–8. doi: 10.1249/JSR.0b013e31824330b6
73. Owens K, Pearson A, Mason G. Pubic Symphysis Separation. *Fetal Maternal Med Rev* (2002) 13(2):141–55. doi: 10.1017/S0965539502000244
74. Pires R, Labronici PJ, Giordano V, Kojima KE, Kfuri M, Barbisan M, et al. Intrapartum Pubic Symphysis Disruption. *Ann Med Health Sci Res* (2015) 5 (6):476–9. doi: 10.4103/2141-9248.177980
75. Pokorny MJ, Smith TD, Calus SA, Dennison EA. Self-Reported Oral Contraceptive Use and Peripheral Joint Laxity. *J Orthop Sports Phys Ther* (2000) 30(11):683–92. doi: 10.2519/jospt.2000.30.11.683
76. Ren XF, Zhao H, Gong XC, Wang LN, Ma JF. RLN2 Regulates *In Vitro* Invasion and Viability of Osteosarcoma MG-63 Cells *via* S100A4/MMP-9 Signal. *Eur Rev Med Pharmacol Sci* (2015) 19(6):1030–6.
77. Samuel CS, Unemori EN, Mookerjee I, Bathgate RA, Layfield SL, Mak J, et al. Relaxin Modulates Cardiac Fibroblast Proliferation, Differentiation, and Collagen Production and Reverses Cardiac Fibrosis In Vivo. *Endocrinology* (2004) 145(9):4125–33. doi: 10.1210/en.2004-0209
78. Sanders AE, Jain D, Sofer T, Kerr KF, Laurie CC, Shaffer JR, et al. GWAS Identifies New Loci for Painful Temporomandibular Disorder: Hispanic Community Health Study/Study of Latinos. *J Dent Res* (2017) 96(3):277–84. doi: 10.1177/0022034516686562
79. Snith FW, Smith PA. Musculoskeletal Differences Between Males and Females. *Sports Med Arthroscopy Rev* (2002) 10(1):98–100. doi: 10.1097/00132585-200210010-00014
80. Steinetz BG, Manning JP. Influence of Growth Hormone, Steroids and Relaxin on Acid Phosphatase Activity of Connective Tissue. *Proc Soc Exp Biol Med Soc Exp Biol Med (New York NY)* (1967) 124(1):180–4. doi: 10.3181/00379727-124-31695
81. Szalay EA. Sexual Dimorphism in Musculoskeletal Medicine. *Eur Musculoskeletal Rev* (2012) 7(3):162–4.
82. Toth AP, Cordasco FA. Anterior Cruciate Ligament Injuries in the Female Athlete. *J Gend Specif Med* (2001) 4(4):25–34.
83. van der MC. Experiments on the Mechanism of Action of Relaxin. *Acta Endocrinol* (1950) 4(4):325–42. doi: 10.1530/acta.0.0040325
84. Veitia R, Laurent A, Quintana-Murci L, Ottolenghi C, Fellous M, Vidaud M, et al. The INSL4 Gene Maps Close to WI-5527 at 9p24.1→P23.3 Clustered With Two Relaxin Genes and Outside the Critical Region for the Monosomy 9p Syndrome. *Cytogenetics Cell Genet* (1998) 81(3-4):275–7. doi: 10.1159/000015045
85. Warren MP, Fried JL. Temporomandibular Disorders and Hormones in Women. *Cells Tissues Organs* (2001) 169(3):187–92. doi: 10.1159/000047881
86. Weinberg A. An X-Ray Pelvimetric Study of Relaxin Extract in Pelvic Expansion. *Surg Gynecol Obstetr* (1956) 103(3):303–6.
87. Freeman BM, Mountain DJ, Brock TC, Chapman JR, Kirkpatrick SS, Freeman MB, et al. Low Testosterone Elevates Interleukin Family Cytokines in a Rodent Model: A Possible Mechanism for the Potentiation of Vascular Disease in Androgen-Deficient Males. *J Surg Res* (2014) 190(1):319–27. doi: 10.1016/j.jss.2014.03.017
88. Henmi H, Endo T, Nagasawa K, Hayashi T, Chida M, Akutagawa N, et al. Lysyl Oxidase and MMP-2 Expression in Dehydroepiandrosterone-Induced Polycystic Ovary in Rats. *Biol Reprod* (2001) 64(1):157–62. doi: 10.1095/biolreprod64.1.157
89. Dhollander AA, Lambrecht S, Verdonk PC, Audenaert EA, Almqvist KF, Pattyn C, et al. First Insights Into Human Acetabular Labrum Cell Metabolism. *Osteoarthr Cartil* (2012) 20(7):670–7. doi: 10.1016/j.joca.2012.03.023

Conflict of Interest: All authors have completed the ICMJE uniform disclosure form at www.icmje.org/coi_disclosure.pdf and declare as follows: MW reports personal fees from Depuy Synthes Sales Inc, other from Smith & Nephew, personal fees from Zimmer Biomet Inc, personal fees from Stryker Corp; outside the submitted work. RW reports personal fees, non-financial support and other from Smith and Nephew, other from Arthrex, personal fees from Medical Device Business Systems, personal fees from Linvatec Corporation, other from Wardlow Enterprises; outside the submitted work.

The remaining authors declare that the research was conducted in the absence of any commercial or financial relationships that could be construed as a potential conflict of interest.

frontiers in Endocrinology

ORIGINAL RESEARCH
published: 24 February 2022
doi: 10.3389/fendo.2022.817146

Water Extract of *Rhizoma Drynaria* Selectively Exerts Estrogenic Activities in Ovariectomized Rats and Estrogen Receptor-Positive Cells

Liping Zhou[1,2†], Ka-Ying Wong[2†], Christina Chui-Wa Poon[2,3], Wenxuan Yu[2], Huihui Xiao[2,3], Chi-On Chan[2,4], Daniel Kam-Wah Mok[2,4] and Man-Sau Wong[2,3,4]*

[1] Cell Therapy Center, Xuanwu Hospital Capital Medical University, Beijing, China, [2] Department of Applied Biology and Chemical Technology, The Hong Kong Polytechnic University, Hong Kong, Hong Kong SAR, China, [3] Research Center for Chinese Medicine Innovation, The Hong Kong Polytechnic University, Kowloon, Hong Kong SAR, China, [4] State Key Laboratory of Chinese Medicine and Molecular Pharmacology (Incubation), The Hong Kong Polytechnic University Shenzhen Research Institute, Shenzhen, China

OPEN ACCESS

Edited by:
Sadiq Umar,
University of Illinois at Chicago,
United States

Reviewed by:
Abdul Syed,
University of Illinois at Chicago,
United States
Yan Zhang,
Shanghai University of Traditional Chinese Medicine, China

***Correspondence:**
Man-Sau Wong
bcmswong@polyu.edu.hk

[†]These authors have contributed equally to this work

Specialty section:
This article was submitted to Bone Research, a section of the journal Frontiers in Endocrinology

Received: 17 November 2021
Accepted: 27 January 2022
Published: 24 February 2022

Citation:
Zhou L, Wong K-Y, Poon CC-W, Yu W, Xiao H, Chan C-O, Mok DK-W and Wong M-S (2022) Water Extract of Rhizoma Drynaria Selectively Exerts Estrogenic Activities in Ovariectomized Rats and Estrogen Receptor-Positive Cells. Front. Endocrinol. 13:817146. doi: 10.3389/fendo.2022.817146

Our previous study demonstrated that the bone protective actions of herbal medicine *Rhizoma Drynariae* (Gusuibu, RD) were mainly mediated by flavonoid phytoestrogens *via* estrogen receptors, raising concerns about the safety of using RD as it may induce estrogen-like risk-benefit profile and interact with other ER ligands, such as selective estrogen receptor modulators (SERMs), when coadministered. The present study evaluated the estrogenic activities of RD and its potential interaction with tamoxifen, a SERM, in estrogen-sensitive tissues by using mature ovariectomized (OVX) rats and ER-positive cells. Similar to but weaker than tamoxifen, RD at its clinical dose dramatically ameliorated OVX-induced changes in bone and dopamine metabolism-related markers in OVX rats. However, tamoxifen, but not RD, induced uterotrophic effects. No significant alteration in mammary gland was observed in OVX rats treated with RD, which was different from the inhibitory actions of tamoxifen. The two-way ANOVA results indicated the interactions between RD and tamoxifen in the bone, brain, and uterus of OVX rats while RD did not alter their responses to tamoxifen. Our results demonstrate that RD selectively exerts estrogenic actions in a different manner from tamoxifen. Moreover, RD interacts with tamoxifen without altering its effects in OVX rats.

Keywords: tissue selectivity, selective estrogen receptor modulators (SERMs), rhizoma drynaria, phytoestrogen, estrogen receptors, estrogenic activities

Abbreviations: BMD, bone mineral density; BV/TV, bone volume over total volume; DAT, dopamine transporter; DPD, deoxypyridinoline; Conn.D, connectivity density; C3, complement component 3; ER, estrogen receptors; ERE, estrogen response element; FSH, follicle-stimulating hormone; HH3, histone H3; HPG, hypothalamus-pituitary-gonadal; HPLC, high-performance liquid chromatography; HRT, hormone replacement therapy; LC-MS, liquid chromatography-mass spectrometry; LH, luteinizing hormone; OCN, osteocalcin; OVX, ovariectomized; SERMs, selective estrogen receptor modulators; Tb.Sp, trabecular bone separation; Tb.Th, trabecular bone thickness; Tb.N, trabecular bone number; TCMs, traditional Chinese medicine; TH, tyrosine hydroxylase.

INTRODUCTION

Hormone replacement therapy (HRT) carries considerable benefits for treatment of menopausal syndrome, like vasomotor symptoms and postmenopausal osteoporosis. However, HRT significantly increases the risk of breast cancer, endometrial cancer, and cardiovascular disease, making HRT a subject of argument (1). Selective estrogen receptor modulators (SERMs) act as either estrogen receptor (ER) antagonist or agonist depending on the tissue type and are clinically prescribed to postmenopausal women as an alternative to HRT. Tamoxifen is clinically used for treatment of breast cancer as it is an ER antagonist in breast. On the other hand, it exerts antiosteoporotic effects in menopausal women as an ER agonist in bone (2). However, due to undesirable uterine abnormalities, depression, and increased risk of endometrial cancer after tamoxifen administration, menopausal women try to seek help from alternative approaches (3).

Phytoestrogens derived from plants are also called natural estrogen and are the most popular alternative approach (4). They act in the same way as SERMs as they could activate ERs and exhibit various estrogenic and antiestrogenic effects in different tissues. As a main source of phytoestrogens, herbal medicines are vigorously promoted because of their perceived health benefits and minimal side effects (4). Indeed, the demands for herbal medicine for management of menopausal symptoms are increasing worldwide.

Rhizoma drynariae (*Gusuibu*, RD or GSB), the dried rhizome of perennial pteridophyte *Drynaria fortunei*, was first recorded in "Ben Cao Shi Yi" over 1,000 years ago and is recognized as a "kidney-tonifying" herb for bone-related disorders such as osteoporosis and bone fracture for many years in China. RD extract has been reported to mimic estrogen and increase bone formation in OVX mice and promote osteoblastic differentiation in pre-osteoblastic MC3T3-E1 cells (5). The major bioactive constituents of RD are demonstrated to be flavonoids, among which naringin and neoeriocitrin are the two richest flavonoids (6). Our previous works confirmed the antiosteoporotic activity of RD in preclinical model and further reported that total flavonoids of RD and naringin could mimic estrogen in stimulating cell proliferation and alkaline phosphatase (ALP) activity *via* activating ER in rat osteoblastic UMR106 cells (7, 8). These results suggest that RD contains phytoestrogens, which mediate the bone-protective effects of RD *via* ERs.

As more and more postmenopausal women are using phytoestrogens and phytoestrogen-containing herbal medicine for relieving their menopausal symptoms, concerns about their safety have been raised whether they will bring similar risk-benefit profile as estrogen and SERMs. Therefore, it is of particular importance to investigate whether these phytoestrogen-containing herbal medicines, like RD, could selectively induce estrogen-like activities in target tissues without inducing undesirable actions. Moreover, it will be crucial to determine if RD interacts with SERMs to either increase or decrease their pharmacological activities, which is of fundamental significance to the medical community and those postmenopausal women with breast cancer who simultaneously take supplements, like herbal medicines, together with their standard treatment.

Our current work defined and compared the possible estrogenic or antiestrogenic effects of RD with those of tamoxifen in the bone, brain, uterus, and breast by using both *in vivo* mature OVX rats and ER-positive cell lines. In addition, the potential interactions between RD and tamoxifen were also determined.

METHODS

Preparation and Chemical Analysis of RD Extract

Dry aerial part of *rhizoma drynariae* was purchased from mainland China and authenticated by Dr. Chen Sibao at the State Key Laboratory of Chinese Medicine and Molecular Pharmacology (Incubation) in Shenzhen (No.: SZ2016HEP01). High-performance liquid chromatography (HPLC) assays were conducted to ensure that the quality of the raw herb fulfill the requirement of the China Pharmacopoeia and/or the Hong Kong Chinese Materia Medica Standards. Upon authentication, raw herb was delivered to Xi'an Pincredit Bio-tech Co., Ltd. for extract preparation. Briefly, RD was boiled in 10 volumes of water (v/w) for 20 min and for another 1 h in triplicate. The extract was obtained by filtration and dried under vacuum and stored at −20°C. The amount of naringin extract, the main active compound of RD, was quantified in RD extract by liquid chromatography-mass spectrometry (LC-MS).

Animal Experiment and Sample Collection

All procedures involving animals in the present study were approved by the Hong Kong Polytechnic University Animal Subjects Ethics Sub-committee (ASESC Case: 15-16/31-ABCT-R-HMRF). Six-month-old female Sprague-Dawley rats were ovariectomized or sham-operated (Sham). After a 2-week recovery, the OVX rats were randomly subjected into 5 treatment groups (10 rats/group) and orally given double-distilled water (OVX), water suspension of 17ß-estradiol (E2, 1.0 mg/kg/day), RD (0.2 g/kg/day), tamoxifen (Tamo, 0.1 mg/kg/day), or the combined use of RD and tamoxifen for 3 months. During the whole treatment period, the animals were paired fed with phytoestrogen-free AIN-93M diet (composition was provided in **Supplementary Table S1**) to avoid the influence of phytoestrogens in the diet. At euthanasia, urine, serum, uterus, breast tissue, lumbar spine, and striatum were collected to evaluate the specific estrogenic parameters in each tissue.

Biochemical Assay of Serum and Urine

Serum estradiol, follicle-stimulating hormone (FSH) and luteinizing hormone (LH), and osteocalcin (OCN), as well as urinary deoxypyridinoline (DPD) were measured by using EIA or ELISA commercial kits (EIA Estradiol Kit, CayMan; FSH and LH ELISA Kits, CloudClone, Katy, TX, USA; Osteocalcin ELISA Kit, Alfa Aesar, Royston, UK; MicroVue DPD EIA Kit, Quidel Corporation, San Diego, CA, USA).

BMD and Micro-CT Analysis

Bone properties of the trabecular bone at the lumbar vertebra (L2–L5) were determined by micro-CT (μCT40, Scanco Medical, Wangen-Brüttisellen, Switzerland) as described in our previous study (9). The source energy selected for this study was 70 kVp and 114 μA with a resolution of 21 μm. Approximately 200 slices were done for each scan. Bone mineral density (BMD, mg HA/ccm) and bone morphometric properties, including bone volume over total volume (BV/TV), connectivity density (Conn.D, 1/mm^3), trabecular bone number (Tb.N, mm^{-1}), trabecular bone thickness (Tb.Th, mm), and trabecular bone separation (Tb.Sp, mm), were evaluated by contoured volume of interest images.

Hematoxylin-Eosin Staining

Uterus and breast tissues were fixed in 4% paraformaldehyde for 6 h. Tissues were embedded in paraffin, and 8-μm-thick sections were produced for each sample after dehydration (Leica TP1020). Five sections from each sample were observed using ×400 (uterus) or ×100 (breast) magnification and photographed using a photoscope (Olympus BX51).

Real-Time PCR Assay

Collected tissues were homogenized in Trizol reagent by using Precellys 24 homogenizer (Bertin, Fontaine, France). A total of 2.0 μg of total RNA was used to generate cDNA by using High-Capacity cDNA Reverse Transcription Kits (Applied Biosystems, Cheshire, UK) following the manufacturers' instruction. Furthermore, 20 μl of PCR reaction system consisting of 1 μl cDNA, 0.4 μl of forward and reverse primers, 8.2 μl of DNase and RNase-free water, and 10 μl of Applied Biosystems® SYBR® Green PCR Master Mix (Applied Biosystems) was performed by using 7500 Fast Real-time PCR System (Applied Biosystems). Sequences for primers are provided in **Supplementary Table S2**.

Immunohistochemistry

Upon dehydration by sequential soaking in 20% and 30% sucrose solution, 18 μm serial coronal section of the substantia nigra was prepared by using a cryostat (Leica, Wetzlar, Germany). The sections were then boiled in citrate buffer for 15 min using a microwave for antigen retrieval, followed by removal of endogenous peroxidases in 0.3% H_2O_2-methanol (v/v) for 15 min at room temperature. Nonspecific binding was blocked with 3% donkey serum for 30 min at room temperature. The slides were then incubated with polyclonal rabbit anti-tyrosine hydroxylase (TH) antibody (1:4,000, AB152, Sigma-Aldrich, St. Louis, MO, USA) overnight at 4°C, followed by washing with PBS and incubation with goat anti-rabbit IgG at room temperature for 1 h and subsequently in streptavidin peroxidase for 30 min at 37°C. TH-positive neurons were visualized by diaminobenzidine (DAB). Images of TH-positive cells were observed under ×100 magnification and captured using a photoscope (Olympus BX51, Olympus Corporation, Tokyo, Japan). The average number of TH-positive neurons from four fields of view was compared between groups.

Preparation of RD-Treated Serum

Young adult OVX rats were given vehicle or RD at 2.0 g/kg day (10 times of its clinical equivalent dose) for 3 consecutive days and pair-fed with phytoestrogen-free AIN-93 diet. Upon the last oral administration on day 3, the rats were fasted overnight and given drugs one more time in the following morning. Rats were euthanized an hour after administration and blood samples were collected. Serum was prepared upon centrifugation and stored at −80°C. LC-MS analysis of the serum was performed to confirm the presence of a major chemical marker from RD. Methanol extract of serum was prepared, and extract of 1 ml serum was dissolved in 1 ml of ethanol; the concentration of this solution was defined as "1." Microsep™ Advance Centrifugal Device (3K, PALL. Cor., Port Washington, NY, USA) was used to remove small molecules including steroid in serum extract, and the solution was sterilized with a 0.22-μm membrane. Final dilution of the serum extract (10^{-5}, 10^{-4}, 10^{-3}, and 10^{-2}) was used for cell studies.

Cell Culture and Measurement

Four ER-positive cell lines, including human breast MCF-7 cells (ATCC® HTB-22™, passage 8-15), endometrial Ishikawa cells (kindly provided by Dr. Lihui Wei at Peking University People's Hospital, passage 12-18), neuroblastoma SHSY5Y cells (ATCC®CRL-2266™, kindly provided by Prof. Wenfang Chen at Qingdao University, passage 15-25), and osteosarcoma MG-63 cell (ATCC® CRL-1427™, passage 3-10) were routinely cultured according to ATCC (Gaithersburg, MD, USA) instruction. Cells were seeded in 96-well or 24-well plate at a density of 0.8×10^3 and 2.0×10^4/well, respectively, for different assays. The medium was changed to phenol red-free medium containing charcoal-stripped FBS for another 24 h. Cells were treated with extract of serum treated with vehicle or RD at various dilutions (10^{-5}, 10^{-4}, 10^{-3}, and 10^{-2}), tamoxifen (10^{-12} to 10^{-6} M) and their combinations at optimal concentrations for 48 h. Cell viability or ALP activity were measured by MTS assay or ALP assay, respectively. Briefly, upon treatment, medium was discarded and replaced with 100 μl of MTS/phenazine methosulfate working solution (Promega, Madison, WI, USA). Absorbance at 490 nm was measured with a microplate reader (CLARIOstar, BMG LABTECH, Ortenberg, Germany) after incubation at 37°C for 1 to 4 h. Relative absorbance to control group was analyzed and compared between treatment groups and controls. For ALP assay, upon treatment, 100 μl of passive lysis buffer (PLB) was added to each well to lyse cell. The ALP activity of cell lysate was measured by a LabAssayTM ALP Kit (Wako, Japan) following manufacturer's instruction. Total protein concentrations of the cell lysate were measured *via* Bradford method to normalize ALP activity.

Statistical Analysis

Data were expressed as mean ± SEM. The differences between groups of *in vivo* study were analyzed by one-way ANOVA with Tukey's *post-hoc* test. The differences between treatment groups and control in *in vitro* study were determined by Independent

t-test. Two-way ANOVA with Bonferroni as *post-hoc* test was performed to analyze the interaction between RD and tamoxifen. A p-value <0.05 was considered statistically significant.

RESULTS

Herbal Extract Preparation and Authentication

HPLC assay confirmed that the quality of *rhizoma drynariae* raw herb has fulfilled the requirements on the presence of naringin (**Supplementary Data 3A**). The amount of naringin in RD extract was 0.394 mg/g. The datasets presented in this study can be found in online repositories. The names of the repository/repositories and accession number(s) can be found below: (Figshare https://doi.org/10.6084/m9.figshare.17084834.v5)

Estrogenic Activities of RD and Its Combination With Tamoxifen in Mature OVX Rats

In response to OVX, a significant increase in body weight was observed in OVX rats in comparison with Sham rat ($p < 0.01$ vs. Sham), which was reversed by the treatments with E2, tamoxifen, or cotreatment of tamoxifen and RD ($p < 0.001$, vs. OVX) but not RD alone (**Figure 1A**). Cotreatment with RD attenuated the inhibitory effects of tamoxifen on body weight gain. Results of two-way ANOVA indicated that RD did not interact with tamoxifen but decreased the inhibitory effect of tamoxifen on body weight gain without significance (RD × Tamo: $p = 0.7253$).

Decreased estrogen production was believed to be the sole reason for menopausal symptoms. However, recent findings suggest that dramatic increase in FSH appears much earlier than the drop of estrogen before the onset of menopause and accounts for the appearance of menopausal symptoms (10). The results of the present study showed that the dramatic decrease in serum estradiol in OVX rats was accompanied with the significant increase in circulating levels of FSH and LH (**Figures 1B–D**, $p < 0.01$ vs. Sham). As expected, the treatment of OVX rats with estradiol significantly reversed serum level of estradiol and completely suppressed FSH and LH levels to comparable level with those of Sham rats. The increases in serum estradiol were also observed in OVX rats treated with tamoxifen, RD, as well as their combinations while the changes did not reach statistical significance (**Figure 1B**, vs. OVX). Similar to estrogen, tamoxifen, RD alone, and their combination all dramatically suppressed the increase in both circulating FSH and LH level in OVX rats (**Figures 1C, D**, $p < 0.01$ vs. OVX). No statistical difference in reproductive hormone level was detected between OVX rats treated with tamoxifen and OVX rats treated with its combination with RD, indicating RD did not alter actions of tamoxifen on reproductive hormones. The two-way ANOVA analysis indicated the interactions between RD and SERMs on inhibiting FSH and LH levels (RD × tamoxifen, FSH: $p = 0.0239$, LH: $p = 0.0331$) but not on restoring estradiol level, in OVX rats.

In response to estrogen deficiency and probable increased FSH, OVX rats experienced severe bone loss as indicated by the deteriorated bone structure (**Figure 2A**), the decreased BMD (**Figure 2B**, $p < 0.001$), and degradation in trabecular bone properties, such as the decreases in BV/TV, Tb.N, Conn.D, and Tb.Th, as well as the increase in Tb.Sp (**Table 1**, $p < 0.001$ vs. Sham) at the lumbar vertebra. Estrogen or tamoxifen alone exerted potent antiosteoprotective activity and attenuated OVX-induced bone loss as expected (**Figures 2A, B** and **Table 1**, $p < 0.001$ vs. OVX). RD alone and in combination with tamoxifen significantly restored OVX-induced changes in bone structure, BMD, and bone properties ($p < 0.001$ vs. OVX). The result of two-way ANOVA confirmed the interaction between tamoxifen and RD on promoting BMD (RD × Tamo: $p = 0.0013$) and improving trabecular bone properties (RD × Tamo: $p = 0.0014$ for BV/TV, $p = 0.0002$ for Conn.D, $p = 0.0049$ for Tb.N, $p = 0.0022$ for Tb.Th, $p = 0.0017$ for Tb.Sp) in OVX rats. Despite the interactions, RD did not induce alteration in the stimulatory activities of tamoxifen on BV/TV, Tb.N, and Tb.Th and inhibitory effect on Tb.Sp.

Serum OCN is an osteoblast-produced biomarker for bone formation while urinary DPD, generated from the breakdown, is a biomarker for bone resorption (11). Serum OCN (28.9 ± 1.291 ng/ml) and urinary DPD (670.1 ± 98.7 nmol/mmol) were significantly increased in OVX rats (**Table 1**, $p < 0.001$ vs. Sham). All treatments exhibited inhibitory effects on the increases in bone turnover biomarkers (**Table 1**, $p < 0.05$ vs. OVX), suggesting their bone protective actions might be mediated by suppressing bone turnover. RD interacted with tamoxifen on decreasing serum level of OCN (RD × Tamo: $p = 0.0128$) but not on urinary DPD (RD × Tamo: $p = 0.1974$). However, RD did not alter the responses of either OCN or DPD to treatment with tamoxifen in OVX rats (SERMs alone vs. TCMs+SERMs).

To investigate if RD also exerted estrogenic activities in the central nervous system, the mRNA expressions of *TH* (12), *dopamine transporter* (*DAT*) in the striatum and TH-positive neurons in the substantia nigra were measured by real-time PCR and immunohistochemistry (IHC), respectively. Six months upon OVX, *TH* mRNA (**Figure 3A**) was downregulated while the mRNA expression of *DAT* (**Figure 3B**, $p<0.001$ vs. Sham) was noticeably upregulated in the striatum in OVX rats. IHC result confirmed the downregulated expression of TH as advised by the decreased numbers of TH-positive neurons in the substantia nigra of OVX rats (**Figures 3C, D**). The treatments with E2, tamoxifen, or RD alone, as well as their combination produced pronounced increase in *TH* mRNA expression and decrease in *DAT* mRNA expression (**Figures 3A, B**, $p < 0.05$). RD, tamoxifen, or their combination appeared to stimulate the TH-positive neurons while changes did not reach a statistical significance (**Figures 3C, D**). These results suggested the potential valuable effects of RD in the CNS. The two-way ANOVA results demonstrated that RD interacted with tamoxifen to suppress *DAT* mRNA expression in the striatum of OVX rats (RD × Tamo: $p < 0.0001$) without affecting TH expression (RD × Tamo: $p = 0.4257$ for *TH* mRNA, $p = 0.3551$ for TH-positive neuron number).

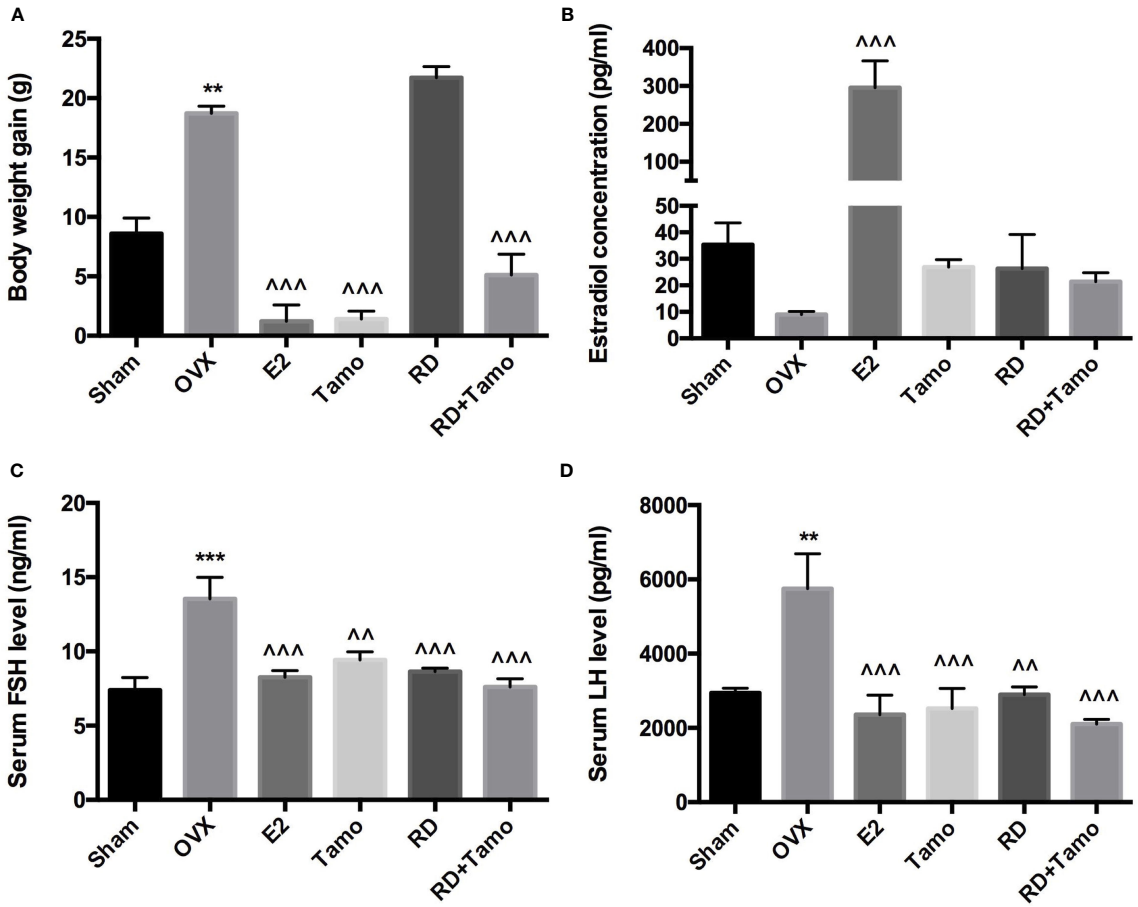

FIGURE 1 | Estrogenic effects of RD, tamoxifen, and their combinations on body weight gain and circulating hormone level in mature ovariectomized rats. Six-month-old mature Sprague Dawley sham-operated (Sham) or ovariectomized (OVX) rats were treated with either vehicle, E2 (1.0 mg/kg/day), RD (0.2 g/kg/day), tamoxifen (Tamo, 0.1 mg/kg/day), or their combination for 12 weeks. **(A)** Body weight gain of OVX rats after 12-week treatments. **(B–D)** Circulating level of estradiol, FSH, and LH was measured by using EIA kit (CayMan). Data were expressed as mean ± SEM. $n = 6$ to 10. $^{***}p < 0.001$, $^{**}p < 0.01$ vs. Sham; $^{\wedge\wedge}p < 0.01$, $^{\wedge\wedge\wedge}p < 0.001$ vs. OVX. p-value of two-way ANOVA: 0.7253 for body weight, 0.1104 for estradiol concentration, 0.0239 for serum FSH, and 0.0331 for serum LH.

In response to OVX, uterine weight of OVX rats was significantly decreased to about 25% of Sham rats (**Figure 4A**, $p < 0.001$ vs. Sham) and a dramatic atrophy was observed in the uterus of OVX rats as revealed by the shrunken endometrium (**Figure 4B**, indicated by the red line). The treatment with E2, tamoxifen alone, or its combinations with RD, but not RD alone, significantly increased the weight of the uterus in OVX rats ($p < 0.05$ vs. OVX rats), confirming the uterotrophic effects of tamoxifen. The changes in weight of the uterus in response to different treatments were in consistence with the increase in the thickness of the endometrium (**Figure 4B**). Similar to estradiol, tamoxifen alone or its combination with RD, but not RD alone, stimulated the mRNA expression of *complement component 3* (*C3*, **Figure 4C**, $p < 0.05$) and *histone H3* (*HH3*, **Figure 4D**, $p < 0.001$), two estrogen-responsive genes, in the uterus of OVX rats. The two-way ANOVA results suggested the interaction between RD and tamoxifen on stimulating *HH3* mRNA expression (RD × Tamo: $p = 0.0003$). Ovariectomy also induced atrophy of breast tissue as indicated by the reduced number of mammary ducts in OVX rats, which was reversed by estrogen (**Figure 5**). Tamoxifen enhanced the atrophy in the mammary gland of OVX rats (**Figure 5**). Unlike either estrogen or tamoxifen, RD did not induce any growth of the mammary duct in OVX rats alone or in combination with tamoxifen. Our results suggest that RD did not induce estrogenic effects in either the uterus or mammary gland in OVX rats while tamoxifen promoted the growth of the endometrium.

Direct Estrogenic Activities of DBT and Combination With Tamoxifen *In Vitro*

Four ER-positive cell lines in line with the four estrogen-sensitive tissues characterized in the OVX rats, including human breast cancer MCF-7 cells, endometrial cancer Ishikawa cells, neuroblastoma SHSY5Y cells, as well as osteosarcoma MG-63 cells, were employed to investigate the estrogenic activities of RD *in vitro*. The results of LC-MS confirmed the presence of

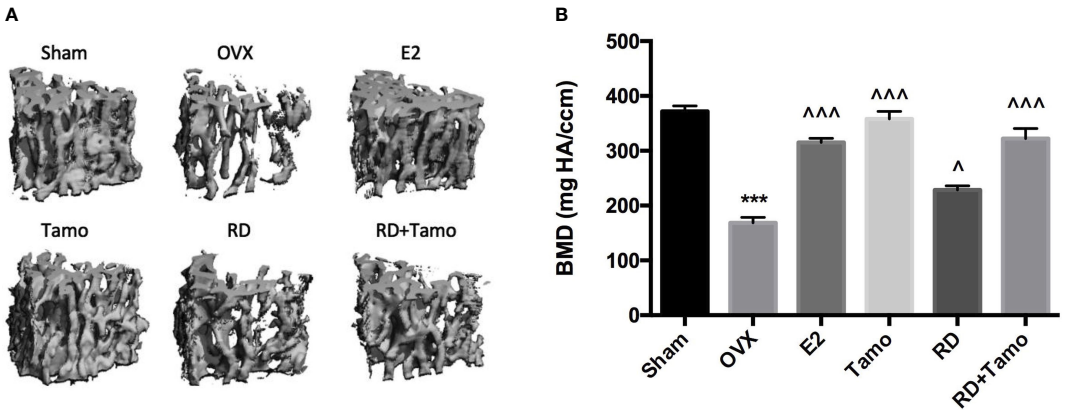

FIGURE 2 | Estrogenic effects of RD, tamoxifen, and their combinations on bone microarchitecture and bone mineral density of the lumbar spine in mature ovariectomized rats. Upon treatment, lumbar vertebra was collected. Bone microarchitecture **(A)** and bone mineral density (BMD) of the lumbar vertebra **(B)** were measured by micro-CT. Data were expressed as mean ± SEM. $n = 6$ to 10. $^{***}p < 0.001$ vs. Sham; $^{\wedge}p < 0.05$, $^{\wedge\wedge\wedge}p < 0.001$ vs. OVX. p-value of two-way ANOVA: 0.0013 for BMD.

naringin and naringenin 5,7-di-*O*-glucoside in RD-treated serum extract, suggesting that RD and its metabolites were absorbed and transported in rat circulation (**Supplementary Data 3B**). The datasets presented in this study can be found in online repositories. The names of the repository/repositories and accession number(s) can be found below: (Figshare https://doi.org/10.6084/m9.figshare.17084834.v5). Compared with the extract of the vehicle-treated serum, RD-treated serum extract dose-dependently increased cell viability [**Figure 6A** (MCF-7), **B** (SH-SY5Y)] and/or ALP activity [**Figure 6C** (Ishikawa), **Figure 6D** (MG-63)], of which RD exerted the most potent effects at 10^{-3} dilution. Tamoxifen exerted inhibitory effect on MCF-7 cell proliferation (**Figure 7A**, $p < 0.05$) but stimulatory effects on SHSY5Y cell proliferation (**Figure 7B**, $p < 0.05$) as well as ALP activity in Ishikawa (**Figure 7C**, $p < 0.05$) and MG-63 cells (**Figure 7D**, $p < 0.05$). The two-way ANOVA results suggested that RD at 10^{-3} dilution interacted with tamoxifen at certain concentrations in all the four cell lines (**Figures 7A–D**, RD × Tamo: $p < 0.05$). RD markedly reversed the inhibitory effects of tamoxifen at 10^{-12}, 10^{-10}, and 10^{-8} M on cell proliferation in MCF-7 cells (**Figure 7A**, $p < 0.05$) but does not affect the actions of tamoxifen in either SHSY5Y, Ishikawa, or MG-63 cells.

DISCUSSION

The use of "kidney-tonifying" herb, RD, is an alternative to SERMs or HRT in managing osteoporosis in China. Our previous studies demonstrated the estrogenic effect of RD in promoting bone health in OVX rats. The present study further addressed the in vivo and in vitro drug-herb interactions of RD at its clinical dose with SERMs in four estrogen-sensitive tissues, including bone, brain, uterus and breast, what are one of the major clinical concerns when patients are cotreated with them. Our results also showed that RD did interact with SERMs but did not alter the action of tamoxifen in all tissues. Unlike tamoxifen, RD alone exerted estrogenic effects in tissue-selective manner, by which RD did not cause side effects on the uterus and breast but has stimulatory impact in the bone and brain.

TABLE 1 | The effect of RD, tamoxifen, or their combination on trabecular bone properties and bone turnover markers in mature ovariectomized rats.

	Lumbar Vertebra					Turnover Biomarkers	
	BV/TV	Conn.D	Tb.N (1/mm)	Tb.Th (mm)	Tb.Sp (mm)	OCN (ng/ml)	DPD (nmol/mmol)
Sham	0.452 ± 0.009	33.97 ± 2.70	3.50 ± 0.06	0.129 ± 0.003	0.245 ± 0.005	11.4 ± 0.419	224.0 ± 16.4
OVX	0.117 ± 0.006***	9.57 ± 1.47***	1.91 ± 0.04***	0.087 ± 0.003***	0.495 ± 0.015***	28.9 ± 1.291***	670.1 ± 98.7***
E2	0.379 ± 0.027^^^	25.70 ± 2.34^^^	3.36 ± 0.06^^^	0.123 ± 0.008^^^	0.295 ± 0.025^^^	14.6 ± 0.790^^^	370.4 ± 32.9^^^
Tamo	0.409 ± 0.023^^^	33.00 ± 2.30^^^	3.32 ± 0.09^^^	0.135 ± 0.005^^^	0.266 ± 0.011^^^	15.9 ± 0.591^^^	463.9 ± 23.7^
RD	0.199 ± 0.010^	18.99 ± 1.10^	2.38 ± 0.09^	0.105 ± 0.002^	0.407 ± 0.015^^	23.8 ± 0.789^^^	484.5 ± 37.3
RD+Tamo	0.354 ± 0.029^^^	25.78 ± 2.04^^^	3.10 ± 0.13^^^	0.127 ± 0.004^^^	0.288 ± 0.016^^^	15.4 ± 0.441^^^	412.5 ± 26.9^^
p value of Two-way ANOVA							
RD × Tamo	0.0014	0.0002	0.0049	0.0022	0.0017	0.0128	0.1974

*BV/TV, bone volume over total volume; DPD, deoxypyridinoline; Conn.D, connectivity density; OCN, osteocalcin; Tb.Sp, trabecular bone separation; Tb.Th, trabecular bone thickness; Tb.N, trabecular bone number. n = 6 to 12. **p < 0.01, ***p < 0.001 vs. Sham; ^^p < 0.01, ^^^p < 0.001 vs. OVX.*

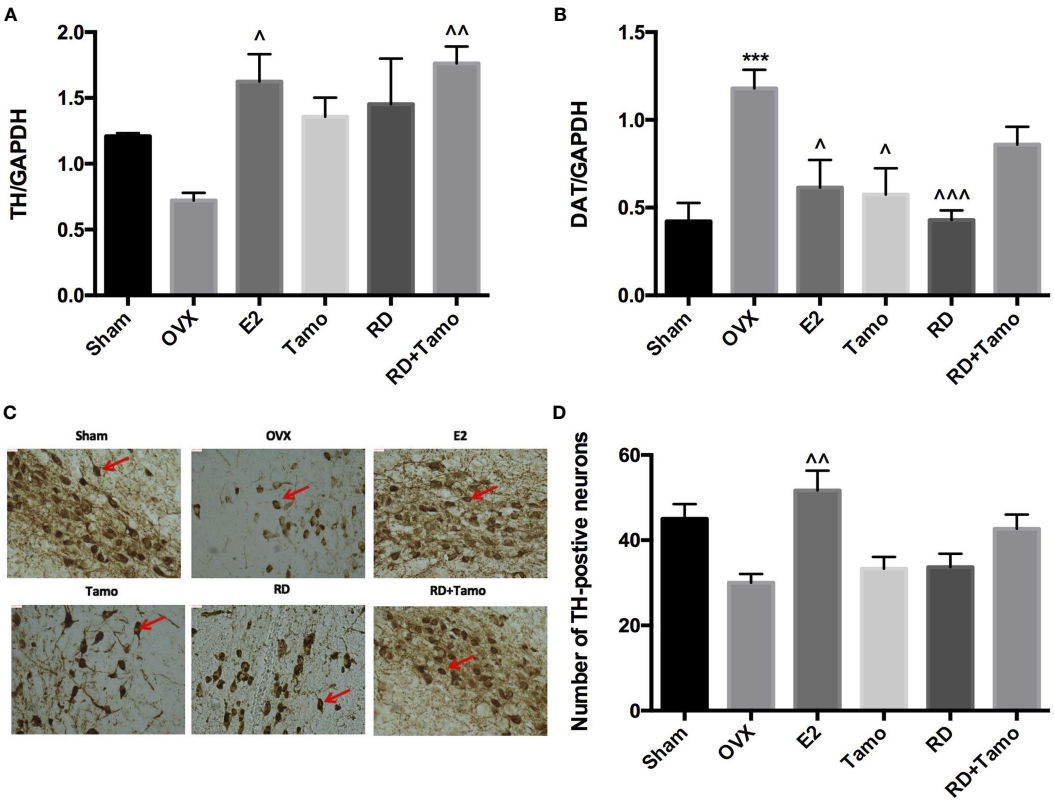

FIGURE 3 | Estrogenic effects of RD, tamoxifen, and their combinations in the central nervous system of mature ovariectomized rats. Upon treatment, striatum was collected at euthanasia. mRNA expression of *tyrosine hydroxylase* (*TH*) **(A)** and *dopamine transporter* (*DAT*) **(B)** were measured by real-time PCR. TH-positive cells in the substantia nigra were visualized by IHC (×100) **(C)** and quantified **(D)**. Data were expressed as mean ± SEM. $n = 6$ to 10. ***p <0.001 vs. Sham; ^$p < 0.05$, ^^$p < 0.01$, ^^^$p < 0.001$ vs. OVX. p-value of two-way ANOVA: 0.4257 for TH/GAPDH, <0.0001 for DAT/GAPDH, 0.35531 for TH-positive neurons.

Dramatic changes in hormonal secretions, including estradiol, FSH, and LH, during menopause cause various negative physiological consequences, including breast, uterus, skeletal, and neuronal tissues (13). The present *in vivo* study showed that OVX in rats caused a remarkable reduction in serum estradiol level but an induction in serum FHS and LH levels. RD treatment or cotreatment of RD with tamoxifen could restore both FSH and LH levels but not E2. It indicated that RD and SERMs might modulate sex hormone level and exert hormonal effect on breast, uterus, skeletal, and neuronal tissues. Further study is needed to confirm if RD has any impact on hypothalamus-pituitary-gonad axis which is the major signaling pathway controlling the releases of sex hormone.

Postmenopausal osteoporosis is the second cause of osteoporosis in women. OVX model in rats mimic the metabolic modification related to deficiency of estradiol in women. Our results demonstrated a significant reduction in serum estradiol level and uterus weight in OVX rats. Such changes were accompanied with bone loss in the lumbar spine in rats. As expected, RD and tamoxifen, like E2, were effective in attenuating bone loss at three bone sites by increasing BMD and improving bone microarchitecture which are in line with our previous studies (7, 9). Also, RD significantly restored serum OCN level, an osteoblastic biomarker in bone remodeling (14), while tamoxifen restored both serum OCN and DPD levels, a collagen breakdown biomarker during bone resorption (9) in OVX rats. These results suggested the estrogen-like effect of RD and tamoxifen in osteoporotic rats, in which RD acted mainly on bone formation while tamoxifen governed both bone formation and resorption. Also, our previous study demonstrated a positive correlation between BMD and serum E2 and a negative correlation between BMD and serum FSH or LH at the distal femur in OVX rats (15). FSH has also been reported to regulate osteoclastogenesis, bone resorption, and bone turnover biomarkers in postmenopausal women (16, 17). Thus, our results suggested that the bone protective effects of RD and tamoxifen might be mediated by the modulation of sex hormone level.

Epidemiological evidence suggests postmenopausal women are at high risk of Parkinson's disease. Circulating estradiol level was reported to act as a neuroprotective agent on the dopaminergic system in women (18, 19). In the present study, OVX in rats was shown to affect the TH level for dopamine production and higher DAT level for dopamine resorption in the striatum.

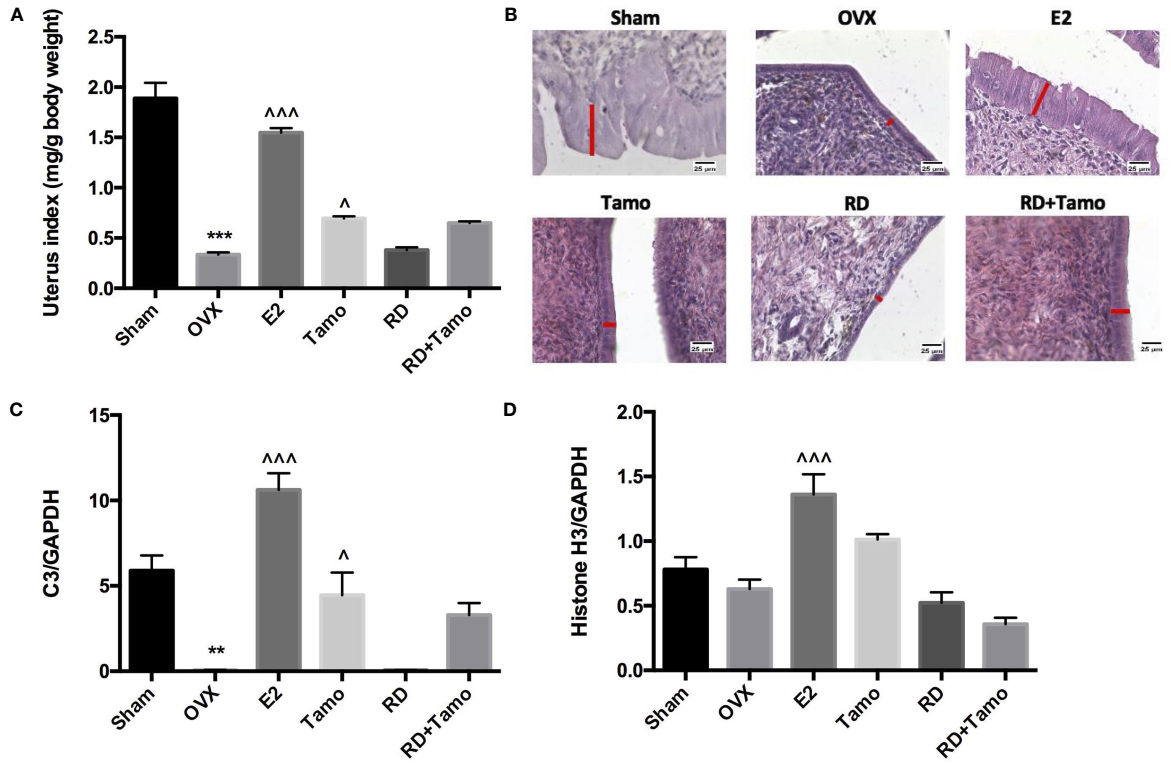

FIGURE 4 | Estrogenic effects of RD, tamoxifen, and their combinations on uterine index, mRNA expression of estrogen-responsive gene, and endometrial morphology in mature ovariectomized rats. Upon treatment, uterus was collected and weighed at euthanasia. Ratio of the uterus weight to body weight was recorded as uterine index (mg/g) and compared between groups **(A)**. Morphology of endometrium (×400, thickness of endometrium was indicated by the length of the red line) was visualized by H&E staining **(B)**. mRNA expression of *complement component 3* (*C3*) and *histone H3* were measured by real-time PCR **(C, D)**. Data were expressed as mean ± SEM. $n = 6$ to 10. $^{**}p < 0.01$, $^{***}p < 0.001$ vs. Sham; $^{\wedge}p < 0.05$, $^{\wedge\wedge\wedge}p < 0.001$ vs. OVX. p-value of two-way ANOVA: 0.0847 for uterine index, 0.4800 for C3/GAPDH, and 0.0003 for histone H3/GAPDH.

The increases in DAT in OVX rats could be reversed by the treatment of RD or tamoxifen alone, indicating their neuroprotective effects. These are in consistence with other studies indicating that tamoxifen directly interacted with the DAT to prevent dopamine uptake and blocked dopamine efflux in rats (20). Also, the hypothalamic dysfunction in PD patients could lead to the disruption of pituitary hormone secretion (FSH, LH, and testosterone) and dopamine content (21). Therefore, the reclamation of serum FSH or LH level in OVX rats after RD or tamoxifen treatment might also be a sign of their neuroprotective effects on the hypothalamus.

Estrogenic side effects on reproductive organs, like the breast and uterus, are always the main concerns when using phytoestrogen-containing drug or SERMs because they could stimulate the growth of reproductive tissues through estrogen receptors (22–24). In the present study, tamoxifen treatment did exert stimulatory effects on endometrium layer and uterus weight and estrogen-responsive gene but not in breast tissues. These results are comparable with those of others that tamoxifen acts as an ER antagonist in breast and is clinically prescribed for the treatment of ER-positive breast cancer (2). However, it was shown to elevate the risk of endometrium cancer in women (25). In contrast to tamoxifen, although RD contains flavonoid, naringin being known as a phytoestrogen, which was reported to act on estrogen receptors (26), RD treatment did not show any stimulatory effect in both the breast and uterus in OVX rats in the present study. It advocated the use of RD as its clinical dose was safer than tamoxifen in OVX rats. Our results suggest that RD might serve as an alternative SERM that could selectively exert agonistic estrogenic protection in the bone and brain and antagonist action in reproductive organs.

Systemic activation of TCM after administration *via* metabolism produces metabolites, which are usually considered to be the bioactive component of the herbal medicine in the body. Thus, the direct effect of RD-treated serum was evaluated in estrogen-sensitive cell lines from four tissues. The results indicated that RD-treated serum, acting like E2 but weaker, promoted the cell viability of MCF-7 cells and SH-SY5Y cells as well as the ALP activity in MG-63 cells and Ishikawa cells. However, these seem to be in contrast with the *in vivo* results that RD did not stimulate reproductive tissues. The discrepancy between *in vitro* and *in vivo* might be due to the differences in the dosages of RD used in cells and animals. The effects of

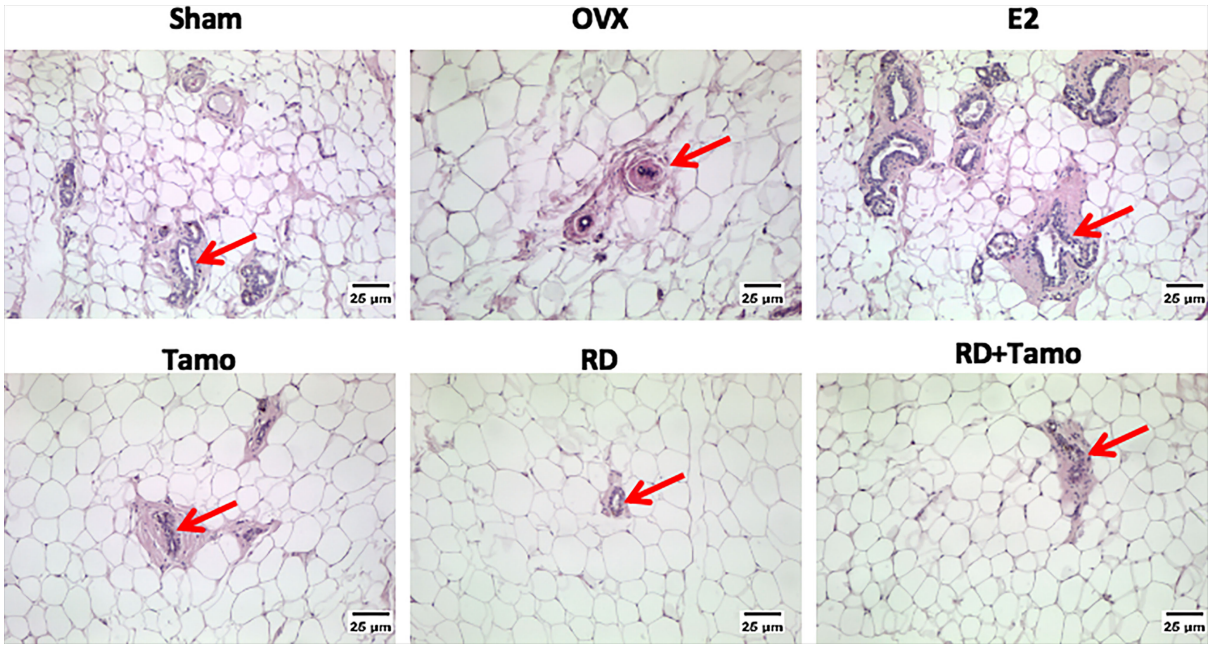

FIGURE 5 | Estrogenic effects of RD, tamoxifen, and their combinations on the morphology of breast tissue in mature ovariectomized rats. Upon treatment, breast tissue was collected in 4% paraformaldehyde and the morphology of mammary gland (as indicated by the red arrow, ×100) was visualized by H&E staining.

phytoestrogen has been demonstrated to be either agonistic or antagonistic depending on its own concentrations and the estrogen concentrations of the environment (27). For the *in vivo* study, the dosage of RD used was converted from its clinical dosage and the level of phytoestrogens and their metabolites in RD is not high enough to compete with SERMs to bind with ERs. In contrast, RD-treated serum used in the *in vitro* studies was prepared by treatment of OVX rats with high dosage of RD (10 times to its *in vivo* dose), potentially enabling the major phytoestrogen components and main metabolites in RD-

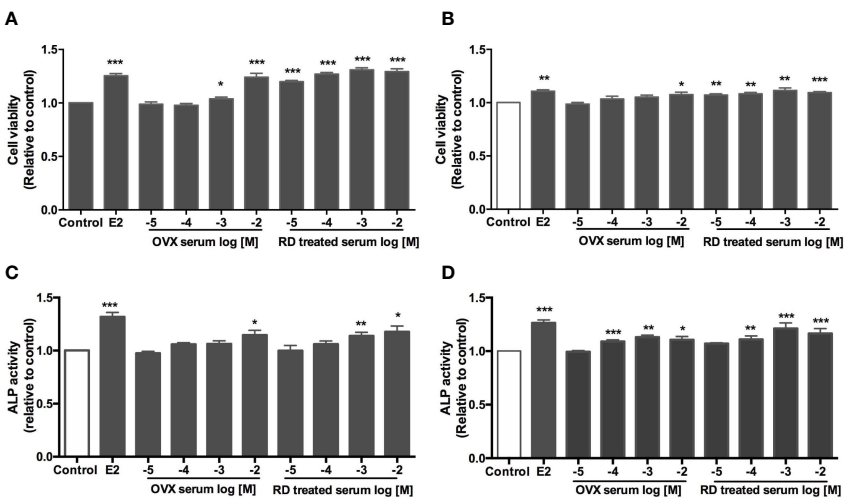

FIGURE 6 | Direct estrogenic effects of OVX serum or RD-treated serum in ER-positive cells. Human breast cancer MCF-7 **(A)** neuroblastoma SHSY5Y **(B)** endometrial cancer Ishikawa **(C)** and osteosarcoma MG-63 cells **(D)** were treated with E2 (10 nM), OVX serum (10^{-5}–10^{-2} dilution) or RD-treated serum (10^{-5}–10^{-2} dilution) for 48 h. MTS assays were performed in MCF-7 and SH-SY5Y cells while ALP activities were measured in MG-63 cells and Ishikawa cells. Results were expressed as ratio to control. $n = 3$ or more. $^{*}p < 0.05$, $^{**}p < 0.01$, $^{***}p < 0.001$ vs. control.

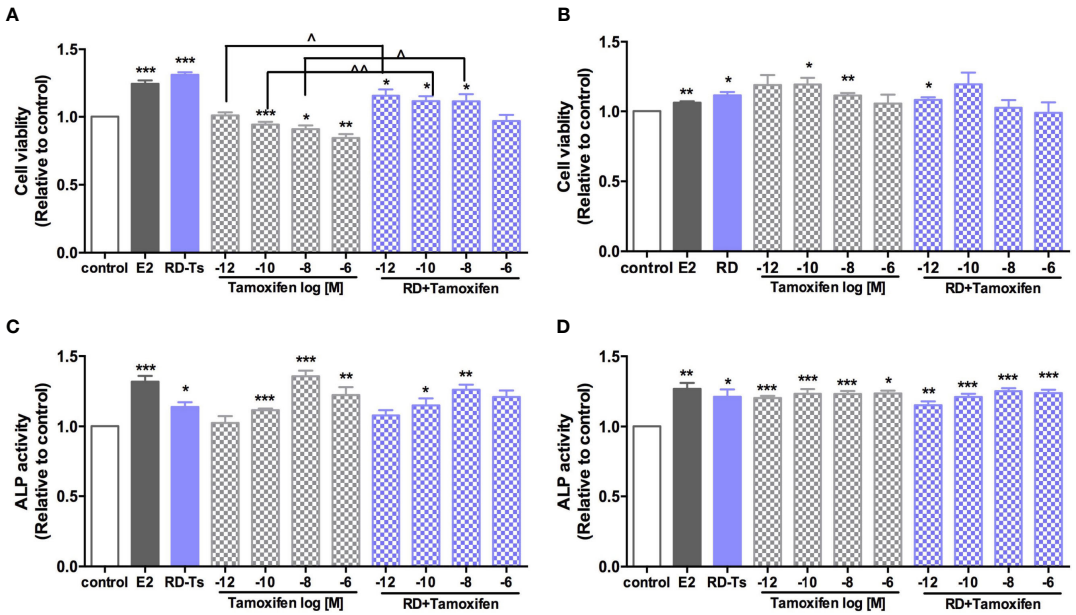

FIGURE 7 | Direct estrogenic effects of RD-treated serum, tamoxifen, and their combinations in ER-positive cells. Human breast cancer MCF-7 **(A)**, neuroblastoma SHSY5Y **(B)**, endometrial cancer Ishikawa **(C)**, and osteosarcoma MG-63 cells **(D)** were treated with E2 (10 nM), tamoxifen (10^{-12}–10^{-6} M) or RD-treated serum (10^{-3} dilution) for 48 h. MTS assays were performed in MCF-7 and SH-SY5Y cells while ALP activities were measured in MG-63 cells and Ishikawa cells. Results were expressed as ratio to control. $n = 3$ or more. $^{*}p < 0.05$, $^{**}p < 0.01$, $^{***}p < 0.001$ vs. control; $^{\wedge}p < 0.05$, $^{\wedge\wedge}p < 0.01$ vs. tamoxifen alone. p-value for interaction between RD and tamoxifen at 10^{-12}, 10^{-10}, 10^{-8}, and 10^{-6} M of two-way ANOVA: 0.0045, 0.0089, 0.0728, and 0.0028 for cell viability in MCF-7 cell; 0.0141, 0.2393, 0.0068, and 0.0816 for cell viability in SH-SY5Y cell; 0.2598, 0.1249, 0.0059, and 0.1098 for ALP activity in Ishikawa cell; and 0.1080, 0.258, 0.0222, and 0.5987 for ALP activity in MG-63 cell.

treated serum to reach the level to activate ERs and induce stimulatory effects in Ishikawa and MCF-7 cells.

With the increased use of TCM worldwide, the concern on drug–herb interaction is exaggerating, especially when both drug and herb target estrogen receptors. Our two-way ANOVA analysis showed that RD could interact with tamoxifen in promoting bone health, exerting neuroprotection, increasing uterine index in OVX rats, and stimulating ALP or cell viability in cells. However, cotreatment with RD did not significantly alter the responses to tamoxifen in estrogen-sensitive tissues. It might be due to their weak binding affinity to ERs compared with tamoxifen. Further study is needed to compare the binding affinity of tamoxifen and major flavonoid as well as their metabolites in RD.

To the best of our knowledge, this is the first investigation on the drug–herb interaction between RD and tamoxifen in OVX model and using biologically activated RD in four ER-positive human cell lines. We confirmed that RD could tissue-selectively exert estrogenic protection in the bone and neuron without causing side effects on the breast and uterus, which differentiates RD from tamoxifen. The drug–herb interaction of RD and tamoxifen did not weaken or strengthen the action of tamoxifen in all tissues, suggesting that RD alone and in combination with tamoxifen might be considered effective and safe alternative methods for the management of menopause-related symptoms. However, further clinical investigation should be made to confirm the preclinical observations in the present study.

DATA AVAILABILITY STATEMENT

The datasets presented in this study can be found in online repositories. The names of the repository/repositories and accession number(s) can be found below: https://doi.org/10.6084/m9.figshare.17084834.v5

ETHICS STATEMENT

The animal study was reviewed and approved by the Hong Kong Polytechnic University Animal Subjects Ethics Sub-committee (ASESC Case: 15-16/31-ABCT-R122 HMRF).

AUTHOR CONTRIBUTIONS

LZ and K-YW are the major contributors of the present study, performing experiments, analyzing the data, and preparing the

manuscript. WY, CP, and HX helped in performing and sample collection of animal experiments. C-OC and DM performed the chemical analysis of the RD extract. M-SW conceived and supervised the experiments and finalized the manuscript. All authors listed have made a substantial, direct, and intellectual contribution to the work and approved it for publication.

FUNDING

This work was supported by the Health and Medical Research Fund (HMRF) grant (Ref. No. 13143771) of Hong Kong.

ACKNOWLEDGMENTS

We thank the University Research Facility in Life Sciences at the Hong Kong Polytechnic University for the technical support.

SUPPLEMENTARY MATERIAL

The Supplementary Material for this article can be found online at: https://www.frontiersin.org/articles/10.3389/fendo.2022.817146/full#supplementary-material

REFERENCES

1. Shook LL. An Update on Hormone Replacement Therapy: Health and Medicine for Women: A Multidisciplinary, Evidence-Based Review of Mid-Life Health Concerns. *Yale J Biol Med* (2011) 84(1):39–42.
2. Maximov PY, Lee TM, Jordan VC. The Discovery and Development of Selective Estrogen Receptor Modulators (SERMs) for Clinical Practice. *Curr Clin Pharmacol* (2013) 8(2):135–55. doi: 10.2174/1574884711308020006
3. Peng W, Adams J, Hickman L, Sibbritt DW. Complementary/alternative and Conventional Medicine Use Amongst Menopausal Women: Results From the Australian Longitudinal Study on Women's Health. *Maturitas* (2014) 79 (3):340–2. doi: 10.1016/j.maturitas.2014.08.002
4. Moreira AC, Silva AM, Santos MS, Sardao VA. Phytoestrogens as Alternative Hormone Replacement Therapy in Menopause: What Is Real, What Is Unknown. *J Steroid Biochem Mol Biol* (2014) 143:61–71. doi: 10.1016/j.jsbmb.2014.01.016
5. Jeong JC, Lee JW, Yoon CH, Kim HM, Kim CH. Drynariae Rhizoma Promotes Osteoblast Differentiation and Mineralization in MC3T3-E1 Cells Through Regulation of Bone Morphogenetic Protein-2, Alkaline Phosphatase, Type I Collagen and Collagenase-1. *Toxicol In Vitro* (2004) 18(6):829–34. doi: 10.1016/j.tiv.2004.05.002
6. Xu T, Wang L, Tao Y, Ji Y, Deng F, Wu X-H. The Function of Naringin in Inducing Secretion of Osteoprotegerin and Inhibiting Formation of Osteoclasts. *Evid-Based Complement Altern Med* (2016) 2016:8981650. doi: 10.1155/2016/8981650
7. Pang W-Y, Wang X-L, Wong K-C, Leung PC, Yao X-S, Wong M-S. Total Flavonoid Fraction of Rhizoma Drynaria Improves Bone Properties in Ovariectomized Mice and Exerts Estrogen-Like Activities in Rat Osteoblast-Like (UMR-106) Cells. *J Food Drug Anal* (2020) 20:265–9. doi: 10.38212/2224-6614.2136
8. Pang WY, Wang XL, Mok SK, Lai WP, Chow HK, Leung PC, et al. Naringin Improves Bone Properties in Ovariectomized Mice and Exerts Oestrogen-Like Activities in Rat Osteoblast-Like (UMR-106) Cells. *Br J Pharmacol* (2010) 159(8):1693–703. doi: 10.1111/j.1476-5381.2010.00664.x
9. Zhou LP, Wong KY, Yeung HT, Dong XL, Xiao HH, Gong AG, et al. Bone Protective Effects of Danggui Buxue Tang Alone and in Combination With Tamoxifen or Raloxifene *In Vivo* and *In Vitro*. *Front Pharmacol* (2018) 9:779. doi: 10.3389/fphar.2018.00779
10. García-Martín A, Reyes-García R, García-Castro JM, Rozas-Moreno P, Escobar-Jiménez F, Muñoz-Torres M. Role of Serum FSH Measurement on Bone Resorption in Postmenopausal Women. *Endocrine* (2012) 41(2):302–8. doi: 10.1007/s12020-011-9541-7
11. Jain S, Camacho P. Use of Bone Turnover Markers in the Management of Osteoporosis. *Curr Opin Endocrinol Diabetes Obes* (2018) 25(6):366–72. doi: 10.1097/MED.0000000000000446
12. Latourelle JC, Dybdahl M, Destefano AL, Myers RH, Lash TL. Risk of Parkinson's Disease After Tamoxifen Treatment. *BMC Neurol* (2010) 10 (1):23. doi: 10.1186/1471-2377-10-23
13. Sievert LL, Obermeyer CM, Saliba M. Symptom Groupings at Midlife: Cross-Cultural Variation and Association With Job, Home, and Life Change. *Menopause (New York NY)* (2007) 14(4):798–807. doi: 10.1097/gme.0b013e31804f8175
14. Nowacka-Cieciura E, Sadowska A, Pacholczyk M, Chmura A, Tronina O, Durlik M. Bone Mineral Density and Bone Turnover Markers Under Bisphosphonate Therapy Used in the First Year After Liver Transplantation. *Med Sci Monitor* (2016) 21:241–9. doi: 10.12659/AOT.895413
15. Wong KY, Zhou L, Yu W, Poon CC, Xiao H, Chan CO, et al. Water Extract of Er-Xian Decoction Selectively Exerts Estrogenic Activities and Interacts With SERMs in Estrogen-Sensitive Tissues. *J Ethnopharmacol* (2021) 275:114096. doi: 10.1016/j.jep.2021.114096
16. Zaidi M, Lizneva D, Kim S-M, Sun L, Iqbal J, New MI, et al. FSH, Bone Mass, Body Fat, and Biological Aging. *Endocrinology* (2018) 159(10):3503–14. doi: 10.1210/en.2018-00601
17. Sun L, Peng Y, Sharrow AC, Iqbal J, Zhang Z, Papachristou DJ, et al. FSH Directly Regulates Bone Mass. *Cell* (2006) 125(2):247–60. doi: 10.1016/j.cell.2006.01.051
18. Cerri S, Mus L, Blandini F. Parkinson's Disease in Women and Men: What's the Difference? *J Parkinsons Dis* (2019) 9(3):501–15. doi: 10.3233/JPD-191683
19. Ascherio A, Schwarzschild MA. The Epidemiology of Parkinson's Disease: Risk Factors and Prevention. *Lancet Neurol* (2016) 15(12):1257–72. doi: 10.1016/S1474-4422(16)30230-7
20. Mikelman SR, Guptaroy B, Schmitt KC, Jones KT, Zhen J, Reith MEA, et al. Tamoxifen Directly Interacts With the Dopamine Transporter. *J Pharmacol Exp Ther* (2018) 367(1):119–28. doi: 10.1124/jpet.118.248179
21. Carpenter C, Zestos AG, Altshuler R, Sorenson RJ, Guptaroy B, Showalter HD, et al. Direct and Systemic Administration of a CNS-Permeant Tamoxifen Analog Reduces Amphetamine-Induced Dopamine Release and Reinforcing Effects. *Neuropsychopharmacology* (2017) 42(10):1940–9. doi: 10.1038/npp.2017.95
22. Lupo M, Dains JE, Madsen LT. Hormone Replacement Therapy: An Increased Risk of Recurrence and Mortality for Breast Cancer Patients? *J Adv Pract Oncol* (2015) 6(4):322–30. doi: 10.6004/jadpro.2015.6.4.3
23. Morello KC, Wurz GT, DeGregorio MW. SERMs: Current Status and Future Trends. *Crit Rev Oncol/Hematol* (2002) 43(1):63–76. doi: 10.1016/S1040-8428(02)00022-7
24. Anderson GL, Judd HL, Kaunitz AM, Barad DH, Beresford SA, Pettinger M, et al. Effects of Estrogen Plus Progestin on Gynecologic Cancers and Associated Diagnostic Procedures: The Women's Health Initiative Randomized Trial. *Jama* (2003) 290(13):1739–48. doi: 10.1001/jama.290.13.1739
25. Bergman L, Beelen ML, Gallee MP, Hollema H, Benraadt J, van Leeuwen FE. Risk and Prognosis of Endometrial Cancer After Tamoxifen for Breast Cancer. Comprehensive Cancer Centres' ALERT Group. Assessment of Liver and Endometrial Cancer Risk Following Tamoxifen. *Lancet* (2000) 356 (9233):881–7. doi: 10.1016/S0140-6736(00)02677-5
26. Guo D, Wang J, Wang X, Luo H, Zhang H, Cao D, et al. Double Directional Adjusting Estrogenic Effect of Naringin From Rhizoma Drynariae (Gusuibu). *J Ethnopharmacol* (2011) 138(2):451–7. doi: 10.1016/j.jep.2011.09.034
27. Kim SH, Park MJ. Effects of Phytoestrogen on Sexual Development. *Korean J Pediatr* (2012) 55(8):265. doi: 10.3345/kjp.2012.55.8.265

Conflict of Interest: The authors declare that the research was conducted in the absence of any commercial or financial relationships that could be construed as a potential conflict of interest.

this article, or claim that may be made by its manufacturer, is not guaranteed or endorsed by the publisher.

frontiers | Frontiers in Endocrinology

ORIGINAL RESEARCH
published: 14 April 2022
doi: 10.3389/fendo.2022.874748

Molecular Regulators of Muscle Mass and Mitochondrial Remodeling Are Not Influenced by Testosterone Administration in Young Women

Oscar Horwath[1*], *Marcus Moberg*[1,2], *Angelica Lindén Hirschberg*[3,4], *Björn Ekblom*[1] *and William Apró*[1,5]

[1] Department of Physiology, Nutrition and Biomechanics, Åstrand Laboratory, Swedish School of Sport and Health Sciences, Stockholm, Sweden, [2] Department of Physiology and Pharmacology, Karolinska Institutet, Stockholm, Sweden, [3] Department of Women´s and Children´s Health, Division of Neonatology, Obstetrics and Gynaecology, Karolinska Institutet, Stockholm, Sweden, [4] Department of Gynaecology and Reproductive Medicine, Karolinska University Hospital, Stockholm, Sweden, [5] Department of Clinical Science, Intervention and Technology, Karolinska Institutet, Stockholm, Sweden

OPEN ACCESS

Edited by:
Sadiq Umar,
University of Illinois at Chicago,
United States

Reviewed by:
Michaël R. Laurent,
University Hospitals Leuven, Belgium
Mohd Salman,
University of Tennessee Health Science Center (UTHSC),
United States

***Correspondence:**
Oscar Horwath
oscar.horwath@gih.se

Specialty section:
This article was submitted to Bone Research, a section of the journal Frontiers in Endocrinology

Received: 12 February 2022
Accepted: 18 March 2022
Published: 14 April 2022

Citation:
Horwath O, Moberg M, Hirschberg AL, Ekblom B and Apró W (2022) Molecular Regulators of Muscle Mass and Mitochondrial Remodeling Are Not Influenced by Testosterone Administration in Young Women. Front. Endocrinol. 13:874748. doi: 10.3389/fendo.2022.874748

Testosterone (T) administration has previously been shown to improve muscle size and oxidative capacity. However, the molecular mechanisms underlying these adaptations in human skeletal muscle remain to be determined. Here, we examined the effect of moderate-dose T administration on molecular regulators of muscle protein turnover and mitochondrial remodeling in muscle samples collected from young women. Forty-eight healthy, physically active, young women (28 ± 4 years) were assigned in a random double-blind fashion to receive either T (10 mg/day) or placebo for 10-weeks. Muscle biopsies collected before and after the intervention period were divided into sub-cellular fractions and total protein levels of molecular regulators of muscle protein turnover and mitochondrial remodeling were analyzed using Western blotting. T administration had no effect on androgen receptor or 5α-reductase levels, nor on proteins involved in the mTORC1-signaling pathway (mTOR, S6K1, eEF2 and RPS6). Neither did it affect the abundance of proteins associated with proteasomal protein degradation (MAFbx, MuRF-1 and UBR5) and autophagy-lysosomal degradation (AMPK, ULK1 and p62). T administration also had no effect on proteins in the mitochondria enriched fraction regulating mitophagy (Beclin, BNIP3, LC3B-I, LC3B-II and LC3B-II/I ratio) and morphology (Mitofilin), and it did not alter the expression of mitochondrial fission- (FIS1 and DRP1) or fusion factors (OPA1 and MFN2). In summary, these data indicate that improvements in muscle size and oxidative capacity in young women in response to moderate-dose T administration cannot be explained by alterations in total expression of molecular factors known to regulate muscle protein turnover or mitochondrial remodeling.

Keywords: androgen receptor, mTORC1-signaling, ubiquitin-proteasome system, fission, fusion

INTRODUCTION

Testosterone (T) is a well-known anabolic agent which promotes dose-dependent increases of lean mass and muscle hypertrophy in young and old men (1–3). Similarly, we and others have previously shown that administration of exogenous T promotes muscle anabolism and lean mass accretion in pre- and post-menopausal women (4–6). However, despite compelling evidence of its anabolic effect, the molecular events underlying muscle hypertrophy following T exposure in humans are not well understood and data from female-only cohorts are lacking.

Given its role as a critical regulator of muscle protein synthesis (7, 8), the mechanistic target of rapamycin complex 1 (mTORC1) pathway is considered a candidate mediator of T-induced muscle growth (9). Indeed, provision of T in cultured muscle cells stimulates hypertrophy *via* mTORC1-dependent signaling (10, 11). This is further supported by rodent data showing reduced signaling activity downstream of mTORC1 after androgen deprivation, while restoring androgen levels by nandrolone injections (6 mg/kg bw) reversed this effect (12). Studies seeking to depict the role of mTORC1-signaling in human muscle following T provision are scarce and have provided mixed results. Howard et al., 2020 showed that weekly injections of T enanthate (200 mg) during 28-days of severe energy deficit did not alter mTORC1-signaling following exercise and protein intake in young men (13). On the other hand, Gharahdaghi and colleagues showed that biweekly T injections (Sustanon, 250 mg) in combination with resistance training potentiated exercise-induced mTORC1-signaling in old men (14). More research in human muscle is although required to verify whether a similar mechanism of action is present in other cohorts.

Changes in muscle mass are dictated by the finely tuned balance between synthesis and degradation of muscle protein (15). Suppression of the latter is assumed to be central for driving lean mass accretion in humans following T exposure (16–18). Mechanistically, protein degradation occurs primarily through the autophagy-lysosomal and the ubiquitin-proteasomal system (UPS) (19). The UPS involves two well characterized muscle specific ubiquitin ligases; Muscle Atrophy F-box (MAFbx) and Muscle RING-finger 1 (MuRF-1) (20, 21). The existing knowledge of how T provision influences markers of UPS-mediated protein degradation is although limited, and inconclusive results have been reported. In the study by Gharahdaghi and colleagues, MAFbx or MuRF-1 protein levels remained unchanged (14), whilst a reduction of these markers were observed in hypogonadal men following T replacement therapy (TRT) (50-100 mg daily) (22). Moreover, whether the autophagy-lysosomal pathway is influenced by androgen levels in human muscle remains to be explored. The increased re-utilization of intracellular amino acids observed after T provision might however represent a putative mechanism for how autophagy could prevent a negative protein balance in the fasted state and thereby contribute to muscle growth (17, 23). In rodents, muscle atrophy induced by castration is associated with elevated levels of microtubule-associated protein 1A/B-light chain 3B (LC3B)-II and polyubiquitin-binding protein 62 (p62), whilst the re-introduction of androgens to the circulation restored their expression levels (24, 25). As such, there is evidence that the autophagy pathway is responsive to changes in systemic androgen concentrations, however, these findings may not be readily translatable to human physiology under *in vivo* conditions where androgen concentrations are less altered in response to exogenous supplementation.

We have previously demonstrated that administration of T increased oxidative capacity in human muscle by improving respiration in isolated mitochondria, a measure of mitochondrial quality (26). However, since this was not paralleled by concomitant increases in mitochondrial protein abundance, i.e., citrate synthase and respiratory chain complex I-V, other factors, such as alterations in mitochondrial remodeling, may underlie these changes. Intriguingly, systemic androgen levels are shown to impact the abundance of proteins involved in mitochondrial quality control in mouse muscle (27, 28), and exposure to high doses of T (50 mg/kg bw) upregulated several key proteins associated with mitophagy as well as fission and fusion (29). While prior work has focused on mitochondrial biogenesis in human muscle following T provision (14, 30), molecular regulators of the remodeling machinery have previously not been addressed in this context.

The molecular mechanisms responsible for adaptations in human skeletal muscle following T administration are not fully understood and the translatability from cell and rodent studies is often limited. Furthermore, understanding how mitochondrial turnover is affected by alternating T concentrations may have clinical implications for mitigating declines in muscle mass and function during aging. Therefore, in the present study we sought to investigate if the previously observed increases in muscle size and oxidative capacity following 10 weeks of T administration in young women are mediated by alterations in protein levels of molecular markers regulating muscle protein turnover and mitochondrial remodeling.

MATERIAL AND METHODS

Ethical Approval

This study is part of a larger project investigating the impact of T administration on physical performance and muscle mass in young physically active women, registered at ClinicalTrials.gov (NCT03210558). This study was approved by the local ethics committee in Stockholm (2016/1485-32, amendment 2017/779-32), and was conducted in line with the principles outlined in the Declaration of Helsinki. All participants received detailed information about the design of the study and associated risks before providing their written consent.

Study Design

The design of the present study has been described in detail in our previous publications (4, 26, 31). Briefly, this was a randomized, double-blinded, placebo-controlled trial. Following initial screening procedures, participants were randomly allocated to 10-weeks of either T or placebo

treatment. T was administered by manually applying a gel (10 mg, Andro-Feme 1) to the outer thigh every evening. This dose was chosen to increase serum levels of T significantly above the physiological level without inducing harmful side effects. Participants were instructed to keep their habitual activity levels throughout the study period, and they were also informed not to make any changes to their diet.

Participants

Forty-eight young (28 ± 4 years), physically active, women participated in the present study. Physical characteristics and serum levels of T have been reported previously (4, 26, 31).

Muscle Biopsy Sampling

Muscle samples were collected ~ 60 min after the participants finished a physical testing session (26, 31). Muscle biopsies were obtained from the middle portion of *m. vastus lateralis* after administration of local anesthesia using the Weil-Blakesley conchotome technique (32). Tissue samples were immediately blotted free of blood and rapidly frozen in liquid nitrogen until further processing.

Muscle Tissue Processing

Muscle samples were freeze-dried overnight and dissected free of blood, fat, and connective tissue under a stereo microscope (VisiScope, VWR). Fibre bundles were then mixed carefully and stored in -80°C before further processing.

Immunoblotting Sample Preparation

To study protein levels in whole muscle homogenates, ~ 2 mg of freeze-dried muscle was homogenized in ice-cold buffer (100 µl · mg^{-1} dry weight) containing 250 mM Sucrose, 20 mM HEPES (pH 7.4), 10 mM KCl, 1.5 mM $MgCl_2$, 1 mM EDTA, 1 mM EGTA, 10 mM β-glycerophosphate, 1% phosphatase inhibitor cocktail (Sigma P-2850) and 1% (v/v) Halt Protease Inhibitor Cocktail (Thermo Scientific, Rockford, USA) using a Bullet-Blender™ (NextAdvance, New York, USA) and 0.5 mm Zirconium Oxide Beads (NextAdvance, New York, USA). The supernatant was collected after lysates had been rotating for 60 min at 4°C and centrifuged at 10,000 g for 15 min. Protein concentration was determined from a small aliquot of the supernatant using Pierce™ 660 nm protein assay (Thermo Scientific, Rockford, USA). The samples were diluted in 4x Laemmli sample buffer (Bio-Rad Laboratories, Richmond, USA) and homogenization buffer, rendering a protein concentration of 0.75 µg $µl^{-1}$. The samples were heated to 95°C for 5 min before being stored in -30°C.

To study protein levels specifically in the mitochondrial compartment, we fractionated muscle according to a previously described protocol with minor adjustments (33). In brief, ~ 6 mg of freeze-dried muscle was homogenized in ice-cold buffer (100 µl · mg^{-1} dry weight) containing 250 mM Sucrose, 20 mM HEPES (pH 7.4), 10 mM KCl, 1.5 mM $MgCl_2$, 1 mM EDTA, 1 mM EGTA, 10 mM β-glycerophosphate, 1% phosphatase inhibitor cocktail (Sigma P-2850) and 1% (v/v) Halt Protease Inhibitor Cocktail (Thermo Scientific, Rockford, USA), using a 2 ml glass Dounce tissue grinder set (Sigma, D8938), applying 10 and 30 strokes with pestle A and B, respectively. The tissue lysate was then transferred into new tubes, rotated for 60 min at 4°C and centrifuged at 1000 g for 10 min to allow for the formation of a myofibrillar pellet. The supernatant was then carefully transferred into new tubes and centrifuged at 16,000 g for 20 min, resulting in a cytosolic protein fraction. The remaining pellet was washed twice by carefully resuspending the pellet in homogenization buffer. Following the final centrifugation, the pellet was dissolved in 60 µl of homogenization buffer containing 1% TritonX-100, resulting in a membrane fraction (hereafter referred to as the mitochondrial fraction). This fraction was then combined with 20 µl of 4x Laemmli sample buffer (Bio-Rad Laboratories, Richmond, USA) and 400 mM dithiothreitol, heated to 37°C for 30 min, before being stored in -30°C. Protein concentration was determined using Ionic Detergent Compatibility Reagent (Thermo Scientific, Rockford, USA) and Pierce™ 660 nm protein assay (Thermo Scientific, Rockford, USA). To determine the purity of the mitochondrial fraction, 5 ug of protein from this fraction and the cytosolic fraction were loaded side-by-side on a gel and immunoblotted for Porin (VDAC1) and translocase of outer mitochondrial membrane 20 (TOM20), two proteins found in the outer mitochondrial membrane, and the eukaryotic elongation factor 2 (eEF2), a protein dispersed throughout the cytoplasm. As demonstrated in **Figure 3G**, eEF2 was only present in the cytosolic fraction whereas Porin and TOM20 were only detected in the mitochondrial fraction.

SDS-PAGE and Immunoblotting

From each sample, 15 µg and 3 µg of protein from whole muscle homogenate and the mitochondrial fraction was loaded on 26-well Criterion TGX gradient gels (4-20% acrylamide; Bio-Rad Laboratories), respectively. Electrophoresis was performed on ice at 300 V for ~ 30 min. The gels were then equilibrated for 30 min in transfer buffer (25 mM Tris base, 192 mM glycine, and 10% methanol) after which proteins were transferred to PVDF membranes (Bio-Rad Laboratories) at constant current (300 mA) for 180 min at 4°C. Membranes were then stained using MemCode™ Reversible Protein Stain Kit (Thermo Scientific, Rockford, USA) to confirm even transfer of proteins. After destaining, membranes were blocked for 1h in Tris-buffered saline (TBS; 20 mM Tris base, 137 mM NaCl, pH 7.6) containing 5% non-fat dry milk followed by incubation overnight (4°C) with primary antibodies diluted in TBS supplemented with 0.1% Tween-20 and 2.5% non-fat dry milk (TBS-TM). Next morning, membranes were washed after which secondary antibodies conjugated to horseradish peroxidase were applied for 1h. Membranes were then washed again in TBS-TM (2 x 1 min, 3 x 10 min) followed by 3 x 5 min with TBS. Lastly, membranes were incubated with Super Signal™ Femto Chemiluminescent Substrate (Thermo Scientific) for 5 min to allow for band detection in the molecular imager (ChemiDoc™MP, Bio-Rad Laboratories). Before the blocking step, membranes were cut into strips and later assembled to expose all samples to the same blotting conditions. Due to limited quantity the mitochondrial fraction samples, following visualization, membranes were stripped using Restore Western Blot Stripping Buffer (Thermo Scientific) for 30 min at 37°C, washed and re-probed with a new primary antibody. For whole muscle

homogenates, protein levels of each sample were normalized to their total protein stain. For the mitochondrial fraction, protein levels were normalized to the corresponding protein level of Porin, which remained unchanged throughout the intervention (data not shown). Quantification of bands were performed using the Image Lab™ software (Bio-Rad Laboratories).

Antibodies

For immunoblotting, primary antibodies against androgen receptor (#D6F11XP®), mTOR (#2983), S6K1 (#2708), eEF2 (#2332), AMPK (#2532), ULK1 (#6439), p62 (#8025), LC3B (#2775), Beclin (#3495) and BNIP3 (#44060), were purchased from Cell Signaling Technology (Beverly, USA). Primary antibodies against 5α-reductase 2 (#293232), MuRF-1 (#sc-398608), UBR5 (#sc-515494), TOM20 (sc-136211) and RPS6 (#sc-74459), were purchased from Santa Cruz Biotechnology (Heidelberg, Germany). Primary antibodies against MAFbx (#92281), Porin (#154856), OPA1 (#157457), DRP1 (#184247), FIS1 (#156865), MFN2 (#56889) and Mitofilin (#137057), were purchased from Abcam (Cambridge, UK). All antibodies were diluted 1:1000 except for 5α-reductase, MuRF-1, UBR5, S6, Beclin, LC3B, OPA1, MFN2 which were diluted 1:500, and eEF2 and Porin which were diluted 1:2000. Secondary anti-mouse (#7076, 1:10000) and secondary anti-rabbit (#7074, 1:10000) were purchased from Cell Signaling Technology.

Statistical Analyses

Data are presented as means ± standard deviation (SD). Statistical analyses were performed using GraphPad Prism version 9.1.2 for Windows (San Diego, California, USA). Data were analyzed with a two-way ANOVA with factors for group (T *vs.* placebo) and time (pre *vs* post intervention). Bonferroni multiple comparison was applied in case of significant interaction to localize differences. The significance level for all statistical tests was two-tailed and set at $P < 0.05$.

RESULTS

Androgen Receptor, 5-α Reductase and Anabolic Signaling

Administration of T had no effect on AR protein content but levels of 5-α reductase increased on average by 15% over time (main effect of time, $P<0.05$) (**Figures 1A, B**). In a similar fashion, administration of T did not influence the abundance of mTOR, S6K1 or eEF2, but levels of RPS6 increased on average by 11% over time and was overall higher in the group receiving T (main effect of time and group, $P<0.05$) (**Figures 1C–F**).

Ubiquitin-Proteasomal and Lysosomal-Autophagy Pathway

Administration of T did not alter protein levels of MAFbx, MuRF1 or UBR5 in the ubiquitin-proteasomal pathway or AMPK, ULK1 or p62 in the lysosomal-autophagy pathway (**Figures 2A–F**).

Mitochondrial Remodeling

Administration of T had no effect on protein levels of Beclin and Mitofilin (**Figures 3A, F**) and OPA1, 225 MFN2, FIS1 or DRP1 (**Figures 4A–D**) in the mitochondrial fraction. LC3B-I (**Figure 3C**) also remained unchanged while LC3B-II increased on average by 30% over time, (main effect of time, $P<0.05$; **Figure 3D**). In a similar fashion, BNIP3 increased on average by 25% in the mitochondrial fraction (main effect of time, $P<0.05$ **Figure 3B**). The ratio between LC3B-II and LC3B-I remained unaltered in response to the intervention (**Figure 3E**).

DISCUSSION

We and others have previously reported that administration of T increases lean mass and aerobic capacity in human subjects (4, 26). However, the molecular mechanisms by which T elicits adaptations in skeletal muscle remains poorly understood. Here we report that T provision in young women did not modulate total levels of key proteins involved in androgen signaling/metabolism, mTORC1-signaling, ubiquitin and autophagy-mediated protein degradation and mitochondrial remodeling. Our findings thus suggest that increases in skeletal muscle size and mitochondrial function following T exposure are not related to altered expression of key factors regulating these processes.

In skeletal muscle, ARs are dispersed throughout the cytoplasm but predominantly located in resident muscle stem cells and myonuclei (34, 35). ARs are not only responsible for mediating the anabolic effects of T (10, 36), but are also critical for muscle fiber remodeling following chronic RT (37, 38). In males, administration of T is commonly accompanied by increased intramuscular AR content (13, 14, 17, 35, 39), but no study has previously examined whether such change occur in young women. In the present study, despite raising T serum concentrations ~ fivefold above basal levels, AR protein expression remained unchanged, a somewhat unexpected finding given that basal muscle AR content is lower in women than in men (40). The lack of change could however be related to the moderate dosage provided (10 mg daily), the route of administration (transdermal), or that AR levels were altered in a transient manner and had returned to a basal state at the post-biopsy timepoint. The latter is supported by work from Ferrando and colleagues showing elevated AR protein levels 4-weeks after the onset of T administration, but these had returned to pre-treatment levels 20 weeks later (17). Nonetheless, in accordance with our findings, AR protein levels were unaltered also in old women receiving oral oxandrolone (7.5 mg twice a day) for 14 consecutive days, whereas men in the same study displayed significant increases (39). Accordingly, rodent data suggest that ARs are dispensable for normal muscle development in females, but not in males (41). It is from our data therefore evident that an augmented intramuscular AR content is not critical in women for mediating the anabolic effects of elevated T levels. This finding may highlight a sexual dimorphism given that male subjects consistently display contrasting results. Furthermore, with regard to T metabolism, we also measured intramuscular

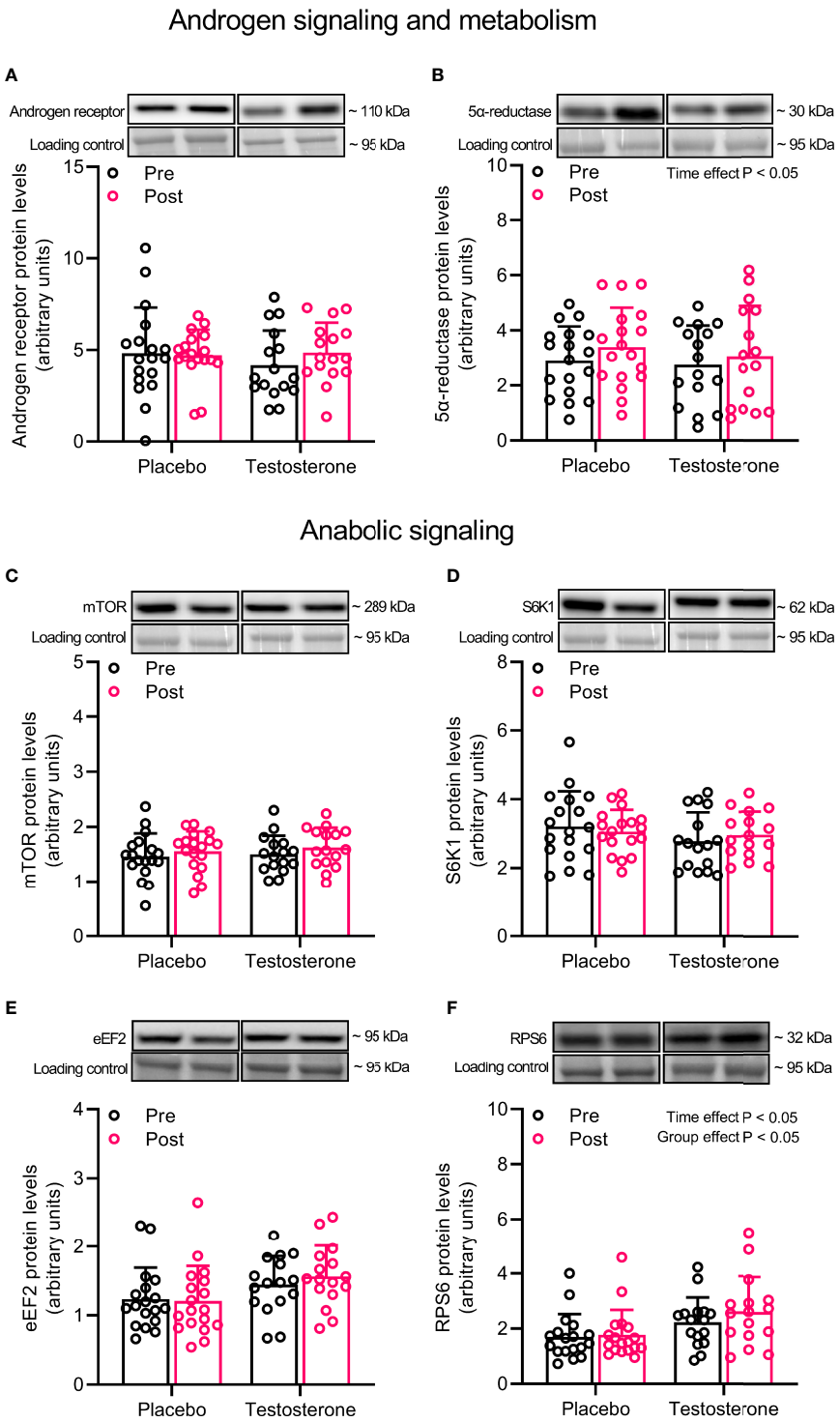

FIGURE 1 | Protein levels of androgen receptor **(A)**, 5α-reductase **(B)**, mTOR **(C)**, S6K1 **(D)**, eEF2 **(E)** and RPS6 **(F)** before (black dots) and after the intervention (red dots). Representative blots for each individual protein target are shown above each graph. Loading control is represented by a band at ~ 95 kDa from the corresponding total protein stain (Memcode™). The values presented are means ± SD and individual data points from 18 and 16 individuals (DF 32) in the placebo group and T group, respectively. The ANOVA revealed a significant main effect of time with respect to changes in protein levels for 5α-reductase and a significant main effect of time and group for RPS6.

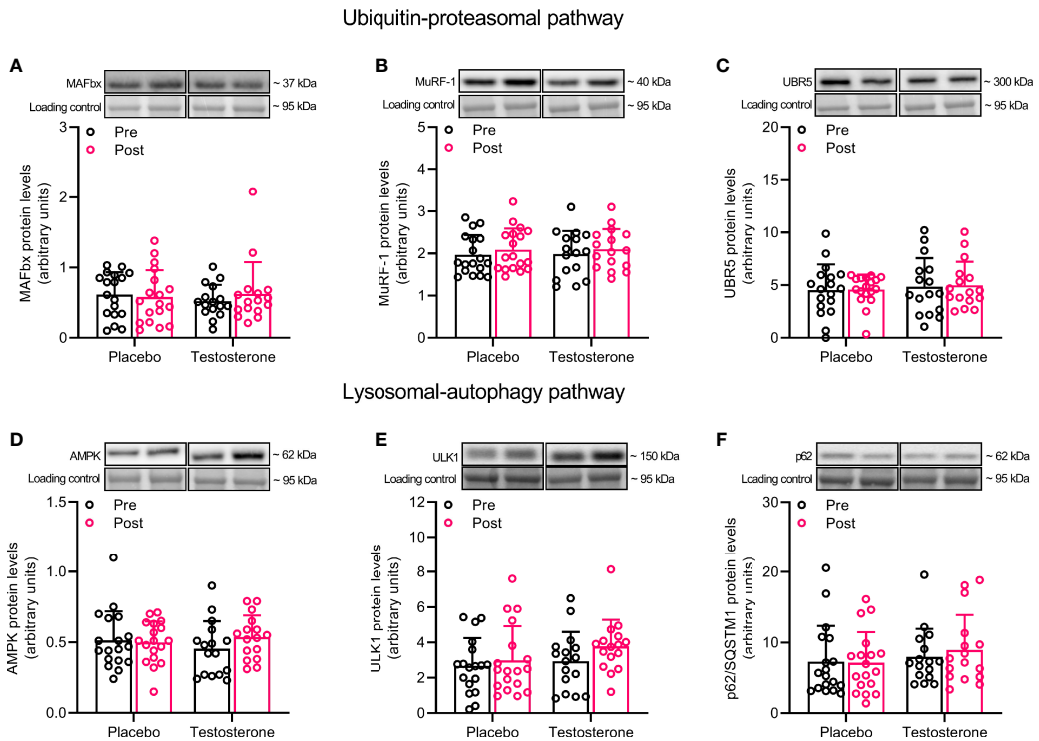

FIGURE 2 | Protein levels of MAFbx **(A)**, MuRF-1 **(B)**, UBR5 **(C)**, AMPK **(D)**, ULK1 **(E)** and p62 **(F)** before (black dots) and after the intervention (red dots). Representative blots for each individual protein target are shown above each graph. Loading control is represented by a band at ~ 95 kDa from the corresponding total protein stain (Memcode™). The values presented are means ± SD and individual data points from 18 and 16 individuals (DF 32) in the placebo group and T group, respectively.

content of 5α-reductase, the enzyme responsible for converting T into the highly potent metabolite dihydrotestosterone (DHT) (42). As both groups displayed slightly increased 5α-reductase protein content (main effect of time), we interpreted this as an effect not specific to T provision and that changes in muscle size cannot be explained by an altered capacity to metabolize T locally in the tissue. This aligns well with other studies questioning the anabolic effect of DHT in human subjects (43). On the other hand, we cannot completely rule out that other enzymes involved in androgen metabolism were affected by the current treatment, i.e., aromatase. Another factor that may have played a critical role for muscle adaptation here is the intramuscular concentration of T and other androgens, as discussed in a recent review (44). We did however not measure intramuscular levels of androgens in the present study but this is an important aspect that needs to be addressed by future work.

Studies in cultured cells and animal muscle have provided compelling evidence that T provision stimulates anabolism in an mTORC1-dependent manner (10–12), whereas data gathered from human trials have yielded inconsistent results (13, 14). To improve our understanding of how anabolic signaling may regulate muscle growth following T exposure, we measured the total expression of key proteins involved in the mTORC1-pathway. While most protein targets remained unchanged, only RPS6 displayed a significant pre-to-post increase in the T group, but this finding should be interpreted with caution as no interaction effect was present (main effect of time and group). Nevertheless, this may represent a potential mechanism by which T administration stimulates an increase in muscle mass. However, it is still possible that acute activation of this signaling cascade in response to anabolic stimuli, such as contractile activity and/or nutrients, was altered with T provision. In this regard, Gharahdaghi et al., 2019 demonstrated that T therapy potentiated acute resistance exercise-induced $mTOR^{Ser2448}$ and $RPS6^{Ser235/236}$ phosphorylation in older men (14). An enhanced response to each exercise session performed during the intervention may therefore explain how T provision stimulated muscle growth in our cohort. However, the observations of Gharahdaghi et al., 2019 were in a cohort of elderly men, in which a blunted signaling response due to potential anabolic resistance may have confounded the results. Future studies are therefore warranted to determine if a similar effect also exists in young individuals who are sensitive to anabolic stimuli. Similarly, whether T provision has a synergistic effect on the acute signaling response following nutrient intake is yet to be determined, but it has been reported that T provision does not further enhance the stimulatory role of amino acids on rates of muscle protein synthesis in human muscle (18), indicating that such effect would be of less importance to the present findings.

In humans, T provision is suggested to increase muscle mass in part by suppressing rates of muscle protein degradation

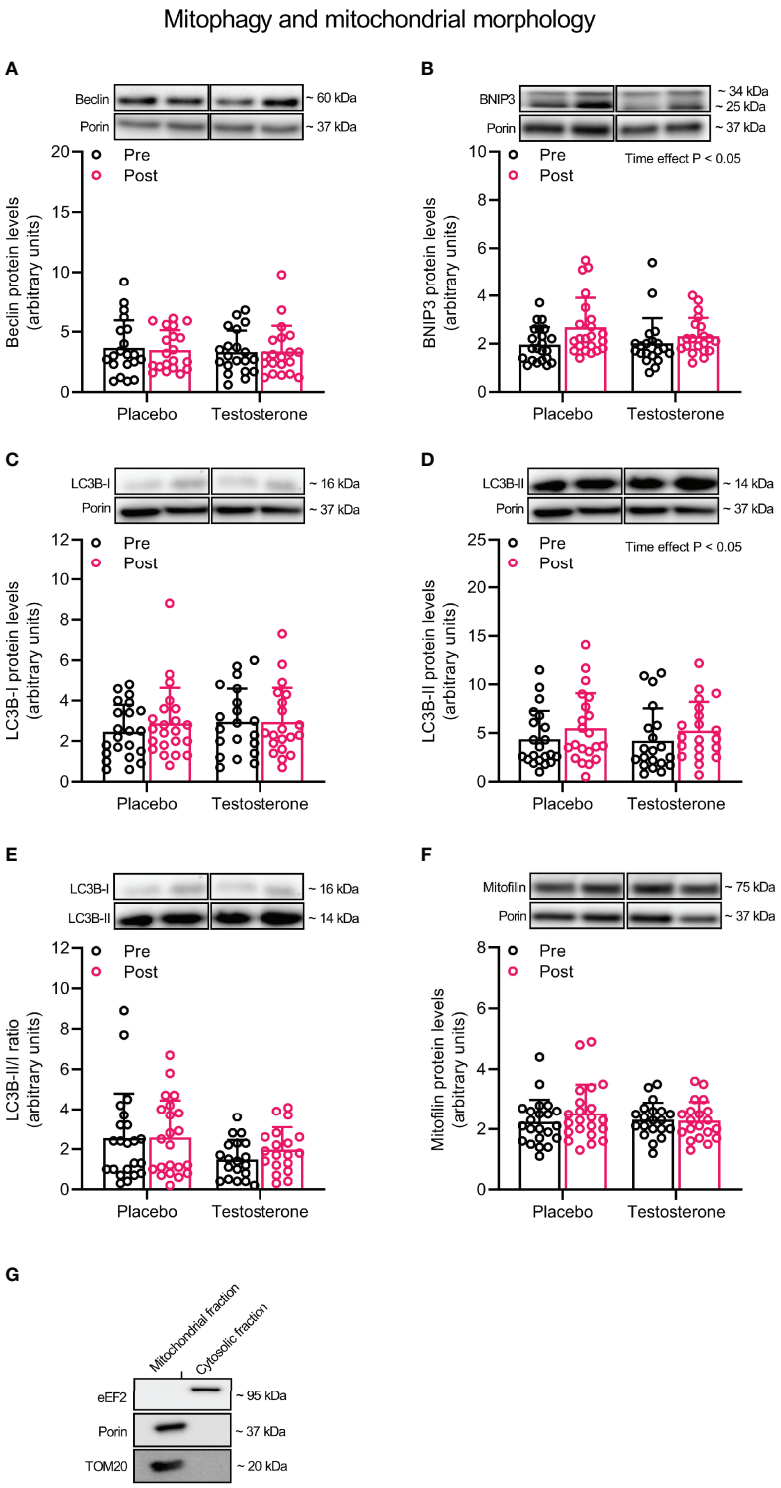

FIGURE 3 | Protein levels of Beclin **(A)**, BNIP3 **(B)**, LC3B-I **(C)**, LC3B-II **(D)**, LC3B-II/I ratio **(E)** and Mitofilin **(F)** in the mitochondrial fraction before (black dots) and after the intervention (red dots), as well as the assessment of mitochondrial fraction purity **(G)**. Representative blots for each individual protein target and Porin are shown above each graph. The values presented are means ± SD and individual data points from 22 and 20 individuals (DF 40) in the placebo group and T group, respectively. The ANOVA revealed a significant main effect of time with respect to changes in protein levels for BNIP3 and LC3B-II. For illustrative purposes, two subjects from the placebo group displaying extreme values were removed from **(A)** (pre-post; 6.7 to 18.5 and 12.3 to 23.6, respectively) and one subject from the placebo group was removed from **(D)** (pre-post; 6.1 to 19.4), but these values were included in the statistical analysis.

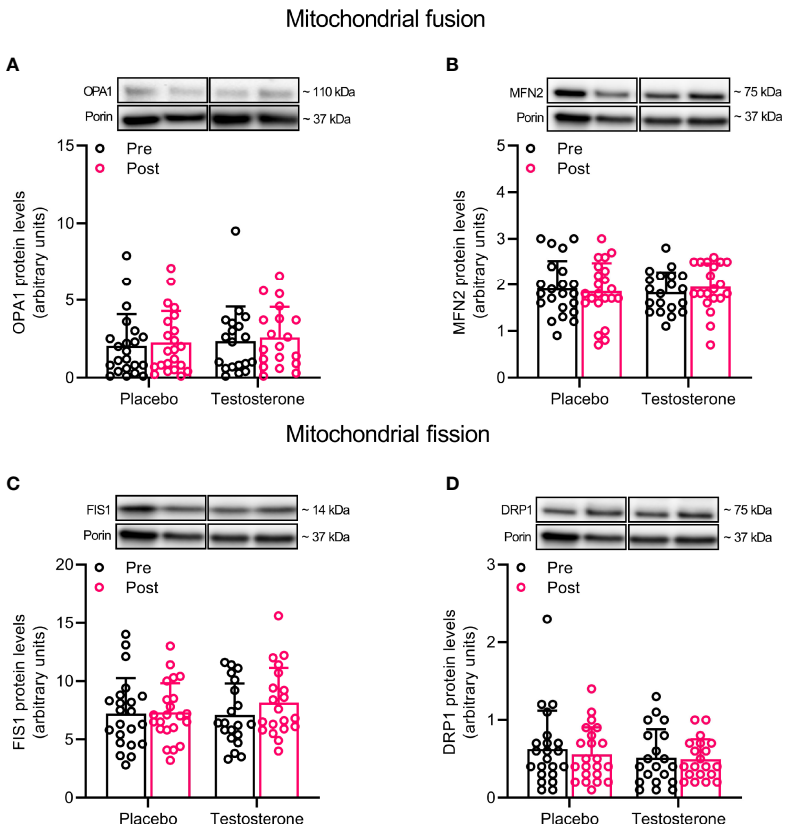

FIGURE 4 | Protein levels of OPA1 **(A)**, MFN2 **(B)**, FIS1 **(C)**, and DRP1 **(D)** in the mitochondrial fraction before (black dots) and after the intervention (red dots). Representative blots for each individual protein target and Porin are shown above each graph. The values presented are means ± SD and individual data points from 22 and 20 individuals (DF 40) in the placebo group and T group, respectively. For illustrative purposes, one subject from the placebo group displaying extreme values was removed from **(A)** (pre-post; 6.1 to 19.4), but these values were included in the statistical analysis.

(16–18), a process largely governed by muscle-specific E3 ligases MAFbx and MuRF-1 (20, 21). We therefore assessed the expression of these proteins together with the newly discovered E3 ligase UBR5. However, none of these targets were altered in response to T treatment. This would either indicate that transient changes in protein abundance were missed due to the current study design, or that muscle hypertrophy following T exposure is not related to changes in UPS-mediated protein breakdown (45). Regardless, our findings contrast recent work, in which reduced levels of MAFbx and MuRF-1 were found in hypogonadal men after they underwent 24-weeks of TRT (22). However, discrepancies between studies may be explained by differences in study population (young active women *vs* old hypogonadal men) and the dosage provided (10 mg *vs* 50-100 mg daily). Beyond this, conflicting findings may also be explained by endogenous androgen production. As such, it seems that rates of protein breakdown are suppressed by T provision only if endogenous concentrations are in the hypogonadal range and not when subjects are transitioning from the physiological to the supraphysiological range (9). Given that T levels were raised ~ fivefold above basal levels here, this notion seems to hold true also for women. It is however important to consider that the expression pattern of these E3-ligases might not fully reflect changes in proteasomal protein breakdown or muscle mass (46).

Another contributor to the overall protein balance in skeletal muscle is the lysosomal-autophagy pathway (47). Whether administration of T alters the autophagic process remains poorly understood and has, to our knowledge, not previously been investigated in human muscle. Current literature consists exclusively of animal studies where markers of autophagy have been assessed in response to surgical castration, which evokes rapid and profound changes in muscle mass, therefore providing little relevance to human subjects under free-living conditions. Nonetheless, castration-induced muscle atrophy is associated with increased phosphorylation of $AMPK^{Thr172}$ and elevated LC3B-II content, as well as decreased phosphorylation of $ULK1^{Ser757}$ and decreased p62 expression, which together indicate robust activation of the autophagy pathway (24, 25). The link between androgen levels and autophagy is further strengthened by the complete reversal of this effect once androgen levels are restored following castration (24, 25). In the present study, we did not find any alterations in total protein expression of AMPK, ULK1 or p62, which implies that the autophagy-lysosomal pathway did not mediate changes in muscle size following exogenous T

provision. The present observation also opposes the notion that this pathway could be involved in the improved capacity to re-utilize amino acids in the fasted state, as previously observed here (17, 23). It must however be pointed out, once again, that the present study does not entail any information on the activation of this pathway in relation to acute stimuli, i.e., exercise, nor does it contain data on the transcriptional level. Thus, some aspects of this pathway with regards to muscle adaptation following T administration remains unanswered and requires additional study.

Mitochondrial remodeling through increased mitophagy, is crucial for maintaining a healthy mitochondrial network and impairments of this process are associated with declines in muscle size and function (48). During mitophagy, mitochondria are first separated from each other through fission, then tagged for removal by specific receptor proteins and later engulfed by autophagosomes for transport to the lysosome (48, 49). Interestingly, mice deprived of androgens displayed attenuated increases in oxidative capacity following chronic exercise, a phenomenon thought to be related to disrupted BNIP3-mediated mitophagy (50). While exercise training itself is sufficient to promote remodeling of the mitochondrial network (51, 52), preliminary evidence in mice suggest that exercise in combination with T provision promotes even greater activation of this system (29). Based on this, we reasoned that previously observed improvements in muscle oxidative capacity could be explained by a similar mechanism (26). We therefore assessed if markers of mitochondrial remodeling were influenced by T exposure. However, we did not observe any changes in markers associated with mitophagy or mitochondrial fission on the subcellular level. There were however some increases of BNIP3 and LC3B-II protein content (main effect of time), but these changes were not related to T provision *per se* and could potentially be related to subtle changes in subject´s training status, although we find this unlikely since exercise habits were well-maintained throughout the intervention (31). In addition, no effects were observed in MFN2 and OPA1 protein levels, two key regulators of mitochondrial fusion shown to be highly responsive to T exposure in rodent skeletal muscle (29). However, in this case, conflicting findings are likely due to profound differences in dosing regimens across species, in which serum T concentrations were raised 25-100 times above control level in the previously mentioned study (29).

Despite assessing several well-known regulators of muscle protein turnover, mitophagy and mitochondrial fission-fusion in the present study, it still remains to be determined by which molecular events T administration elicits hypertrophy and improved mitochondrial quality as we were unable to provide any clear mechanistic links here. One of the limitations of the present study is that we only reported chronic effects in muscle samples collected pre-post intervention. We therefore cannot exclude out that T administration, 1) transiently altered total protein abundance, 2) modulated the acute signaling response to exercise and/or nutrients, 3) influenced these regulating factors in a muscle fiber-type specific manner, 4) induced changes only at the transcriptional level. It is also possible that the sample size in the present study precluded us from detecting small but biologically relevant changes in total protein levels. To put our findings in light of the current literature is difficult as several inconsistences exist, which is reflective of the large variability among studies in terms of sex (men *vs* women), age (old *vs* young), endogenous androgens (hypo- *vs* eugonadal), route of administration (injections *vs* transdermal) and length of treatment. Nonetheless, the present study sheds important light on the effects of T provision on skeletal muscle in females and provides insights into their molecular underpinnings.

In summary, improvements in muscle size and oxidative capacity following 10-weeks of T administration in young women (4, 26, 31), cannot be explained by changes in protein expression related to muscle protein turnover or mitochondrial remodeling.

DATA AVAILABILITY STATEMENT

The original contributions presented in the study are included in the article/supplementary material. Further inquiries can be directed to the corresponding author.

ETHICS STATEMENT

The studies involving human participants were reviewed and approved by Stockholm (2016/1485-32, amendment 2017/779-32). The patients/participants provided their written informed consent to participate in this study.

AUTHOR CONTRIBUTIONS

AL, BE, and WA were responsible for the conception and design of the study. OH, MM, and WA were responsible for data acquisition, data analysis and interpretation. OH drafted the manuscript. All authors provided intellectual content, contributed to the revision of the manuscript, and approved the final version to be published.

FUNDING

This work was supported by the International Athletics Foundation, the Swedish Research Council (2017–02051), the Swedish Research Council for Sport Science (P2018-0197 and P2019-0098), the Karolinska Institute, and the Swedish Military Research Authority (Grant No. AF 922 0916). MM and WA were supported by Early Career Research Grants from the Swedish Research Council for Sport Science (D2017-0012 and D2019-0050, respectively).

ACKNOWLEDGMENTS

The authors are grateful to all the participants for their time and efforts throughout the study.

REFERENCES

1. Sinha-Hikim I, Artaza J, Woodhouse L, Gonzalez-Cadavid N, Singh AB, Lee MI, et al. Testosterone-Induced Increase in Muscle Size in Healthy Young Men Is Associated With Muscle Fiber Hypertrophy. *Am J Physiol Endocrinol Metab* (2002) 283(1):E154–64. doi: 10.1152/ajpendo.00502.2001
2. Sinha-Hikim I, Cornford M, Gaytan H, Lee ML, Bhasin S. Effects of Testosterone Supplementation on Skeletal Muscle Fiber Hypertrophy and Satellite Cells in Community-Dwelling Older Men. *J Clin Endocrinol Metab* (2006) 91(8):3024–33. doi: 10.1210/jc.2006-0357
3. Bhasin S, Storer TW, Berman N, Callegari C, Clevenger B, Phillips J, et al. The Effects of Supraphysiologic Doses of Testosterone on Muscle Size and Strength in Normal Men. *N Engl J Med* (1996) 335(1):1–7. doi: 10.1056/NEJM199607043350101
4. Hirschberg AL, Elings Knutsson J, Helge T, Godhe M, Ekblom M, Bermon S, et al. Effects of Moderately Increased Testosterone Concentration on Physical Performance in Young Women: A Double Blind, Randomised, Placebo Controlled Study. *Br J Sports Med* (2020) 54(10):599–604. doi: 10.1136/bjsports-2018-100525
5. Huang G, Basaria S, Travison TG, Ho MH, Davda M, Mazer NA, et al. Testosterone Dose-Response Relationships in Hysterectomized Women With or Without Oophorectomy: Effects on Sexual Function, Body Composition, Muscle Performance and Physical Function in a Randomized Trial. *Menopause* (2014) 21(6):612–23. doi: 10.1097/GME.0000000000000093
6. Smith GI, Yoshino J, Reeds DN, Bradley D, Burrows RE, Heisey HD, et al. Testosterone and Progesterone, But Not Estradiol, Stimulate Muscle Protein Synthesis in Postmenopausal Women. *J Clin Endocrinol Metab* (2014) 99(1):256–65. doi: 10.1210/jc.2013-2835
7. Dickinson JM, Fry CS, Drummond MJ, Gundermann DM, Walker DK, Glynn EL, et al. Mammalian Target of Rapamycin Complex 1 Activation Is Required for the Stimulation of Human Skeletal Muscle Protein Synthesis by Essential Amino Acids. *J Nutr* (2011) 141(5):856–62. doi: 10.3945/jn.111.139485
8. Drummond MJ, Fry CS, Glynn EL, Dreyer HC, Dhanani S, Timmerman KL, et al. Rapamycin Administration in Humans Blocks the Contraction-Induced Increase in Skeletal Muscle Protein Synthesis. *J Physiol* (2009) 587(Pt 7):1535–46. doi: 10.1113/jphysiol.2008.163816
9. Rossetti ML, Steiner JL, Gordon BS. Androgen-Mediated Regulation of Skeletal Muscle Protein Balance. *Mol Cell Endocrinol* (2017) 447:35–44. doi: 10.1016/j.mce.2017.02.031
10. Basualto-Alarcon C, Jorquera G, Altamirano F, Jaimovich E, Estrada M. Testosterone Signals Through mTOR and Androgen Receptor to Induce Muscle Hypertrophy. *Med Sci Sports Exerc* (2013) 45(9):1712–20. doi: 10.1249/MSS.0b013e31828cf5f3
11. Wu Y, Bauman WA, Blitzer RD, Cardozo C. Testosterone-Induced Hypertrophy of L6 Myoblasts Is Dependent Upon Erk and mTOR. *Biochem Biophys Res Commun* (2010) 400(4):679–83. doi: 10.1016/j.bbrc.2010.08.127
12. White JP, Gao S, Puppa MJ, Sato S, Welle SL, Carson JA. Testosterone Regulation of Akt/mTORC1/FoxO3a Signaling in Skeletal Muscle. *Mol Cell Endocrinol* (2013) 365(2):174–86. doi: 10.1016/j.mce.2012.10.019
13. Howard EE, Margolis LM, Berryman CE, Lieberman HR, Karl JP, Young AJ, et al. Testosterone Supplementation Up-Regulates Androgen Receptor Expression and Translational Capacity During Severe Energy Deficit. *Am J Physiol Endocrinol Metab* (2020) 319(4):E678–88. doi: 10.1152/ajpendo.00157.2020
14. Gharahdaghi N, Rudrappa S, Brook MS, Idris I, Crossland H, Hamrock C, et al. Testosterone Therapy Induces Molecular Programming Augmenting Physiological Adaptations to Resistance Exercise in Older Men. *J Cachexia Sarcopenia Muscle* (2019) 10(6):1276–94. doi: 10.1002/jcsm.12472
15. Brook MS, Wilkinson DJ, Phillips BE, Perez-Schindler J, Philp A, Smith K, et al. Skeletal Muscle Homeostasis and Plasticity in Youth and Ageing: Impact of Nutrition and Exercise. *Acta Physiol (Oxf)* (2016) 216(1):15–41. doi: 10.1111/apha.12532
16. Ferrando AA, Sheffield-Moore M, Wolf SE, Herndon DN, Wolfe RR. Testosterone Administration in Severe Burns Ameliorates Muscle Catabolism. *Crit Care Med* (2001) 29(10):1936–42. doi: 10.1097/00003246-200110000-00015
17. Ferrando AA, Sheffield-Moore M, Yeckel CW, Gilkison C, Jiang J, Achacosa A, et al. Testosterone Administration to Older Men Improves Muscle Function: Molecular and Physiological Mechanisms. *Am J Physiol Endocrinol Metab* (2002) 282(3):E601–7. doi: 10.1152/ajpendo.00362.2001
18. Ferrando AA, Sheffield-Moore M, Paddon-Jones D, Wolfe RR, Urban RJ. Differential Anabolic Effects of Testosterone and Amino Acid Feeding in Older Men. *J Clin Endocrinol Metab* (2003) 88(1):358–62. doi: 10.1210/jc.2002-021041
19. Sandri M. Protein Breakdown in Muscle Wasting: Role of Autophagy-Lysosome and Ubiquitin-Proteasome. *Int J Biochem Cell Biol* (2013) 45(10):2121–9. doi: 10.1016/j.biocel.2013.04.023
20. Bodine SC, Baehr LM. Skeletal Muscle Atrophy and the E3 Ubiquitin Ligases MuRF1 and MAFbx/atrogin-1. *Am J Physiol Endocrinol Metab* (2014) 307(6):E469–84. doi: 10.1152/ajpendo.00204.2014
21. Bodine SC, Latres E, Baumhueter S, Lai VK, Nunez L, Clarke BA, et al. Identification of Ubiquitin Ligases Required for Skeletal Muscle Atrophy. *Science* (2001) 294(5547):1704–8. doi: 10.1126/science.1065874
22. Kruse R, Petersson SJ, Christensen LL, Kristensen JM, Sabaratnam R, Ortenblad N, et al. Effect of Long-Term Testosterone Therapy on Molecular Regulators of Skeletal Muscle Mass and Fibre-Type Distribution in Aging Men With Subnormal Testosterone. *Metabolism* (2020) 154347. doi: 10.1016/j.metabol.2020.154347
23. Ferrando AA, Tipton KD, Doyle D, Phillips SM, Cortiella J, Wolfe RR. Testosterone Injection Stimulates Net Protein Synthesis But Not Tissue Amino Acid Transport. *Am J Physiol* (1998) 275(5):E864–71. doi: 10.1152/ajpendo.1998.275.5.E864
24. Serra C, Sandor NL, Jang H, Lee D, Toraldo G, Guarneri T, et al. The Effects of Testosterone Deprivation and Supplementation on Proteasomal and Autophagy Activity in the Skeletal Muscle of the Male Mouse: Differential Effects on High-Androgen Responder and Low-Androgen Responder Muscle Groups. *Endocrinology* (2013) 154(12):4594–606. doi: 10.1210/en.2013-1004
25. Steiner JL, Fukuda DH, Rossetti ML, Hoffman JR, Gordon BS. Castration Alters Protein Balance After High-Frequency Muscle Contraction. *J Appl Physiol* (2017) 122(2):264–72. doi: 10.1152/japplphysiol.00740.2016
26. Cardinale DA, Horwath O, Elings-Knutsson J, Helge T, Godhe M, Bermon S, et al. Enhanced Skeletal Muscle Oxidative Capacity and Capillary-To-Fiber Ratio Following Moderately Increased Testosterone Exposure in Young Healthy Women. *Front Physiol* (2020) 11:585490. doi: 10.3389/fphys.2020.585490
27. Rossetti ML, Esser KA, Lee C, Tomko RJJr., Eroshkin AM, Gordon BS. Disruptions to the Limb Muscle Core Molecular Clock Coincide With Changes in Mitochondrial Quality Control Following Androgen Depletion. *Am J Physiol Endocrinol Metab* (2019) 317(4):E631–E45. doi: 10.1152/ajpendo.00177.2019
28. Rossetti ML, Steiner JL, Gordon BS. Increased Mitochondrial Turnover in the Skeletal Muscle of Fasted, Castrated Mice Is Related to the Magnitude of Autophagy Activation and Muscle Atrophy. *Mol Cell Endocrinol* (2018) 473:178–85. doi: 10.1016/j.mce.2018.01.017
29. Guo W, Wong S, Li M, Liang W, Liesa M, Serra C, et al. Testosterone Plus Low-Intensity Physical Training in Late Life Improves Functional Performance, Skeletal Muscle Mitochondrial Biogenesis, and Mitochondrial Quality Control in Male Mice. *PloS One* (2012) 7(12):e51180. doi: 10.1371/journal.pone.0051180
30. Petersson SJ, Christensen LL, Kristensen JM, Kruse R, Andersen M, Hojlund K. Effect of Testosterone on Markers of Mitochondrial Oxidative Phosphorylation and Lipid Metabolism in Muscle of Aging Men With Subnormal Bioavailable Testosterone. *Eur J Endocrinol* (2014) 171(1):77–88. doi: 10.1530/EJE-14-0006
31. Horwath O, Apro W, Moberg M, Godhe M, Helge T, Ekblom MM, et al. Fiber Type-Specific Hypertrophy and Increased Capillarization in Skeletal Muscle Following Testosterone Administration in Young Women. *J Appl Physiol* (2020) 1985). doi: 10.1152/japplphysiol.00893.2019
32. Ekblom B. The Muscle Biopsy Technique. Historical and Methodological Considerations. *Scand J Med Sci Sports* (2017) 27(5):458–61. doi: 10.1111/sms.12808
33. Schwalm C, Deldicque L, Francaux M. Lack of Activation of Mitophagy During Endurance Exercise in Human. *Med Sci Sports Exerc* (2017) 49(8):1552–61. doi: 10.1249/MSS.0000000000001256
34. Kadi F, Bonnerud P, Eriksson A, Thornell LE. The Expression of Androgen Receptors in Human Neck and Limb Muscles: Effects of Training and Self-

Administration of Androgenic-Anabolic Steroids. *Histochem Cell Biol* (2000) 113(1):25–9. doi: 10.1007/s004180050003
35. Sinha-Hikim I, Taylor WE, Gonzalez-Cadavid NF, Zheng W, Bhasin S. Androgen Receptor in Human Skeletal Muscle and Cultured Muscle Satellite Cells: Up-Regulation by Androgen Treatment. *J Clin Endocrinol Metab* (2004) 89(10):5245–55. doi: 10.1210/jc.2004-0084
36. Singh R, Artaza JN, Taylor WE, Gonzalez-Cadavid NF, Bhasin S. Androgens Stimulate Myogenic Differentiation and Inhibit Adipogenesis in C3H 10T1/2 Pluripotent Cells Through an Androgen Receptor-Mediated Pathway. *Endocrinology* (2003) 144(11):5081–8. doi: 10.1210/en.2003-0741
37. Morton RW, Sato K, Gallaugher MPB, Oikawa SY, McNicholas PD, Fujita S, et al. Muscle Androgen Receptor Content But Not Systemic Hormones Is Associated With Resistance Training-Induced Skeletal Muscle Hypertrophy in Healthy, Young Men. *Front Physiol* (2018) 9:1373. doi: 10.3389/fphys.2018.01373
38. Ferry A, Schuh M, Parlakian A, Mgrditchian T, Valnaud N, Joanne P, et al. Myofiber Androgen Receptor Promotes Maximal Mechanical Overload-Induced Muscle Hypertrophy and Fiber Type Transition in Male Mice. *Endocrinology* (2014) 155(12):4739–48. doi: 10.1210/en.2014-1195
39. Sheffield-Moore M, Paddon-Jones D, Casperson SL, Gilkison C, Volpi E, Wolf SE, et al. Androgen Therapy Induces Muscle Protein Anabolism in Older Women. *J Clin Endocrinol Metab* (2006) 91(10):3844–9. doi: 10.1210/jc.2006-0588
40. Nicoll JX, Fry AC, Mosier EM. Sex-Based Differences in Resting MAPK, Androgen, and Glucocorticoid Receptor Phosphorylation in Human Skeletal Muscle. *Steroids* (2019) 141:23–9. doi: 10.1016/j.steroids.2018.11.004
41. MacLean HE, Chiu WS, Notini AJ, Axell AM, Davey RA, McManus JF, et al. Impaired Skeletal Muscle Development and Function in Male, But Not Female, Genomic Androgen Receptor Knockout Mice. *FASEB J* (2008) 22 (8):2676–89. doi: 10.1096/fj.08-105726
42. Lakshman KM, Kaplan B, Travison TG, Basaria S, Knapp PE, Singh AB, et al. The Effects of Injected Testosterone Dose and Age on the Conversion of Testosterone to Estradiol and Dihydrotestosterone in Young and Older Men. *J Clin Endocrinol Metab* (2010) 95(8):3955–64. doi: 10.1210/jc.2010-0102
43. Bhasin S, Travison TG, Storer TW, Lakshman K, Kaushik M, Mazer NA, et al. Effect of Testosterone Supplementation With and Without a Dual 5alpha-Reductase Inhibitor on Fat-Free Mass in Men With Suppressed Testosterone Production: A Randomized Controlled Trial. *JAMA* (2012) 307(9):931–9. doi: 10.1001/jama.2012.227
44. Alexander SE, Pollock AC, Lamon S. The Effect of Sex Hormones on Skeletal Muscle Adaptation in Females. *Eur J Sport Sci* (2021), 1–11. doi: 10.1080/17461391.2021.1921854
45. Baehr LM, Tunzi M, Bodine SC. Muscle Hypertrophy Is Associated With Increases in Proteasome Activity That Is Independent of MuRF1 and MAFbx Expression. *Front Physiol* (2014) 5:69. doi: 10.3389/fphys.2014.00069
46. Tipton KD, Hamilton DL, Gallagher IJ. Assessing the Role of Muscle Protein Breakdown in Response to Nutrition and Exercise in Humans. *Sports Med* (2018) 48(Suppl 1):53–64. doi: 10.1007/s40279-017-0845-5
47. Sandri M. Autophagy in Skeletal Muscle. *FEBS Lett* (2010) 584(7):1411–6. doi: 10.1016/j.febslet.2010.01.056
48. Drake JC, Yan Z. Mitophagy in Maintaining Skeletal Muscle Mitochondrial Proteostasis and Metabolic Health With Ageing. *J Physiol* (2017) 595 (20):6391–9. doi: 10.1113/JP274337
49. Guan Y, Drake JC, Yan Z. Exercise-Induced Mitophagy in Skeletal Muscle and Heart. *Exerc Sport Sci Rev* (2019) 47(3):151–6. doi: 10.1249/JES.0000000000000192
50. Rossetti ML, Gordon BS. The Role of Androgens in the Regulation of Muscle Oxidative Capacity Following Aerobic Exercise Training. *Appl Physiol Nutr Metab* (2017) 42(9):1001–7. doi: 10.1139/apnm-2017-0230
51. Balan E, Schwalm C, Naslain D, Nielens H, Francaux M, Deldicque L. Regular Endurance Exercise Promotes Fission, Mitophagy, and Oxidative Phosphorylation in Human Skeletal Muscle Independently of Age. *Front Physiol* (2019) 10:1088. doi: 10.3389/fphys.2019.01088
52. Mesquita PHC, Lamb DA, Parry HA, Moore JH, Smith MA, Vann CG, et al. Acute and Chronic Effects of Resistance Training on Skeletal Muscle Markers of Mitochondrial Remodeling in Older Adults. *Physiol Rep* (2020) 8(15): e14526. doi: 10.14814/phy2.14526

Conflict of Interest: The authors declare that the research was conducted in the absence of any commercial or financial relationships that could be construed as a potential conflict of interest.

Publisher's Note: All claims expressed in this article are solely those of the authors and do not necessarily represent those of their affiliated organizations, or those of the publisher, the editors and the reviewers. Any product that may be evaluated in this article, or claim that may be made by its manufacturer, is not guaranteed or endorsed by the publisher.

frontiers | Frontiers in Endocrinology

ORIGINAL RESEARCH
published: 25 April 2022
doi: 10.3389/fendo.2022.871380

Additive Effect of Parathyroid Hormone and Zoledronate Acid on Prevention Particle Wears-Induced Implant Loosening by Promoting Periprosthetic Bone Architecture and Strength in an Ovariectomized Rat Model

Chenhe Zhou[1,2,3†], Yangxin Wang[1,2,3†], Jiahong Meng[1,2,3], Minjun Yao[1,2,3], Huikang Xu[4], Cong Wang[1,2,3], Fanggang Bi[5], Hanxiao Zhu[1,2,3], Guang Yang[1,2,3], Mingmin Shi[1,2,3], Shigui Yan[1,2,3*] and Haobo Wu[1,2,3*]*

[1] Department of Orthopedic Surgery, The Second Affiliated Hospital, Zhejiang University School of Medicine, Hangzhou, China, [2] Orthopedic Research Institute of Zhejiang University, Hangzhou, China, [3] Key Laboratory of Motor System Disease Research and Precision Therapy of Zhejiang Province, The Second Affiliated Hospital, Zhejiang University, Hangzhou, China, [4] State Key Laboratory for Diagnosis and Treatment of Infectious Diseases, National Clinical Research Center for Infectious Diseases, Collaborative Innovation Center for Diagnosis and Treatment of Infectious Diseases, The First Affiliated Hospital, College of Medicine, Zhejiang University, Hangzhou, China, [5] Department of Orthopaedic Surgery, The First Affiliated Hospital of Zhengzhou University, Zhengzhou, China

Implant-generated particle wears are considered as the major cause for the induction of implant loosening, which is more susceptible to patients with osteoporosis. Monotherapy with parathyroid hormone (PTH) or zoledronate acid (ZOL) has been proven efficient for preventing early-stage periprosthetic osteolysis, while the combination therapy with PTH and ZOL has exerted beneficial effects on the treatment of posterior lumbar vertebral fusion and disuse osteopenia. However, PTH and ZOL still have not been licensed for the treatment of implant loosening to date clinically. In this study, we have explored the effect of single or combined administration with PTH and ZOL on implant loosening in a rat model of osteoporosis. After 12 weeks of ovariectomized surgery, a femoral particle-induced periprosthetic osteolysis model was established. Vehicle, PTH (5 days per week), ZOL (100 mg/kg per week), or combination therapy was utilized for another 6 weeks before sacrifice, followed by micro-CT, histology, mechanical testing, and bone turnover examination. PTH monotherapy or combined PTH with ZOL exerted a protective effect on maintaining implant stability by elevating periprosthetic bone mass and inhibiting pseudomembrane formation. Moreover, an additive effect was observed when combining PTH with ZOL, resulting

OPEN ACCESS

Edited by:
Sadiq Umar,
University of Illinois at Chicago,
United States

Reviewed by:
Supriya Jagga,
Harvard Medical School,
United States
Mohd Salman,
University of Tennessee Health Science Center (UTHSC),
United States

***Correspondence:**
Haobo Wu
2505014@zju.edu.cn
Shigui Yan
zrjwsj@zju.edu.cn
Mingmin Shi
shimingmin@zju.edu.cn

†These authors have contributed equally to this work

Specialty section:
This article was submitted to Bone Research, a section of the journal Frontiers in Endocrinology

Received: 08 February 2022
Accepted: 16 March 2022
Published: 25 April 2022

Citation:
Zhou C, Wang Y, Meng J, Yao M, Xu H, Wang C, Bi F, Zhu H, Yang G, Shi M, Yan S and Wu H (2022) Additive Effect of Parathyroid Hormone and Zoledronate Acid on Prevention Particle Wears-Induced Implant Loosening by Promoting Periprosthetic Bone Architecture and Strength in an Ovariectomized Rat Model. Front. Endocrinol. 13:871380. doi: 10.3389/fendo.2022.871380

in better fixation strength, higher periprosthetic bone mass, and less pseudomembrane than PTH monotherapy. Taken together, our results suggested that a combination therapy of PTH and ZOL might be a promising approach for the intervention of early-stage implant loosening in patients with osteoporosis.

Keywords: implant loosening, osteolysis, osteoporosis, parathyroid hormone (1-34), zoledronate (ZOL)

INTRODUCTION

Arthroplasty has been widely utilized to improve the life quality of patients with end-stage osteoarthritis. However, the occurrence of complications still impacts some patients. Among those complications, implant failure is the most severe one, which might result in revision surgeries eventually. The survival rate of implants is reported to be only 71% at 20 years (1). Aseptic loosening, the major reason for arthroplasty failure, is caused by an inflammatory response to the debris generated from the prosthesis, leading to a promotion of periprosthetic bone loss and pseudomembrane formation, as well as a reduction of prosthesis stability (2, 3). So far, the only treatment for arthroplasty failure is revision surgery, which requires higher technical demand and higher costs but results in a higher complication rate and lower satisfaction rate (4, 5). In the meantime, there is also an essential concern that those patients with revision surgery are likely to be older and frailer, which might result in a higher surgical risk. Therefore, an effective tactic with minimal invasion to prevent prosthetic loosening is of great value.

As reported previously, over 50% of patients undergoing total hip arthroplasty (THA) are combined with osteoporosis (6). Nevertheless, osteoporosis has been proven to negatively regulate implant osseointegration and further increase prosthetic migration (7, 8). Moreover, poor bone quality also increases the prevalence of periprosthetic osteolysis. A study has shown that aseptic loosening is associated with low lumbar bone mineral density (BMD) (9). Additionally, more significant bone loss has been observed in the femoral component in female patients associated with low systemic BMD (10). Excessive osteoclast activities are confirmed to be responsible for both periprosthetic osteolysis and osteoporosis, which are characterized by increasing bone remodeling, especially increasing bone loss (11, 12). Due to the vital role of and similar mechanism with osteoporosis, the utilization of agents with a capacity of regulating bone remodeling has the potential to be an effective approach for implant-loosening prevention.

Many systemic antiosteoporotic agents have been tested to prevent implant loosening by inhibiting periprosthetic osteolysis or improving periprosthetic osseointegration (13). Bisphosphonates, generally regarded as the first-line treatment for osteoporosis, have been verified to demonstrate a beneficial effect on suppressing periprosthetic osteolysis in animal models (14, 15). A clinical study also confirmed that a single infusion of zoledronic acid (ZOL) could reduce the early implant migration in hip arthroplasty (16). Additionally, intermittent parathyroid hormone (PTH) 1-34 is another classical mediation for the treatment of osteoporosis, with the capacity of anabolic effects. Our and other research groups have revealed that intermittent PTH treatment could prevent particle-induced osteolysis *in vivo* (17–19). Recently, several cases reported that PTH has a protective effect on prosthetic loosening clinically (20–22). Therefore, both PTH and ZOL are promising to be therapeutic options for implant loosening. In addition, the combined use of PTH and ZOL has been found to have an additive-promoting effect in several animal models of skeletal diseases, such as posterior lumbar vertebral fusion in ovariectomized (OVX) rats and fracture healing (23, 24). However, to date, PTH and ZOL still have not been licensed to treat implant loosening. Also, bisphosphonate use was found to increase the incidence rate of periprosthetic fractures after THA in patients with normal bone quality (25). As the crucial role of osteoporosis mentioned above in implant loosening, it is reasonable and meaningful to detect the effects of approved antiosteoporotic agents, PTH and ZOL, on early-stage periprosthetic osteolysis in patients with poor bone quality. In this study, we established a particle-induced periprosthetic osteolysis model in OVX rats and further investigated and compared the effects of combined PTH and ZOL with monotherapy on preventing implant loosening.

METHOD AND MATERIALS

Preparation of Agents and Materials

PTH (1-34) was obtained from Bachem (Bubendorf, Switzerland) and dissolved at a concentration of 60 μg/ml with distilled water. ZOL (Sigma–Aldrich, St. Louis, MO, United States) was dissolved to 100 μg/ml with distilled water. Titanium (Ti) rods and the suspension of 30 mg Ti particles (Johnson Matthey, Ward Hill, MA, United States) were gained and prepared as reported in our previous study (26).

Animal Experiment

All animal care and the entire experiment protocols followed the Guide for the Care and Use of Laboratory Animal published by the United States National Institutes of Health and were approved by the Institutional Animal Care and Use Committee of the Second Affiliated Hospital, Zhejiang University School of Medicine. Female Sprague–Dawley (SD) rats were purchased from Shanghai SLAC Laboratory Animal Co. Ltd, (Shanghai, China) and were maintained in a room with a temperature of 24 ± 2°C, humidity of 60%, and light/dark cycle rhythm of 12 h. Animals were free to access to water and food with a number of two per cage. All rats were assessed every day for visual signs of pain, morbidity, or depression during the whole experiment period. Animals were

sacrificed humanely with symptoms above or an acute loss of 10% weight. All efforts we made in this study aimed to minimize the number of animals used and animal suffering.

A total of sixty-six female SD rats weighing 200–250 g were randomly assigned into the sham group (n=13) and OVXS group (n=53). All rats were anesthetized with an intraperitoneal injection of pentobarbital sodium (50 mg/kg). Both the sham surgery and OVX surgery were processed as we reported previously (27). Twelve weeks postoperatively, three rats in each group were selected randomly and sacrificed for radiological and histological analysis to confirm the successful establishment of the osteoporosis model.

The remaining sixty rats were used for the following experiment, including 10 in the sham group and 50 in the OVXS group. Ti rod implantation was performed in the remaining animals. Rats in the sham group were identified as the normal control (NC) group, while rats in the OVXS group were randomly divided into 5 groups (n=10 per group): the OVX group, O+T group, PTH group, ZOL group, and P+Z group. The rat model of implant loosening was established as we reported previously (26). Briefly, Ti rods were implanted into the medullary canal of distal femurs bilaterally after the injection of PBS or 30 mg Ti suspension in the canal. Postoperatively, intra-articular PBS or Ti particle suspension injection was performed at weeks 2 and 4. Ti particles were used in the O+T group, PTH group, ZOL group, and P+Z group, while vehicles were used in the other two groups. One week after surgery, rats were administrated with PTH (60 mg/kg 5 days per week, subcutaneous injection) in the PTH group, or with ZOL (100 μg/kg per week, intraperitoneal injection) in the ZOL group, or with combined PTH (60 mg/kg 5 days per week) and ZOL (100 μg/kg every week) in the P+Z group (combination therapy), and vehicle injection was used in the remaining three groups. After 6 weeks of treatment, rats were euthanasia with an overdose injection of pentobarbital sodium (90 mg/kg), and specimens were collected for further analysis, including biomechanical testing, X-ray examination, micro-CT, histomorphology, and bone turnover analysis. Subcutaneous injections of 10 mg/kg calcein green and 30 mg/kg alizarin red were performed 14 and 4 days before euthanasia, respectively.

X-Ray Examination and Micro-CT Analysis

Femurs were fixed in 4% (w/v) paraformaldehyde (PFA) for 48 h and used for X-ray examination and micro-CT analysis. X-ray examination was performed using 40 kV and 25 mAs to detect the general radiological manifestations. After X-ray examination, the specimens were subsequently transported for micro-CT scanning. A Scanco μCT100 instrument (Scanco Medical, Bassersdorf, Switzerland) was utilized at 14.8 μm isometric resolution. All parameters of micro-CT scanning and the selection of the region of interest (ROI) were referred to in our previous study (26). The data of bone mineral density (BMD) bone volume/total volume (BV/TV), bone surface/bone volume (BS/BV), connective density (Conn.D), structural model index (SMI), trabecular number (Tb.N), trabecular thickness (Tb.Th), and trabecular separation (Tb.Sp) were collected for quantitative analysis.

Histomorphological Analysis

Methylmethacrylate-embedded femurs were fixed in 70% alcohol and processed without demineralization as described before (28). Followed by being grounded to 50 μm thick slices, sample blocks were cut into 1 mm thick pieces *via* the cross-section using the IsoMet 5000 instrument (Buehler, Lake Bluff, IL, United States) and attached to plastic slides. Sections located 1 mm below the distal femoral growth plate were recorded under fluorescence microscopy (Leica DM5 500B; Leica Microsystems, Bensheim, Germany), and the parameters for bone formation were calculated with Image J software, including the mineral apposition rate (MAR) and mineral surface/bone surface (MS/BS).

Paraffin-embedded femurs were fixed in 4% PFA for 48 h and decalcified for 2 months in 10% (w/v) ethylene diamine tetraacetic acid (EDTA). Samples collected beyond implant-loosening surgery were cut along the coronal plane, and the others were sliced perpendicularly to the long axis after removing Ti rods. Five-micron-thick sections were cut in the similar region as methylmethacrylate-embedded samples above, followed by being performed with hematoxylin and eosin (H&E) and Masson and tartrate-resistant acid phosphatase (TRAP) staining as previously reported (26). The observation and measurement of samples were performed under light microscopy (Olympus BX51, Tokyo, Japan), and the histological images were evaluated by bone–implant contact (BIC), the ratio of bone area/total area (B.Ar/T.Ar), and mean thickness of the pseudomembrane according to our previous study (26).

Immunohistochemistry (IHC) staining was performed to detect the expression of osteocalcin (OCN) and receptor activator of NF-κB ligand (RANKL) around the Ti rods. The staining was processed according to the suggested protocol of an immunohistochemistry staining accessory kit (Boshide, Wuhan, China).

Bone Turnover Biomarkers

Before sacrifice, all rats fasted for 12 h. After anesthesia, blood was drawn from the abdominal aorta, and serum was subsequently obtained from the upper layer after blood centrifugation at 425× g for 5 min. Serum type I collagen cross-linked C-terminal telopeptide (CTX-1) and Gla-osteocalcin (GLA-OCN) levels were detected using Ratlaps (CTX-1) enzyme immunoassay (EIA) kit (Immunodiagnostic Systems Limited, Boldon, United Kingdom) and Rat Gla-Osteocalcin High Sensitive EIA Kit (TaKaRa Bio, Otsu, Japan) following the manufacturers' protocol, respectively.

Mechanical Testing

Femurs from each group were collected and stored at -20°C, covered with gauze soaked in normal saline. A biomechanical test was performed after specimens were melted completely at 4°C. All samples were prepared, and the subsequent pull-out testing was performed as shown in **Figure 2A** using a Zwick/Roell 2.5 material testing system (Zwick, Ulm, Germany), as we described previously (26). The maximum fixation strength (N) and stiffness (N/m) were recorded and analyzed from the load–displacement curve (29).

Statistical Analysis

All data were collected and analyzed by two independent researchers blinded to grouping and treatment. ROUT was conducted on the data to identify outliers with GraphPad Prism Version 9.0, and no data points were excluded. Results were shown as mean ± standard deviation (SD) and processed using GraphPad Prism Version 9.0 software. An unpaired t-test was used to analyze the differences between two groups, while one-way ANOVA with *post-hoc* Tukey's multiple comparison test was used to compare multiple groups. The values (*$p < 0.05$ and **$p < 0.01$) were set as the threshold of statistical significance.

RESULTS

Confirmation of Ovariectomized-Induced Osteoporosis Model

To validate whether osteoporosis was induced successfully, three rats from each group (the sham group and OVXS group) were selected randomly for analysis. As shown in **Figures 1A–C** and **Figure S1**, micro-CT and H&E staining data demonstrated a decreased bone mass in the OVXS group compared to the sham group (BMD: t=4.3, df 4, $p<0.05$; BV/TV: t=4.83, df 4, $p<0.01$). In addition, bodyweight elevation and uterus atrophy (t=4.964, df 4, $p<0.01$) further revealed that the OVX-induced osteoporosis model was established successfully (**Figures 1D–F**).

Preventive Effects of Combined Therapy and Monotherapy on Particle-Induced Implant Fixation

A biomechanical test was performed to investigate the effect of combination therapy and monotherapy on implant fixation stability. The results were presented as the maximal pull-out force and stiffness. As shown in **Figures 2C, D**, reduced maximal implant pull-out strength was observed in the OVX group compared to the NC group, while no difference was demonstrated in stiffness between the two groups. The lowest maximal implant pull-out strength and stiffness were found in the O+T group compared with the NC and OVX groups. These data indicated that the implant loosening model had been constructed based on the OVX model. After the treatment of PTH alone, or ZOL alone, or combination therapy, significantly improved implant fixation was manifested with increased maximal pull-out force (F=23.4, df 5 and 24, $p<0.01$) and stiffness (F=4.696, df 5 and 24, $p<0.01$) in the PTH group and P+Z group, whereas no difference but an increasing trend was found under ZOL alone (**Figures 2C, D**). Moreover, the combination therapy of PTH and ZOL demonstrated a better preventive effect on the maximal pull-

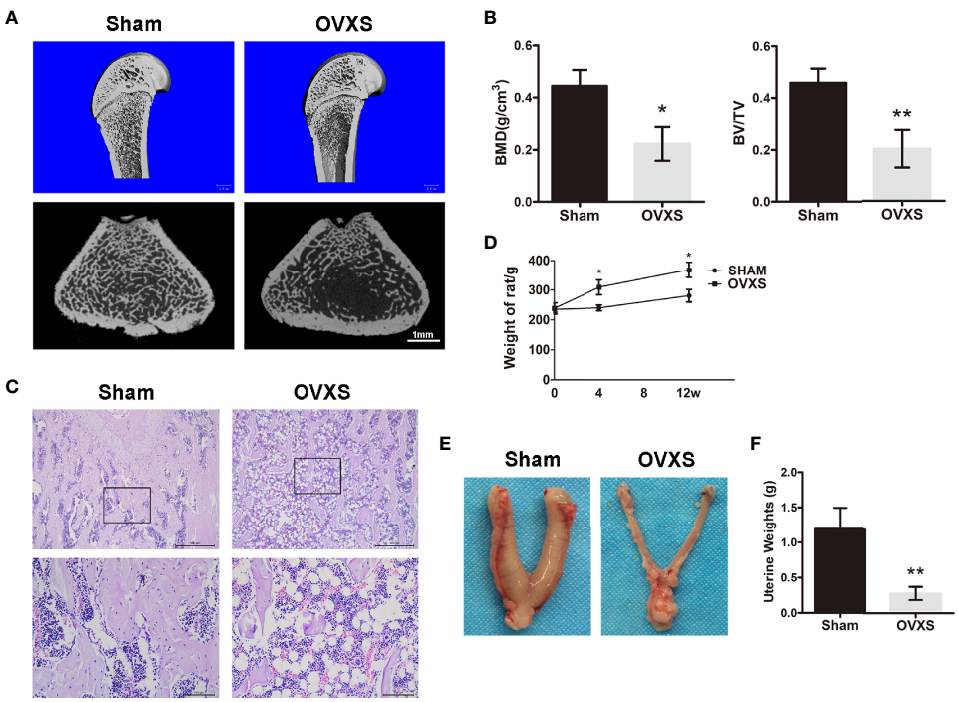

FIGURE 1 | The establishment of the OVX model was confirmed by radiological and histomorphological analysis. **(A)** The representative 3D and 2D micro-CT images of distal femurs were demonstrated from the sham group and the OVXS groups. **(B)** The BMD and BV/TV values of micro-CT images were quantified. **(C)** The representative images of H&E staining from both groups were performed. Upper ×40, lower ×200 magnification. Scale bar = 500 μm (upper) and 100 μm (lower). **(D)** The bodyweight of rats from 0 to 12 weeks after OVX in both groups. The representative images of the uterus **(E)** and weight **(F)** were obtained at the time of sacrifice in both groups. Values are expressed as mean ± SD, n=3; *$p<0.05$, **$p<0.01$, compared with the sham group.

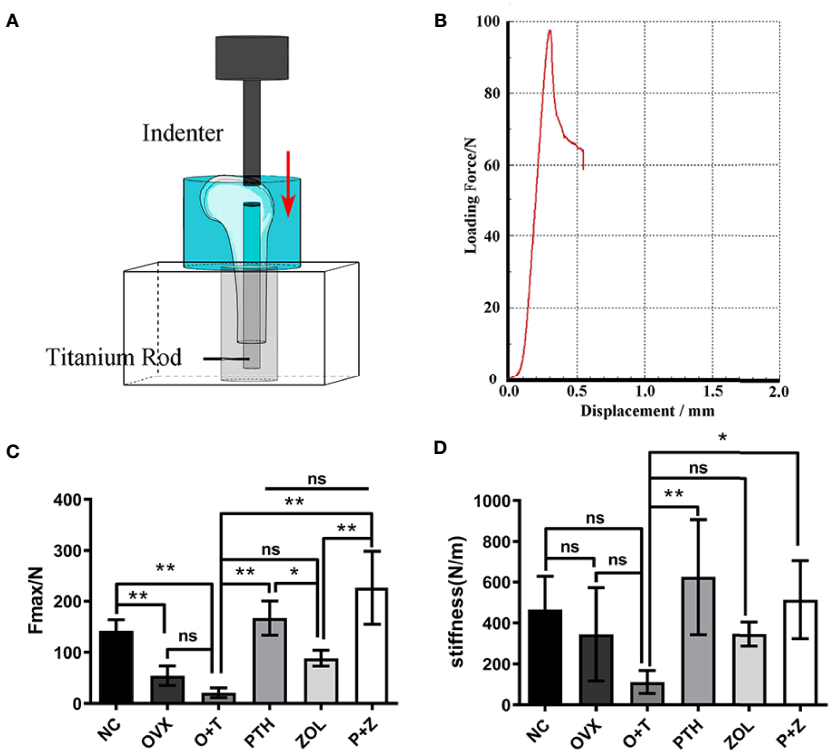

FIGURE 2 | The positive effects of combined or single treatment with PTH and ZOL on inhibiting particle-induced fixation strength loss of the implant in OVX rats. The schematic image of the biomechanical testing device **(A)** and the representative loading force–displacement curve **(B)** were displayed. The maximal fixation strength **(C)** and stiffness **(D)** of samples were collected and analyzed. Values expressed are means ± SD; *p < 0.05, n=5; **p < 0.01, significantly different compared between two groups. "ns", no significant difference.

out force than the ZOL group. However, no differences have been observed between combination therapy and PTH alone on the maximal pull-out strength. Also, combination therapy has not shown any differences in stiffness among PTH alone and ZOL alone mechanically.

Effects of Combined Therapy and Monotherapy on Blocking Periprosthetic Destruction of Bone Architecture

Radiological examinations were further utilized to explore the effects of combined therapy and monotherapy on bone architecture. General manifestations were demonstrated using X-ray examination. Implants were appropriately inserted into the medullary canals in **Figure 3A**, and noticeable bone mass loss and radiolucent regions were observed around the implant in the O+T group. After combination or monotherapy of PTH and ZOL, greater peri-implant bone mass in the distal femurs and reduced radiolucent lines were exhibited (**Figure 3A**).

To further confirm the therapeutic effects of combination and monotherapy, distal femurs were analyzed by micro-CT scanning. As revealed in **Figures 3B, C**, significantly decreased peri-implant bone mass was found in the OVX group in comparison with the NC group. Lower peri-implant bone mass in a trend was observed after Ti particle treatment in the OVX rats, compared to rats in the OVX group, according to 3D micro-CT-reconstructed images (**Figure 3B**). Notably, combination therapy and the monotherapy of PTH and ZOL significantly increased peri-implant bone mass, resulting in improved bone architecture (**Figure 3B**). The quantification of micro-CT scanning data was next performed and displayed as BMD, BV/TV, BS/BV, Conn.D, SMI, Tb.N, Tb.Th, and Tb.Sp. As indicated in **Figure 3C**, increased Tb.Sp was observed with the treatment of Ti particles in OVX rats. However, no considerable differences were found between the OVX group and the O+T group in BMD, BV/TV, Tb.N, Tb.Th, and Conn.D ($F=10.99$, df 5 and 24, $p<0.01$); a decreased trend could still be observed after the administration of Ti particles. In contrast, with the treatment of combined PTH and ZOL, or monotherapy, remarkable elevations were demonstrated in BMD ($F=21.15$, df 5 and 24, $p<0.01$), BV/TV ($F=39.03$, df 5 and 24, $p<0.01$), Tb.N ($F=18.77$, df 5 and 24, $p<0.01$) and Tb.Th ($F=55.72$, df 5 and 24, $p<0.01$), while BS/BV ($F=50.71$, df 5 and 24, $p<0.01$) and Tb.Sp ($F=24.90$, df 5 and 24, $p<0.01$)values were significantly decreased in comparison with those in the O+T group. Moreover, combined PTH and ZOL therapy exhibited a better preventive effect than PTH alone or ZOL alone on peri-implant bone loss, presented as greater enhancement in BMD, BV/TV, Tb.Th, and reduction in SMI ($F=28.87$, df 5 and 24, $p<0.01$). In addition, no differences

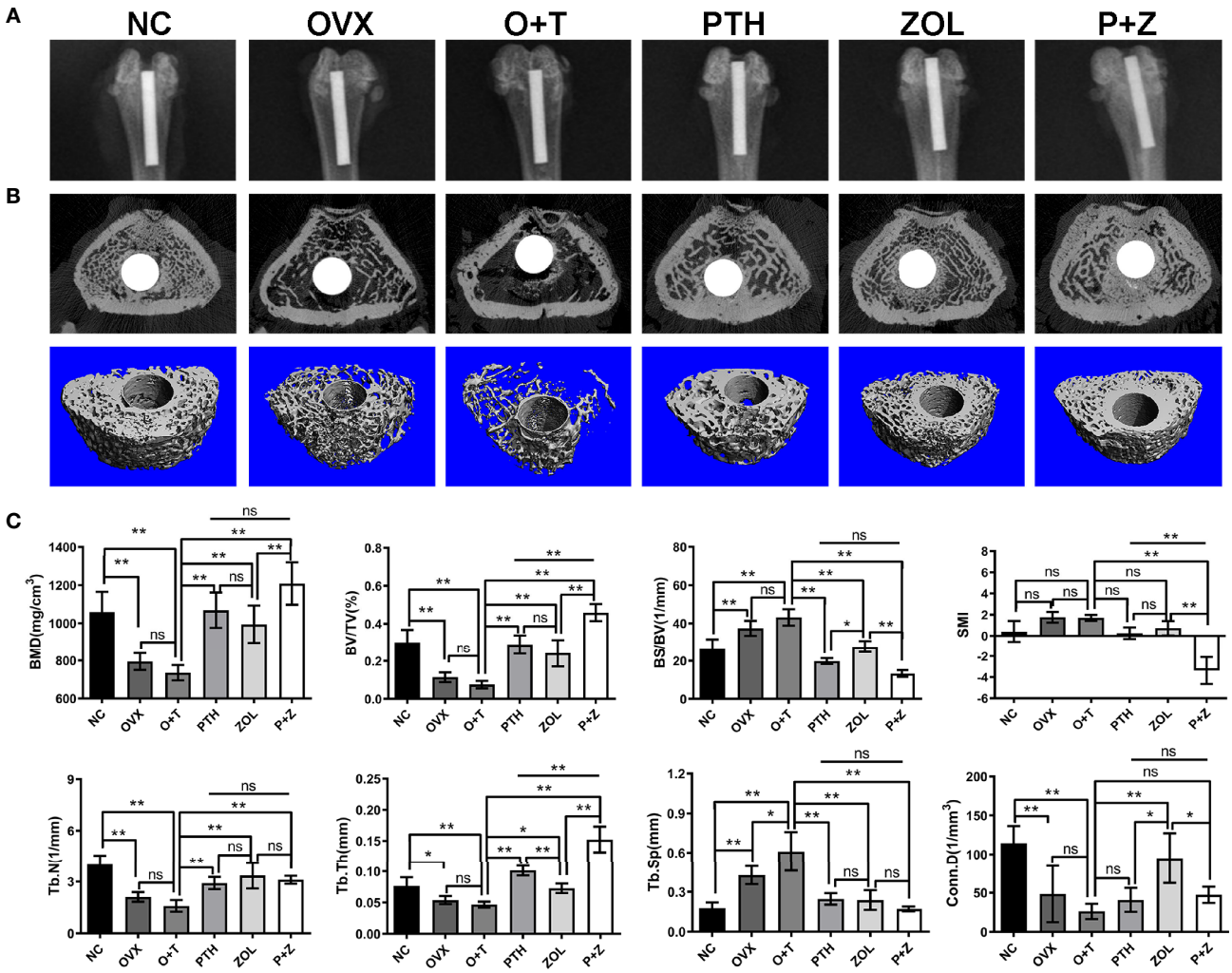

FIGURE 3 | The beneficial effect of combined therapy or monotherapy on preventing particles-induced peri-implant bone loss was observed radiologically in OVX rats. **(A)** The representative X-ray images from the NC, OVX, O+T, PTH, ZOL, and P+Z groups were exhibited. **(B)** The representative 3D and 2D micro-CT images of peri-implant bone mass in distal femurs were demonstrated from the six groups. **(C)** The quantification of the BMD, BV/TV, BS/BV, Conn.D, SMI, Tb.N, Tb.Th and Tb.Sp values was analyzed. Values expressed are means ± SD, n=5; *p < 0.05, **p < 0.01, significantly different compared between two groups. "ns", no significant difference.

were observed in most of the parameters in the comparison between the PTH group and the ZOL group, whereas higher BS/BV and Conn.D and lower Tb.Th were shown in the ZOL group (**Figure 3C**).

After decalcification, histological manifestations of peri-implant bone were assessed. **Figure 4** shows that diminished BIC ($F=255.07$, df 5 and 24, $p<0.01$) and B.Ar/T.Ar ($F=19.59$, df 5 and 24, $p<0.01$) were observed in the OVX group compared with the NC group, whereas a similar fibrous pseudomembrane formation was found in the two groups ($F=60.34$, df 5 and 24, $p<0.01$). Consistent with micro-CT results above, H&E staining and Masson staining revealed that less and thinner bone mass was exhibited around the implant in the O+T group, with abundant fibrous pseudomembrane formation and reduced bone-implant contact when compared with other groups (**Figure 4**). Restored trabecular bone and enhanced interface contact were observed after combination therapy and monotherapy, as well as decreased pseudomembrane appearance. Histomorphological quantification was further performed, confirming the results above. Moreover, pseudomembrane and BIC in the P+Z group were thinner than in the PTH group, while no difference was found between the ZOL and P+Z groups. In addition, no considerable differences were observed in B.Ar/T.Ar among these three groups (**Figure 4C**).

Effects of Combined Therapy and Monotherapy on Bone Formation and Bone Resorption

To investigate the effects of different treatments on bone formation, calcein green and alizarin red were injected successively before euthanasia. As a classical marker for bone

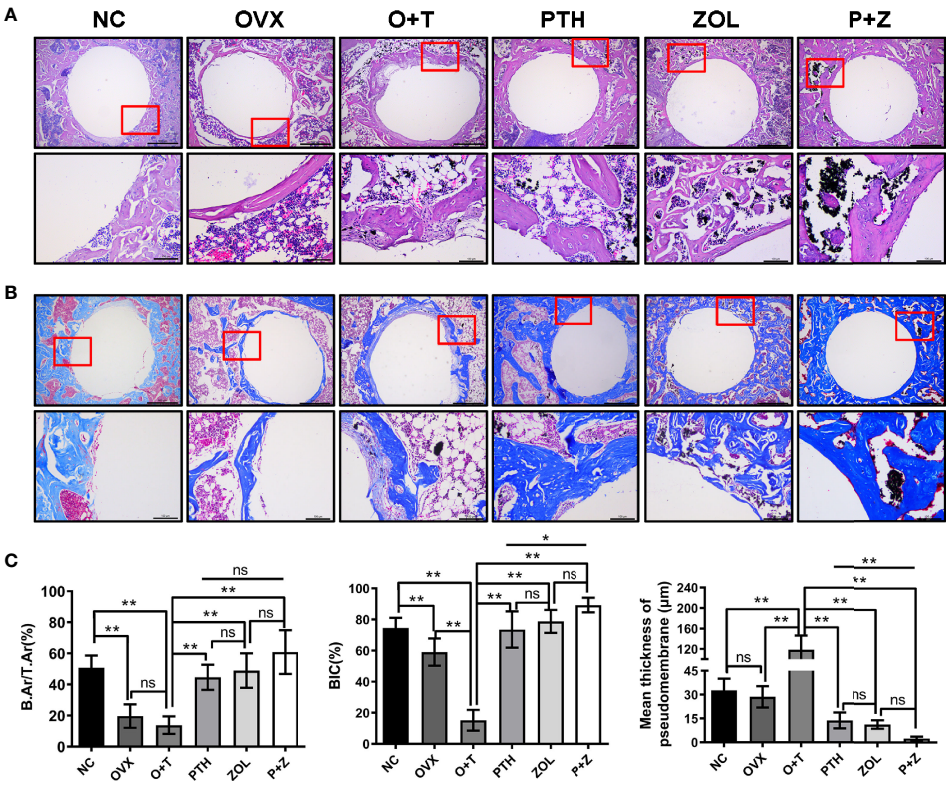

FIGURE 4 | Histomorphology of combined therapy or monotherapy on protecting particle-induced peri-implant osteolysis. **(A)** H&E staining (upper ×40, lower ×200 magnification) and **(B)** Masson staining (upper 40×, lower ×200 magnification) were used for the histological analysis. Scale bar= 500 μm (upper) and 100 μm (lower). **(C)** BIC, B.Ar/T.Ar, and mean thickness of the pseudomembrane were quantified. Values expressed are means ± SD, n=5; **p < 0.01, significantly different compared between two groups. "ns", no significant difference.

formation, double fluorescence labeling was visualized using undecalcified bone section, and MAR (F=12.19, df 5 and 24, p<0.01) and MS/BS (F=13.85, df 5 and 24, p<0.01) were quantified in all groups. As shown in **Figure 5A**, fewer labels were found in the NC group, OVX group, and O+T group than the other groups, whereas Ti particles with drug stimulation enhanced labels. Quantification data indicated no obvious differences in mineral apposition found among the NC, OVX, and O+T groups (**Figures 5C, D**). However, elevated MAR and MS/BS were observed in the PTH and P+Z groups compared to the O+T group, while declined MAR was found in the ZOL group. The immunochemistry staining of OCN further indicated that peri-implant osteoblast activities, inhibited by Ti particles, were reversed by the PTH treatment, with or without ZOL (**Figure 6**). Furthermore, a serum bone formation marker, GLA-OCN, was measured to evaluate the systemic effects of combined therapy and monotherapy (30). **Figure 7A** revealed that, compared with the O+T group, increased serum GLA-OCN levels (F=13.79, df 5 and 27, p<0.01) were found under PTH alone treatment, while ZOL monotherapy decreased the level, consistent with the fluorescence labeling results. Interestingly, no differences were observed between the O+T group and the P+Z group, unlike the mineral apposition data.

TRAP staining was used to examine the influence on periprosthetic osteoclast formation under different treatments. As presented in **Figures 5B**, **E, F**, no difference but an increasing trend of osteoclasts was found in the OVX group in comparison with the NC group. Ti particles significantly stimulated osteoclast formation in the OVX rats, resulting in the elevation of N.OC/BS (F=7.971, df 5 and 24, p<0.01) and OC.S/BS (F=9.520, df 5 and 24, p<0.01). However, a considerable inhibition on the osteoclast number and size was observed with the treatment of ZOL monotherapy, while no differences were demonstrated with combined therapy or PTH monotherapy. Due to the critical role RANKL plays during osteoclastogenesis, we investigated the expression of RANKL around the implants (31). An increased expression of RANKL was found in the peri-implant region in the O+T group, compared with that in the other groups, while combined or single treatment of PTH and ZOL reduced the expression (**Figure 6**). Moreover, serum CTX-1 levels (F=8.667, df 5 and 28, p<0.01) were measured to confirm this further. Unexpectedly, as shown in **Figure 7B**, Ti particle-induced serum CTX-1 level elevation was reversed by both single PTH and single ZOL treatment, whereas no changes were observed in the P+Z group.

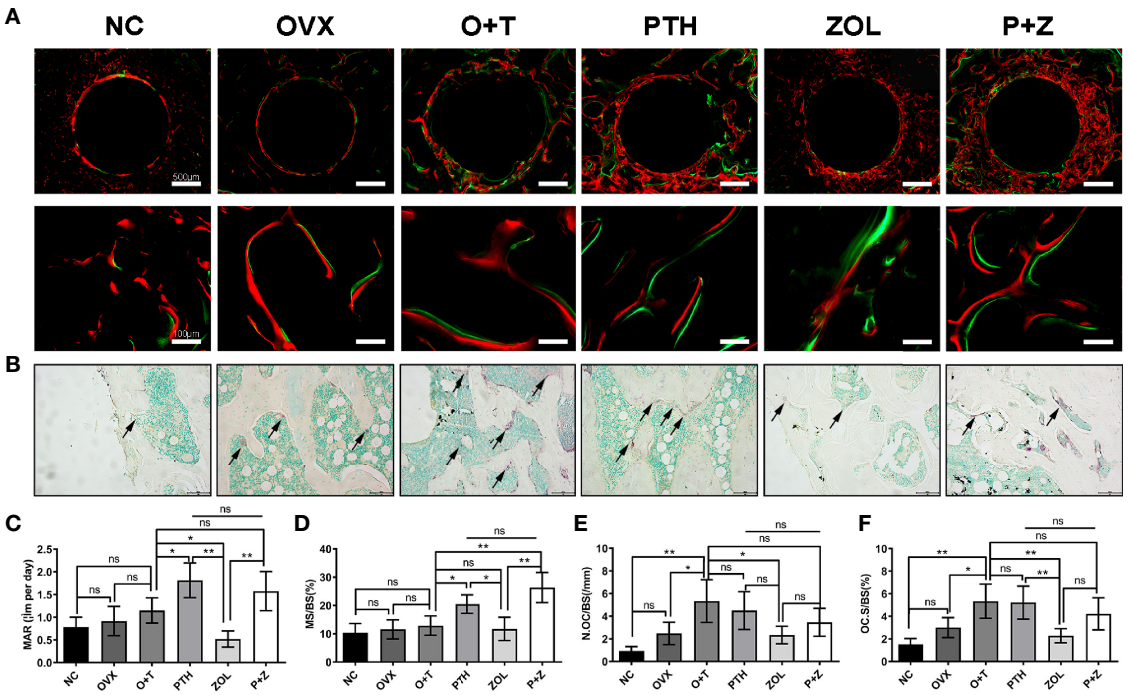

FIGURE 5 | Different effects of combined therapy or monotherapy on bone formation and osteoclast formation in the animal model. **(A)** Representative images of alizarin red (red) and calcein (green) labels were observed. **(B)** Representative images of TRAP staining were presented. The **(C)** MAR, **(D)** MS/BS, **(E)** N.Oc/BS and **(F)** OcS/BS were analyzed with sections. Values expressed are means ± SD, n=5; *p<0.05, **p<0.01, significantly different compared with the O+T group. "ns", no significant difference.

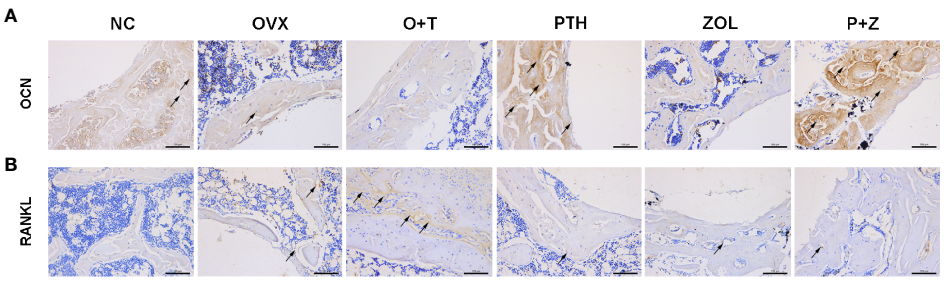

FIGURE 6 | The effects of combined therapy or monotherapy on the expression of OCN **(A)** and RANKL **(B)** in peri-implant bone. Representative IHC staining images of OCN and RANKL were visualized.

DISCUSSION

In the present study, the combined treatment and monotherapy of PTH and ZOL enhanced periprosthetic bone volume and bone-implant contact and intramedullary implant stability in a debris wear-induced periprosthetic osteolysis under a condition of osteoporosis. Moreover, combined PTH and ZOL therapy revealed an additive effect on preventing periprosthetic osteolysis and improving prosthetic anchorage, exhibiting a greater improvement than monotherapy, even similar or higher than the NC group. Thus, our findings indicated that combination or monotherapy with PTH and/or ZOL might be a promising strategy for preventing early-stage implant loosening in patients with severe osteoporosis.

Various strategies have been attempted to attenuate periprosthetic osteolysis and subsequently implant loosening, including prosthesis modification and systemic agent administration (13). Particularly, agents targeting at regulating bone metabolism have been found effective on implant loosening prevention in animal models, such as sclerostin antibody, alendronate (14, 29). Our group has previously proved the protective effect of intermittent PTH administration or weekly

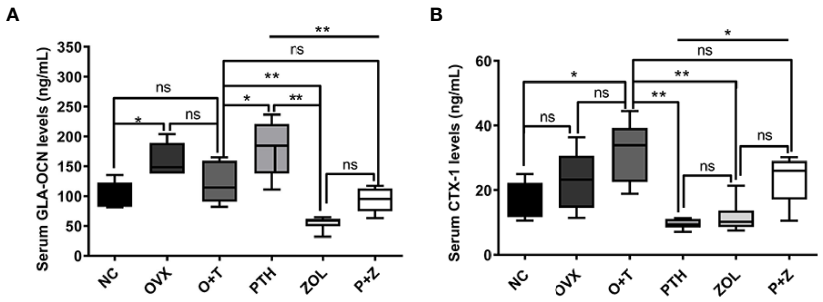

FIGURE 7 | The effects of combined or single treatment on serum levels of GLA-OCN and CTX-1 in the animal model. The serum levels of GLA-OCN **(A)** and CTX-1 **(B)** were measured using ELISA. Values expressed are means ± SD; n=5~6; *p<0.05, **p<0.01, significantly different compared between two groups. "ns", no significant difference.

ZOL injection on periprosthetic osteolysis, indicating that these were potential ways to prevent implant loosening (17, 19, 32). Additionally, clinical case reports and trials also provided evidence that agents (such as denosumab and PTH) inhibited periprosthetic bone loss and improved early-stage implant loosening after arthroplasty (20, 21, 33). However, considerable concern should be taken into account, as all these agents are only approved for osteoporosis treatment rather than the treatment of implant loosening. Osteoporosis has been found to increase the morbidity of implant loosening and accelerate the disease progression due to the poor periprosthetic bone quality (8, 9). In this study, we performed the OVX surgery 12 weeks before establishing the debris wear-induced periprosthetic osteolytic model. Female SD rats weighing 200–250 g are regarded as sexually mature preoperatively, in which bone remodeling prevails to bone modeling and is suitable for OVX surgery (34). Simultaneously, constant bone mass was reported to be observed in rats 12 weeks after OVX previously, with a significant bone loss, indicating that the animal model was approaching to aged- or postmenopausalrelated osteoporosis clinically (35). Reduced bone mass, atrophic uterus, and elevated weight observed 12 weeks after OVX surgery in our study certified the successful establishment of the animal model of osteoporosis, meeting the indications of anti-osteoporotic drugs. The subsequent surgery for implant loosening was performed based on the osteoporotic model afterward. A clinical study has shown that osteoporosis is found to be a comorbidity with aseptic loosening (9). Consistent with this clinical study, our research demonstrated that significantly decreased maximal pull-out force and peri-implant bone mass were observed in the OVX group, further confirming that osteoporosis might increase the chance of aseptic loosening. Moreover, a murine study proved that osteoporosis aggravated Ti particle-induced calvarial osteolysis *in vivo* (18). In our research, increased pseudomembrane and decreased BIC were observed between the OVX group and the O+T group, while no significant differences but downregulated trends were found in biomechanical strength and periprosthetic bone mass. The dense pseudomembrane formation and reduced bone contact confirmed that the periprosthetic osteolytic model has also been built successfully. By contrast, biomechanical strength and periprosthetic bone mass results exhibited no differences but reduced trends, which might be caused by 12-week OVX-induced severe bone loss. Although debris wears accelerated bone loss, it might attenuate the variation between the OVX groups with and without Ti particles.

ZOL, a representative bisphosphonate, serves as the first-line antiosteoporotic agent clinically worldwide. Several nationwide clinical studies clarified that bisphosphonate in patients with THA exhibited a lower risk for revision surgery, indicating that bisphosphonate use is encouraged in patients suffering from osteoporosis and candidates for THA (25, 36). Animal studies also proved that both local and system administrations of bisphosphonate displayed a capacity to prevent particle-induced osteolysis by diminishing bone loss and fiber formation (18, 19, 32). In this study, the systemic administration of ZOL has not improved implant anchorage compared with the O+T group. However, micro-CT and histological results demonstrated that periprosthetic bone loss induced by the synergistic effect of osteoporosis and particles was reversed markedly under ZOL treatment *via* manifesting the increased BMD, BV/TV, Tb.N, Tb.Th, and Conn.D, as well as reduced BS/BV and Tb.Sp. Inflammation and osteoclastic resorption play crucial roles in osteoporosis and particle-induced osteolysis, resulting in excessive bone destruction. ZOL has confirmed the suppressive effects on bone loss in several animal models, aiming to inhibit osteoclast differentiation and osteoclastic function and induce apoptosis by modulating the mevalonate pathway and diminishing adherence to osteoclast onto the bone surface (37, 38). According to those studies above, in our research, the obviously elevated number and size of osteoclasts were confirmed under the synergistic action of osteoporosis and periprosthetic osteolysis while they were impaired after ZOL treatment. Mechanically, RANKL initiates the activation of signaling cascades and drives osteoclast differentiation and function (39). Ramage et al. indicated that RANKL was highly expressed in fibroblast cells located at the periprosthetic membrane, regulating focalized bone resorption (40). Our IHC results showed the abundant expression of RANKL in the pseudomembrane, whereas ZOL administration attenuated RANKL expression in fibrous tissues. In addition, reduced fibrous pseudomembrane formation was observed under ZOL administration. Since bisphosphonates have not exhibited

inhibitory effects on wear debris-induced inflammation in a dog model and human specimens, the explanation was that ZOL decreased osteoclastic resorptive regions, which was presumably filled with fibrous tissues formed by ongoing inflammation-facilitated cell necrosis and fibrosis (41, 42). The inhibition of bone formation by ZOL has been reported previously that ZOL downregulates the proliferation, differentiation, maturation, and function of osteoblasts (23, 43). Our findings further demonstrated a similar result that ZOL reduced the bone formation rate and OCN expression in this animal model. Simultaneously, the serum level of GLA-OCN and CTX-1 further confirmed the suppressive effects of ZOL on both bone formation and bone resorption. Thus, our result demonstrated that ZOL could inhibit peri-implant bone loss but played a limited role in preventing implant loosening.

A considerable enhancement on implant fixation was exhibited under daily PTH treatment, compared with that in the O+T group, with improved stiffness and maximal pull-out force. Several studies from our group and other groups have exhibited beneficial effects on improving prosthetic fixation (17, 32, 44). Recently, some case reports also indicated the clinical efficacy of PTH on the improvement of early-stage implant loosening, with the disappearance of the radiographic line, which is consistent with our findings (20–22). Moreover, PTH showed a more substantial beneficial effect on the biomechanical test than ZOL in this study, which has been proven in other studies before (45). On the contrary, the local administration of ZOL contributed a better potential than PTH on the maximal push-out force in a rat model of initial stability, suggesting that different methods of administration might produce different efficiencies (44). Increased periprosthetic bone mass and decreased pseudomembrane formation are considered to contribute to the enhancement of implant stability (26). PTH is a commonly used anabolic agent on bone remodeling regulation, demonstrating accelerative effects on osteoblastic bone formation and osteoclastic resorption (46). Furthermore, intermittent administration of PTH has shown a greater promotive effect on bone formation than bone resorption, resulting in an elevation of bone mass (47). In this study, elevated trabecular bone and reduced periprosthetic fibrous membrane formed around the implants after PTH treatment, with a significantly raised bone formation rate. The presence of wear debris stimulates the process of chronic inflammation, which disrupts bone formation by impairing osteoblastic proliferation, differentiation, and maturation, as well as inducing apoptosis (48). PTH has been reported to enhance cell activity, prolong the lifespan, reduce the apoptosis of osteoblasts, and promote osteogenic differentiation of MSCs, which greatly supports our findings (49, 50). A higher expression of OCN in peri-implant bone and serum with PTH treatment further confirmed the anabolic effects on bone formation. In addition, less fibrous tissue was observed in the BIC region under PTH treatment, providing better contact between bone and the implant. This finding was consistent with the results reported in a previous study, in which the authors found that PTH exerted a suppressive effect on fibrosis (51).

The exact effects of combined administration with PTH and ZOL remain controversial. No additive effect of PTH and alendronate was exerted in the treatment of osteoporosis in men or postmenopausal women (52, 53); However, Cosman et al. found that the combination therapy of PTH (20 μg daily) and ZOL (5 mg per year) showed an additive effect and a substantial increments in the BMS of spine and hip (54). In addition, some animal studies also confirmed the beneficial effects of combination therapy on promoting implant fixation, preventing disuse-induced osteopenia, and improving posterior lumbar vertebral fusion, compared with PTH or ZOL monotherapy (23, 24, 44). Thus, we hypothesized that conjunctive use of PTH and ZOL exhibited a better preventive effect than PTH or ZOL alone on particle-induced implant loosening in a rat model with osteoporosis. In the present study, the combined PTH with ZOL was found to be effective in maintaining peri-implant bone mass and facilitating the stability of the implant, which is in accordance with the previous studies. Outstanding improvement of maximal pull-out force and stiffness was observed in the combination therapy group, with a similar efficiency with PTH alone but higher than in the ZOL and NC groups. The additive effect on bone mass raise was also exhibited in micro-CT and histomorphological results, along with significantly decreased pseudomembrane thickness. Nevertheless, the major concern is whether the anabolic effect of PTH would be blunted when combined with bisphosphonates (55). Our study demonstrated a similar anabolic effect with the PTH group, which is not impaired obviously by ZOL administration. On the other hand, ZOL-induced inhibition of osteoclasts was slightly counteracted by the utilization of PTH, which is confirmed by the serum results and TRAP staining, resulting in good bone homeostasis. Unexpectedly, the inhibited serum CTX-1 level by PTH or ZOL was reversed with the combination therapy at the level of the NC group. There is no plausible explanation for the interesting phenomenon. Taken together, the combination therapy of PTH and ZOL exerted a superior effect than monotherapy, with better fixation strength and peri-implant bone mass and restoring the bone turnover to the normal level.

Various cells are involved in the process of periprosthetic osteolysis, such as osteoclasts, osteoblasts, fibroblasts, and osteocytes. Osteoblasts and osteoclasts play crucial roles in regulating bone metabolism, and reactions were observed in osteoblasts and osteoclasts after particle wear stimulation during the process of prosthetic osteolysis. Chemokines and proinflammatory cytokines, including tumor necrosis factor (TNF)-α, interleukin (IL)-1β, IL-6, IL-11, and macrophage colony-stimulating factor (M-CSF), were secreted in the presence of debris wears, which is in response to an innate host immune stimulation, resulting in excessive osteoclast formation and activity (56, 57). RANKL-RANK-osteoprotegerin (OPG) axis plays an essential role in osteoclastogenesis, while TNF-α and IL-1β support the survival, differentiation, and activation of osteoclasts (58, 59). When RANKL binds to RANK, a series of downstream signaling cascades are initiated, including the ERK,

p38, JNK, and NF-κB pathways, subsequently promoting the auto-amplification of the nuclear factor of activated T cells, cytoplasmic, calcineurin-dependent 1 (NFATc1, the key molecule of osteoclastogenesis), resulting in osteoclastogenesis (26). ZOL has been widely used to treat osteoporosis with preventive effects on osteoclastogenesis. Inhibiting farnesyl diphosphate (FPP) synthase, a key enzyme of the mevalonate pathway, is generally considered the main molecular mechanism of ZOL on suppressing osteoclast formation antiresorptive potency (60). With a similar mechanism of osteoclastogenesis in periprosthetic osteolysis and osteoporosis, the suppression of the mevalonate pathway might also be the mechanism of ZOL on preventing periprosthetic osteolysis. In the meantime, osteoblast functions are impaired under particle wear stimulation, exhibiting supranuclear vacuolization, cell cycle arrest, and elevated DNA damage (61). Moreover, the adverse effects of viability, proliferation, adhesion, migration, osteogenic differentiation, and mineralization on osteoblasts were also observed in the presence of particle wear (48). In the mechanism, wnt/β-catenin and BMP/Smad signaling pathways were impaired by particles during osteogenic differentiation (62). In addition, OPG, secreted by osteoblasts, is found to be suppressed in periprosthetic osteolysis, resulting in the imbalance of OPG/RANK/RANKL axis (63). Teriparatide (PTH 1-34) has exhibited its capacity to improve bone formation *via* PKA (protein kinase A) and Wnt/b-catenin pathways and also stimulate OPG secretion (64). Here, we think that the Wnt/β-catenin pathways and OPG/RANK/RANKL axis might be involved in the mechanism of PTH-treated periprosthetic osteolysis by improving osteogenic differentiation, viability, proliferation, adhesion, and migration, as well as attenuating DNA damage.

Some limitations are worth being concerned to our study. Although polyethylene wear particles are considered the leading cause for implant loosening rather than metal particles, metal particles still play a role. They are confirmed to be effective during the initiation and process of peri-implant osteolysis *in vivo* and *in vitro* (65). Thus, we used Ti particles here to establish the animal model. In addition, the 6-week duration of particle-induced osteolysis could not represent the entire process of pathological changes. A study with a long period is needed further. Moreover, as the maximum treatment duration with PTH is approved to 24 months in lifespan and the withdrawal of PTH has been proven to lead to the deterioration of implant fixation in a particle-induced osteolytic model, it would be valuable to explore whether the usage of ZOL should be continued when withdrawing PTH, after a period of combined PTH with ZOL (32, 66).

In conclusion, Ti particles deteriorated implant fixation strength, along with periprosthetic bone loss and increased pseudomembrane formation in an OVX rat model. PTH monotherapy or combined PTH with ZOL exerted a protective effect on maintaining implant stability by elevating periprosthetic bone mass and inhibiting pseudomembrane formation *via* regulating bone metabolism. Moreover, an additive effect was observed when combining PTH with ZOL, resulting in better fixation strength, higher periprosthetic bone mass, and less pseudomembrane than PTH monotherapy. Taken together, our results suggested that combination therapy of PTH and ZOL might be a promising approach for the intervention of early-stage implant loosening in patients with osteoporosis.

DATA AVAILABILITY STATEMENT

The original contributions presented in the study are included in the article/**Supplementary Material**. Further inquiries can be directed to the corresponding authors.

ETHICS STATEMENT

The animal study was reviewed and approved by the Institutional Animal Care and Use Committee of the Second Affiliated Hospital of Zhejiang University School of Medicine.

AUTHOR CONTRIBUTIONS

CZ, SY, HW, and MS: designed the experiment. CZ, YW, JM, FB and HZ: performed the experiment. MY and HX: performed the measurement and analysis. CZ, GY, and CW: drafted the manuscript. CZ and MS: revised the manuscript. All authors contributed to the article and approved the submitted version.

FUNDING

This study was supported by research grants from Zhejiang Natural Science Foundation (No.LQ21H060006), the National Natural Science Foundation of China (No.82001461, No.81902279, No.82102628), and the fellowship of China Postdoctoral Science Foundation (No.2020M671758, No. 2021M692795).

SUPPLEMENTARY MATERIAL

The Supplementary Material for this article can be found online at: https://www.frontiersin.org/articles/10.3389/fendo.2022.871380/full#supplementary-material

REFERENCES

1. Wroblewski BM, Fleming PA, Siney PD. Charnley Low-Frictional Torque Arthroplasty of the Hip. 20-to-30 Year Results. *J Bone Joint Surg Br* (1999) 81 (3):427–30. doi: 10.1302/0301-620x.81b3.9521
2. Athanasou NA. The Pathobiology and Pathology of Aseptic Implant Failure. *Bone Joint Res* (2016) 5(5):162–8. doi: 10.1302/2046-3758.55.BJR-2016-0086
3. Holt G, Murnaghan C, Reilly J, Meek RM. The Biology of Aseptic Osteolysis. *Clin Orthop Relat Res* (2007) 460:240–52. doi: 10.1097/BLO.0b013e31804b4147

4. Eisler T, Svensson O, Tengstrom A, Elmstedt E. Patient Expectation and Satisfaction in Revision Total Hip Arthroplasty. *J Arthroplasty* (2002) 17 (4):457–62. doi: 10.1054/arth.2002.31245
5. Vanhegan IS, Malik AK, Jayakumar P, Ul Islam S, Haddad FS. A Financial Analysis of Revision Hip Arthroplasty: The Economic Burden in Relation to the National Tariff. *J Bone Joint Surg Br* (2012) 94(5):619–23. doi: 10.1302/0301-620X.94B5.27073
6. Lacko M, Schreierova D, Cellar R, Vasko G. [the Incidence of Osteopenia and Osteoporosis in Patients With Cementless Total Hip Arthroplasty]. *Acta Chir Orthop Traumatol Cech* (2015) 82(1):61–6.
7. Aro HT, Alm JJ, Moritz N, Makinen TJ, Lankinen P. Low Bmd Affects Initial Stability and Delays Stem Osseointegration in Cementless Total Hip Arthroplasty in Women: A 2-Year Rsa Study of 39 Patients. *Acta Orthop* (2012) 83(2):107–14. doi: 10.3109/17453674.2012.678798
8. Finnila S, Moritz N, Svedstro ME, Alm JJ, Aro HT. Increased Migration of Uncemented Acetabular Cups in Female Total Hip Arthroplasty Patients With Low Systemic Bone Mineral Density. A 2-Year Rsa and 8-Year Radiographic Follow-Up Study of 34 Patients. *Acta Orthop* (2016) 87 (1):48–54. doi: 10.3109/17453674.2015.1115312
9. Nixon M, Taylor G, Sheldon P, Iqbal SJ, Harper W. Does Bone Quality Predict Loosening of Cemented Total Hip Replacements? *J Bone Joint Surg Br* (2007) 89(10):1303–8. doi: 10.1302/0301-620X.89B10.19038
10. Lacko M, Schreierova D, Cellar R, Vasko G. [Bone Remodelling in the Proximal Femur After Uncemented Total Hip Arthroplasty in Patients With Osteoporosis]. *Acta Chir Orthop Traumatol Cech* (2015) 82(6):430–6.
11. Archibeck MJ, Jacobs JJ, Roebuck KA, Glant TT. The Basic Science of Periprosthetic Osteolysis. *Instr Course Lect* (2001) 50:185–95.
12. Raisz LG. Pathogenesis of Osteoporosis: Concepts, Conflicts, and Prospects. *J Clin Invest* (2005) 115(12):3318–25. doi: 10.1172/Jci27071
13. Apostu D, Lucaciu O, Berce C, Lucaciu D, Cosma D. Current Methods of Preventing Aseptic Loosening and Improving Osseointegration of Titanium Implants in Cementless Total Hip Arthroplasty: A Review. *J Int Med Res* (2018) 46(6):2104–19. doi: 10.1177/0300060517732697
14. Millett PJ, Allen MJ, Bostrom MP. Effects of Alendronate on Particle-Induced Osteolysis in a Rat Model. *J Bone Joint Surg Am* (2002) 84(2):236–49. doi: 10.2106/00004623-200202000-00011
15. Wise LM, Waldman SD, Kasra M, Cheung R, Binnington A, Kandel RA, et al. Effect of Zoledronate on Bone Quality in the Treatment of Aseptic Loosening of Hip Arthroplasty in the Dog. *Calcif Tissue Int* (2005) 77(6):367–75. doi: 10.1007/s00223-005-0062-3
16. Friedl G, Radl R, Stihsen C, Rehak P, Aigner R, Windhager R. The Effect of a Single Infusion of Zoledronic Acid on Early Implant Migration in Total Hip Arthroplasty. A Randomized, Double-Blind, Controlled Trial. *J Bone Joint Surg Am* (2009) 91(2):274–81. doi: 10.2106/JBJS.G.01193
17. Bi F, Shi Z, Zhou C, Liu A, Shen Y, Yan S. Intermittent Administration of Parathyroid Hormone [1-34] Prevents Particle-Induced Periprosthetic Osteolysis in a Rat Model. *PloS One* (2015) 10(10):e0139793. doi: 10.1371/journal.pone.0139793
18. Fu G, Li S, Ouyang N, Wu J, Li C, Liu W, et al. Antiresorptive Agents Are More Effective in Preventing Titanium Particle-Induced Calvarial Osteolysis in Ovariectomized Mice Than Anabolic Agents in Short-Term Administration. *Artif Organs* (2018) 42(9):E259–E71. doi: 10.1111/aor.13271
19. Wang P, Shang GQ, Xiang S, Zhang HN, Wang YZ, Xu H. Zoledronic Acid and Teriparatide Have a Complementary Therapeutic Effect on Aseptic Loosening in a Rabbit Model. *BMC Musculoskelet Disord* (2021) 22(1):580. doi: 10.1186/s12891-021-04458-4
20. Oteo-Alvaro A, Matas JA, Alonso-Farto JC. Teriparatide (Rh [1-34] Pth) Improved Osteointegration of a Hemiarthroplasty With Signs of Aseptic Loosening. *Orthopedics* (2011) 34(9):e574–7. doi: 10.3928/01477447-20110714-50
21. Suzuki T, Ryu K, Kojima K, Saito S, Nagaoka H, Tokuhashi Y. Teriparatide Treatment Improved Loosening of Cementless Total Knee Arthroplasty: A Case Report. *J Orthop Case Rep* (2017) 7(1):32–5. doi: 10.13107/jocr.2250-0685.676
22. Zati A, Sarti D, Malaguti MC, Pratelli L. Teriparatide in the Treatment of a Loose Hip Prosthesis. *J Rheumatol* (2011) 38(4):778–80. doi: 10.3899/jrheum.100980
23. Vegger JB, Nielsen ES, Bruel A, Thomsen JS. Additive Effect of Pth (1-34) and Zoledronate in the Prevention of Disuse Osteopenia in Rats. *Bone* (2014) 66:287–95. doi: 10.1016/j.bone.2014.06.020
24. Yishake M, Yasen M, Jiang L, Liu W, Xing R, Chen Q, et al. Effects of Combined Teriparatide and Zoledronic Acid on Posterior Lumbar Vertebral Fusion in an Aged Ovariectomized Rat Model of Osteopenia. *J Orthop Res* (2018) 36(3):937–44. doi: 10.1002/jor.23682
25. Khatod M, Inacio MCS, Dell RM, Bini SA, Paxton EW, Namba RS. Association of Bisphosphonate Use and Risk of Revision After Tha: Outcomes From a Us Total Joint Replacement Registry. *Clin Orthop Relat R* (2015) 473(11):3412–20. doi: 10.1007/s11999-015-4263-4
26. Zhou CH, Shi ZL, Meng JH, Hu B, Zhao CC, Yang YT, et al. Sophocarpine Attenuates Wear Particle-Induced Implant Loosening by Inhibiting Osteoclastogenesis and Bone Resorption *Via* Suppression of the Nf-Kappab Signalling Pathway in a Rat Model. *Br J Pharmacol* (2018) 175(6):859–76. doi: 10.1111/bph.14092
27. Zhou CH, Meng JH, Yang YT, Hu B, Hong JQ, Lv ZT, et al. Cepharanthine Prevents Estrogen Deficiency-Induced Bone Loss by Inhibiting Bone Resorption. *Front Pharmacol* (2018) 9:210. doi: 10.3389/fphar.2018.00210
28. Lotinun S, Kiviranta R, Matsubara T, Alzate JA, Neff L, Luth A, et al. Osteoclast-Specific Cathepsin K Deletion Stimulates S1p-Dependent Bone Formation. *J Clin Invest* (2013) 123(2):666–81. doi: 10.1172/JCI64840
29. Liu S, Virdi AS, Sena K, Sumner DR. Sclerostin Antibody Prevents Particle-Induced Implant Loosening by Stimulating Bone Formation and Inhibiting Bone Resorption in a Rat Model. *Arthritis Rheum* (2012) 64(12):4012–20. doi: 10.1002/art.37697
30. Li H, Zhou Q, Bai BL, Weng SJ, Wu ZY, Xie ZJ, et al. Effects of Combined Human Parathyroid Hormone (1-34) and Menaquinone-4 Treatment on the Interface of Hydroxyapatite-Coated Titanium Implants in the Femur of Osteoporotic Rats. *J Bone Miner Metab* (2018) 36(6):691–9. doi: 10.1007/s00774-017-0893-9
31. Kong YY, Feige U, Sarosi I, Bolon B, Tafuri A, Morony S, et al. Activated T Cells Regulate Bone Loss and Joint Destruction in Adjuvant Arthritis Through Osteoprotegerin Ligand. *Nature* (1999) 402(6759):304–9. doi: 10.1038/46303
32. Hu B, Wu H, Shi Z, Ying Z, Zhao X, Lin T, et al. Effects of Sequential Treatment With Intermittent Parathyroid Hormone and Zoledronic Acid on Particle-Induced Implant Loosening: Evidence From a Rat Model. *J Orthop Res* (2019) 37(7):1489–97. doi: 10.1002/jor.24217
33. Nystrom A, Kiritopoulos D, Ullmark G, Sorensen J, Petren-Mallmin M, Milbrink J, et al. Denosumab Prevents Early Periprosthetic Bone Loss After Uncemented Total Hip Arthroplasty: Results From a Randomized Placebo-Controlled Clinical Trial. *J Bone Miner Res* (2020) 35(2):239–47. doi: 10.1002/jbmr.3883
34. Thomas ML, Ibarra MJ. Developmental Changes in Duodenal Calcium Transport in Female Rats Related to Ovarian Hormone Status and Growth Rate. *Mech Ageing Dev* (1986) 37(3):221–9. doi: 10.1016/0047-6374(86)90039-4
35. Yamauchi H, Kushida K, Yamazaki K, Inoue T. Assessment of Spine Bone Mineral Density in Ovariectomized Rats Using Dxa. *J Bone Miner Res* (1995) 10(7):1033–9. doi: 10.1002/jbmr.5650100707
36. Thillemann TM, Pedersen AB, Mehnert F, Johnsen SP, Soballe K. Postoperative Use of Bisphosphonates and Risk of Revision After Primary Total Hip Arthroplasty: A Nationwide Population-Based Study. *Bone* (2010) 46(4):946–51. doi: 10.1016/j.bone.2010.01.377
37. Goodman SB, Trindade M, Ma T, Genovese M, Smith RL. Pharmacologic Modulation of Periprosthetic Osteolysis. *Clin Orthop Relat Res* (2005) 430):39–45. doi: 10.1097/01.blo.0000149998.88218.05
38. Luckman SP, Hughes DE, Coxon FP, Graham R, Russell G, Rogers MJ. Nitrogen-Containing Bisphosphonates Inhibit the Mevalonate Pathway and Prevent Post-Translational Prenylation of Gtp-Binding Proteins, Including Ras. *J Bone Miner Res* (1998) 13(4):581–9. doi: 10.1359/jbmr.1998.13.4.581
39. Boyle WJ, Simonet WS, Lacey DL. Osteoclast Differentiation and Activation. *Nature* (2003) 423(6937):337–42. doi: 10.1038/nature01658
40. Ramage SC, Urban NH, Jiranek WA, Maiti A, Beckman MJ. Expression of Rankl in Osteolytic Membranes: Association With Fibroblastic Cell Markers. *J Bone Joint Surg Am* (2007) 89(4):841–8. doi: 10.2106/JBJS.F.00655
41. Shanbhag AS, Hasselman CT, Rubash HE. The John Charnley Award. Inhibition of Wear Debris Mediated Osteolysis in a Canine Total Hip Arthroplasty Model. *Clin Orthop Relat Res* (1997) 344):33–43. doi: 10.1097/00003086-199711000-00005

42. Holt G, Reilly J, Meek RM. Effect of Alendronate on Pseudomembrane Cytokine Expression in Patients With Aseptic Osteolysis. *J Arthroplasty* (2010) 25(6):958–63. doi: 10.1016/j.arth.2009.07.029
43. Goodman SB, Gallo J. Periprosthetic Osteolysis: Mechanisms, Prevention and Treatment. *J Clin Med* (2019) 8(12). doi: 10.3390/jcm8122091
44. Li YF, Li XD, Bao CY, Chen QM, Zhang H, Hu J. Promotion of Peri-Implant Bone Healing by Systemically Administered Parathyroid Hormone (1-34) and Zoledronic Acid Adsorbed Onto the Implant Surface. *Osteoporos Int* (2013) 24(3):1063–71. doi: 10.1007/s00198-012-2258-5
45. Aspenberg P, Wermelin K, Tengwall P, Fahlgren A. Additive Effects of Pth and Bisphosphonates on the Bone Healing Response to Metaphyseal Implants in Rats. *Acta Orthop* (2008) 79(1):111–5. doi: 10.1080/17453670710014851
46. Qin L, Raggatt LJ, Partridge NC. Parathyroid Hormone: A Double-Edged Sword for Bone Metabolism. *Trends Endocrinol Metab* (2004) 15(2):60–5. doi: 10.1016/j.tem.2004.01.006
47. Liu CC, Kalu DN. Human Parathyroid Hormone-(1-34) Prevents Bone Loss and Augments Bone Formation in Sexually Mature Ovariectomized Rats. *J Bone Miner Res* (1990) 5(9):973–82. doi: 10.1002/jbmr.5650050911
48. Zhang L, Haddouti EM, Welle K, Burger C, Wirtz DC, Schildberg FA, et al. The Effects of Biomaterial Implant Wear Debris on Osteoblasts. *Front Cell Dev Biol* (2020) 8:352. doi: 10.3389/fcell.2020.00352
49. Jilka RL, Weinstein RS, Bellido T, Roberson P, Parfitt AM, Manolagas SC. Increased Bone Formation by Prevention of Osteoblast Apoptosis With Parathyroid Hormone. *J Clin Invest* (1999) 104(4):439–46. doi: 10.1172/JCI6610
50. Yu B, Zhao X, Yang C, Crane J, Xian L, Lu W, et al. Parathyroid Hormone Induces Differentiation of Mesenchymal Stromal/Stem Cells by Enhancing Bone Morphogenetic Protein Signaling. *J Bone Miner Res* (2012) 27(9):2001–14. doi: 10.1002/jbmr.1663
51. Dhillon RS, Xie C, Tyler W, Calvi LM, Awad HA, Zuscik MJ, et al. Pth-Enhanced Structural Allograft Healing Is Associated With Decreased Angiopoietin-2-Mediated Arteriogenesis, Mast Cell Accumulation, and Fibrosis. *J Bone Miner Res* (2013) 28(3):586–97. doi: 10.1002/jbmr.1765
52. Black DM, Greenspan SL, Ensrud KE, Palermo L, McGowan JA, Lang TF, et al. The Effects of Parathyroid Hormone and Alendronate Alone or in Combination in Postmenopausal Osteoporosis. *New Engl J Med* (2003) 349(13):1207–15. doi: 10.1056/NEJMoa031975
53. Finkelstein JS, Hayes A, Hunzelman JL, Wyland JJ, Lee H, Neer RM. The Effects of Parathyroid Hormone, Alendronate, or Both in Men With Osteoporosis. *New Engl J Med* (2003) 349(13):1216–26. doi: 10.1056/NEJMoa035725
54. Cosman F, Eriksen EF, Recknor C, Miller PD, Guanabens N, Kasperk C, et al. Effects of Intravenous Zoledronic Acid Plus Subcutaneous Teriparatide [Rhpth(1-34)] in Postmenopausal Osteoporosis. *J Bone Mineral Res* (2011) 26(3):503–11. doi: 10.1002/jbmr.238
55. Wu X, Pang L, Lei W, Lu W, Li J, Li Z, et al. Inhibition of Sca-1-Positive Skeletal Stem Cell Recruitment by Alendronate Blunts the Anabolic Effects of Parathyroid Hormone on Bone Remodeling. *Cell Stem Cell* (2010) 7(5):571–80. doi: 10.1016/j.stem.2010.09.012
56. Gallo J, Goodman SB, Konttinen YT, Raska M. Particle Disease: Biologic Mechanisms of Periprosthetic Osteolysis in Total Hip Arthroplasty. *Innate Immun* (2013) 19(2):213–24. doi: 10.1177/1753425912451779
57. Drees P, Eckardt A, Gay RE, Gay S, Huber LC. Mechanisms of Disease: Molecular Insights Into Aseptic Loosening of Orthopedic Implants. *Nat Clin Pract Rheum* (2007) 3(3):165–71. doi: 10.1038/ncprheum0428
58. Boyce BF, Rosenberg E, de Papp AE, Duong LT. The Osteoclast, Bone Remodelling and Treatment of Metabolic Bone Disease. *Eur J Clin Invest* (2012) 42(12):1332–41. doi: 10.1111/j.1365-2362.2012.02717.x
59. Crotti TN, Smith MD, Findlay DM, Zreiqat H, Ahern MJ, Weedon H, et al. Factors Regulating Osteoclast Formation in Human Tissues Adjacent to Peri-Implant Bone Loss: Expression of Receptor Activator Nf Kappa B, Rank Ligand and Osteoprotegerin. *Biomaterials* (2004) 25(4):565–73. doi: 10.1016/S0142-9612(03)00556-8
60. Roelofs AJ, Thompson K, Gordon S, Rogers MJ. Molecular Mechanisms of Action of Bisphosphonates: Current Status. *Clin Cancer Res* (2006) 12(20 Pt 2):6222s–30s. doi: 10.1158/1078-0432.CCR-06-0843
61. Ribeiro AR, Gemini-Piperni S, Travassos R, Lemgruber L, Silva RC, Rossi AL, et al. Trojan-Like Internalization of Anatase Titanium Dioxide Nanoparticles by Human Osteoblast Cells. *Sci Rep* (2016) 6:23615. doi: 10.1038/srep23615
62. Nam JS, Sharma AR, Jagga S, Lee DH, Sharma G, Nguyen LT, et al. Suppression of Osteogenic Activity by Regulation of Wnt and Bmp Signaling During Titanium Particle Induced Osteolysis. *J BioMed Mater Res A* (2017) 105(3):912–26. doi: 10.1002/jbm.a.36004
63. Granchi D, Amato I, Battistelli L, Ciapetti G, Pagani S, Avnet S, et al. Molecular Basis of Osteoclastogenesis Induced by Osteoblasts Exposed to Wear Particles. *Biomaterials* (2005) 26(15):2371–9. doi: 10.1016/j.biomaterials.2004.07.045
64. Tian Y, Xu Y, Fu Q, He M. Parathyroid Hormone Regulates Osteoblast Differentiation in a Wnt/Beta-Catenin-Dependent Manner. *Mol Cell Biochem* (2011) 355(1-2):211–6. doi: 10.1007/s11010-011-0856-8
65. Hirakawa K, Bauer TW, Stulberg BN, Wilde AH. Comparison and Quantitation of Wear Debris of Failed Total Hip and Total Knee Arthroplasty. *J BioMed Mater Res* (1996) 31(2):257–63. doi: 10.1002/(SICI)1097-4636(199606)31:2<257::AID-JBM13>3.0.CO;2-I
66. Compston JE, McClung MR, Leslie WD. Osteoporosis. *Lancet* (2019) 393(10169):364–76. doi: 10.1016/S0140-6736(18)32112-3

Conflict of Interest: The authors declare that the research was conducted in the absence of any commercial or financial relationships that could be construed as a potential conflict of interest.

frontiers | Frontiers in Endocrinology

ORIGINAL RESEARCH
published: 20 May 2022
doi: 10.3389/fendo.2022.891217

Association of Sex Hormones and Sex Hormone-Binding Globulin Levels With Bone Mineral Density in Adolescents Aged 12–19 Years

Ke Xu[1,2†], *Yicheng Fu*[3†], *Buzi Cao*[4] *and Mingyi Zhao*[1*]

[1] Department of Pediatrics, The Third Xiangya Hospital, Central South University, Changsha, China, [2] Xiangya School of Medicine, Central South University, Changsha, China, [3] Department of Pediatrics, Wuhan University Renmin Hospital, Wuhan University, Wuhan, China, [4] Medical School, Hunan Normal University, Changsha, China

Background: Sex hormones are recognized to play a significant role in increasing bone mineral density (BMD) and promoting bone maturation during adolescence. The purpose of our study was to use a database with large population data to evaluate the association of BMD with sex hormones (including testosterone and estradiol) and sex hormone-binding globulin (SHBG) in adolescent boys and girls aged 12–19 years.

Methods: The data for our study were taken from the National Health and Nutrition Examination Survey 2013-2016, and we used weighted multiple linear regression models to assess the relationship between testosterone, estradiol, and SHBG and total BMD. We use weighted generalized additive models and smooth curve fitting to discover underlying nonlinear relationships.

Results: A total of 1648 teenagers (853 boys, 795 girls) were selected for the final analysis. In boys, testosterone and estradiol levels were positively associated with total BMD, whereas SHBG levels were negatively associated with total BMD after adjusting for covariates [$P < 0.05$; 95% confidence interval (CI)]. In addition, there was a point between estradiol and total BMD, after which the positive correlation between estradiol and total BMD was relatively insignificant in boys. In girls, there was a positive association between estradiol and total BMD ($P < 0.05$; 95% CI), but there was no significant association between the testosterone (β 0.0004; 95% CI -0.0001 to 0.0008) or SHBG (β -0.0001; 95% CI -0.0002 to 0.0001) levels and total BMD. We also found an inverted U-shaped association between testosterone and total BMD with the inflection point at 25.4 ng/dL of testosterone.

OPEN ACCESS

Edited by:
Sadiq Umar, University of Illinois at Chicago, United States

Reviewed by:
Mohd Salman, University of Tennessee Health Science Center (UTHSC), United States
Mohammad Faraz Zafeer, University of Miami, United States
Md Zahid Akhter, University of Illinois at Chicago, United States

***Correspondence:**
Mingyi Zhao
zhao_mingyi@csu.edu.cn

†These authors have contributed equally to this work and share first authorship

Specialty section:
This article was submitted to Bone Research, a section of the journal Frontiers in Endocrinology

Received: *07 March 2022*
Accepted: *19 April 2022*
Published: *20 May 2022*

Citation:
Xu K, Fu Y, Cao B and Zhao M (2022) Association of Sex Hormones and Sex Hormone-Binding Globulin Levels With Bone Mineral Density in Adolescents Aged 12–19 Years. Front. Endocrinol. 13:891217. doi: 10.3389/fendo.2022.891217

Conclusions: We found differences in the association of sex hormones with total BMD in boys and girls. Based on our findings, an appropriate increase in serum testosterone levels may be beneficial for skeletal development in girls because of the inverted U-shaped relationship (with the inflection point at 25.4 ng/dL of testosterone), and a high testosterone level might be detrimental to BMD. Furthermore, keeping estradiol levels below a certain level in boys (24.3 pg/mL) may be considered.

Keywords: sex hormones, testosterone, estradiol, sex hormone-binding globulin, adolescents, bone mineral density

INTRODUCTION

Osteoporosis is a major public health issue that threatens the health of millions of people globally (1). It is characterized by very low bone mass and destruction of the microstructure of the bone, which greatly increases the risk of fracture. It is well known that adolescence is an important period of bone growth, development, and maturation. During adolescence, bone builds up and grows rapidly. By the end of puberty, the bone mass approaches approximately 90% of the adult peak bone mass (2). Obtaining a higher bone mineral density (BMD) during adolescence is essential for bone mass gain and bone maturation to achieve a higher peak bone mass for prevention of osteoporosis in old age (3).

Sex hormones and growth hormone (GH) are the main determinants of BMD, and sex hormones are recognized to play a significant role in increasing BMD and promoting bone maturation during adolescence. Estrogens modulate changes in bone geometry during puberty and stimulate periosteal bone deposition while inhibiting cortical bone resorption (4). Testosterones increase bone diameter by increasing periosteal apposition (5). A marked increase in sex hormone levels occurs during puberty, as boys and girls develop differences in their skeletal development owing to the differences in sex hormone levels in their bodies.

Sex hormone-binding globulin (SHBG) is synthesized by the liver and released into the bloodstream, where it regulates the bioavailability of sex hormones by binding to them (6). Studies have thus far evaluated the association of SHBG with BMD in adults, postmenopausal women, and older adults (7–9). However, the association in adolescent boys and girls remains inconclusive. The purpose of our study was to use a database with large population data to evaluate the association of BMD with sex hormones (including testosterone and estradiol) and SHBG in adolescent boys and girls aged 12–19 years.

MATERIALS AND METHODS

Data Source

The National Health and Nutrition Examination Survey (NHANES) is a large, population-based cross-sectional survey aimed at gathering information on the health and nutrition of the general American population. The National Center for Health Statistics (NCHS) authorized and conducted these surveys.

The data for our study were gathered from the NHANES 2013-2016. The population of this study was restricted to adolescents aged 12–19 years. After filtering according to the flow chart (**Figure 1**), 1648 participants (853 boys, 795 girls) aged 12–19 years were selected for the final analysis.

The NHANES was approved by the NCHS Ethical Review Board, and informed consent was obtained from all participants. For those under the age of 18, informed consent was provided by their parents/guardians and those aged 18 and over provided their own consent.

Study Variables

The exposure variables of this study were testosterone, estradiol and SHBG levels. Testosterone and estradiol were measured by isotope dilution liquid chromatography tandem mass spectrometry (ID-LC–MS/MS). SHBG was measured based on its reaction with immuno-antibodies and chemo-luminescence. The outcome variable was total BMD, which was measured using dual-energy X-ray absorptiometry. The following categorical variables were included in our analysis as covariates: race and moderate activities. The continuous covariates in our study were as follows: age, body mass index, the family income-to-poverty ratio, and blood urea nitrogen, serum uric acid, total protein, total cholesterol, serum phosphorus, and serum calcium levels. The family income-to-poverty ratio was calculated by dividing the annual family income by the poverty guideline. More information on testosterone, estradiol, SHBG, total BMD and all covariates can be found at https://www.cdc.gov/nchs/nhanes/.

Statistical Analyses

All analyses were calculated based on the weights of the NHANES samples. The participants in the study were divided into quartiles based on testosterone, estradiol or SHBG levels. In accordance with the Strengthening the Reporting of Observational Studies in Epidemiology (STROBE) statement (10), we developed three models: Model 1: no covariates were adjusted; Model 2: age and race were adjusted; and Model 3: all covariates were adjusted. We assessed the independent association of testosterone, estradiol, and SHBG with total BMD separately using weighted multiple linear regression models. We revealed underlying nonlinear associations by using weighted generalized additive models and smooth curve fitting. In addition, we used a two-piecewise linear regression model to calculate the threshold effects when nonlinear associations existed.

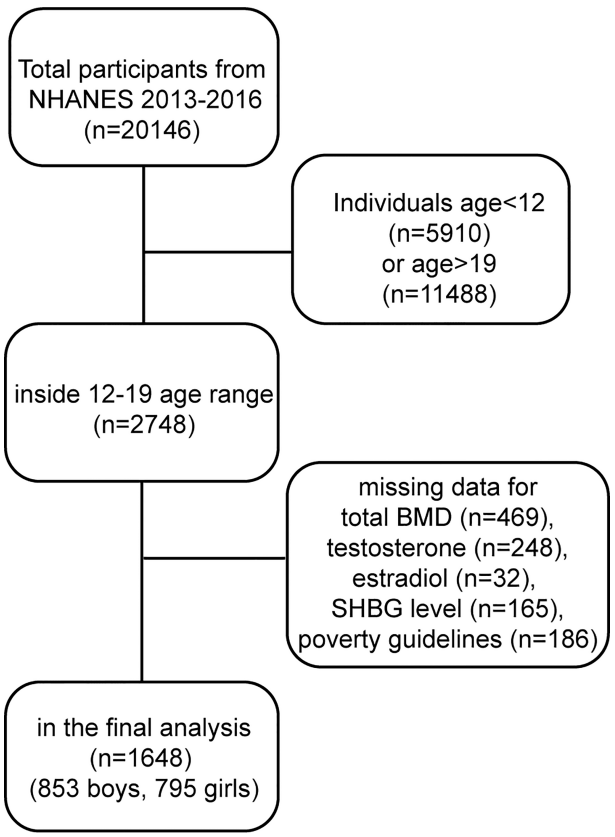

FIGURE 1 | Research flow chart.

The continuous and categorical variables are presented as the mean ± standard deviation and percentage, respectively. The statistical significance was set at P<0.05 for this study. All statistical analyses were carried out by EmpowerStats software (http://www.empowerstats.com) and R software (version 3.4.3).

RESULTS

Tables 1, **2** show the descriptions of the sociodemographic and medical characteristics of boys and girls, respectively. In **Table 1**, we divided the testosterone, estradiol and SHBG levels of 853 boys into quartiles (Q1-Q4; from Q1 to Q4, the levels gradually increase). For testosterone levels, boys with higher testosterone levels had higher levels of total BMD than boys in the Q1 group. For estradiol levels, from Q1 to Q4, estradiol levels increased, with a corresponding increase in total BMD levels. However, this trend was reversed for SHBG levels, and boys with higher SHBG levels had lower total BMD levels. In **Table 2**, the testosterone, estradiol and SHBG levels of 795 girls were divided into quartiles. For testosterone levels, girls with higher testosterone levels had higher total BMD levels. For estradiol levels, girls in the Q2 group had the lowest total BMD. Among the SHBG level groups, the total BMD level was lowest in the Q3 group.

Association Between Testosterone and Total BMD

In boys (**Table 3**; **Figure 2**), the association between testosterone and total BMD was positive in all three regression models (**Table 3**): Model 1 [0.0003 (0.0002, 0.0003)]; Model 2 [0.0001 (0.0000, 0.0001)]; and Model 3 [0.0001 (0.0001, 0.0002)]. The P values were all statistically significant (P<0.001).

In girls (**Table 4**; **Figure 3**), the association of testosterone with total BMD was positive in Model 1 [0.0014 (0.0008, 0.0019)] and Model 2 [0.0006 (0.0000, 0.0011)], whereas in Model 3, the association was not significant [0.0004 (-0.0001, 0.0008)] (**Table 4**). The P values for all three models were statistically significant (P < 0.05). The nonlinear association between testosterone and total BMD is presented in **Figure 3B**. The inflection point of the inverted U-shaped curve between testosterone and total BMD was calculated to be a testosterone level of 25.4 ng/dL by using a two-piecewise linear regression model (**Table 5**).

Association Between Estradiol and Total BMD

In boys (**Table 3**; **Figure 2**), estradiol was positively associated with total BMD in all three models (**Table 3**): Model 1 [0.0070 (0.0063, 0.0078)]; Model 2 [0.0032 (0.0024, 0.0040)]; and Model 3 [0.0029 (0.0021, 0.0037)]. The P values were all statistically significant (P<0.001). There was a specific point between estradiol and total BMD (24.3 pg/mL of estradiol), after which the positive correlation between estradiol and total BMD was relatively insignificant (**Figure 2D**).

In girls (**Table 4**; **Figure 3**), the association between estradiol and total BMD was positive in all three models (**Table 4**): Model 1 [0.0002 (0.0001, 0.0003)]; Model 2 [0.0001 (0.0000, 0.0002)]; and Model 3 [0.0001 (0.0001, 0.0002)] (P for trend < 0.05 for each).

Association Between SHBG and Total BMD

In boys (**Table 3**; **Figure 2**), SHBG was negatively associated with total BMD in all three regression models (**Table 3**): Model 1 [-0.0024 (-0.0027, -0.0021)]; Model 2 [-0.0011 (-0.0015, -0.0008)]; and Model 3 [-0.0007 (-0.0011, -0.0004)] (P for trend < 0.01 for each).

In girls (**Table 4**; **Figure 3**), we did not find a significant correlation between SHBG and total BMD (**Table 4**): Model 1 [-0.0001 (-0.0002, 0.0000)]; Model 3 [-0.0001 (-0.0002, 0.0001)]. The P value for Model 3 was not significant (P>0.05).

DISCUSSION

The population of adolescent boys and girls selected for our study was nationally representative. The association of sex hormones with total BMD differed in boys and girls. In boys, testosterone and estradiol levels were positively associated with total BMD, whereas SHBG levels were negatively associated with total BMD. In girls, estradiol was positively associated with total

TABLE 1 | Descriptions of 853 boys included in the present study.

	Testosterone					Estradiol					Sex hormone-binding globulin					
	Q1	Q2	Q3	Q4	P value	Q1	Q2	Q3	Q4	P value		Q1	Q2	Q3	Q4	P value
Age (years)	13.42 ± 1.58	15.52 ± 2.09	16.27 ± 2.01	16.12 ± 1.92	<0.0001	13.19 ± 1.38	15.11 ± 1.87	16.27 ± 2.00	16.82 ± 1.66	<0.0001	Age (years)	16.36 ± 2.11	15.95 ± 1.99	15.15 ± 1.90	13.96 ± 2.07	<0.0001
Race/Ethnicity (%)					0.7371					0.1357	Race/Ethnicity (%)					<0.0001
Mexican American	12.19	18.13	18.62	15.73		12.21	15.35	19.64	17.78		Mexican American	25.03	18.62	12.42	9.82	
Other Hispanic	8.72	6.02	6.00	9.14		7.72	6.17	8.34	7.78		Other Hispanic	9.41	9.26	5.63	5.87	
Non-Hispanic White	57.46	57.86	55.57	52.49		61.48	61.43	49.80	49.77		Non-Hispanic White	44.42	52.78	56.75	67.35	
Non-Hispanic Black	13.14	9.91	10.92	13.90		12.97	10.24	11.22	13.45		Non-Hispanic Black	9.77	10.09	15.50	12.34	
Other Race/ Ethnicity	8.50	8.07	8.88	8.74		5.61	6.81	10.99	11.23		Other Race/ Ethnicity	11.37	9.25	9.69	4.62	
Body mass index (kg/m^2)	23.86 ± 7.16	25.59 ± 7.70	24.15 ± 4.94	22.14 ± 3.60	<0.0001	21.23 ± 4.70	23.16 ± 5.61	25.63 ± 7.03	26.27 ± 6.37	<0.0001	Body mass index (kg/m^2)	30.36 ± 6.86	24.47 ± 5.36	22.09 ± 3.82	19.95 ± 3.37	<0.0001
Income to poverty ratio	4.75 ± 1.79	4.93 ± 3.68	4.91 ± 2.62	5.15 ± 5.43	0.7277	4.81 ± 1.81	4.84 ± 3.50	5.10 ± 4.79	5.00 ± 3.88	0.8183	Income to poverty ratio	4.94 ± 2.59	4.73 ± 2.93	5.28 ± 5.41	4.81 ± 2.91	0.4334
Moderate activities (%)					0.1443					0.0014	Moderate activities (%)					0.6156
Yes	59.08	58.54	56.35	55.27		56.99	63.67	49.74	58.31		Yes	55.43	55.83	61.46	56.90	
No	38.31	39.85	43.32	44.73		39.61	35.77	49.61	41.69		No	43.14	43.93	36.94	41.62	
Not recorded	2.61	1.61	0.33			3.39	0.56	0.65			Not recorded	1.43	0.24	1.60	1.48	
Blood urea nitrogen (mg/dL)	11.86 ± 3.63	12.32 ± 3.48	11.92 ± 3.08	11.77 ± 3.74	0.3781	12.08 ± 3.48	12.20 ± 3.54	11.62 ± 3.55	11.96 ± 3.41	0.3641	Blood urea nitrogen (mg/dL)	11.64 ± 3.23	12.20 ± 3.43	12.46 ± 3.83	11.63 ± 3.43	0.0310
Serum uric acid (mg/dL)	5.18 ± 1.30	5.83 ± 1.33	5.83 ± 1.03	5.60 ± 0.97	<0.0001	4.77 ± 1.05	5.70 ± 1.12	5.96 ± 1.04	6.05 ± 1.16	<0.0001	Serum uric acid (mg/dL)	6.47 ± 1.16	5.78 ± 0.97	5.51 ± 1.07	4.83 ± 1.01	<0.0001
Total protein (g/L)	71.40 ± 4.16	72.16 ± 4.29	72.99 ± 4.37	73.29 ± 4.35	<0.0001	70.78 ± 4.27	72.45 ± 4.32	72.81 ± 4.06	73.82 ± 4.16	<0.0001	Total protein (g/L)	73.36 ± 4.30	72.95 ± 4.38	72.53 ± 4.33	71.12 ± 4.07	<0.0001
Total cholesterol (mg/dL)	155.75 ± 31.15	155.53 ± 29.27	153.24 ± 28.10	154.98 ± 28.85	0.8190	154.01 ± 30.00	150.38 ± 26.92	154.50 ± 28.79	161.42 ± 30.94	0.0013	Total cholesterol (mg/dL)	162.22 ± 33.74	153.26 ± 28.94	150.59 ± 24.46	154.14 ± 28.89	0.0006
Serum phosphorus (mg/ dL)	4.94 ± 0.65	4.45 ± 0.67	4.25 ± 0.75	4.28 ± 0.61	<0.0001	5.03 ± 0.62	4.54 ± 0.67	4.28 ± 0.64	4.07 ± 0.57	<0.0001	Serum phosphorus (mg/ dL)	4.19 ± 0.58	4.36 ± 0.68	4.55 ± 0.75	4.81 ± 0.71	<0.0001
Serum calcium (mg/dL)	9.61 ± 0.31	9.66 ± 0.29	9.68 ± 0.29	9.69 ± 0.29	0.0115	9.63 ± 0.28	9.67 ± 0.30	9.62 ± 0.32	9.72 ± 0.28	0.0047	Serum calcium (mg/dL)	9.67 ± 0.32	9.66 ± 0.29	9.65 ± 0.31	9.66 ± 0.27	0.9330
Total BMD (g/cm^2)	0.94 ± 0.12	1.04 ± 0.13	1.07 ± 0.12	1.09 ± 0.12	<0.0001	0.91 ± 0.10	1.03 ± 0.12	1.09 ± 0.11	1.11 ± 0.11	<0.0001	Total BMD (g/cm^2)	1.09 ± 0.11	1.08 ± 0.12	1.02 ± 0.12	0.94 ± 0.13	<0.0001

Mean ± SD for continuous variables: P-value was calculated by weighted linear regression model. % for categorical variables: P-value was calculated by weighted chi-square test.

TABLE 2 | Descriptions of 795 girls included in the present study.

	Testosterone					Estradiol					Sex hormone-binding globulin					
	Q1	Q2	Q3	Q4	P value	Q1	Q2	Q3	Q4	P value		Q1	Q2	Q3	Q4	P value
Age (years)	14.65 ± 2.19	15.28 ± 2.07	15.44 ± 2.10	15.86 ± 1.98	<0.0001	15.23 ± 2.31	14.95 ± 2.13	15.30 ± 2.04	15.85 ± 1.87	0.0004	Age (years)	15.35 ± 2.23	15.35 ± 2.01	15.20 ± 2.26	15.41 ± 2.02	0.7709
Race/Ethnicity (%)					0.8543					0.0075	Race/Ethnicity (%)					<0.0001
Mexican American	15.18	17.67	14.99	12.20		11.42	17.25	12.57	19.24		Mexican American	25.57	13.81	17.74	5.59	
Other Hispanic	10.59	9.36	6.46	7.94		4.46	10.29	13.20	6.83		Other Hispanic	9.94	11.54	5.84	7.19	
Non-Hispanic White	53.97	54.99	56.55	56.00		66.19	52.36	51.65	49.47		Non-Hispanic White	43.75	49.07	53.31	71.09	
Non-Hispanic Black	10.79	10.53	10.52	12.86		8.09	11.94	11.58	13.77		Non-Hispanic Black	9.88	11.69	13.59	9.79	
Other Race/ Ethnicity	9.47	7.46	11.47	11.00		9.85	8.17	11.00	10.68		Other Race/ Ethnicity	10.86	13.90	9.52	6.35	
Body mass index (kg/m^2)	23.75 ± 5.65	23.81 ± 5.57	25.50 ± 7.15	25.14 ± 5.71	0.0050	24.46 ± 5.61	24.87 ± 6.69	24.75 ± 6.15	24.31 ± 6.12	0.7984	Body mass index (kg/m^2)	29.98 ± 6.94	25.29 ± 4.94	22.23 ± 4.19	21.98 ± 4.85	<0.0001
Income to poverty ratio	5.42 ± 6.79	5.63 ± 6.32	4.65 ± 1.82	4.69 ± 3.56	0.1077	4.75 ± 3.96	5.45 ± 7.33	5.31 ± 4.96	4.85 ± 2.40	0.4134	Income to poverty ratio	6.25 ± 7.93	4.80 ± 3.79	5.03 ± 4.16	4.45 ± 2.98	0.0025
Moderate activities (%)					0.0164					<0.0001	Moderate activities (%)					0.0267
Yes	56.69	54.11	56.38	52.33		65.11	56.86	45.96	49.41		Yes	52.62	59.69	53.67	53.58	
No	42.74	45.22	39.94	47.67		34.89	42.12	49.91	50.37		No	46.77	40.31	42.68	45.60	
Not recorded	0.58	0.66	3.68				1.02	4.13	0.22		Not recorded	0.61		3.65	0.82	
Blood urea nitrogen (mg/dL)	162.04 ± 26.82	10.75 ± 3.40	10.65 ± 4.94	10.29 ± 2.72	0.2949	10.74 ± 3.00	10.85 ± 5.11	10.04 ± 2.80	10.18 ± 3.18	0.0649	Blood urea nitrogen (mg/dL)	9.88 ± 2.55	10.66 ± 2.67	10.58 ± 3.38	10.65 ± 4.92	0.1106
Serum uric acid (mg/dL)	4.49 ± 1.02	4.33 ± 1.07	4.63 ± 1.07	4.41 ± 1.04	0.0249	4.40 ± 0.97	4.68 ± 1.24	4.43 ± 0.94	4.37 ± 1.04	0.0157	Serum uric acid (mg/dL)	5.20 ± 1.18	4.41 ± 0.97	4.27 ± 0.86	4.14 ± 0.91	<0.0001
Total protein (g/L)	162.04 ± 26.82	158.57 ± 29.32	158.60 ± 29.11	164.69 ± 30.73	0.0970	163.93 ± 28.82	161.98 ± 29.23	161.37 ± 29.80	156.04 ± 28.43	0.0463	Total protein (g/L)	165.54 ± 32.69	155.81 ± 26.67	155.91 ± 25.26	165.94 ± 30.04	<0.0001
Total cholesterol (mg/dL)	71.45 ± 3.76	71.98 ± 3.97	72.37 ± 4.33	71.76 ± 4.01	0.1392	71.80 ± 3.75	72.27 ± 4.06	72.02 ± 4.56	71.56 ± 3.79	0.3584	Total cholesterol (mg/dL)	72.30 ± 4.08	72.61 ± 4.03	72.15 ± 3.76	70.85 ± 4.06	<0.0001
Serum phosphorus (mg/ dL)	4.39 ± 0.62	4.26 ± 0.56	4.18 ± 0.55	4.16 ± 0.52	0.0003	4.28 ± 0.61	4.35 ± 0.59	4.19 ± 0.53	4.12 ± 0.50	0.0004	Serum phosphorus (mg/ dL)	4.20 ± 0.63	4.19 ± 0.51	4.32 ± 0.54	4.25 ± 0.59	0.1179
Serum calcium (mg/dL)	9.56 ± 0.32	9.53 ± 0.27	9.54 ± 0.32	9.52 ± 0.29	0.6382	9.55 ± 0.34	9.56 ± 0.27	9.55 ± 0.28	9.50 ± 0.31	0.2507	Serum calcium (mg/dL)	9.56 ± 0.30	9.50 ± 0.27	9.60 ± 0.27	9.50 ± 0.34	0.0009
Total BMD (g/cm^2)	0.98 ± 0.11	1.02 ± 0.10	1.03 ± 0.10	1.04 ± 0.10	<0.0001	1.01 ± 0.12	1.00 ± 0.10	1.02 ± 0.10	1.04 ± 0.10	0.0023	Total BMD (g/cm^2)	1.04 ± 0.11	1.04 ± 0.10	1.00 ± 0.10	1.01 ± 0.10	<0.0001

Mean ± SD for continuous variables: P-value was calculated by weighted linear regression model. % for categorical variables: P-value was.

TABLE 3 | Association of serum testosterone, estradiol, and sex hormone-binding globulin levels with total bone mineral density in boys.

	Model 1 β (95% CI)	Model 2 β (95% CI)	Model 3 β (95% CI)
Testosterone	0.0003 (0.0002, 0.0003) <0.000001	0.0001 (0.0000, 0.0001) 0.000035	0.0001 (0.0001, 0.0002) <0.000001
Testosterone categories			
Q1	0	0	0
Q2	0.0980 (0.0751, 0.1209) <0.000001	0.0277 (0.0071, 0.0483) 0.008421	0.0273 (0.0078, 0.0468) 0.006311
Q3	0.1322 (0.1086, 0.1558) <0.000001	0.0350 (0.0128, 0.0573) 0.002100	0.0494 (0.0279, 0.0709) 0.000008
Q4	0.1454 (0.1218, 0.1689) <0.000001	0.0513 (0.0294, 0.0732) 0.000005	0.0788 (0.0571, 0.1006) <0.000001
P for trend	<0.001	<0.001	<0.001
Estradiol	0.0070 (0.0063, 0.0078) <0.000001	0.0032 (0.0024, 0.0040) <0.000001	0.0029 (0.0021, 0.0037) <0.000001
Estradiol categories			
Q1	0	0	0
Q2	0.1125 (0.0917, 0.1333) <0.000001	0.0603 (0.0403, 0.0802) <0.000001	0.0563 (0.0361, 0.0764) <0.000001
Q3	0.1784 (0.1569, 0.1999) <0.000001	0.0922 (0.0696, 0.1147) <0.000001	0.0852 (0.0622, 0.1082) <0.000001
Q4	0.1959 (0.1745, 0.2173) <0.000001	0.0929 (0.0692, 0.1166) <0.000001	0.0833 (0.0588, 0.1077) <0.000001
P for trend	<0.001	<0.001	<0.001
Sex hormone-binding globulin	-0.0024 (-0.0027, -0.0021) <0.000001	-0.0011 (-0.0015, -0.0008) <0.000001	-0.0007 (-0.0011, -0.0004) 0.000072
Sex hormone-binding globulin categories			
Q1	0	0	0
Q2	-0.0056 (-0.0294, 0.0181) 0.642019	0.0080 (-0.0117, 0.0277) 0.425053	0.0312 (0.0104, 0.0520) 0.003420
Q3	-0.0648 (-0.0889, -0.0408) <0.000001	-0.0278 (-0.0482, -0.0074) 0.007671	0.0063 (-0.0166, 0.0293) 0.587642
Q4	-0.1451 (-0.1682, -0.1220) <0.000001	-0.0662 (-0.0872, -0.0452) <0.000001	-0.0210 (-0.0463, 0.0042) 0.102539
P for trend	<0.001	<0.001	0.008

Model 1, no covariates were adjusted. Model 2, age, race were adjusted. Model 3, age, race, body mass index, ratio of family income to poverty, moderate activities, blood urea nitrogen, serum uric acid, total protein, total cholesterol, serum phosphorus, and serum calcium were adjusted.

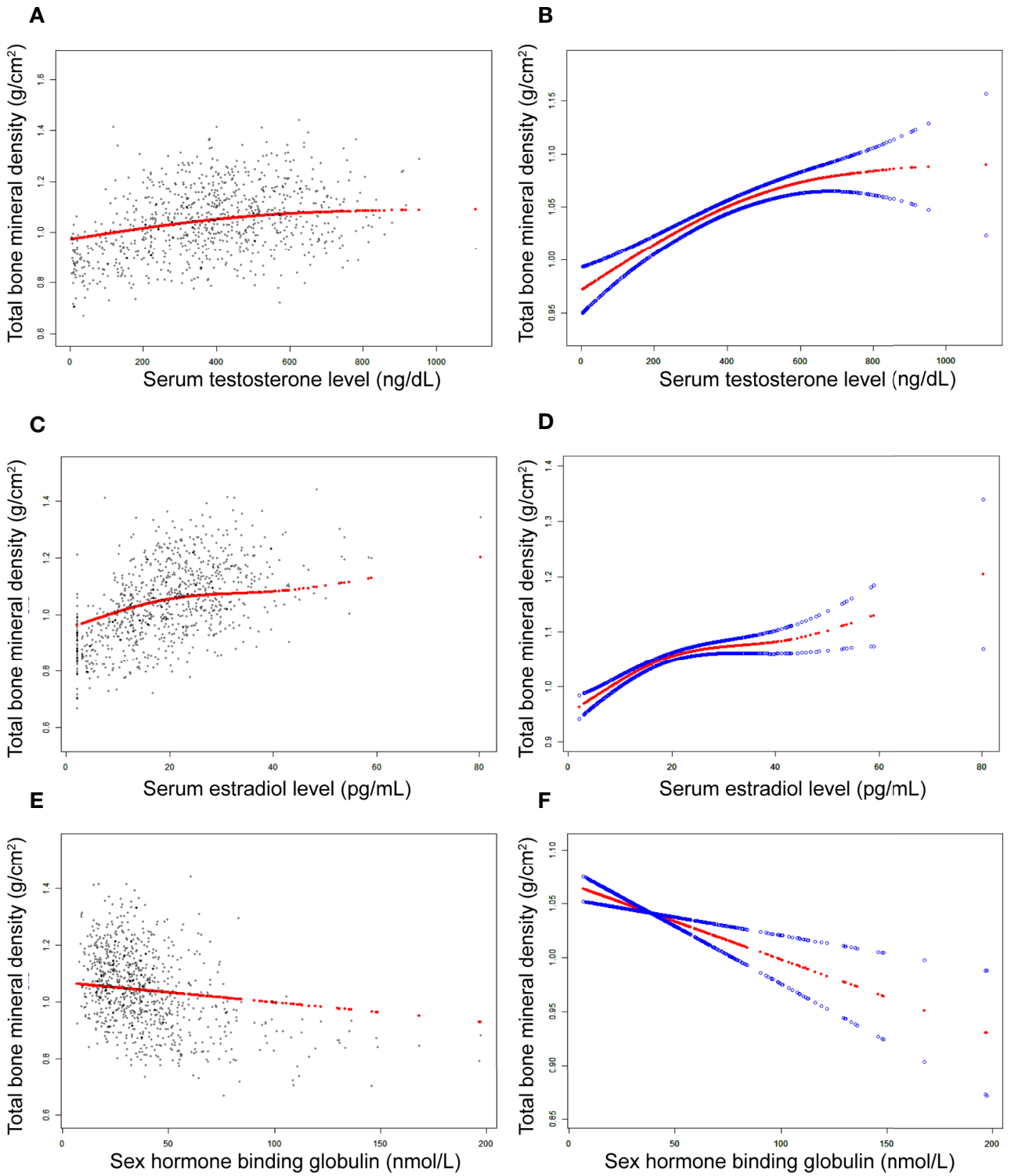

FIGURE 2 | The association between testosterone **(A, B)**, estradiol **(C, D)**, and SHBG **(E, F)** and total bone mineral density in boys, respectively. **(A, C, E)** Each black point represents a sample. **(B, D, F)** Solid red line represents the smooth curve fit between variables. Blue bands represent the 95% of confidence interval from the fit. Adjusted for age, race, body mass index, ratio of family income to poverty, moderate activities, blood urea nitrogen, serum uric acid, total protein, total cholesterol, serum phosphorus, and serum calcium.

TABLE 4 | Association of serum testosterone, estradiol, and sex hormone-binding globulin levels with total bone mineral density in girls.

	Model 1 β (95% CI)	Model 2 β (95% CI)	Model 3 β (95% CI)
Testosterone	0.0014 (0.0008, 0.0019) 0.000001	0.0006 (0.0000, 0.0011) 0.032395	0.0004 (-0.0001, 0.0008) 0.129161
Testosterone categories			
Q1	0	0	0
Q2	0.0317 (0.0108, 0.0526) 0.003052	0.0183 (-0.0003, 0.0370) 0.054683	0.0153 (-0.0020, 0.0326) 0.084278
Q3	0.0495 (0.0291, 0.0699) 0.000002	0.0320 (0.0137, 0.0504) 0.000655	0.0203 (0.0031, 0.0375) 0.020724
Q4	0.0546 (0.0341, 0.0751) <0.000001	0.0268 (0.0082, 0.0455) 0.004953	0.0210 (0.0038, 0.0383) 0.017147
P for trend	<0.001	0.002	0.017
Estradiol	0.0002 (0.0001, 0.0003) 0.000058	0.0001 (0.0000, 0.0002) 0.004228	0.0001 (0.0001, 0.0002) 0.000257
Estradiol categories			
Q1	0	0	0
Q2	-0.0066 (-0.0267, 0.0135) 0.521140	-0.0001 (-0.0180, 0.0178) 0.990773	0.0017 (-0.0149, 0.0182) 0.845114
Q3	0.0116 (-0.0085, 0.0317) 0.258851	0.0105 (-0.0074, 0.0285) 0.250676	0.0112 (-0.0055, 0.0280) 0.189114
Q4	0.0312 (0.0111, 0.0513) 0.002435	0.0167 (-0.0013, 0.0347) 0.069677	0.0189 (0.0022, 0.0357) 0.027236
P for trend	<0.001	0.041	0.017
Sex hormone-binding globulin	-0.0001 (-0.0002, 0.0000) 0.133284	-0.0002 (-0.0003, -0.0001) 0.000132	-0.0001 (-0.0002, 0.0001) 0.242211
Sex hormone-binding globulin categories			
Q1	0	0	0
Q2	0.0054 (-0.0159, 0.0267) 0.620522	0.0026 (-0.0161, 0.0213) 0.784763	0.0105 (-0.0085, 0.0295) 0.277503
Q3	-0.0340 (-0.0551, -0.0129) 0.001645	-0.0354 (-0.0539, -0.0169) 0.000191	-0.0085 (-0.0285, 0.0115) 0.405766
Q4	-0.0314 (-0.0517, -0.0112) 0.002442	-0.0384 (-0.0566, -0.0202) 0.000038	-0.0075 (-0.0281, 0.0131) 0.476320
P for trend	<0.001	<0.001	0.160

Model 1, no covariates were adjusted. Model 2, age, race were adjusted. Model 3, age, race, body mass index, ratio of family income to poverty, moderate activities, blood urea nitrogen, serum uric acid, total protein, total cholesterol, serum phosphorus, and serum calcium were adjusted.

TABLE 5 | Threshold effect analysis of serum testosterone level on total bone mineral density using two-piecewise linear regression model.

Total bone mineral density	Adjusted β (95% CI), P value
Serum testosterone level	
Fitting by standard linear model	0.0004 (-0.0001, 0.0008) 0.129161
Fitting by two-piecewise linear model	
Inflection point	25.4 (ng/dL)
Serum testosterone level < 25.4 (ng/dL)	0.0021 (0.0009, 0.0034) 0.0008
Serum testosterone level > 25.4 (ng/dL)	-0.0003 (-0.0010, 0.0003) 0.3095
Log likelihood ratio	0.002

Age, race, body mass index, ratio of family income to poverty, moderate activities, blood urea nitrogen, serum uric acid, total protein, total cholesterol, serum phosphorus, and serum calcium were adjusted.

BMD, whereas testosterone and SHBG levels were not significantly associated with total BMD. Notably, we found that in boys, there was a point between estradiol and total BMD (24.3 pg/mL of estradiol), after which the positive correlation between estradiol and total BMD was relatively insignificant. In girls, there was an inverted U-shaped association between total BMD and testosterone with the inflection point at 25.4 ng/dL of testosterone.

A cross-sectional study of 1070 Korean men reported that both total testosterone and free testosterone were positively correlated with BMD, and genetic effects played an important part in the association of testosterone with BMD (11). A cross-sectional study of adults aged 40-60 years reported that testosterone levels were negatively associated with total BMD (12). Furthermore, total testosterone levels were not significantly associated with total BMD in adolescent girls. However, we found that too much testosterone can not only cause virilization and infertility but also reduce BMD and affect bone health in women. However, we need more prospective intervention studies to support our findings.

A growing number of studies have reported that decreased estradiol levels are associated with decreased BMD. A study of postmenopausal women with and without osteoporosis found that serum estradiol levels were markedly lower in those with osteoporosis than in those without osteoporosis, suggesting that there was a positive association between estradiol and BMD (13). A previous study of male college athletes found that free and total estradiol levels were important positive determinants of BMD (14). Moreover, a previous genome-wide study confirmed the role of estradiol on BMD and bone health in men and women (15). In our study, we found that the relationship between estradiol and total BMD in boys was not always significantly positive.

A cross-sectional study of US adults reported that the value of SHBG for predicting bone loss in adults may improve (7). A previous cross-sectional study of 142 Moroccan men with no prior diagnosis of osteoporosis reported that BMD at the total hip was negatively correlated with SHBG (16). A study of Chinese men over 45 years old reported a negative correlation between serum SHBG levels and BMD (17). Additionally, a study of premenopausal women reported a negative relationship between SHBG levels and bone mass (18). The evidence mentioned above suggests that higher SHBG levels may play a significant role in the development of osteoporosis. In our study, this relationship was not significant in girls.

Our data were obtained from the NHANES, and NHANES data were acquired according to standard protocols, which ensures that our findings are consistent and accurate. However, we should clearly recognize the limitations of our study. First, the NHANES is a large cross-sectional survey and therefore cannot determine causal relationships between exposure factors and outcome variables, and more cohort studies are needed to confirm our conclusions. Second, the samples in the NHANES were only assessed once, and some data were missing, which may lead to potential bias. Therefore, it is recommended that further

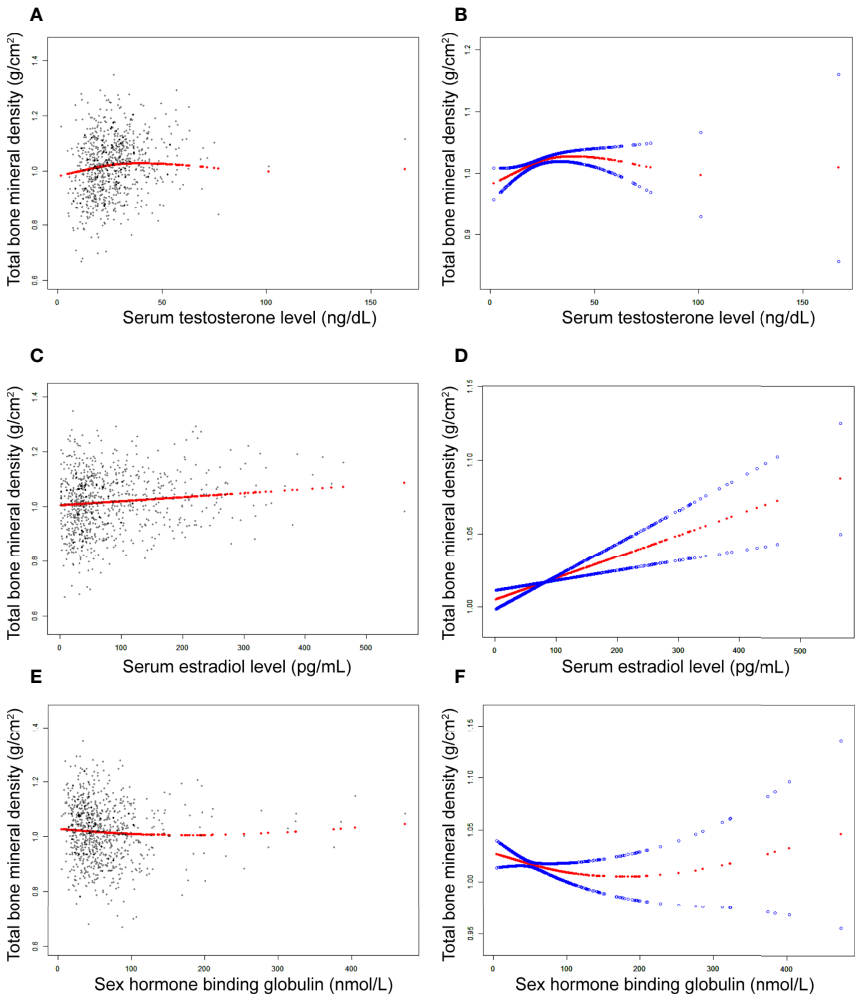

FIGURE 3 | The association between testosterone **(A, B)**, estradiol **(C, D)**, and SHBG **(E, F)** and total bone mineral density in girls, respectively. **(A, C, E)** Each black point represents a sample. **(B, D, F)**, Solid red line represents the smooth curve fit between variables. Blue bands represent the 95% of confidence interval from the fit. Adjusted for age, race, body mass index, ratio of family income to poverty, moderate activities, blood urea nitrogen, serum uric acid, total protein, total cholesterol, serum phosphorus, and serum calcium.

studies are required to perform multiple tests. Third, although we used nationally representative population data, the study was limited to adolescent boys and girls aged 12–19 years. Consequently, the study's conclusions may not be applicable to children and other populations.

CONCLUSION

We found differences in the association of sex hormones with total BMD in boys and girls. An inverted U-shaped association between testosterone levels and total BMD in girls with the inflection point at 25.4 ng/dL of testosterone suggests that an appropriate increase in serum testosterone levels may be beneficial for skeletal development, whereas a high testosterone level may be detrimental to BMD. Furthermore, keeping estradiol levels below a certain level in boys (24.3 pg/mL) may be considered.

DATA AVAILABILITY STATEMENT

The original contributions presented in the study are included in the article/**Supplementary Material**. Further inquiries can be directed to the corresponding author.

AUTHOR CONTRIBUTIONS

KX and MZ conceptualized and designed the study. KX collected data, performed data analysis, and participated in

the writing the manuscript. KX and YF revised the manuscript. KX and MZ reviewed the manuscript. KX, YF and BC produced figures and tables. All authors approved the final manuscript and agreed to be responsible for all aspects of the study.

REFERENCES

1. Torres-Costoso A, López-Muñoz P, Martínez-Vizcaíno V, Álvarez-Bueno C, Cavero-Redondo I. Association Between Muscular Strength and Bone Health From Children to Young Adults: A Systematic Review and Meta-Analysis. *Sports Med (Auckland N.Z.)* (2020) 50:1163–90. doi: 10.1007/s40279-020-01267-y
2. Bland VL, Bea JW, Blew RM, Roe DJ, Lee VR, Funk JL, et al. Influence of Changes in Soft Tissue Composition on Changes in Bone Strength in Peripubertal Girls: The STAR Longitudinal Study. *J Bone Mineral Res* (2021) 36:123–32. doi: 10.1002/jbmr.4168
3. Weaver CM, Gordon CM, Janz KF, Kalkwarf HJ, Lappe JM, Lewis R, et al. The National Osteoporosis Foundation's Position Statement on Peak Bone Mass Development and Lifestyle Factors: A Systematic Review and Implementation Recommendations. *Osteoporosis Int* (2016) 7:1281–386. doi: 10.1007/s00198-015-3440-3
4. Bachrach LK. Hormonal Contraception and Bone Health in Adolescents. *Front Endocrinol* (2020) 11:603. doi: 10.3389/fendo.2020.00603
5. Vescini F, Chiodini I, Falchetti A, Palermo A, Salcuni AS, Bonadonna S, et al. Management of Osteoporosis in Men: A Narrative Review. *Int J Mol Sci* (2021) 22:13460. doi: 10.3390/ijms222413640
6. Simó R, Sáez-López C, Barbosa-Desongles A, Hernández C, Selva DM. Novel Insights in SHBG Regulation and Clinical Implications. *Trends Endocrinol Metab* (2015) 26:376–83. doi: 10.1016/j.tem.2015.05.001
7. Yang F, Yang D, Zhou Y, Wu J. Associations of Sex Hormone-Binding Globulin With Bone Mineral Density Among US Adults, NHANES 2013-2016. *Int J Gen Med* (2021) 14:7707–17. doi: 10.2147/IJGM.S329992
8. Zhu Z, Zhao J, Fang Y, Hua R. Association Between Serum Estradiol Level, Sex Hormone Binding Globulin Level, and Bone Mineral Density in Middle-Aged Postmenopausal Women. *J Orthop Surg Res* (2021) 16:648. doi: 10.1186/s13018-021-02799-3
9. Woods GN, Huang MH, Cawthon PM, Laughlin GA, Schousboe JT, McDaniels-Davidson C, et al. SHBG, Sex Steroids, and Kyphosis in Older Men: The MrOS Study. *J Bone Miner Res* (2016) 31:2123–8. doi: 10.1002/jbmr.2901
10. von Elm E, Altman DG, Egger M, Pocock SJ, Gøtzsche PC, Vandenbroucke JP. The Strengthening the Reporting of Observational Studies in Epidemiology (STROBE) Statement: Guidelines for Reporting Observational Studies. *Lancet (London England)* (2007) 370:1453–7. doi: 10.1016/S0140-6736(07)61602-X
11. Shin J, Sung J, Lee K, Song YM. Genetic Influence on the Association Between Bone Mineral Density and Testosterone in Korean Men. *Osteoporosis Int* (2016) 27:643–51. doi: 10.1007/s00198-015-3298-4
12. Wang N, Wang L, Huang C. Association of Total Testosterone Status With Bone Mineral Density in Adults Aged 40-60 Years. *J Orthopaedic Surg Res* (2021) 16:612. doi: 10.1186/s13018-021-02714-w
13. Mederle OA, Balas M, Ioanoviciu SD, Gurban CV, Tudor A, Borza C. Correlations Between Bone Turnover Markers, Serum Magnesium and Bone Mass Density in Postmenopausal Osteoporosis. *Clin Interv Aging* (2018) 13:1383–9. doi: 10.2147/CIA.S170111
14. Ackerman KE, Skrinar GS, Medvedova E, Misra M, Miller KK. Estradiol Levels Predict Bone Mineral Density in Male Collegiate Athletes: A Pilot Study. *Clin Endocrinol* (2012) 76:339–45. doi: 10.1111/j.1365-2265.2011.04212.x
15. Schmitz D, Ek WE, Berggren E, Höglund J, Karlsson T, Johansson Å. Genome-Wide Association Study of Estradiol Levels and the Causal Effect of Estradiol on Bone Mineral Density. *J Clin Endocrinol Metab* (2021) 106:e4471–86. doi: 10.1210/clinem/dgab507
16. Maataoui AE, Benghabrite A, Maghraoui AE, Chabraoui L, Ouzzif Z. Relationship Between Sex Hormone Levels, Bone Mineral Density and Bone Turnover Markers in Healthy Moroccan Men: A Cross-Sectional Study. *Pan Afr Med J* (2015) 22:206. doi: 10.11604/pamj.2015.22.206.6066
17. Zha XY, Hu Y, Pang XN, Zhu JH, Chang GL, Li L. Sex Hormone-Binding Globulin (SHBG) as an Independent Determinant of Bone Mineral Density (BMD) Among Chinese Middle-Aged and Elderly Men. *Endocrine* (2014) 47:590–7. doi: 10.1007/s12020-013-0155-0
18. Wei S, Jones G, Thomson R, Otahal P, Venn A. Menstrual Irregularity and Bone Mass in Premenopausal Women: Cross-Sectional Associations With Testosterone and SHBG. *BMC Musculoskeletal Disord* (2010) 11:288. doi: 10.1186/1471-2474-11-288

SUPPLEMENTARY MATERIAL

The Supplementary Material for this article can be found online at: https://www.frontiersin.org/articles/10.3389/fendo.2022.891217/full#supplementary-material

Conflict of Interest: The authors declare that the research was conducted in the absence of any commercial or financial relationships that could be construed as a potential conflict of interest.

Publisher's Note: All claims expressed in this article are solely those of the authors and do not necessarily represent those of their affiliated organizations, or those of the publisher, the editors and the reviewers. Any product that may be evaluated in this article, or claim that may be made by its manufacturer, is not guaranteed or endorsed by the publisher.

Advantages of publishing in Frontiers

OPEN ACCESS
Articles are free to read for greatest visibility and readership

FAST PUBLICATION
Around 90 days from submission to decision

HIGH QUALITY PEER-REVIEW
Rigorous, collaborative, and constructive peer-review

TRANSPARENT PEER-REVIEW
Editors and reviewers acknowledged by name on published articles

Frontiers
Avenue du Tribunal-Fédéral 34
1005 Lausanne | Switzerland

Visit us: www.frontiersin.org
Contact us: frontiersin.org/about/contact

REPRODUCIBILITY OF RESEARCH
Support open data and methods to enhance research reproducibility

DIGITAL PUBLISHING
Articles designed for optimal readership across devices

FOLLOW US
@frontiersin

IMPACT METRICS
Advanced article metrics track visibility across digital media

EXTENSIVE PROMOTION
Marketing and promotion of impactful research

LOOP RESEARCH NETWORK
Our network increases your article's readership